VILNIUS GEDIMINAS TECHNICAL UNIVERSITY

Mindaugas MELAIKA

RESEARCH OF A COMBUSTION PROCESS IN A SPARK IGNITION ENGINE, FUELLED WITH GASEOUS FUEL MIXTURES

DOCTORAL DISSERTATION

TECHNOLOGICAL SCIENCES,
TRANSPORT ENGINEERING (03T)

VGTU
LEIDYKLA TECHNIKA
Vilnius 2016

Doctoral dissertation was prepared at Vilnius Gediminas Technical University in 2012–2016.

Supervisor

Assoc. Prof. Dr Saugirdas PUKALSKAS (Vilnius Gediminas Technical University, Transport Engineering – 03T).

The Dissertation Defense Council of Scientific Field of Transport Engineering of Vilnius Gediminas Technical University:

Chairman

Assoc. Prof. Dr Gintautas BUREIKA (Vilnius Gediminas Technical University, Transport Engineering – 03T).

Members:

Assoc. Prof. Dr Raimundas JUNEVIČIUS (Vilnius Gediminas Technical University, Transport Engineering – 03T),
Prof. Dr Gvidonas LABECKAS (Aleksandras Stulginskis University, Transport Engineering – 03T),
Prof. Dr Habil. Gintautas MILIAUSKAS (Kaunas University of Technology, Energetics and Power Engineering – 06T),
Dr Adam TOROK (Budapest University of Technology and Economics, Transport Engineering – 03T).

The dissertation will be defended at the public meeting of the Dissertation Defense Council of Transport Engineering in the Senate Hall of Vilnius Gediminas Technical University at **10 a. m. on 24 January 2017**.

Address: Saulėtekio al. 11, LT-10223 Vilnius, Lithuania.
Tel.: +370 5 274 4956; fax +370 5 270 0112; e-mail: doktor@vgtu.lt

A notification on the intend defending of the dissertation was send on 23 December 2016.
A copy of the doctoral dissertation is available for review at VGTU repository http://dspace.vgtu.lt and at the Library of Vilnius Gediminas Technical University (Saulėtekio al. 14, LT-10223 Vilnius, Lithuania), Klaipėda University (K. Donelaičio g. 3, LT-92144 Klaipėda, Lithuania) and Aleksandras Stulginskis University (Studentų g. 11, LT-53361 Akademija, Kauno raj.).

VGTU leidyklos TECHNIKA 2403-M mokslo literatūros knyga

ISBN 978-609-457-996-7

mindaugas.melaika@gmail.com

VILNIAUS GEDIMINO TECHNIKOS UNIVERSITETAS

Mindaugas MELAIKA

DUJINIŲ DEGALŲ MIŠINIŲ DEGIMO PROCESO KIBIRKŠTINIO UŽDEGIMO VARIKLYJE TYRIMAI

DAKTARO DISERTACIJA

TECHNOLOGIJOS MOKSLAI,
TRANSPORTO INŽINERIJA (03T)

VGTU
LEIDYKLA
Vilnius TECHNIKA 2016

Disertacija rengta 2012–2016 metais Vilniaus Gedimino technikos universitete.

Vadovas

doc. dr. Saugirdas PUKALSKAS (Vilniaus Gedimino technikos universitetas, transporto inžinerija – 03T).

Vilniaus Gedimino technikos universiteto Transporto inžinerijos mokslo krypties disertacijos gynimo taryba:

Pirmininkas

doc. dr. Gintautas BUREIKA (Vilniaus Gedimino technikos universitetas, transporto inžinerija – 03T).

Nariai:

doc. dr. Raimundas JUNEVIČIUS (Vilniaus Gedimino technikos universitetas, transporto inžinerija – 03T),
prof. dr. Gvidonas LABECKAS (Aleksandro Stulginskio universitetas, transporto inžinerija – 03T),
prof. habil. dr. Gintautas MILIAUSKAS (Kauno technologijos universitetas, energetika ir termoinžinerija – 06T),
dr. Adam TOROK (Budapešto technologijos ir ekonomikos universitetas, transporto inžinerija – 03T).

Disertacija bus ginama viešame Transporto inžinerijos mokslo krypties disertacijos gynimo tarybos posėdyje **2017 m. sausio 24 d. 10 val.** Vilniaus Gedimino technikos universiteto senato posėdžių salėje.

Adresas: Saulėtekio al. 11, LT-10223 Vilnius, Lietuva.
Tel.: (8 5) 274 4956; faksas (8 5) 270 0112; el. paštas doktor@vgtu.lt

Pranešimai apie numatomą ginti disertaciją išsiusti 2016 m. gruodžio 23 d.

Disertaciją galima peržiūrėti VGTU talpykloje http://dspace.vgtu.lt ir Vilniaus Gedimino technikos universiteto bibliotekoje (Saulėtekio al. 14, LT-10223 Vilnius, Lietuva), Klaipėdos universiteto bibliotekoje (K. Donelaičio g. 3, LT-92144 Klaipėda, Lithuania) ir Aleksandro Stulginskio Universiteto bibliotekoje (Studentų g. 11, LT-53361 Akademija, Kauno raj.).

Abstract

Research work relevance is concerned with global energy saving, alternative fuel use and environmental pollution reduction issues in wide world, which is especially important for the transport sector. Dissertation work presents study of efficient and ecological indicators, combustion process behaviour and its parameters of different gaseous fuels and their mixtures in the spark ignition internal combustion engine, which has such adaptations of duel fuel supply, gas direct injection or dual coil ignition systems. Different theoretical evaluations and analysis, experimental investigation and numerical simulation methods are applied in order to have a complex research, to suggest efficiency improving implements and to get a better understanding of gaseous fuels, like biogas, natural gas, hydrogen influence on the engine work cycle.

Introduction chapter presents the importance of the thesis, goal and the tasks of this work. In addition, scientific novelty, theoretical and practical significance of achieved results, defendable statements and authors published scientific papers presented in the chapter.

An overview of scientific literature according to thesis theme represented in the first chapter. Different features, like fuel composition, lower heating value, chemical combustion reactions of different gas fuels were reviewed according other scientist's works and the influence of these indicators on engine efficient and ecological parameters and combustion behaviour were discussed.

Second chapter represents different research work methodologies, which were applied for the theoretical analysis and calculations, numerical simulation and experimental tests with different research type spark ignition engines.

Experimental test results of biogas, natural gas, natural gas and hydrogen fuel mixtures, numerical analysis and simulation of mentioned gas fuels presented in the third chapter. Furthermore, test results of methane direct injection system with combustion process imaging and combustion light emission spectroscopy given in the result part. Research of different gas fuels and different types of fuel injection systems revealed that it is possible to achieve promising results, which are concerned with improved gaseous fuel combustion process, higher engine efficiency and lower exhaust gas emissions in spark ignition engine.

12 scientific papers according to the thesis subject have been published: one – in scientific journal, included in *Thomson ISI Web of Science* data base; two – in editions of international conferences, referred in *Thomson Reuters data base Proceedings*; four – in other international data base publications; one – in periodical reviewable scientific publication; four – in conferences materials.

Reziumė

Disertacijos darbo aktualumas yra susijęs su globaliu energijos tausojimu, alternatyvių degalų panaudojimu bei aplinkos užterštumo, kuris ypatingai aktualus transporto sektoriui, mažinimu visame pasaulyje. Rengiant darbą buvo siekiama kompleksiškai ištirti dujinius degalus, pasiūlyti vidaus degimo variklio efektyvumą bei ekologinius rodiklius gerinančias priemones. Šiam tikslui pasiekti atliktas teorinis vertinimas, analizė, eksperimentiniai tyrimai bei skaitinis modeliavimas. Disertacijoje pateikiami efektyviųjų ir ekologinių rodiklių, degimo proceso ir jo parametrų tyrimai bei jų rezultatai. Eksperimentai atlikti kibirkštinio uždegimo varikliui veikiant su skirtingais dujiniais degalais ir jų mišiniais, pritaikyti dvigubos degalų sistemos tiekimo technologiniai sprendimai, tiesioginis dujų įpurškimas, dvigubos apvijos uždegimo sistema.

Įvadiniame skyriuje pateiktas disertacinio darbo aktualumas, tikslas ir uždaviniai. Šiame skyriuje taip pat pateiktas darbo mokslinis naujumas, teorinis ir praktinis gautų rezultatų pritaikomumas, ginamieji teiginiai bei paskelbtos autoriaus publikacijos.

Mokslinės literatūros apžvalga disertacijos tema pateikta pirmajame skyriuje. Apžvelgti skirtingi dujinių degalų rodikliai, t. y. degalų sudėtis, žemutinis degalų šilumingumas, cheminės degimo reakcijos, šių rodiklių įtaka variklio efektyviesiems, ekologiniams parametrams bei degimo procesui.

Antrajame skyriuje pateiktos skirtingos teorinei analizei ir skaičiavimams, skaitiniam modeliavimui bei eksperimentiniams bandymams, kai buvo naudojami skirtingų tipų varikliai, pritaikytos tyrimų metodikos.

Trečiajame skyriuje pateikti eksperimentinių tyrimų, kurių metu buvo išbandytos biodujos, gamtinės dujos, gamtinių dujų ir vandenilio mišiniai, rezultatai bei analizės ir skaitinio modeliavimo rezultatai. Šiame skyriuje kartu su degimo proceso vaizdine medžiaga bei šviesos emisijos spektroskopijos rezultatais taip pat pateikti rezultatai, gauti atliekant metano tiesioginio įpurškimo sistemos bandymus. Šie tyrimų rezultatai rodo, kad naudojant minėtų dujinių degalų mišinius bei naujos kartos įpurškimo sistemas, pagerėja dujinių degalų degimo procesas kibirkštiniame variklyje, padidėja variklio efektyvumas, sumažėja išmetamųjų deginių emisijos.

Disertacinio darbo tematika yra paskelbta 12 mokslinių straipsnių: vienas – mokslo žurnale, įtrauktame į *Thomson ISI Web of Science* duomenų bazę, du – tarptautinių konferencijų recenzuotų darbų leidiniuose (*Thomson Reuters data base Proceedings*); keturi – kitų tarptautinių duomenų bazių leidiniuose; vienas – periodiniame recenzuojamame moksliniame žurnale; keturi – konferencijų medžiagose.

Notations

Symbols

$\%_{fuel\ comp.}$ – percentage of certain fuel component in fuel mixture according to mass;
$\overline{x}$ – mean value of observed values;
A – Ampere;
a_d – rectangular distribution parameter;
a – Vibe constant when 99.9% of fuel is burned;
A_i – surface area (cylinder head, piston, liner);
$a_{i,j}$ – coefficient values of partial ternary systems which is given by EN standard;
B_d – hourly fuel consumption;
B_{d_P} – petrol hourly consumption;
b_e – brake specific fuel consumption;
C – Carbon atom;
C_2* – carbon radical;
CH^* – carbon hydrogen radical;
CH_2O – formaldehyde;
c_m – mean piston speed;
CN^* – cyano radical;
CO – carbon monoxide;

CO_2 – carbon dioxide;
c_u – circumferential velocity;
D – cylinder bore;
d – degree of freedom;
dm_e – mass element flowing out of the cylinder;
dm_i – mass element flowing into the cylinder;
dQ – released heat;
$d\Phi$ – crank angle variation;
E_c – cyclic energy amount;
f – fraction of evaporation heat from the cylinder charge;
H – hydrogen element;
H_0, H_1 – hypothesis;
H_2 – hydrogen atom;
HC – hydrocarbon;
HCO* – formyl radical;
h_e – enthalpy of the mass leaving the cylinder;
h_i – enthalpy of the in-flowing mass;
J – Joules;
m_{aC} – atomic mass of C element in gaseous fuel mixture.
m_{aH} – atomic mass of H_2 element in gaseous fuel mixture;
M_e – engine torque;
m_{ev} – evaporating fuel;
$m_{fuel\ comp.}$ – mass of fuel component;
$M_{fuel\ comp.}$ – molar mass of the component, g/mol;
m_i – i sample empirical mean value;
m_v – combustion intensity shape parameter;
n – engine speed;
N – normal distribution;
N_2 – nitrogen;
N_A – Avogadro constant ($6.022140857 \cdot 10^{23}$ mol^{-1});
$n_{fuel\ comp.}$ – mole number of additive in gaseous fuel mixture;
$n_{fuel\ comp.}$ – mole number of fuel component in 1 gram, moles;
NH* – amino radical;
n_i – sample size;
n_m – the number of components in a simplified mixture;
NO_x – nitrous oxide;
$n_{V\ fuel}$ – mole number in chosen volume;
O – oxygen atom;
O_2 – oxygen;
°C – degrees of Celsium;
OH^* – hydroxyl radical;
p_{crit} – critical value;

p_{cyl} – cylinder pressure of the motored engine;
p_{inj} – injection pressure;
p_{max} – maximum cylinder pressure;
Q – released heat amount from fuel which was used during engine work cycle;
q_{ev} – evaporation heat of the fuel;
Q_{wi} – wall heat flow (cylinder head, piston, liner);
s – evaluation of standard deviation;
T_c – gas temperature in the cylinder;
$T_{cyl.}$ – temperature in the cylinder;
$T_{Exh.}$ – exhaust gas temperature;
$t_{p,d}$ – Student distribution;
T_{wi} – wall temperature (cylinder head, piston, liner);
T_z – maximum combustion temperature;
$u(x_i)$ – directly measured value standard uncertainties;
$u_c^2(f)$ – dispersion of whole uncertainty;
V – electrical voltage;
V_D – displacement per cylinder;
V_{fuel} – gaseous fuel mixture volume;
$V_{fuel\ comp.}$ – volume of certain fuel additive in gaseous fuel;
V_i – the volume fraction of component *i* in a simplified mixture;
$V_{max\ i,j}$ – the maximum content of component *i* for the range of applicability;
$V_{sum\ i}$ – the sum of all maximum contents of component *i* for the range of applicability of all systems;
W_j – fitness value for methane number calculation;
X – random value;
$X_{fuel\ comp.}$ – number of element atoms in fuel component;
α – crank angle relative to TDC;
α_s – significance level;
α_w – heat transfer coefficient;
β – certain quintile for Student or Standad Normal Distribution;
γ – adiabatic index;
Δp – pressure difference;
δ_{P1} – the pressure difference across the injector holes;
δ_{P2} – the pressure drop inside the injector;
Δp_{max} – maximum pressure alteration;
Δp_{mi} – minimum pressure alteration;
$\Delta\varphi_c$ – combustion duration;
η_e – efficient engine efficiency coefficient;
η_i – indicated engine efficiency coefficient;
η_v – volumetric efficiency;
Θ – advanced ignition angle (spark timing);
λ – lambda, coefficient of air / fuel ratio;

μ – mean value;
σ – standard deviation;
φ – crank angle;
φ_0 – start of combustion;
φ_{comb} – combustion duration;
φ_{Pmax} – angle at which maximum pressure is achieved;
φ_z – combustion duration;
ε – compression ratio.

Abbreviations

A/F – air / fuel ratio;
aTDC – after top dead center;
AVL – *germ.* AnstaltfürVerbrennungskraftmaschinen;
BMEP – brake mean effective pressure;
BSFC – brake specific fuel consumption;
$BSFC_P$ – brake specific petrol fuel consumption;
bTDC – before top dead center;
CA10 – crank angle degree where 10% of fuel is burned;
CA50 – crank angle degree where 50% of fuel is burned;
CAD – crank angle degree;
CARB – California Air Resources Board;
CI – compression ignition;
CNG – compressed natural gas;
CNG + 10% H_2 – compressed natural gas and hydrogen of 10% in the fuel mixture;
CNG + 20% H_2 – compressed natural gas and hydrogen of 20% in the fuel mixture;
CNG + 30% H_2 – compressed natural gas and hydrogen of 30% in the fuel mixture;
CNG + 50% H_2 – compressed natural gas and hydrogen of 50% in the fuel mixture;
CNG + 70% H_2 – compressed natural gas and hydrogen of 70% in the fuel mixture;
CNG + 90% H_2 – compressed natural gas and hydrogen of 90% in the fuel mixture;
CoV – coefficient of variation;
CoV_{IMEP} – coefficient of variation of indicated mean effective pressure;
CP – combustion potential;
CR – compression ratio;
DI – direct injection;
DISI – direct injection spark ignition;
DME – dimethyl ether;
EGR – exhaust gas recirculation;
EOI – end of injection;
EU – European Union;
EVO – exhaust valve open;
F_t – the fraction of the partial mixture;

H/C – hydrogen / carbon atom ratio;
HCCI – homogeneous charge compression ignition;
HHV – higher heating value;
HP – horse power;
ICE – internal combustion engine;
IDI – indirect injection;
IMEP – indicated mean effective pressure;
ISFC – indicated specific fuel consumption;
ISO – International Organization of Standardization;
IVC – intake valve close;
kJ – kilo Joules;
LHV – lower heating value;
LNG – liquefied natural gas;
LPG – liquefied petroleum gas;
MBF – mass burned fuel;
MBT – maximum brake torque;
MN' – methane number of simplified mixture;
MN – methane number;
MN_{inerts} – methane number of inert gas;
$MN_{methane}$ – methane number of 100% CH_4
MN_t – methane number of a partial mixture;
MON – motored octane number;
NG – natural gas;
NGV – natural gas vehicle;
NMHC – non-methane hydrocarbons;
N_{sys} – the number of ternary systems selected;
P – petrol fuel;
P + *Bio* 20 – petrol and 20 *l*/min. of biogas fuel mixture;
P + *Bio* 25 – petrol and 25 *l*/min. of biogas fuel mixture;
P + *Bio* 30 – petrol and 30 *l*/min. of biogas fuel mixture;
PFI – port fuel injection;
PM – particulate matter;
RME – rapeseed methyl ester;
RoHR – rate of heat release;
RON – research octane number;
rpm – revolutions per minute;
SE – standard error;
SG – specific gravity;
SI – spark ignition;
SOI – start of injection;
STP – standard conditions for temperature and pressure;
UV – ultraviolet;

VGTU – Vilnius Gediminas Technical University;
WI – Wobbe index;
WN – Wobbe number;
WOT – wide open throttle.

Notions

Biogas – renewable gas fuel produced from wastes, agriculture, plant materials. Biogas mainly contains of CH_4 with some diluents in the fuel like CO_2, N_2.

Natural gas – fossil fuel obtained from different land sources and supplied for in-house use as a transport fuel. Natural gas composition is usually composed of CH_4, C_2H_6, C_3H_8, C_4H_{10}, N_2.

Methane gas – gas containing 100% CH_4.

Diluents – some certain concentration of elements (CO_2, N_2), which can be in a composition of a gaseous fuels and which has an influence on fuel physical and chemical features.

Stratified combustion – combustion type when the fuel is injected during the compression stroke and the combustible mixture is formed around the spark plug. The combustible area around spark plug is very rich of fuel and other area in cylinder is very lean.

Misfire – combustion process in ICE when combustible mixture is not ignited in some certain amount of combustion cycles.

Pool-fires – intense combustion of fuel rich area, usually coming from the injector after the ignition. Typical for petrol DI systems.

Contents

[1]The annexes are supplied in the enclosed compact disc

Introduction

Problem Formulation

Increasing population growth of people lead to high demand of fossil fuels, especially when the improvement in the standard of people living is getting higher and it results in the total energy consumption (Korakianitis *et al*. 2011; Wasiu *et al*. 2012).

The industry is trying to move towards alternative fuels due to climate change from the increase of greenhouse gas emission, the increase of health problems in the cities and the oil supply and price issues. Upcoming humanity's strategic objectives is to significantly reduce the fossil fuels (oil) consumption, as a radical reduction way of the greenhouse gases, especially CO_2. This gas is not the most dangerous greenhouse effect "shapers", but the worldwide emission of it from the ICEs is enormous. Sudden transition to a global use of electromobiles and alternative fuel sources is not possible, so one of the most acceptable alternatives to the "transition period" is a wider use of simple molecular structure fuel – natural gas of which resources will be sufficient for 300–400 years. What is more, to expand alternative fuel range, it is attractive to use energetically potential and clean fuel – hydrogen. The research and development of new generation engine control and fuel supply systems let to improve both engine efficient and engine ecological

parameters. Efficient fuel use in the ICE has a great impact on CO_2 and greenhouse effect reduction.

It is widely known that there are two types of alternative gaseous fuels mostly used in the world: LPG and CNG. Vehicles running on the natural gas fuel have such advantages that engines emit low particle numbers and nitrous oxide emissions comparing to other fuel type vehicles. The one major advantage of such ICEs is that, it can be adopted to use biogas from municipal waste, agriculture or plant materials. Natural gas engines can achieve higher thermal efficiency because gas has higher octane number and it is possible to use engines with a higher compression ratio. Though the natural gas and biogas have disadvantage – these fuels have lower flame speed and worse combustion at higher A/F ratio, which can lead to misfires.

The increasing amount of the NGVs force to search for the new and innovative ICE technologies, which can improve the fuel economy. One of the main problem concerned with gaseous fuel is that the gas, which is injected into the intake air manifold, can occupy some certain volume, which can result in worse cylinder filling. Furthermore, there is high heat loss to the cylinder walls when the homogeneous mixture is used, so it is hard to achieve higher engine efficiency. There are two ways to improve gas engines characteristics:

1. Engine technical improvement – fuel control system, fuel injection system research and development.
2. Fuel features improvement – use of new generation fuels or fuel mixtures composed from traditional and renewable fuel sources.

Theoretical and experimental researches of both mentioned issues will be presented in this thesis work. The fuel mixtures of traditional fossil fuels (CNG) and additive (H_2) having better combustion characteristics (LHV, higher flame speed, wider lean limits) were scientifically investigated. Also, the research results of biogas addition in duel fuel system together with petrol fuel will be presented. In addition, the gas direct injection (DI) with relatively low injection pressure was tested and analysed in this work.

Relevance of the Thesis

Over past twenty years, the growing concern about the climate changes and the future energy supply were caused by unsustainable energy use (Malenshek *et al*. 2009). Since the first European emission standards in the European Union and the European Economic Area in 1993 appeared and the Kyoto Protocol (signed in 1997), which commit all participating countries to reduce greenhouse gases, alternative fuels are being developed and used in order to replace the traditional fuels in ICE.

The European Commission states that long-range strategy of the alternative fuels must satisfy all transport vehicles demands using either liquid or gas fuels. It states that there is no single fuel solution for the future of mobility, because the availability and the cost of the alternative fuels differ between modes. A long-term strategy on alternative fuels has to meet the energy needs of all transport modes, therefore different types of liquid biofuels and gaseous fuels have to be applied in order to support the EU 2020 strategy (European Commission 2013). One of the ways is to use LPG, CNG or even H_2.

Present natural gas engines running on stoichiometric A/F ratio usually have stable combustion, but they face with quite high fuel consumption and emissions comparing with the lean burn engines ($\lambda > 1.4$). However, lean burn engines face with combustion stability, loss issues of engine power. In order to improve lean burn engines, one of the ways is to use better physical and chemical properties having element – hydrogen. Hydrogen is having higher flame speed, higher LHV. In addition, it has no carbon bonds if comparing to liquid fuels – petrol or diesel. These features could let to achieve better engine efficiency and ecological parameters. However, more deep investigation of different CNG / H_2 mixture concentrations should be done as hydrogen has low density, which can affect the engine cylinder volumetric efficiency and engine achievable power level.

In order to improve ICE efficient parameters there is a need to research and develop more advanced fuel supply technologies. One of the ways to avoid mentioned gaseous fuel disadvantages is natural gas DI system. DI ensures a better volumetric efficiency, better mixture formation and it can achieve better torque and power output, reduce pumping and heat losses. Therefore, gaseous fuel DI should be investigated and developed more deeply with applied different combustion cases: homogeneous stoichiometric, homogeneous lean burn and stratified lean burn.

The thesis work is valuable for full-scale research, which involves both: new type of fuel mixtures, which can be used for present and upcoming light and heavy-duty vehicles, and new type of gaseous fuel supply technologies, which can be applied in a new generation engines. The different research directions mentioned above are closely related to each other as different types of fuel mixture can be used with DI systems in the near future.

The Object of Research

The combustion process of gaseous fuels and gas fuel mixtures, containing methane as a base component in the fuel, in the spark ignition internal combustion engine with duel fuel supply, gas direct injection or dual coil ignition systems.

The Aim of the Thesis

To determine improving implements for the efficient, ecological indicators and gas combustion process of the spark ignition internal combustion engine, running on gaseous fuels, by applying the algorithm of theoretical evaluation, numerical simulation and experimental research methodology.

The Tasks of the Thesis

In order to achieve the aim of the research, the following tasks are formed:

1. To evaluate features and apply assessment methods for the different gaseous fuels and fuel mixture types and develop the experimental and numerical investigation methodology, when the different fuel supply and ignition systems are applied in the spark ignition engine.
2. To evaluate the comparison of LHV, H/C atom ratio and theoretical MON (MN) calculations for the standard petrol, natural gas fuel and their fuel mixtures with alternative fuel – biogas or highly reactive element – H_2 additive, and compare the obtained data with the experimental investigations.
3. To apply the dual fuel injection control system for the petrol and biogas fuel mixtures and using the numerical simulation methodology, evaluate the influence on the rate of heat release, combustion duration, intensity and their influence on the engine ecological and efficient indicators when the different engine control adjustments are used in the spark ignition engine.
4. To asses the highly reactive element – H_2 influence on the petrol and natural gas fuel combustion process, for the engine efficient and ecological indicators, using experimental investigation with the port fuel injection system in the spark ignition engine and apply developed theoretical and numerical simulation methodology to determine the most optimal fuel mixture in an aspect of engine efficiency.
5. To apply optical investigation methodology and evaluate low-pressure (18 bar) gas direct injection system influence on the methane gas combustion process and combustion product formation in the optical cylinder when different combustion strategies and ignition systems are applied.

Research Methodology

Theoretical, experimental and numerical simulation investigation methods are applied in presented dissertation. Lower heating value, hydrogen / atom ratio calculations are presented. Also, theoretical MON, MN, experimental data sample normality and errors for calculated parameters were determined according to ISO EN standards and given in the thesis. Experiments with the natural gas and hydrogen also petrol and biogas fuel mixtures were carried out with – 4 cylinder SI engine with port fuel injection system. *LabView, AVL DiTest* and *AVL Indicom* software was used for in-cylinder pressure measurements' aquisition, also *MoTEC* for PFI, spark timing adjustmens and *LabView* was used for DI system control. Numerical simulation model was developed with *AVL BOOST* software and was applied in order to get combustion process data and simulate engine work process with the different fuel mixtures. The natural gas and hydrogen mixtures were also tested with heavy duty vehicle on dyno test bench. Methane direct injection experimental investigations were carried out using optical single cylinder SI ICE. The combustion process and combustion light emission spectroscopy were captured through the glass piston surface and glass cylinder liner with high speed cameras and later analysed using *MATLAB* code.

Scientific Novelty of the Thesis

1. Applied theoretical calculation methodology of MON and MN for the fuels and the fuel mixtures according to the EN ISO standards for the experimental research data support and analysis.
2. Developed and applied experimental research methodology of duel fuel injection system for the liquid and gaseous fuels (petrol / biogas, petrol / natural gas, petrol / hydrogen) in SI ICE.
3. Developed and applied experimental research methodology for the engine bench testing with the natural gas / hydrogen fuel mixtures, which contain H_2 from 10% to 90% concentration according to volume in the fuel mixture, and developed numerical simulation methodology for the optimum natural gas / hydrogen fuel mixture determination.
4. Applied methane DI system with relatively low gas fuel injection pressure – 18 bar and researched its influence on engine efficient parameters applying different combustion cases.
5. Adaptation of stratified combustion type at low injection pressure (18 bar) and optical research methodology application for the methane direct injection and dual coil ignition system investigation.

Practical Value of the Research Findings

1. Different petrol / biogas, petrol / hydrogen, natural gas / hydrogen mixtures were researched in SI engine with PFI system. Results revealed that lower brake specific fuel consumptions, lower exhaust gas emissions can be achieved using different alternative gaseous fuels, therefore such fuels can be adapted for the light duty and heavy duty vehicles. However, engine adjustments, like spark timing or air / fuel ratio, have to be done, in order to achieve the highest engine efficiency. These findings show that further development and research of engine control systems and fuel supply systems should be applied in order to achieve lower NO_x and soot emissions.
2. Obtained theoretical and experimental investigation results can be adapted for the optimization of internal combustion engines for cogeneration power plants, urban fleets and other vehicles which are running on natural gas, biogas fuels. Also, obtained results give a reason to continue researches of gaseous fuel mixtures, advanced injection and ignition systems which will let to obtain even higher efficiency and lower ecological indicators of internal combustion engines.
3. Numerical model of SI engine was developed using the *AVL BOOST* software in order to analyse different fuel mixtures influence on the combustion process and determine the most optimum fuel mixture. Developed model and methodology are suitable for the investigation of different concentrations or compositions of gaseous fuels' (biogas, petrol / biogas, natural gas / hydrogen) influence for engine work process.
4. Obtained optical imaging and emission spectra data from the methane DI experiments in the single cylinder engine let to improve the injection system, compare different combustion types, and develop more efficient natural gas engines with the DI systems.

The Defended Statements

1. Fuel octane number increases up to 96 when biogas amount is increased up to 30 *l*/min. in petrol and biogas fuel mixture. 90% addition of reactive element H_2 in natural gas decrease the octane number up to 80. The change of fuel knock characteristics have an influence on combustion processes in experimentally researched spark ignition engines.
2. Developed and applied ICE experimental research and numerical simulation methodology lets to determine the optimum natural gas / hydrogen fuel mixture, which lets to achieve better engine efficient indicators.

3. It is possible to achieve HC, NO_x and CO_2 limits, which will be still under the liquid petrol exhaust gas emission limits, using stoichiometric or lean burn conditions and low H_2 concentrations in the fuel mixtures.
4. Engine torque and efficiency decrease using very high H_2 concentration (90%) in the natural gas / hydrogen fuel mixture and NO_x formation increases strongly (>4000 ppm) at stoichiometric conditions.
5. Theoretical calculations and numerical simulation method proved that the highest engine torque can be achieved with ~ 65% H_2 addition in natural gas.
6. Low pressure (18 bar) DI injector use in SI ICE with CH_4 gas fuel in stratified combustion is a feasible solution in order to achieve up to ~ 30% lower indicated specific fuel consumptions and up to ~ 36 % higher engine indicated efficiency comparing with results obtained from tested homogeneous stoichiometric and homogeneous lean burn combustion.
7. The formation of soot due to improper air / fuel mixing was observed during a stratified combustion in a gas DI system by applying light emission spectrum research methodology for the combustion process. Also, intermediate combustion products – OH* and CN* radicals were recorded.

Approval of the Research Findings

12 scientific papers focusing on the subject of the dissertation have been published: one – in scientific journal, included in *Thomson ISI Web of Science* data base; two – in editions of international conferences, referred in *Thomson Reuters data base Proceedings*; four – in other international data base publications; one – in periodical reviewable scientific publications; four – in conferences materials.
The obtained experimental data was presented in eight international conferences:

1. "Innovative technologies in engineering production ITEP 2016". Žilina, Slovakia.
2. "SAE World Congress: Powering Possibilities 2016". SAE International. Detroit city, Michigan State, USA.
3. "Science – Lithuania future: 18th young scientist conference. Transport engineering and management", 2015. Vilnius, Lithuania.
4. "Transbaltica 2015: 9th international scientific conference". Vilnius, Lithuania.
5. International scientific conference "Mobile Machines 2014". Kaunas, Lithuania.
6. "Transport Means 2013: 17th international conference". Kaunas, Lithuania.

7. "Science – Lithuania future: 16th young scientist conference. Transport engineering and management", 2013. Vilnius, Lithuania.
8. "*AVL* Advanced Simulation Technologies International User Conference", 2013. Graz, Austria.

Structure of the Dissertation

Dissertation consists of an introduction, three chapters, general conclusions, a list of references and a list of publications by the author on the topic of the dissertation, a summary in Lithuanian and 4 annexes.

The scope of a dissertation is 157 text pages excluding annexes. 56 numbered formulas, 66 figures and 16 tables were used, 134 literature sources were referenced when preparing a doctoral dissertation.

Acknowledgments

The author would like to acknowledge scientific supervisor Assoc. Prof. Dr Saugirdas Pukalskas for the support and help during PhD studies, Dr Alfredas Rimkus for the valuable advices during researches, Prof. Dr Ingemar Denbratt and Assoc. Prof. Dr Petter Dahlander for the warm welcome and possibility to do researches in Chalmers University of Technology, Paulius Stravinskas (VGTU) and Eugenio De Benito Sienes (Chalmers University of Technology) for the help during preparations for the experiments, company "SG dujos Auto" for the cooperation and possibility to do researches in their laboratory.

1

Analysis of Gaseous Fuel Relevance, Features and Use in Transport

The relevance and perspectives of different gas fuels, like natural gas, biogas, liquefied petrol gas, hydrogen are presented in the first chapter. Features of different gas fuels and their mixtures are analysed and presented. In addition, different gas fuel injection types, combustion strategies and their advantages are being overviewed. According to chapter's theme, several publications were published (Sendžikienė *et al.* 2015), (Pukalskas *et al.* 2014), (Melaika *et al.* 2016), (Melaika *et al.*2013).

1.1. Relevance and Perspective of Natural Gas, Biogas, Hydrogen Gas Use in Transport

Europe is particularly dependent on imported oil for its mobility and transport. In order to reduce Europe's dependence on imported oil and reduce carbon emissions in transport by 60% by 2050, also increase mobility, remove major barriers in key areas and fuel growth and employment, The European Commission accepted "Transport 2050" strategy (European Commission 2013). One of the ideas of "Transport 2050" strategy is to halve the use of 'conventionally fuelled' cars in

urban transport by 2030 and finally eliminate it from the cities by 2050. Moreover, achieve essentially CO_2-free transportation in major urban centers by 2030 (European Commission 2011).

A decision was adopted considering that urban transport is responsible for about a quarter of CO_2 emissions from the transport. Eliminating 'conventionally-fuelled' vehicles from the urban environment is a major contribution to significant reduction of oil dependence, greenhouse gas emissions and local air and noise pollution (European Commission. White paper 2011).

It states that there is no single fuel solution for the future transport because the availability and cost of alternative fuels differ between the modes. The benefits of alternative fuels are initially larger in urban areas where pollutant emissions are greater and options of different alternatives have bigger variety. Table 1.1 presents abilities of different fuel types used for different kind of transport.

Table 1.1. Alternative fuel sources for transportation (European Commission 2013)

Fuel		Transport										
		Road-passenger			Road-freight			Air	Rail	Water		
		Short	Medium	Long	Short	Medium	Long			Inland	Short-sea	Maritime
LPG		+	+	+	+	+	+	–	–	+	+	–
NG	LNG	+	+	+	+	+	+	–	+	+	+	+
	CNG	+	+	+	+	+	–	–	–	–	–	–
Electricity		+	–	–	+	–	–	–	+	–	–	–
Liq. biofuels		+	+	+	+	+	+	+	+	+	+	+
H_2		+	+	+	+	+	–	–	+	+	–	–

A long-term strategy on alternative fuels has to meet the energy needs of all transport modes, therefore different types of liquid biofuels and gaseous fuels have to be applied in order to support EU 2020 strategy (European Commission 2013).

European Commission states the definition for biofuels which means liquid or gaseous fuels for transport, produced from biomass. It also defines that alternative fuel vehicle is a vehicle designed to be capable of running on at least one type of fuel that is either gaseous at atmospheric temperature and pressure, or substantially non-mineral oil derived.

As alternative, gaseous fuels can be adapted for light vehicles and heavy duty vehicles in order to cover some part of crude oil fuels and liquid biofuels use.

Liquefied petroleum gas is one option of gaseous fuels. Currently, it is obtained from crude oil and natural gas. It is stated that in the future, possibly, it can be obtained also from the biomass. LPG is already widely used in Europe but the distribution is still quite uneven. LPG had an advantage as it was low pollutant emissions fuel, however, the new Euro standards progressed to a lower emission limit and LPG has to face it also. On the other hand, it has clear advantage in particulate emissions comparing with diesel engines (European Commission 2013).

Fuel transportation is important aspect of the gas business, since gas reserves are often far away from the main markets. There are several ways of natural gas transportation:

- pipeline system;
- gas to liquids;
- gas to wire;
- gas to solids;
- LNG system;
- CNG system.

CNG system transportation is one of the most promising. It is claimed that energy consumed in operating a CNG project is about 40% of that of an LNG project. Other types of transportation also require a lot of economical and advanced technological effort comparing with simple CNG system (Wasiu *et al.* 2012).

During production process natural gas is being cleaned from high value components like propane, butane, also sulfur, CO_2. These components can influence gas transportation pipes' conditions (MacLeana *et al*. 2003).

Natural gas is the second alternative fuel most widely used in the market (after LPG) (Kakaee *et al*. 2014). Natural gas can be obtained from the large fossil fuel reserves, from biomass and waste as biogas. It is stated that natural gas can fulfill a long-term perspective in terms of security of supply to transport and a diversification of transport fuels. CNG vehicles have low pollutant emissions. The growth in ground urban fleets of buses, utility trucks and taxis is observed. Optimised gas-only vehicles can have higher energy efficiency (European Commission 2013; Brownstein 2015).

Hydrogen is further alternative for transport and it can be produced from all primary energy sources. It can be used as transport fuel or as an energy storage gained from the solar and wind power. The most efficient way to use hydrogen is a fuel cell technology which is twice as efficient as an ICE. Fuel cells could replace diesel engines in trains, ships but the main problem concerned with high fuel cost and refueling infrastructure network remains. However, industry studies indicated that mentioned costs can be reduced to the levels of conventional petrol and diesel vehicles by 2025 (European Commission 2013).

Meanwhile, looking in transitional period until the fuel cells will be used widely, hydrogen could be used as a fuel additive in biofuels or traditional fuels. As it was mentioned before, strict regulations for CO_2 emission and other pollutants forces to search for more efficient combustion systems or fuels. At this moment Euro 6 standard for light vehicles and heavy duty vehicles is being run. These regulations strictly note how much of CO, HC, NMHC, NO_x, PM can be emitted by light and heavy duty vehicles (European Parliament and the Council of the European Union 2007; European Parliament and the Council of the European Union 2009). Fig. 1.1 shows how different emissions were regulated with different Euro standards over the years and Fig. 1.2 presents the dependence of NO_x and PM emissions on different Euro emission standards.

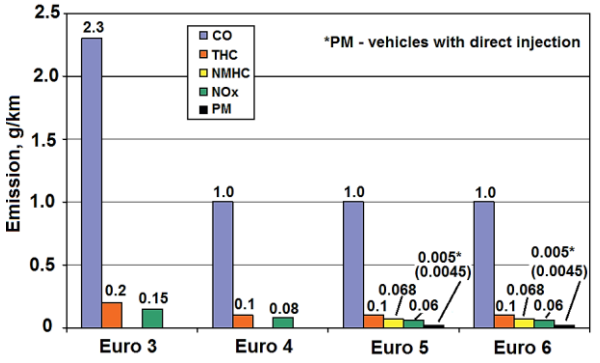

Fig. 1.1. Comparison of Euro emission standards (Bielaczyc *et al.* 2014)

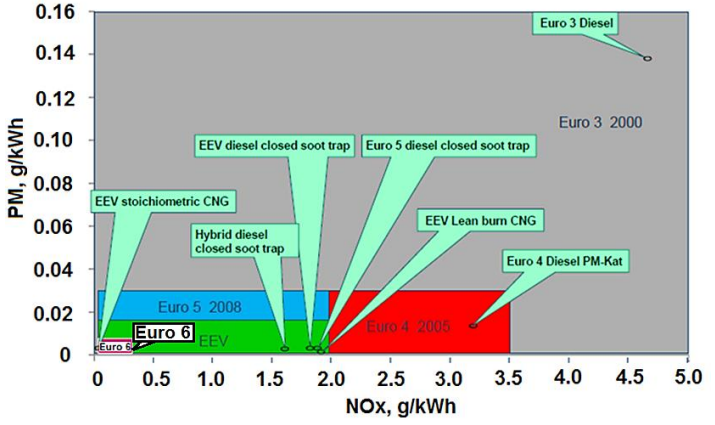

Fig. 1.2. New generation natural gas fuelled vehicles comparison with diesel fuelled vehicles (NGVA Europe 2013)

With Euro 5 and Euro 6 standards regulations the PM regulations appeared for vehicles running with DI systems. It is well known that with DI systems where the fuel is injected in high concentration, the soot formation is appearing in the cylinder. Therefore it is very important to do further researches of DI systems and search for the alternatives, like using different type of fuels (ethanol, biofuels, gaseous fuels) in DI engines.

During last 16 years, more and more attention is payed for the NO_x and PM reduction which is traced now not only in CI engines but also in SI DI engines. From the Fig. 1.2 it is obvious that lowest PM and NO_x emissions can be achieved with CNG engines. In order to reduce CO_2 emissions and improve CNG engine efficiency it is important to investigate alternative fuels (fuel mixtures) or new generation engine management or fuel injection systems and to see how they affect PM and NO_x emission formation, which is also very important when the question is raised about humanity health and global warming.

1.2. Natural Gas, Biogas, Hydrogen Features

1.2.1. Natural Gas Features

Natural gas as energy source is expected to grow steadily in the future as it can provide sustainable energy supplies needed for the social and economic development and reduce the impact on global climate.

It is assumed that natural gas hydrocarbons come from organic matter (the remains of land and aquatic plants, animals and microorganisms). Organic matters were trapped within sediments as they were deposited and transformed over long periods of time into their present form. Natural gas is a complex mixture of hydrocarbon and nonhydrocarbon constituents and exists as a gas under atmospheric conditions (Mokhatab *et al.* 2015).

Natural gas contains mainly methane (CH_4) with additional components such as ethane (C_2H_6), propane (C_3H_8), butane (C_4H_{10}) and diluents – nitrogen (N_2) or carbon dioxide (CO_2) in various concentrations. Sulfur compounds and other hydrocarbon species are also available within NG. Natural gas generally contains 75–98% of methane. The levels of dilutants can vary depending on geographical source, time of the year, and even treatment type applied during the production (Mokhatab *et al*. 2015; Wasiu *et al.* 2012; Karavalakis *et al*. 2012; Kakaee *et al.* 2014).

Natural gas is prepared for supply to the customers within limits of pressure, heating value and Wobbe Index or Wobbe Number (Wasiu *et al*. 2012). Some other investigations showed that most important fuel properties were the mass

based heating value, the energy density per cycle, the WN, the ratio of methane and hydrocarbon ratio (Kakaee *et al.* 2014; Matthews *et al*. 1996).

Natural gas, as mentioned before, is naturally combined of hydrocarbons of the benzene series and it varies in composition in different places (Zachariah-Wolff *et al*. 2007). Generally, the specifications for natural gas sources can be divided into such categories like (Zachariah-Wolff *et al*. 2007):

- energy content;
- combustion properties;
- percentage of impurities (undesirable components such as sulphur, carbon dioxide, oxygen).

Different fuel types have a great impact on engine ecological and efficient parameters which are influenced mainly by the fuel composition (hydrocarbon bonds, different additives – hydrogen, ethane, propane, butane or carbon dioxide) and ability to bring energy per cycle (E_C). It is important to understand the real impact of the fuel on engine parameters changes when the real conditions are taken into account, like injection pressure, fuel temperature, temperature in cylinder, etc. Fig. 1.3 presents the comparison of different fuels (DME, H_2, CNG, methanol, ethanol, RME, petrol) at different conditions and when the LHV is compared by volume and by mass.

Comparing energy density per unit mass and energy density per unit volume, natural gas has a higher combustion enthalpy per unit mass than petrol or diesel at standard conditions. Natural gas has lower energy density in mass and in volume when comparing high pressure injection systems. In order to replace petrol or diesel fuel, advanced CNG fuel storage and supply systems, like LNG, are required. Also modified fuel injectors and systems with higher fuel flow rate are required in order to bring sufficient energy mass to the cylinder (Korakianitis *et al.* 2011).

Combustion properties can be described by the WI. This calculation is regulated and described according ISO standard (Standard ISO 6976 2005). The WI is calculated as follows:

$$\mathrm{WI} = \frac{\text{Calorific value}}{\sqrt{\text{Relative density}}}. \tag{1.1}$$

The WI is a measure of the fuel energy flow rate through a fixed orifice under given inlet conditions. It is calculated as the ratio of the heating value divided by the square root of the specific gravity. Variations in WI of the gas will produce similar variations in the A/F ratio for gas metering systems used on vehicles.

Gas combustion potential (CP) can be evaluated which can give a theoretical burning velocity of a mixed gas based on the burning velocity of hydrogen (Zachariah-Wolff *et al*. 2007):

$$\mathrm{CP} = k\frac{H_2 + 0.6(CO + C_mH_n) + 0.3CH_4}{\sqrt{\mathrm{SG}}}. \qquad (1.2)$$

Here k – correction factor adjusted by the O_2 concentration in the fuel; SG – specific gravity.

Fuel properties such as density, heating value, the stoichiometric air / fuel ratio and knock resistance are important for the engine performance when using natural gas as a fuel (Kakaee *et al.* 2014).

Knock in SI engine is an abnormal combustion process. It appears when there is a sudden ignition of a portion of the end gas, owing to high temperature and pressure conditions. This self-ignition process leads to an instantaneous release of energy stored in the end gas fuel (Heywood 1988; Arunachalam *et al.* 2011).

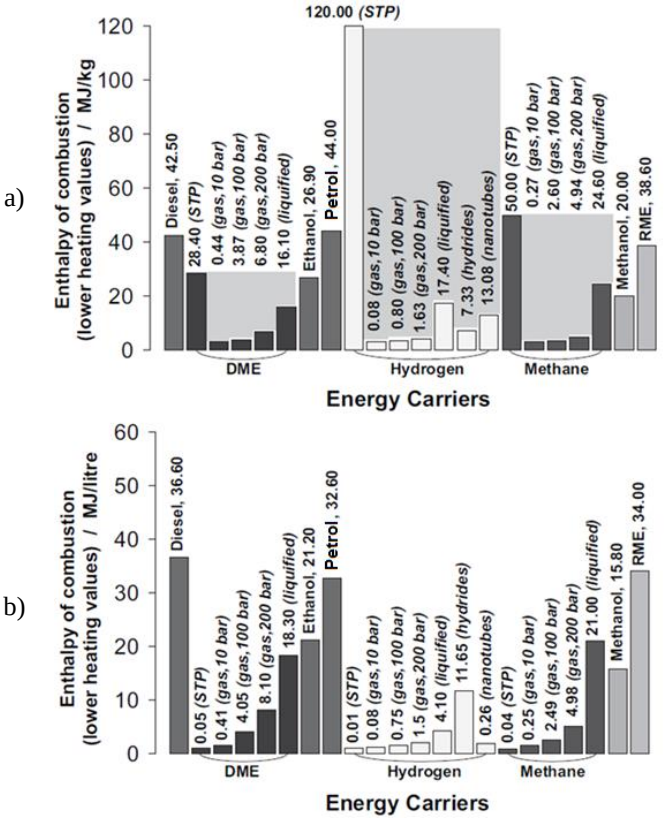

Fig. 1.3. Energy content comparison between different fuels types: a) according to mass; b) according to volume (Korakianitis *et al.* 2011)

It can be identified by a metallic noise which is a result of the high frequency pressure fluctuation in the engine cylinder (Arunachalam *et al*. 2011).

In the middle of the 20th century the interest of gaseous fuels was rising. International Organization of Standardization purposed a standard for LPG motor octane number determination. However this method was suitable just for LPG but not for the investigation of other gaseous fuels as it had upper limit of MON = 120.34. Such method limited the knock rating not only for the methane with higher than 120 MON but with all fuels with greater resistance to knock. The analogous to the MON method for liquid fuels, methane number (MN) scale was suggested by Leiker *et al*. in 1972.

MON and MN calculations were based on Austrian company *AVL* work which was done in 1964–1969 period. It was known that methane and hydrogen have the highest and lowest resistance to knock respectively (Arunachalam *et al*. 2011; Ryan *et al*. 1993; Leiker *et al*. 1972; Malenshek *et al*. 2009).

It was concluded that a mixture of hydrogen and methane should be the standard gaseous reference fuel. This rating system extends the measurable range beyond the MON and was termed as 'methane number' which defined – the percentage by volume of methane blended with hydrogen that exactly matches the knock intensity of the unknown gas mixture under specified operating conditions in a knock testing engine. For the range beyond 100 MN, methane-carbon dioxide mixtures were used as reference mixtures. In this case, in accordance with the definition, the MN is 100 plus the percent CO_2 by volume in the reference methane-carbon dioxide mixture (Leiker *et al*. 1972; Malenshek *et al*. 2009)

Fig. 1.4 presents the MN evaluation guide line depending on different CH_4 / CO_2 and CH_4 / H_2 compositions.

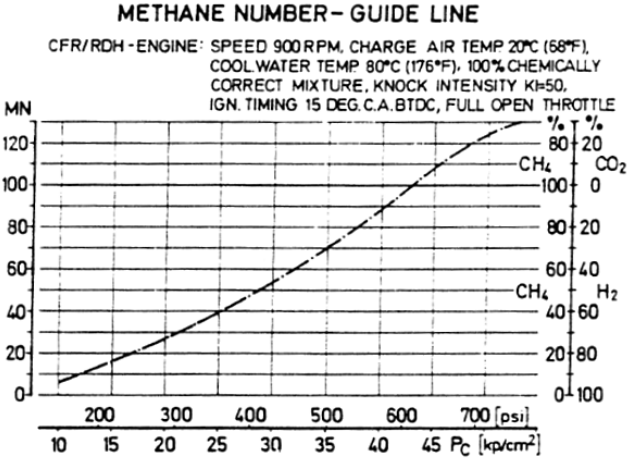

Fig. 1.4. Methane number evaluation (Leiker *et al*. 1972)

Different gas diluents have great impact on knock resistance and MN indicator. Fig. 1.5 shows dependence of MN on different types of natural gas.

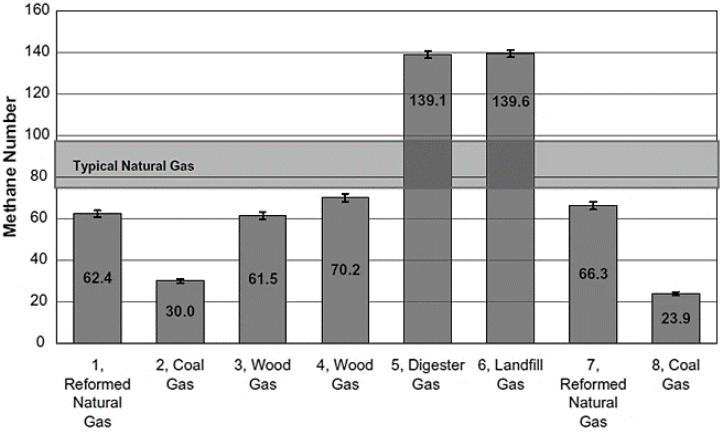

Fig. 1.5. Methane number for different gas fuels (Malenshek *et al.* 2009)

The highest MN is for Digester and Landfill Gases. SI engines with lower compression ratios will have knock with the lower MN gases (Malenshek *et al.* 2009). Typical MN for natural gas is from 75 to 100 MN. Fig. 1.6 presents MN dependence on different natural gas and compression ratios.

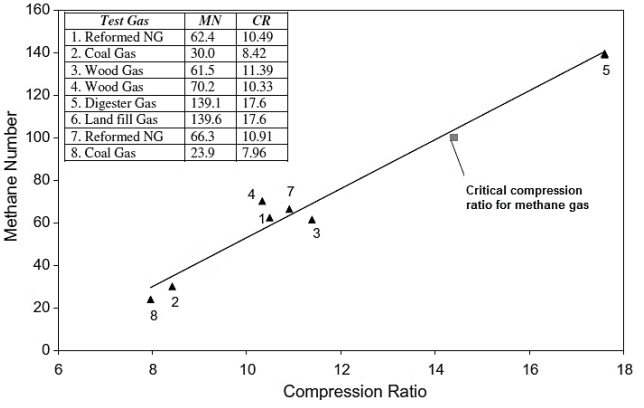

Fig. 1.6. Methane number dependence on different natural gas and compression ratios (Malenshek *et al.* 2009)

It was determined that the critical CR for CNG engines is around 14.5, when methane gas is used (MN equal to 100) (Malenshek *et al.* 2009; Ryan *et al.* 1993).

The CR has to be applied lower than 12:1 with the gas which has lower MN (fuel composition include components which improve combustion process). The biogas let to use engines with very high CR.

The main benefit of the methane gas is that it has much higher octane number (RON > 130) as compared to petrol (RON 86) and this enables substantially higher compression ratios without knock problems. Such fuel property is more suitable for SI engines. The relationship of compression ratio and thermal efficiency of Otto cycle engine is shown below (Heywood 1988):

$$\eta = 1 - \frac{1}{\varepsilon^{(y-1)}}. \tag{1.3}$$

Here ε – compression ratio; γ – adiabatic index.

As CNG engines can operate with higher compression ratio, it is possible to achieve higher thermal efficiency, though some modifications have to be done (Boretti *et al.* 2013; Reynolds *et al.* 2005). Typical compression ratios in gas engines vary from 10:1 to 13:1.

Natural gas has very high self-ignition temperature which is obviously higher than for the petrol or for the diesel fuel. It is admitted that natural gas are safer than petrol or diesel because of high self-ignition temperature (540º C). Lowest energy required to ignite methane is much higher, therefore gas engines requires more efficient ignition systems which could be able to generate at least three time bigger energy than for the petrol engines (Ramadhas 2011).

Methane has certain oxidation characteristics that are different from those of all other hydrocarbons. Bond energy calculations showed, that in order to have a first brake of C–H bond in methane gas, takes more kJ than for the others hydrocarbons. This proves that ignition is more difficult with methane / air mixtures (Glassman 2008). However, methane combustion process is slower, respectively heat losses to the combustion chamber walls are higher. Natural gas has 75% of carbon according to mass, while petrol or diesel has 86–88% of carbon. For this reason, using natural gas there is lower CO_2 concentration in engine exhaust gases (Ramadhas 2011).

Methane stoichiometric combustion balance can be written as following (McAllister *et al*. 2011):

$$CH_4 + (0_2 + \frac{79}{21} N_2) \rightarrow CO_2 + H_2O + N_2; \tag{1.4}$$

$$CH_4 + 2(0_2 + 3.76N_2) \rightarrow CO_2 + 2H_2O + 7.52N_2. \tag{1.5}$$

In order to make the combustion balance, where multiple fuels are used, for example for 95% methane and 5% hydrogen mixture, such chemical equation is used, where stoichiometry relations for CH_4 and H_2 are developed individually:

$$CH_4 + 2(0_2 + 3.76N_2) \rightarrow CO_2 + 2H_2O + 2 \cdot 3.76N_2; \quad (1.6)$$

$$H_2 + 0.5(0_2 + 3.76N_2) \rightarrow H_2O + 0.5 \cdot 3.76N_2. \quad (1.7)$$

Then, the relations are multiplied by the mole fractions of the fuel components and added together:

$$0.95 \cdot \{CH_4 + 2(0_2 + 3.76N_2) \rightarrow CO_2 + 2H_2O + 2 \cdot 3.76N_2\}; \quad (1.8)$$

$$0.05 \cdot \{H_2 + 0.5(0_2 + 3.76N_2) \rightarrow H_2O + 0.5 \cdot 3.76N_2\} \Rightarrow; \quad (1.9)$$

$$\Rightarrow 0.95CH_4 + 0.05H_2 + 1.925(O_2 + 3.76N_2) \rightarrow \quad (1.10)$$
$$\rightarrow 0.95CO_2 + 1.95H_2O + 7.238N_2.$$

Methane has simple hydrogen and carbon bonds which results in less complicated combustion reaction mechanism. Due to the large number of isomers and many possible intermediate species, the number of the species and steps in a detailed mechanism can grow substantially with the size of the fuel molecule for the hydrocarbon fuels. For example, isooctane can contain 860 species and 3.606 reaction steps, while methane chemical kinetics can be described by 53 species and 400 steps (using GRI3.0 combustion mechanism) (McAllister *et al*. 2011).

Emissions of HC, CO, CO_2, NO_x, and PM are significantly lower with natural gas fuel than with diesel fuel in CI engines or sometimes even with petrol fuel in SI engines (Kakae *et al*. 2014). It was noted, that PM emissions are significantly reduced with natural gas fuels because it does not have aromatic and polyaromatic compounds and also contains less sulfur compounds comparing with the liquid fuels (Karavalakis *et al*. 2012).

It should be noted that variation in natural gas composition has also great impact on engine efficiency and pollutant emissions. Diluents can make the great impact on gas ignition and combustion characteristics.

Small concentrations of other hydrocarbons (C_2–C_7+), like higher alkanes such as ethane, propane or butane in the mixture can make the ignition delay lower, because methane normally is resistant to the auto ignition (Khalil *et al*. 2002).

On the other hand, big amount of propane in CNG gases can cause problems related with the propane liquefaction. Typically CNG systems have 200 bar pressure and at such high pressure propane turns from gaseous to liquid phase (Ramadhas 2011).

Other type of diluents – incombustible components like N_2 and CO_2 makes negative influence in engines running on natural gas. Mentioned elements reduce the fuel heating value, flame propagation rate which makes longer combustion duration (Khalil *et al*. 2002; Shrestha *et al*. 2001).

These differences in the fuel composition can have great impact on the fuel consumption and engine performance (Lee *et al*. 2000). But comparing specific heat of CO_2 and N_2, CO_2 has higher specific heat. Energy released during combustion will be taken by CO_2 in much faster rate than by nitrogen or air. Experimental investigation showed that the combustion duration reduced in both cases, with CO_2 and with N_2, but N_2 had greater impact on the combustion duration. Also the indicated power for CO_2 was higher (Shrestha *et al*. 2001).

The results of the studies showed that the fuel features have direct impact on NGVs emissions and fuel economy. Depending on gas composition, A/F ratio varied also. For this reason, engines are preferred to be designed so that they will compensate the variations of the fuel composition (Karavalakis 2012; Lee *et al*. 2000).

1.2.2. Biogas Features

CNG is a fossil fuel and one of the way to reduce fossil fuel use in the globe is biogas solution, which can be produced by anaerobic fermentation of organic material. The raw materials available for the biogas production are abundant (from agriculture, municipal waste, industrial waste and green biomass) and underutilized (Tricase *et al*. 2009; Raheman *et al*. 2012; Li *et al*. 2009; Rulkens 2008). One of the options can be biogas, which is a renewable and produced by anaerobic fermentation of organic material (Bedoya *et al*. 2009).

As a fuel, biogas has an extremely low energy density on the volume basis on account of its high CO_2 content and the flame speed is much lower if compared with methane. The energy value in biogas depends on the methane content, which should be as high as possible for vehicle use. For example, the methane content in the biogas used in Sweden is at least 97%, the hydrogen sulphide content is limited to 23 mg/m^3, and the moisture content must not exceed 32 mg/m^3 (Subramanian *et al.* 2013). The large quantity of CO_2 present in biogas lowers its calorific value, flame velocity and flammability range. On the other hand, the auto ignition temperature of methane, which is present in biogas, is high (Table 1.2) and it resists knocking which is positive property for SI engines.

Scientists have been studying the opportunities of biogas use for the marine and road transport (Porpatham *et al*. 2012). The energy utilization of biogas is maximized when it is converted into electricity via a biogas generator or a gas engine, which makes the process ecological and energy efficient (Chandra *et al*. 2011). The use of purified (at least 90% methane) biogas in diesel engines has been also widely analysed.

The use of biogas with the partially eliminated CO_2, i. e., the content of CO_2 varied from 5% to 35%, has been studied (Makarevičienė *et al*. 2013). It was found that the use of biogas with a low methane content resulted in an increased

CO_2 content in the exhaust gas because, according to V.B. Kovács and A. Torok, this phenomenon depends on the CO_2 content in the biogas (Kovács *et al*. 2010). Therefore, if the carbon dioxide content in the biogas is high, the CO_2 content is also high in the engine combustion products. However, the research results demonstrated that additional use of biogas in a diesel engine can reduce NO_x emissions (Makarevičienė *et al*. 2013; Talal *et al*. 2010). The added mass of non-reacting gas absorbs heat and lowers the combustion temperature which has influence on NO_x formation. The effect of CO_2 variation in the fuel composition is similar to that of exhaust gas recirculation, which is known as the dilution effect (Byun *et al*. 2015).

The biogas influence was also researched by the thesis author with diesel engines. Results showed that the more biogas is supplied together with diesel fuel the more thermal efficiency and fuel consumptions are reduced. The reduction of the thermal efficiency was influenced by worse biogas combustion behavior. Diesel injection timing also had to be advanced in case when the biogas was used. However, it can be faced with few problems when additionally using biogas together with diesel fuel. First of all, engine constructional changes must be done because additional fuel supply system has to be equipped. Secondly, because of different fuel characteristics there is a difference of such fuel blend ignition and combustion process. Such reason requires engine adjustment or changes in engine control software. Because biogas has lower Cetane Number, compared with diesel, mentioned gas ignite worse and slower. In this case, diesel injection time must be earlier. Also it is known, that the thermal and kinetic interaction between the liquid pilot spray and the gaseous fuel leads to an extension of the ignition delay, which influence the following combustion process (Carlucci *et al*. 2011).

Biogas use in SI engines were studied by author by analysing the biogas operating properties and the engine operating mode. As a result, biogas is recommended as a fuel for SI engines. However, the impact of the methane / carbon dioxide ratio in biogas on engine operation is still unclear and further researches has to be done.

1.2.3. Hydrogen Features

With rising environmental problems more and more attention is paid not only to the natural gas but also to other alternative fuel sources. It is agreed that compared to the petrol or diesel fuels, better effect is obtained when natural gas is used in the ICE, because of better H/C ratio, which influences HHV and lower CO_2 amount. However, such fuel is not renewable energy source and its resources are also slowly running out. Therefore it is important to explore alternatives for the natural gas fuel (Rimkus *et al*. 2013; Keršys *et al*. 2013; Ma *et al*. 2009).

Hydrogen is one of the most perspective future energy "accumulators" which can be used for the different variety of vehicles to move. For this reason, there is a great interest of such fuel usage possibilities in recent time. Energy can be obtained from the hydrogen in two ways in the vehicle: using fuel cells device which produces electricity or using as a regular fuel in ICE.

Table 1.2. Physical and chemical features of the different fuel types (Bain *et al.* 1998; Ramadhas 2011)

Feature	Petrol	Methane	Hydrogen
Chemical formula	C_4–C_{12}	CH_4	H_2
Molar mass	100–114	16.04	2.02
Carbon, C	85–88	75	0
Hydrogen, H	12–15	25	100
Oxygen, O	0	–	0
Density, kg/m^3 at 15.5 °C	719–779	0.671	0.084
Boiling temperature, °C	27–225	–164 to –88	–253
RON	88–100	–	130+
MON	80–88	–	–
Freeze temp, °C	–40	–182.2	–259.4
Self-ignition temp, °C	257	482–632	500
HHV, MJ/kg at 15.5 °C	46.53	52.22	139.11
LHV, MJ/kg at 15.5 °C	43.44	45.3–47.13	121.46
A/F ratio (stoichiometric), –	14.7	17.2	34.3
Flame propagation speed, cm/s	41.5	–	237
Ignition energy, mJ	0.24	0.28	0.017
Autoignition temperature, °C	540	650	585

Hydrogen is promising alternative fuel, which gets a lot of attention recently. Sometimes it is called future fuel because it is the most wide spread element in the universe. Industrial hydrogen is mainly produced from the fossil fuel, however such production type is not an alternative way (Ramadhas 2011). Hydrogen can be produced from the renewable and from not renewable sources. Renewable sources can be: water, biomass. Nowadays, H_2 mainly is generated from the steam reforming technology.

Hydrogen is a clean fuel. It is the lightest fuel, having one proton and one electron. It is without color, smell and taste, and it is about 14 times lighter than air (Ramadhas 2011). Chemically hydrogen atoms are very active. When small amount of energy ignite hydrogen and air mixtures, hydrogen molecules react with air very intensively and emits a huge amount of heat and steam. Hydrogen self-ignition temperature is very high. For this reason, it is more suitable for SI engines.

Higher self-ignition temperature lets to use engines with the higher compression ratio (Ramadhas 2011). As hydrogen and air mixture combusts, due to higher flame speed and combustion rate, compared to combustion of petrol and air (Table 1.2), combustion duration significantly decreases (Mardi *et al*. 2014).

Hydrogen flame propagation speed is approximately 5 times higher than the one of other known hydrocarbon fuels (Table 1.2). Mixture combustion range is extremely wide, therefore even a very small additive of hydrogen into liquid or gaseous hydrocarbon fuel can significantly expand the ignition limits of these mixtures. Hydrogen additive reduces the induction period and improves the period of flame propagation. 3% of hydrogen (by volume) increases flame propagation speed from 11.08 m/s (standard engine) to 15.2 m/s (37%), while 6% of hydrogen – up to 17.78 m/s (60%) (Ji *et al*. 2013; Ji *et al*. 2010; Rimkus *et al*. 2013).

The use of pure hydrogen is characterized by some drawbacks because of its extremely low density, e.g., decrease in engine power, torque and coefficient of performance at low engine speed. Air and fuel ratio in petrol engine is 14.7:1, and hydrogen has 34:1 ratio. When hydrogen at gaseous shape enters the combustion chamber, the amount of intake air in cylinder is reduced because hydrogen takes more volume than liquid fuels because of its very low density (Kahraman *et al*. 2006).

1.3. Hydrogen as Additive in Natural Gas, Biogas Fuel Mixture

Hydrogen is carbon-free, renewable, easy (relatively) derived alternative energy "accumulator", which can be easily adapted for use in ICEs. Natural gas and hydrogen fuel blends can be an alternative for vehicle development towards exhaust gas emissions reduction in the future (Ramadhas 2011). Hydrogen as fuel or fuel additive in ICEs can be easily fitted using present fuel supply infrastructure (Mariani *et al*. 2012).

The use of CNG and H_2 fuel blends is especially relevant in public transport because it does not require to use extra fuel additives or expensive and complicated exhaust gas filtering systems, which requires sophisticated and responsible technical maintenance like for the diesel vehicles. Also, the use of natural gas system lets the bus engine to be much quieter than a diesel engine, which makes it possible to reduce urban noise pollution (Mariani *et al*. 2012).

RoHR and MBF have influence on the combustion duration. Combustion duration is an important parameter, when efficient parameters are being investigated. Scientists Karim *et al*. (1996) determined, that comparing hydrogen with other fuels in wide temperature and pressure limits, hydrogen has a high flame propa-

gation intensity in the engine cylinder. This intensity remains even at lean mixtures. Energy release is intense and combustion duration is short, engine efficiency and power are high. The fastest combustion was determined with $\lambda = 1$ (Karim *et al*. 2003).

Performance of engine, which is powered by natural gas, can be further improved by using hydrogen as an additive (Das *et al*. 2000). It was found, that using hydrogen as an additive in natural gas, increased the thermal efficiency of the engine, increased indicated mean effective pressure, and reduced fuel consumption (Das *et al*. 2000).

It was found that the advanced ignition angle is a very important parameter for improving natural gas powered engine performance and combustion. Such adjustment is also important, when using hydrogen and natural gas mixtures. Scientists indicated in their research studies, that the maximum torque reached, when consistently the ignition advanced angle was reduced at higher combustible mixture flame speed (Mariani *et al*. 2012; Huang *et al*. 2007; Nagalingam *et al*. 1983).

Larsen *et al*. (1997) claims that in heavy duty vehicles hydrogen and natural gas fuel mixtures decrease such pollutants like CO, CO_2 and HC.

Das *et al*. (2000) compared ICE work characteristic and combustion characteristics, when CNG and hydrogen is being used. During the investigation it was obvious, that efficiency was higher with hydrogen. In this case, engine performance can be improved, when natural gas is used with hydrogen as an additive.

Also it was determined that hydrogen can increase natural gas laminar combustion speed. For this reason, it can increase engine efficiency (Karim 2003).

CH_4 / H_2 fuel blends cannot be used with too big hydrogen amount, when such fuels are supplied into the SI engine, in case when the engine is not modified. Using more than 5% hydrogen and CH_4 fuel blends there is need for engine operation modification, such as advanced ignition angle. Dimopoulos and Karim determined, that hydrogen increased natural gas combustion speed. Correctly set advanced ignition angle can improve gas engine thermal efficiency (Dimapoulous *et al*. 2007; Karim *et al.* 2003).

Ignition timing is an important parameter in natural gas fuelled engine when the combustion characteristics are improved (Huang *et al*. 2007). It was determined, that at higher flame speeds and retarded spark timing it was possible to achieve better MBT (Nagalingam 1983).

Huang *et al.* (2007) also determined, that advanced ignition angle is important parameter, while improving work process and characteristics of engine with gas fuel control system. Furthermore, because of much faster hydrogen and air blend flame spreading speed, compared to petrol (or CH_4) and air blend, it is possible to ignite much leaner blends with spark, therefore, it is possible to use not only stoichiometric blends in case when hydrogen and CH_4 are used (Soberanis *et al*. 2010).

Lean combustion process of ICE is very promising due to the high efficiency and low nitrous oxide emissions. However, it is hard to ensure a stable combustion process for the lean mixture. It is extremely difficult to achieve it using CNG fuel. One of the ways to achieve a stable combustion of lean mixture is to use a hydrogen as an additive (Mariani *et al.* 2012).

Methane combustible mixture limits are narrower than for the other fuel types. Comparing with methane, air / hydrogen mixtures have very wide combustion limits. When the standard A/F mixture was flowing and the turbulent speed increased beyond certain value, the limits of combustion decreased. Hydrogen can expand combustion limits at different gas flow speeds. Tendencies showed, that hydrogen addition in the methane fuel let to use leaner and fast flowing (turbulent) mixture (Al-Alousi *et al*. 1984).

Karim *et al.* (1996) presented their investigation, where it was claimed, that hydrogen as additive in natural gas can improve such characteristics like power, efficiency and emissions, when engine was working on lean mixtures (Karim *et al*. 1996).

Meanwhile, Rimkus' paper (2011) revealed, that as SI engine run on leaned mixture and ~ 0.15% (of intake air volume) HHO (Brown gas) was supplied, the engine indicated coefficient of efficiency increased up to 5%.

Under high air excess, even a small amount of H_2 (up to 2% by volume) accelerated and improved combustion, which resulted in improvement of process efficiency, however, due to intensified heat release (peak temperature) NO_x concentration increased in combustion products (D'Andrea *et al*. 2004).

However, in experimental research of V8 engine running on natural gas and hydrogen mixtures (from 0% to 30% in mixture), it was noticed that NO_x emission was lower 15–20%. Also HC emission was higher with extremely lean mixtures (Raman *et al*. 1994). However, besides already mentioned characteristics of hydrogen use some of the previous research also mentions the reduction of NO_x (Jingding *et al*., 1998).

1.4. Features, Innovation and Challenge of Engines with Direct Gas Injection

There are already vehicles with indirect injection (IDI) of CNG on the market and the main benefits of these are, that engines ensure high knocking resistance, higher hydrogen and carbon H/C ratio for methane resulting in lowered CO_2 emissions compared to petrol, extremely low particle numbers due to good mixing and high specific power output. On the other hand, using such injection systems the gaseous fuel can occupy from 4 to 15% of intake manifold volume, resulting in notably

reductions in the volumetric efficiency, comparing to liquid fuels (Boretti *et al*. 2013; Reynolds *et al*. 2005; Obiols *et al*. 2011; Kalam *et al*. 2011).

NGV manufacturers search for new or improved technologies, which let to obtain a better fuel economy and lower emissions. There are different ways of using CNG system in ICEs, such as: SI port fuel injection (PFI) homogeneous stoichiometric, SI homogeneous lean burn, CI dual-fuel (with diesel for pilot ignition) and HCCI engines. Also possible is DI homogeneous or stratified combustion systems (Kakae *et al*. 2014; Boretti *et al*. 2013).

One of the ways to avoid mentioned gaseous fuel disadvantages is natural gas DI system use in new generation gas engines. DI ensures better volumetric efficiency, better mixture formation and it can achieve better torque and power output, reduce pumping and heat losses (Zhao 2010). With DI system for a gaseous fuel, it is possible to achieve three different combustion strategies: homogeneous stoichiometric, homogeneous lean burn and stratified lean burn. Each combustion strategy has its own specific performance characteristics. Stratified combustion mode has the greatest potential in fuel savings due to much lower pumping losses and lower heat losses.

Modern DI engines use high fuel pressures and in these engines the pressure difference between the fuel pressure and the cylinder pressure rarely needs to be addressed. However with a gaseous fuel, relative low pressures are interesting and if stratified mode is considered, where the fuel is injected during the compression stroke, this differential pressure will influence the mass injected.

The combustion behavior can be strongly influenced by injector parameters (A-Aziz *et al*. 2009). Nowadays three standard types of nozzles are used for petrol DI injectors. Fig. 1.7 presents different types of DI system injectors.

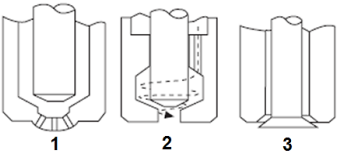

Fig. 1.7. Different types of direct injection injectors: 1 – multi-hole nozzle; 2 – swirl nozzle; 3 – outward-opening nozzle (Zhao 2010)

The injector nozzles differ from the each other by the way it open and close: multi-hole nozzle with inward-opening (I-nozzle); swirl nozzle with inward-opening (I-nozzle); valve type opening with outward-opening nozzle (A-nozzle). Last type of nozzle self-forms the spray shape via the cone (Zhao 2010).

Essential parameter for the injector is injection pressure at the end of compression stroke. It should be considered that backpressure can influence the amount of injected fuel, especially when the injector working pressure range is on

the low side (Zhao 2010). A positive pressure difference between the injection pressure and the cylinder pressure has to be sufficiently large to deliver the fuel to the cylinder in a short time period. Considering the pressure loss inside an injector, injection pressure can be expressed (p_{inj}), as (Zhao 2010):

$$p_{inj} > p_{\max} + \delta_{P1} + \delta_{P2}\,. \tag{1.11}$$

Here p_{max} – the maximum cylinder pressure, δ_{P1} – the pressure difference across the injector holes, δ_{P2} – the pressure drop inside the injector.

In A-Aziz research (2000) the influence of low injection pressure in a CNG DI engine was investigated. They found out that longer fuel injection duration with lower fuel injection pressure (7.5 bar) resulted in lower volumetric efficiency and engine performance. Highest torque and break mean effective pressure (BMEP) was achieved with 18 bar injection pressure. But at some particular engine speeds a lower injection pressure had more benefits because of a sufficient mixing time for the A/F charge.

A comparison of port injection petrol, DI methane at 8 bar and dual fuel (methane / petrol) at homogeneous and stratified lean conditions showed, that methane combustion behavior was different from petrol because of turbulence in the cylinder and combustion reaction rate (Di Iorio *et al*. 2014).

Injection timing and end of injection (EOI) has remarkable influence on the combustion behavior and A/F mixture formation, which influences engine performance and stability. Retarding the fuel injection timing, reduced time and quality of air / fuel mixing. Gas jet penetration distance decreased because of late injection timing after intake valves closed, resulting in more fuel concentrated near injector exit around spark plug (Huang *et al*. 2005).

A multi-dimensional modeling was done for the DI natural gas stratified charge for a poppet valve type injector (Baratta *et al*. 2009). The influence of different parameters such as injection timing, injector tip protrusion, piston and cylinder head geometry on the A/F mixture formation and their ratio distribution were analysed. Piston bowl shape and chamber geometry affects gas mixture formation. Keeping the flammable mixture in a compact area seems to be an important characteristic for stratified charge operation (Yadollahi *et al*. 2011). Also other authors note that main problem of methane DI is due to poor fuel penetration at the injector nozzle, comparing with liquid fuels. It was noticed that even in very high fuel velocities, the mixture homogenization or stratification mainly depends on the charge motion (Chiodi *et al*. 2006).

The injector's back-pressure dependency must be understood; at full load operation the fuel is injected during the intake stroke at lower back-pressures than during compression stroke, and this in combination with the longer injection durations available enables injecting sufficient fuel masses for full load. With CNG injectors it is a challenge to be able to accurately inject small masses and at the

same time being able to inject enough fuel at higher loads. Low pressure DI systems are mainly used in low compression ratio SI engines. CNG with high injection pressure (above 20 bar) is typically used in diesel type engines which requires high fuel rail pressure (Thipse *et al.* 2015). High CNG fuel pressures in the range of 200 bars, like used in CNG Diesel's, are not needed. For a Diesel, very high back-pressures are present and in combination with multi-hole nozzles with small holes they require high fuel pressures in order to inject sufficient masses. In DISI engines however, like the one tested here, only a low fuel pressure is needed. Low dosing accuracy also needs to be considered. A solenoid driven CNG injector is considered reaching its linear relation between duration and mass starting at around 1 ms duration. Shorter injections will therefore occur in the non-linear ballistic area of the injector's duration-mass curve and would thus result in high coefficient of variance in the injected mass, which is not desirable. A 200 bar injector would have great issues with low dosing with high accuracy. In (Liu *et al.* 2013) it was found that high spray velocities were reached when high injection pressure had been used which reduced ignition probability because of quenching of the flame kernel. Another disadvantage with 200 bar injection pressure is that a pump is needed in order to reach 200 bar when the fuel tank pressure is lower than 200 bar (Bohatsch 2011).

Optical engine setup with chemiluminescence imaging with methane port injection system showed that combustion species – OH*, CO_2 and small amount of CH* appeared at typical wavelengths. No obvious soot formation was noticed. With hydrogen addition OH* and CO_2 chemiluminescence emission intensity was higher (Catapano *et al*. 2013). Comparing petrol port injection and methane DI system, chemiluminescence emission intensity was higher for the petrol port injection and the peak values were lowest with methane DI at stoichiometric and lean conditions (Di Iorio *et al*. 2014).

Methane PFI or DI combustion systems can have positive features like previously mentioned but little information is available in the open literature about soot formation during stratified combustion process with methane gases. Soot is an unwelcome combustion product which is for example found in combustion systems which use liquid fuel DI systems, especially in diesel engines and in combustion systems which provide rich fuel conditions (Stanmore *et al*. 2001).

Soot formation can also occur in petrol engines. In (Stojkovic *et al*. 2005) they found that soot is formed first as a partially premixed flame propagates through locally rich zones, but this soot oxidize rapidly due to its high temperature. In a later phase, soot can be formed in pool fires due to thin films of liquid fuel on the piston surface. The pool-fire soot remained until late in the expansion stroke.

1.5. Conclusions of the 1st Chapter and the Formulation of the Thesis Tasks

According to literature overview analysis of gaseous fuels, ICE running on such fuels, the conclusions of this chapter are formed:

1. Alternative fuels are stimulated to use in every transportation sector by EU and Lithuania authorities. Gaseous fuels, like CNG, LNG, LPG, H_2, biogas, can be as alternative choice for liquid based fuels and the research and development of these fuels are motivated in the whole world.
2. During quality evaluation and testing of methane based fuels it is important to pay attention to such fuel characteristics as LHV and HHV, the energy density per cycle, the WN, the ratio of methane and hydrogen, methane number. These values can strongly influence combustion process in ICE and make an impact on efficient and ecological parameters.
3. Biogas use in transport can give advantages for ecological parameters, but the impact on engine operation of CH_4 / CO_2 ratio in biogas is still needed to investigate, especially when dual fuel systems are used.
4. H_2 has a great potential of use in transportation due to its physical and chemical characteristics. Even small amount of H_2 in gaseous fuels can improve combustion process in ICE. However, there are still contradictory conclusions about H_2 influence on engine efficiency and ecological parameters change. In addition, the use of higher amounts (more than 50% of H_2) in the fuel mixtures with stoichiometric and lean combustible mixture preparation is promising in a point of view of ecology.
5. The DI systems is the most promising engine technology in the future for improving engine efficiency and fuel consumptions, but it faces with ecological problem – the soot is being formed during combustion with liquid fuels. Therefore, the alternative solutions, like gaseous fuels having simpler hydrocarbon bonds in fuel composition, should be applied.
6. Literature overview revealed that comprehensive research about gaseous DI is still needed and combustion behavior, stability and soot formation in stratified combustion systems could be further investigated, especially with lower injection pressures.

According to the conclusions of the first chapter, the following tasks of the thesis are formulated:

1. To evaluate features and apply evaluation methods for different types of gaseous fuels, like biogas, H_2, CNG / H_2 fuel mixtures, methane fuel and

develop the experimental and numerical investigation methodology which could reveal and give explanations for engines efficient and ecological parameter changes.

2. To evaluate SI engine combustion process (combustion duration, intensity, combustion temperature) and its influence on the engine ecological and efficient indicators using petrol / biogas fuel mixtures, when the biogas fuel flow rate and spark timing are being changed.
3. To determine the influence of different CNG / H_2 fuel mixtures for SI ICE efficient and ecological parameters using developed experimental methodology, when the combustible mixture composition is being changed from very low to very high H_2 amount in the fuel composition and when engine load, excess air ratio and spark timing are being changed. Also, to determine the optimum fuel mixture by using numerical simulation analysis.
4. To evaluate low-pressure (18 bar) DI system influence on methane gas combustion process and combustion product formation in the cylinder during three different combustion strategies application (homogeneous stoichiometric, homogeneous lean burn, stratified lean burn).

2

Research Methodology of Gaseous Fuel Combustion Processes

During thesis preparation the specific experimental and numerical simulation research methodology was chosen, developed and adopted for the researches presented in the thesis. The used methodology and research results were published in scientific journals and were presented in international scientific conferences (Sendžikienė *et al*. 2015, Rimkus, Melaika *et al.* 2016, Pukalskas *et al*. 2014, Latakas *et al.* 2014, Melaika *et al*. 2016, Rimkus *et al. 2016*, Melaika *et al*. 2013, Pukalskas *et al. 2013*, Melaika *et al.* 2013).

Experiments were carried out during 2012–2016 year in Vilnius Gediminas Technical University and Chalmers University of Technology. Some of the researches were funded by the European Social Fund within the project "Development and application of innovative research methods and solutions for traffic structures, vehicles and their flows", project code VP1-3.1-SMM-08-K-01-020. Experiments were also carried out in company "SG dujos Auto" research laboratory, which was funded by the EU "Intellect LT+" funds.

Experiments were performed using 3 different experimental engines:

- The *HR16DE* model SI ICE (Table 2.1) from the *Nissan Qashqai* vehicle (2007–2013) was used as the test engine in the Internal Combustion Laboratory of Automobile Transport Department, VGTU. 4 cylinder engine

was used for the experimental investigations of *P* / *Bio*, *P* / H_2 and CNG / H_2 fuel mixtures.

- An *AVL* single cylinder SI ICE (Table 2.1) with optical access through the cylinder and through the piston top. The experiments were carried out in Combustion Division of Mechanical Engineering Faculty in Chalmers University of Technology in Gothenburg, Sweden. Single cylinder engine was used for the pure methane (100% CH_4) fuel DI investigation.
- The *Castrosua City Versus* city bus with SI 6 cylinder ICE (engine model *F2BE0642H*) (Table 2.1). Experiments were carried out in "SG dujos Auto" company laboratory "Experimental Research Laboratory of Hydrogen as Fuel or Fuel Additive, Organic Fuel Additives and Fuel Systems", which is situated in Pabradė town, Lithuania. The 6 cylinder engine was used for the CNG / H_2 fuel mixtures tests.

Table 2.1 also presents tested different fuel types, fuel mixtures with different engines, fuel injection types.

Table 2.1. Researched different engines using different fuel mixtures

Tested engines	Fuel injection type	Engine speed, rpm	Tested fuels	Load	A/F mixture preparation type
4 cylinder engine *HR16DE*	PFI	2000	Petrol (*P*)	15% throttle	1. Homog. stoich.; 2. Homog. lean.
			Petrol + Biogas (*P* + *Bio*) (1)	15% throttle	1. Homog. stoich.;
			Petrol + Hydrogen (*P* + H_2)	15% throttle	1. Homog. stoich.; 2. Homog. lean.
			Compressed natural gas (CNG) (2)	15% throttle; BMEP 1.6 bar BMEP 3.2 bar BMEP 6.3 bar	1. Homog. stoich.; 2. Homog. lean.
			Compressed natural gas/ hydrogen (CNG / H_2) (2)		
1 cylinder *AVL* optical engine	DI	1000 1500 2000	Methane (CH_4) (3)	IMEP 2.5 bar IMEP 3.5 bar IMEP 5.0 bar	1. Homog. stoich.; 2. Homog. lean; 3. Stratified.
6 cylinder F2BE0642 H engine	PFI	1500	Compressed natural gas (CNG) (2)	30 kW; 50 kW; 100 kW	1. Homog. stoich.;
			Compressed natural gas/ hydrogen (CNG / H_2) (2)		

Chemical composition of tested fuels:
(1) – 65% CH_4; 35% CO_2.
(2) – 91.8% CH_4; 5.88% C_2H_6; 1.26% C_3H_8; 0.464% C_4H_{10}; 0.596% N_2.
(3) – 100% CH_4.

4 cylinder engine *HR16DE* has two separate PFI fuel injection systems: one is originally mounted by manufacturer for *P* injection and second is aftermarket injectors for gaseous fuel (biogas, CNG, CNG / H_2) injection. Engine is atmospheric type with throttle valve control system.

Optical single cylinder engine was equipped with DI gaseous fuel (CH_4) injection system. Similarly like the first engine, the air was supplied atmospherically through the intake manifold with ability to use throttle valve for controlling intake manifold pressure.

Tested heavy duty vehicle with 6 cylinder engine was turbocharged, but also with PFI fuel injection system for gaseous fuel (CNG) supply, which was originally mounted and setuped by vehicle manufacturer.

Different A/F mixture preparation types were tested with different fuels. Homogeneous stoichiometric ($\lambda = 1$) mixtures were researched with *P* + *Bio*, *P* + H_2 and CNG / H_2 fuel mixtures. Also homogeneous lean burn ($\lambda = 1.4$) conditions were tested with pure methane (100% CH_4) with DI system in single cylinder engine and CNG / H_2 fuel mixtures with 4 cylinder engine. Stratified cases were tested with single cylinder engine (DI system) when pure methane (100% CH_4) was injected directly into the cylinder at the end of the compression stroke.

The experimental setup, measuring and calculation methods for engines, measuring equipment and data analysis are presented more accurately in the next chapter.

2.1. Setups of Experimental Engines

Experiments were performed with three different SI internal combustion engines: light duty 4 cylinder engine, 1 cylinder optical engine and heavy duty 6 cylinder engine. The technical data of tested engines is presented in Table 2.2.

Experiments with petrol and biogas were carried out using 4 cylinder *HR16DE* SI ICE from the *Nissan Qashqai* vehicle. Engine test bench is located in VGTU Internal Combustion Engine laboratory. A schematic diagram of the experimental test bench is provided in Fig. 2.1.

Petrol and gas fuel (biogas, natural gas) were injected separately via the ICE air intake manifold. The engine working parameters (throttle, engine speed), ignition angle, A/F ratio and petrol injection duration was controlled with a *MoTeC M800* programmable electronic engine control unit. The biogas fuel was injected by additional gas fuel injectors using an electronically controlled *OSCAR–N* gas injection system (Annex Fig. A.1.1). Natural gas or natural gas / hydrogen mixtures were also injected into the air intake manifold and the injectors were controlled with *MoTeC M800* programmable electronic engine control unit (Fig. 2.1).

Table 2.2. Technical characteristics of tested engines

Parameter	*Nissan HR16DE*	*AVL* Single Cylinder	*F2BE0642H*
Number of cylinders	4	1	6
Cylinder bore, mm	78	83	115
Piston stroke, mm	83.6	90	125
Displacement, dm^3	1.598	0.487	7.790
Maximum engine power, kW (rpm)	84 (6000)	–	213 (2000)
Maximum engine torque, Nm (rpm)	156 (4400)	–	1100 (1100–1850)
Compression ratio, ε	10.7	9.89	11.5
Con-rod length, mm	130	139.5	–
Number of valves per cylinder	4	4	4
Intake valves open	336° bTDC	355° bTDC	–
Intake valves close	108° bTDC	257° bTDC	–
Exhaust valves open	156° aTDC	125° aTDC	–
Exhaust valves close	308° bTDC	330° bTDC	–

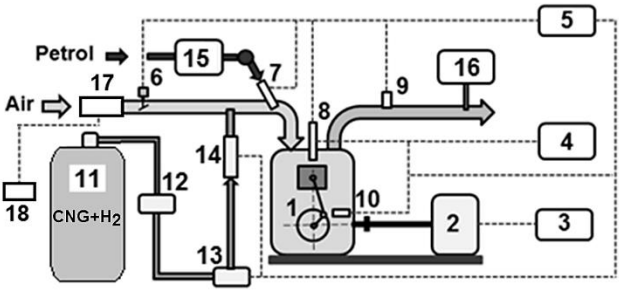

Fig. 2.1. Schematic of engine stand testing equipment for natural gas and hydrogen fuel mixtures investigation: 1 – SI engine *Nissan HR16DE*; 2 – engine load stand *AMX 200/100*; 3 – load stand electronic control unit; 4 – equipment for registration of pressure in the cylinder *LabView Real Time*; 5 – engine electronic control unit *MoTeC M800*; 6 – throttle control servo-motor; 7 – petrol injector; 8 – spark plug with integrated pressure sensor *AVL ZI31*; 9 – wideband oxygen sensor *Bosch LSU 4.9*; 10 – crankshaft position sensor; 11 – natural gas and hydrogen fuel mixtures cylinder at 200 bar pressure; 12 – gas mass flow meter *RHEONIK RHM015*; 13 – high pressure reducer from 200 bar to 1.5 bar; 14 – gas injector; 15 – petrol consumption metering device *AMX 212F*; 16 – exhaust gas analyser *OPUS 40–D*; 17 – air mass flow meter *Bosch HFM 5*; 18 – air mass flow meter indication monitor

Optical combustion investigation experiments were performed in an *AVL* optical single cylinder engine and the engine data are shown in Table 2.2. The schematics of the optical engine is shown in Fig. 2.2. Optical access to the combustion chamber is provided by a glass ring between cylinder head and liner as well as by a Bowditch type flat piston.

Such configuration allows two different views; side view and bottom view and both these views were used in the investigation. The cylinder head was designed for a downsized SI engine and had a medium tumble air motion.

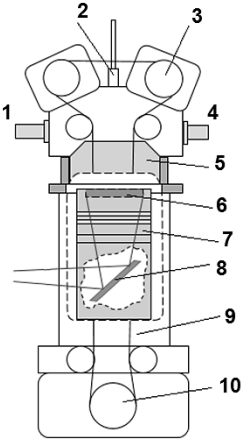

Fig. 2.2. Schematics of the optical single cylinder engine: 1 – exhaust manifold; 2 – gas DI injector; 3 – camshafts; 4 – intake manifold; 5 – quartz cylinder; 6 – quartz piston window; 7 – piston; 8 – mirror; 9 – engine timing belt; 10 – crankshaft

A standard ignition system was used for the homogeneous stoichiometric and homogeneous lean burn combustion modes, whereas a prototype dual coil ignition system was used for the stratified operation mode. The same dual coil system was used in another experimental investigation (Doornbos *et al*. 2015). Pre-experimental tests revealed that combustion in stratified mode had stability issues when a single coil ignition system was used and that misfires occurred. With the dual-coil ignition system however, these issues disappeared. Influence of ignition energy and ignition duration were investigated by Dahlstrom (2013) and Polcyn (2014), also concluding that combustion stability for gaseous fuel is greatly influenced by these parameters.

The optical single cylinder engine was fuelled with pure (100%) CH_4. Methane was supplied from a pressurized 200 bar bottle using a pressure regulator

which reduced the pressure to 18 bar accordingly to the injectors' maximum working pressure (18 bar) and an *ORBITAL* DI CNG injector was used to supply fuel directly into the combustion. A photograph of the injector is shown in Fig. 2.3.

This prototype injector was specially designed for gaseous fuels e. g. CNG. The actuator is a solenoid type and the injector opens outwards creating an A-shaped spray. The pressure range in which the injector operates is between 10–18 bar. In order to be able to inject the methane during the compression stroke and to create maximum pressure difference between the fuel pressure and the cylinder pressure, 18 bar fuel pressure was used. This also resulted in the most stable combustion, thus the lowest coefficient of variation of indicated mean effective pressure (CoV_{IMEP}). The injector parameters are given in Table A.1 (Annexes).

A fuel pressure of 18 bar works for both injecting fuel late during the compression stroke at high back-pressures (stratified operation) but it is also high enough for injecting enough fuel at full load operation.

The cylinder head configuration has a closed-spaced configuration where the fuel injector and the spark plug are mounted close to each other, see Fig. 2.3. This is a suitable configuration for stratified charge. The angle between the injector and the spark plug was ~ 18°. The injector tip was shimmed resulting in 2 mm protrusion from the cylinder head surface. The fuel injector has an umbrella angle of 60°.

The injector was electrically controlled from a *LabView* DI system module in which the injector current peak values (A), power supply voltage (V) and injector opening time in milliseconds (ms) were adjusted and optimized.

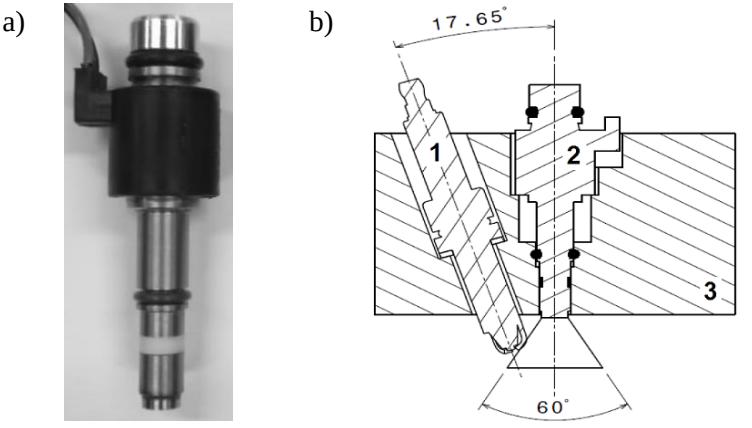

Fig. 2.3. Methane direct injection system: a) prototype injector; b) geometrical layout of the spark plug (1) and methane DI injector (2) in the cylinder head (3)

Experiments were also performed using *Castrosua City Versus* city bus with SI 6 cylinder ICE (engine model *F2BE0642H*) fuelled with CNG. Engine maximum power 213 kW is achieved at 2000 rpm engine speed. Engine meets one of the newest emission standards – Euro 5 EVV. Fig. 2.4 shows the experimental setup of CNG heavy duty vehicle tests.

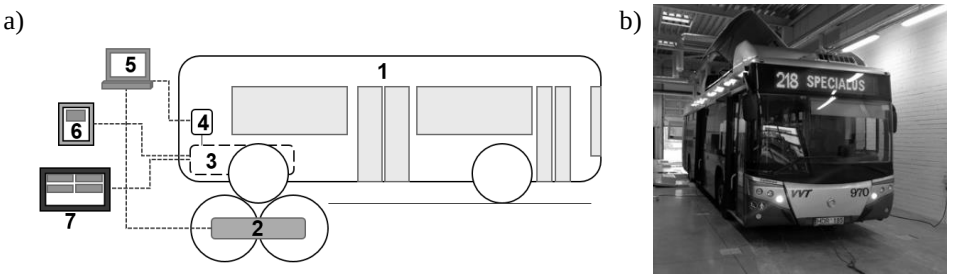

Fig. 2.4. City bus tests: a) test scheme in the "SG dujos Auto" research laboratory (1 – tested city bus; 2 – heavy duty vehicles' dynamometer test bench *V-Tech*; 3 – city bus with SI ICE *F2BE0642H*; 4 – engine control unit; 5 – computer for data acquisition; 6 – gas mass flow meter *RHEONIK RHM015*; 7 – exhaust gas analyser *OPUS 40–D*); b) tested *Castrosua* city bus

Vehicle was equipped with high pressure (up to 200 bar) natural gas fuel tanks, which supply gaseous fuel through the gas reducer to the gas fuel rail, which has a ~ 7 bar gas pressure in the system. Gas fuel injectors injected natural or natural gas and hydrogen mixture into the intake manifold.

2.2. Characteristics of Experimental Measuring Equipment

2.2.1. Engine Load Stands and Test Modes

The *HR16DE* 4 cylinder engine was controlled by a *MoTeC M800* programmable electronic control unit (ECU) which let to change spark timing during the test from 14 CAD bTDC to 30 CAD bTDC in the experimental investigation of biogas fuel addition. During the experiments, the following engine parameters were maintained electronically: crankshaft rotation speed n = 2000 rpm, 15% open engine throttle and stoichiometric mixture $\lambda = 1$. The engine load was generated by Electromagnetic Eddy Current load stand *AMX 200/100* (Table 2.3) where the obtained engine effective torque M_e was measured.

Table 2.3. Parameters of load stands used in experimental investigations

Parameter	Equipment		
	Engine load stand *AUTOMEX AMX200/200*	Engine load stand *AVL 5702*	Heavy duty vehicle dynamometer test bench *V-Tech VT-2/T*
Load mechanism	Electromagnetic Eddy Current brake	Asynchronous motor	Electromagnetic Eddy Current brake
Stand working speed range	0–6000 rpm	0–7000 rpm	up to 250 km/h
Maximum possible load torque	480 Nm	–	–
Maximum possible load power	200 kW	38 kW	600 kW (at const rpm)
Accuracy	±0.9 Nm	±0.1%	±1%

The same engine and load equipment were used in the experimental investigation of natural gas / hydrogen fuel mixtures. The programmable *MoTeC M800* ECU controlled A/F ratio, advanced ignition angle, injection duration. Experiments were done with different amounts of hydrogen in natural gas fuel: 10% H_2, 20 % H_2, 30% H_2, 50% H_2, 70% H_2, and 90% H_2. The percentage shows the H_2 amount by volume in the fuel mixture. All tests were run at engine speed – 2000 rpm. Firstly, different loads (20 Nm / 1.56 bar; 40 Nm / 3.14 bar; 60 Nm / 4.72 bar; 80 Nm / 6.28 bar) were tested at different A/F ratios ($\lambda = 1$; $\lambda = 1.4$) (Table 2.4).

Table 2.4. Natural gas and hydrogen fuel mixture testing modes

Fuel	Engine speed, rpm	λ	Tested engine cases	
P	2000	1;1.4	Engine load, Nm / bar	20 Nm / 1.56 bar; 40 Nm / 3.14 bar; 60 Nm / 4.72 bar; 80 Nm / 6.28 bar
CNG				
CNG + 10% H_2				
CNG + 20% H_2				
CNG + 30% H_2				
CNG + 50% H_2			Throttle, %	15%
CNG + 70% H_2				
CNG + 90% H_2				

Secondly, in order to achieve the best engine efficiency, further tests were done by changing the spark timing at 2000 rpm, 15% opened throttle with all

mentioned fuel mixtures at $\lambda = 1$ and $\lambda = 1.4$. In-cylinder pressure, exhaust gas temperature, exhaust gas emissions, A/F ratio, fuel consumption were captured and analysed.

Heavy duty vehicle tests were performed with 1 axle dyno test bench *V-Tech VT2/T* Dynamometer in "SG dujos Auto" research laboratory (Table 2.3). Dyno test bench was able to measure the maximum power on wheels and torque with inertial brake system. The power on wheels was calculated into engine power by dyno test bench computer. Vehicle engine *F2BE0642H* tests were performed at constant rpm and constant load.

Optical engine tests were made with the engine load stand *AVL5702* (Table 2.3). Engine load stand was working as an electric motor and running the optical engine at constant rpm in cyclic way, which is described in detail later. Experimental tests were carried out using *AVL* optical single cylinder engine, which has a possibility to observe combustion process through the piston top – bottom view and cylinder liner – side view.

During the DI system experiments pure (100%) CH_4 fuel was used. Three different combustion modes (homogeneous stoichiometric, homogeneous lean burn, stratified lean burn) were tested at different engine speeds (1000 rpm, 1500 rpm, 2000 rpm) and with different IMEP (~ 2.5 bar, ~ 3.5 bar, ~ 5 bar), see Table 2.5. Such experimental investigation plan was able to fulfill analysis of combustion on both low speeds and high speeds.

The experiments did not let to achieve BMEP engine load. The maximum stresses of glass cylinder and piston limits the maximum pressure in the cylinder, therefore it is not possible to achieve engine efficient work. The engine is able to create just indicated efficiency and achieve desirable IMEP.

Table 2.5. Parameters adjusted for engine tests with different combustion modes at different engine speeds

Engine speed, rpm	Combustion type	λ	IMEP, bar
1000 1500 2000	Homogeneous stoichiometric	1	2.5; 3.5; 5
	Homogeneous lean burn	1.4	2.5; 3.5; 5
	Stratified lean burn	2.5–2.9	2.5
		1.87–2.2	3.5
		1.37–1.45	5

The engine was running steadily on desired engine rpm because of electric motor rotation without any combustion cycles. When the fuel was injected into the cylinder, the fuel combusted and it created desirable IMEP values, which were calculated by engine test bench control unit *AVL PUMA*.

2.2.2. Fuel Consumption Measuring Equipment

During petrol and biogas tests petrol (*P*) hourly consumption (B_{d_P}) was measured using electronical fuel consumption meter *AMX 212F* which is working as gravitational weight.

Biogas consumption was measured using gas meter KG-0095-G06-94-10 (Table 2.6) (Annex Fig. A.1.1), which was measuring volumetric values. The measuring range was 0.06 m^3/h – 10.00 m^3/h with accuracy of ±0.001 m^3.

Natural gas and natural gas / hydrogen fuels were measured by Coriolis type mass flow meter. The fuel flow meter was *RHEONIK RHM 015* (Table 2.6) which was connected into the high pressure fuel supply system before the gas reducer, which was reducing gas to 1.5 bar pressure. The measuring range of the flow meter was 0.004–0.6 kg/min with high measurement accuracy ±0.10%.

Coriolis type mass flow meter is measuring the force resulting from the acceleration caused by a mass moving toward or away a center of rotation. The mass flow rate of fluid passing through the pipe is proportional to the pipe twist. Sensors measure the twist and generates electronic signal, which is converted into the numerical values and showed by the indicator.

Table 2.6. Parameters of fuel measuring equipment used in experimental investigations

Parameter	Equipment			
	AMX240	*KG-0095-606-94-10*	*RHEONIK RHM 015*	*Micro Motion ELITE CMF010M323NB*
Fuel state	Liquid	Gas	Gas and liquid	Gas and liquid
Measuring type	Gravitational weight	Mechanical gas flow meter	Coriolis Mass Flowmeter	Coriolis Mass Flowmeter
Measuring range	–	0.06–10.00 m^3/h	0.004–0.6 kg/min	0.016–0.75 kg/min
Accuracy	±0.10%	±0.001 m^3	±0.10%	±0.35%
Repeatability	–	–	±0.05%	±0.20%

During methane DI tests the fuel flow was also measured by a Coriolis type mass flow meter. The measuring range of the fuel flow meter was 0.016–0.75 kg/min with high accuracy ±0.35%. The fuel flow meter was a *Micro Motion ELITE* Coriolis mass flow meter *CMF010M323NB* (Table 2.6).

During the optical experiments the methane fuel was supplied from a pressurized 200 bar bottle using a pressure regulator which reduced the pressure to injector working pressure – 18 bar.

2.2.3. Emission Measuring Equipment

The exhaust gas emissions were measured with an *AVL DiCom 4000* exhaust gas analyser during the experimental investigation of biogas (Annex Fig. A.1.1). CNG heavy duty vehicle and *Nissan HR16DE* engine pollutants were measured with *OPUS 40–D* exhaust gas analyser when natural gas / hydrogen fuel mixtures were tested (Table 2.7). Both analysers had a possibility to change the measurement mode according to tested fuel. During tests where the fuel mixture has a CH_4 as a main base element, the analysers where switched to NG fuel measurement mode.

The fuel injection duration and injected mass was adjusted by lambda value during the experimental tests with *HR16DE* engine. The lambda value is calculated by a free oxygen amount in the exhaust pipe. The oxygen was measured with wideband oxygen sensor *BOSCH LSU 4.9* which gives a certain voltage value. Certain value of voltage is equal to a certain value of λ which does not depend on the type of fuel being used (*Motec* 2016). In order to get accurate measurements and to be sure that a certain λ is achieved, the air mass flow meter was used. The comparison of obtained λ value from air mass flow meter and gas analyser are presented in Annexes Fig. B.7.

Table 2.7. Parameters of exhaust gas analysers used in experimental investigations

Parameter	Equipment			
	AVL DiCOM 4000		*OPUS 40-D*	
	Measuring range	Accuracy	Measuring range	Accuracy
CO, % vol.	0–10	±0.01	0–10	±0.02
CO_2, % vol.	0–20	±0.1	0–20	±0.3
HC, ppm vol.	0–20000	±1	0–20000	±4
NO_x, ppm vol.	0–4000	±1	0–5000	±25
O_2, % vol.	0–25	±0.01	0–25%	±0.1
λ	0–9.999	±0.001	0.6–1.7	±0.001

Table 2.8. Parameters of oxygen measurement system used in experimental investigations

Parameter	*Horiba Mexa-110*	
	Measuring range	Accuracy
A/F	10.0–30.0	±0.3 A/F when 12.5 A/F ±0.1 A/F when 14.7 A/F ±0.5 A/F when 23.0 A/F
λ	0.5–2.5	
O_2, % vol.	0–25.0	
Temperature of exhaust gas used by sensor, ° C	–7°–+900	

Engine exhaust A/F ratio was measured using a *Horiba Mexa-110* (Table 2.8) during the optical experiments, which was adapted to work with methane fuel. The methane fuel H/C atom ratio was calculated and has been input in measuring system module in order to obtain the real calculated λ value. The λ value was captured for whole 200 combusting cycles which means that the available window for the measuring sensor was 24 s, enough time to get repeatable and stable measured data. On the other hand, the exhaust gas emission could not be measured due to still little time to get exhaust gas analyser stabilized.

2.2.3. In-Cylinder Pressure Measuring Equipment

In-cylinder pressure was traced by integrated pressure sensor *AVL ZI31_Y7S* in spark plug (sensor nominal sensitivity 12 pC/bar) during petrol / biogas and natural gas / hydrogen experiments, see Table 2.9 and Annexes Fig. A.1.2 a).

The pressure was recorded using *AVL DiTEST DPM 800* and *LabView Real Time* equipment. Average pressure values were obtained from captured 200 combustion cycles.

Table 2.9. Parameters of pressure sensors used in experimental investigations

Parameter	Equipment	
	AVL ZI31	*Kistler 6053CC60*
Measuring range, bar	0–200	0–300
Sensitivity, pC/bar	12	20
Natural frequency, kHz	130	160
Acceleration sensitivity, bar/g	≤0.001	≤0.0002
Shock resistance, g	2000	2000
Insulation resistance, Ω	$>10^{13}$	$>10^{13}$
Operating temperature, ° C	–40°–+350	–20°–+350
Thermal sensitivity change, %	≤±0.6	≤±0.5
Load change drift, mbar/ms	5	–
Cyclic temperature drift, bar	≤±0.6	–
Thermal shock error at 9 bar IMEP and 1500 rpm, bar	Δp ≤ ±0.5	Δp ≤ ±0.5

In-cylinder pressure was measured using a *Kistler 6053CC60* pressure sensor (Table 2.9, Annexes Fig. A.1.2 b)) in methane DI investigation and all pressure data was sampled in an *AVL INDICOM* data acquisition system. The engine was operated in cyclic mode. In overall there were about 200 combustion cycles. The cylinder pressure was sampled between cycles 100–150 (50 cycles). The engine was then motored for at least 30 s allowing temperature especially on the piston glass to cool down.

2.3. Optical Measurements

Images of the combustion process in the dissertation are presented in the third chapter only from the stratified operational mode. The optical cylinder head was un-cooled and due to this and the fact that the piston glass rapidly becomes very hot, the engine was operated cyclic like follows: 200 combusting cycles where camera images were captured between cycles 100–150.

The combustion was captured from the bottom through quartz piston glass (below view). Images were diverted through a 45° mirror towards video cameras through a beam splitter glass which directed the view into two directions: the first direction into a high-speed camera capturing the combustion and the second direction into a spectrometer connected to a second high-speed camera see Fig. 2.5 (Annexes Fig. A.1.3).

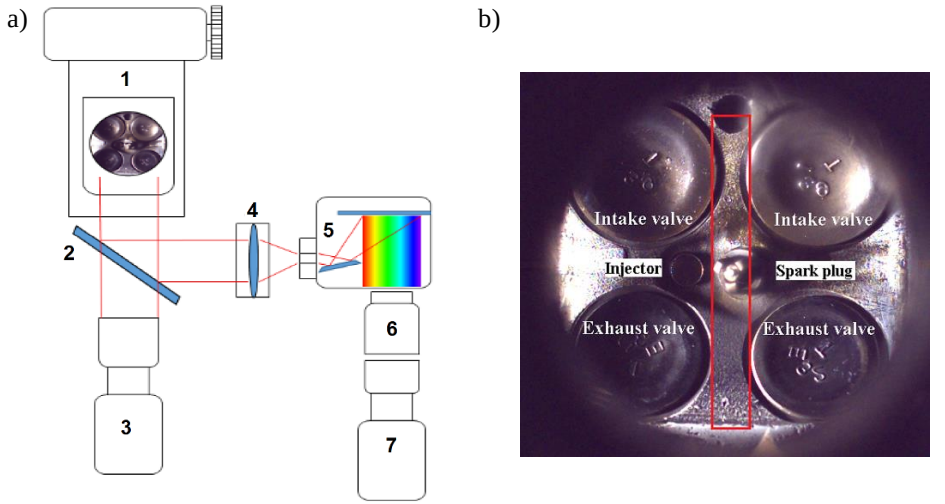

Fig. 2.5. Optical research methodology of methane direct injection system: a) schematics of the optical setup used for the emission spectra and the combustion images (1 – optical single cylinder engine, 2 – beam splitter, 3 – high-speed video camera for combustion visualization, 4 – focal lens, 5 – reflecting diffraction grating, 6 – image intensifier, 7 – high-speed camera for the emission spectrum); b) photograph of the combustion chamber with the red rectangle, which defines the area of the combustion chamber in which the emission spectra were captured

The focusing lens in front of the inlet of the spectrometer focused emitted combustion light to a vertical 0.25 mm slit. The light passed through the slit and was directed to the reflecting diffraction grating. Diffracted light radiation was

diverted into a Hamamatsu C9548-04 image intensifier. The output of intensifier was recorded by an Ametec Vision Research v7.1 high-speed video camera. The wavelength spectrum was calibrated with known wavelength peaks from a Mercury lamp. The area of the captured combustion process through the spectrometer was limited by a vertical slit which covered the area between the valves in the center of the spark plug, see Fig. 2.5. These spectrometer images had a resolution of 656 × 456 pixels, exposure time of 110 μs and the sample rate was 7.407 frames per second.

An Ametec Vision Research Phantom Miro M310 with a Nikon 105 mm f/2 lens was used for the combustion images. The image resolution for these images was 512 × 480, exposure time 98.46 μs and the sample rate was 10.000 frames per second. 50 combustion cycles were captured.

2.4. Methane Number and Motor Octane Number Calculations for Different Gaseous Fuels

In order to get a better understanding about the fuel ability to resist the knock inside the cylinder, it is important to determine the anti-knock parameter – octane number or methane number, depending on fuel type. MON and MN number evaluation for gaseous fuel is impractical as it requires time and economical resources in order to do motor tests. Alternatively mathematical methods were suggested by California Air Resources Board (CARB) and AnstaltfürVerbrennungskraftmaschinen (*AVL*). Further *CARB* method calculation and ISO standard (Standard ISO 15403–2006) calculation for MN is presented. The MON is calculated according H/C ratio (Kakae *et al.* 2014):

$$\text{MON} = -406.14 + 508.04\left(\frac{H}{C}\right) - 173.55\left(\frac{H}{C}\right)^2 + 20.17\left(\frac{H}{C}\right)^3. \qquad (2.1)$$

Here H/C – the ratio of hydrogen atoms to carbon atoms.

The calculated MON value is applied in further MN calculation:

$$\text{MN} = 1.624 \times \text{MON} - 119.1. \qquad (2.2)$$

The calculation of MN is also regulated by ISO standard (Standard ISO 15403–2006) where the MN can be calculated also according to mole fraction of different components in the fuel composition:

$$\begin{aligned}\text{MON} = &\left(137.78 \cdot x_{CH_4}\right) + \left(29.948 \cdot x_{C_2H_6}\right) + \left(-18.193 \cdot x_{C_3H_8}\right) + \\ &+ \left(-167.062 \cdot x_{C_4H_{10}}\right) + \left(181.233 \cdot x_{CO_2}\right) + \left(26.994 \cdot x_{N_2}\right).\end{aligned} \qquad (2.3)$$

Here x – the mole fraction of the corresponding components in the fuel composition.

The third equation which was developed from measured data, can be achieved by correlation between MON and MN according to the same ISO standard:

$$\mathrm{MON} = 0.679 \times \mathrm{MN} + 72.3; \tag{2.4}$$

$$\mathrm{MN} = 1.445 \times \mathrm{MON} - 103.42. \tag{2.5}$$

Research of new fuel mixtures, like biogas, CNG / H_2 fuels or different composition CNG, forced to improve the calculation method as mentioned standards above could not suit calculations of named fuels, because the increase of fuel additions, like H_2, were giving big impact on MN deviation, if using formula (2.1), where the H/C ratio is included in a calculation. According to scientific researches (Genchi *et al.* 2014), mentioned MON calculation formula can be used just in case when H/C atom ratio is between 2 and 5.

Formula (2.3) could not be used either, as the H_2 element is not included in calculation. Therefore, new European standard (EN 16726:2015) was released in 2015 year where the MN calculation methodology was changed and was adopted for different gaseous fuels, which comprises the following gases: carbon monoxide; butadiene; butylene; ethylene; propylene; hydrogen sulfide; hydrogen; propane; ethane; butane; methane; nitrogen and carbon dioxide.

The MN was calculated for different tested fuels in this thesis work: biogas, CNG and CNG / H_2 fuel mixtures. The MN was calculated from its composition in five steps. First, the mixtures were simplified, then subdivided into ternary mixtures. The MN value of each ternary mixture was calculated according to EN standard. The final methane number value was determined according:

$$\mathrm{MN} = \mathrm{MN}' + \mathrm{MN}_{\mathrm{inerts}} - \mathrm{MN}_{\mathrm{methane}}. \tag{2.6}$$

Detailed MN calculation according standard is presented in Annex A.2 (Methane Number calculation methodology for gaseous fuels**)**.

The MON values for tested CNG and CNG / H_2 fuel mixtures were calculated according to formula (1.6). Literature overview also showed that it is possible to calculate MON values for liquid and gaseous fuels (bifuels) like *P* / *Bio* fuel mixtures (Genchi *et al.* 2014). MON calculations for mentioned fuels were obtained by (1.3) formula where the H/C atom ratios were included.

The calculated values of MN and MON for tested different fuels and fuel mixtures are presented in Table 2.10.

Calculations show that with increasing amount of biogas the MON value is increasing from ~ 85 for *P* fuel up to 96 for *P* + *Bio* 30 fuel mixtures. Physical features of CO_2 make influence on combustion process, therefore engines with higher compression ratios could be used in order to obtain higher thermal efficiency.

The fossil CNG fuel has 77 value of MN and 121 value of MON. It shows that CNG fuel has high anti-knock characteristic. Comparing CNG (natural gas) calculated values with pure methane (CH_4) MON (MN) values, the difference is obvious due to different CNG chemical composition, which includes not only CH_4 but also such elements like C_2H_6, C_3H_8, C_4H_{10}, N_2.

Table 2.10. Methane number and Motor Octane number values for different tested fuels

Researched fuels and fuel mixtures	MN	MON
P	–	85
CH_4	100	135
CNG	77	121
H_2	0	–
Biogas (65% CH_4 / 35% CO_2)	135	156
P + *Bio* 20 (65% CH_4 / 35% CO_2)	–	94
P + *Bio* 25 (65% CH_4 / 35% CO_2)	–	95
P + *Bio* 30 (65% CH_4 / 35% CO_2)	–	96
P + 10% H_2	–	–
P + 15% H_2	–	–
CNG + 10% H_2	73	118
CNG + 20% H_2	67	114
CNG + 30% H_2	60	110
CNG + 50% H_2	46	102
CNG + 70% H_2	28	90
CNG + 90% H_2	10	80

The highest amount of H_2 addition (90% H_2) in CNG reduces MN and MON values up to 10 and 80, respectively. It means that the probability of knock phenomena can be expected during testing. Though the value of 80 MON is fairly close to *P* fuel value. The MON could not be calculated for *P* + 10% H_2 and *P* + 15% H_2 investigation because the H/C atom ratio exceeded permissible values and the theoretical calculation model could not be adopted.

2.5. Fuel Lower Heating Value Dependencies on Different Gaseous Fuel Mixtures

Fuel LHV has an influence on the energy amount which is brought by a fuel and for the combustion process. But the LHV level directly depends on the fuel content distribution by mass, therefore, firstly, the distribution according to mass calculations for different tested fuels and fuel mixtures were calculated.

The fuel distribution according to mass is presented in Annex A.3 (Fuel mass distribution in different fuel mixture).

The LHV of fuel mixture can be calculated according to formula:

$$\mathrm{LHV}_{\mathrm{fuelmix}} = \frac{\mathrm{LHV}_1 \cdot \%_{fuelcomp.1}}{100} + \frac{\mathrm{LHV}_2 \cdot \%_{fuelcomp.2}}{100}. \qquad (2.7)$$

Here LHV_1, LHV_2 – lower heating values of the fuel components; $\%_{fuelcomp.1}$, $\%_{fuelcomp.2}$ – percentage of a certain fuel component in a fuel mixture according to mass, %.

Figure 2.6 represent the LHV values for the tested different fuels and fuel mixtures which are depending on the different fuel addition concentrations.

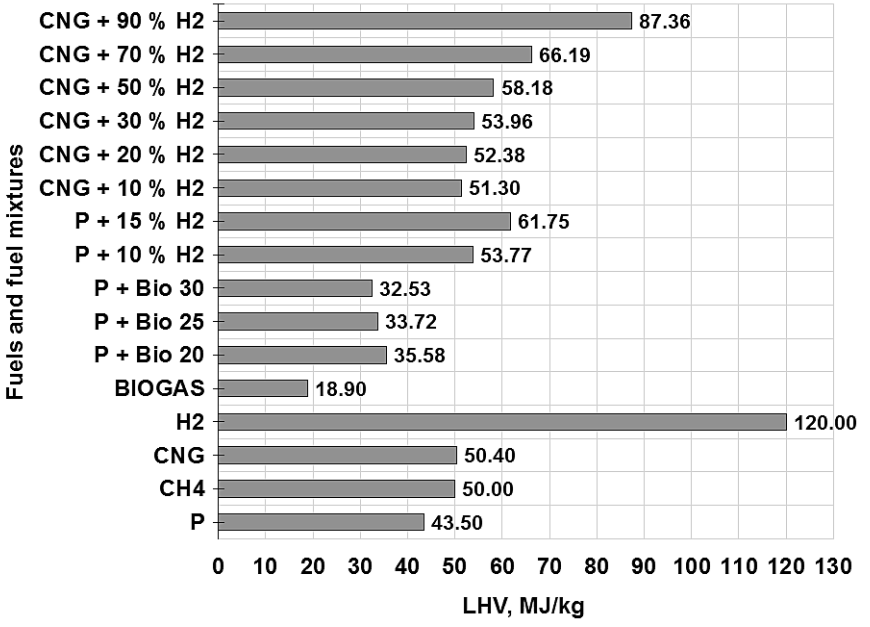

Fig. 2.6. Dependence of lower heating values on different fuels and fuel compositions

First experimental studies were performed with a 4 cylinder SI *HR16DE* engine fuelled with petrol and petrol with additional feeds of biogas. Such system worked as dual fuel system. Different petrol and 20 *l*/min. (*P* + *Bio* 20), 25 *l*/min. (*P* + *Bio* 25) and 30 *l*/min. (*P* + *Bio* 30) of biogas additive were tested.

The lowest LHV value (18.90 MJ/kg) was calculated for pure biogas which contains CO_2 element. Comparing with a pure methane (50 MJ/kg) or fossil CNG

fuel (50.40 MJ/kg), it was even ~ 62.2% lower. Such LHV decrease is influenced by CO_2 element which is present in tested biogas composition.

The addition of biogas together with petrol fuel (*P* + *Bio*) reduced overall fuel mixture LHV up to 32.53 MJ/kg with biggest amount of biogas addition (*P* + *Bio* 30) which was ~ 26% lower comparing with *P* fuel – 43.4 MJ/kg. In this case, the energy amount which is brought with biogas fuel should give the impact on the combustion process which is expected to be less intense and longer in time.

H_2 has the highest LHV (120 MJ/kg) comparing with all tested fuel types. Such high number gives obvious impact on other fuel mixtures where the H_2 is present. 15% H_2 addition with *P* fuel gives 61.75 MJ/kg LHV which is ~ 42% higher if compared with *P* fuel.

H_2 addition into CNG fossil fuel also gives increase of LHV for CNG / H_2 fuel mixtures. With small amounts of H_2, like 10% addition, the LHV increase is just ~ 6.7% (53.77 MJ/kg) comparing with CNG (50.40 MJ/kg). Such small increase is influenced due to small density of H_2 element and according to presented Fig. A.3.3 (Annexes) the mass of H_2 in whole fuel mixture is just 1.29%.

Increasing amount of H_2 gives higher LHV. The highest LHV among CNG / H_2 is obtained with 90% H_2 addition – 87.36 MJ/kg which is ~ 73% higher comparing with 100% CNG. Such LHV increase could give improvement for the engine efficient indicators. The injected fuel mass can bring bigger amount of energy. Such fuel characteristic also could give better combustion features, like shorter combustion duration.

2.6. Hydrogen and Carbon Atom Ratio Dependencies on Different Fuels and Fuel Mixtures

The auto-ignition temperature of gaseous fuel is related to its molecular weight. In this case, it is related with H/C atom ratio. With increasing amount of C element the ratio is getting lower and the auto-ignition temperature decreases. The higher content of H_2 atoms, the lower auto-ignition temperature. H/C atom ratio can be one of the indicators which can give also better understanding about exhaust gas emission formation.

The H/C atom ratio calculation is based on molar volume (V_m) of an ideal gas and calculation of fuel mixtures molecules and atoms. The V_m for all ideal gas is 22.465 dm^3 at 1 bar atmospheric pressure and 25° C. The V_m = 22.465 dm^3 is equal to 1 mole.

Firstly, the mole number of every gaseous fuel mixture composition can be calculated by:

$$n_{fuelcomp.} = \frac{n_{V_{fuel}} \cdot V_{fuel}}{V_{fuelcomp.}}. \quad (2.8)$$

Here $n_{V_{fuel}}$ – mole number in a chosen volume V_{fuel} of gaseous fuel mixture, moles; V_{fuel} – gaseous fuel mixture volume, dm^3; $V_{fuelcomp.}$ – volume of certain fuel additive in a gaseous fuel, dm^3.

Secondly, the number of molecules is calculated by:

$$N_{fuelcomp.} = N_A \cdot n_{fuelcomp.}. \quad (2.9)$$

Here N_A – Avogadro constant ($6.022140857 \cdot 10^{23}$ mol^{-1}); $n_{fuelcomp.}$ – mole number of additive in gaseous fuel mixture.

The atomic mass of each component in the fuel can be calculated by:

$$m_a = N_{fuelcomp.} \cdot X_{fuelcomp.}. \quad (2.10)$$

Here $X_{fuel\ comp.}$ – number of element atoms in a fuel component.

Finally, the H/C atom ratio can be calculated by:

$$\frac{H}{C} = \frac{m_{a_H}}{m_{a_C}}. \quad (2.11)$$

Here m_{a_H} – atomic mass of H_2 element in a gaseous fuel mixture; m_{a_C} – atomic mass of a C element in a gaseous fuel mixture.

Fig 2.7 presents H/C atoms ratio dependence on different fuels and fuel mixtures. The standard *P* fuel (MON = 85) has H/C ratio of 2.25 which is almost half lower comparing with CNG fossil fuel. CNG fuel has H/C atom ratio of ~ 4.

The presence of CO_2 in biogas reduced overall ratio. The biogas has lowest ratio among all researched fuels, which is 1.56. It probably will have an obvious influence on the combustion process and exhaust gas emission formation, though the increasing amount of biogas (*P* + *Bio* 30) showed higher ratio than *P* fuel. It can be explained by increasing amount of CH_4 element in the fuel, which has more H_2 atoms than C atoms in its chemical composition.

The hydrogen addition to the fuel mixtures gave rising tendencies. Hydrogen element has no C atom in his molecular structure. With biggest hydrogen amount (90% H_2) addition the H/C atom ratio was 22. Such ratio change can give presumption that fuel composition is changing and it will have an effect on A/F mixture combustion behavior, exhaust gas emissions formation. The addition of H_2 together with *P* fuel also increased this indicator depending on hydrogen concentration in combustible mixture.

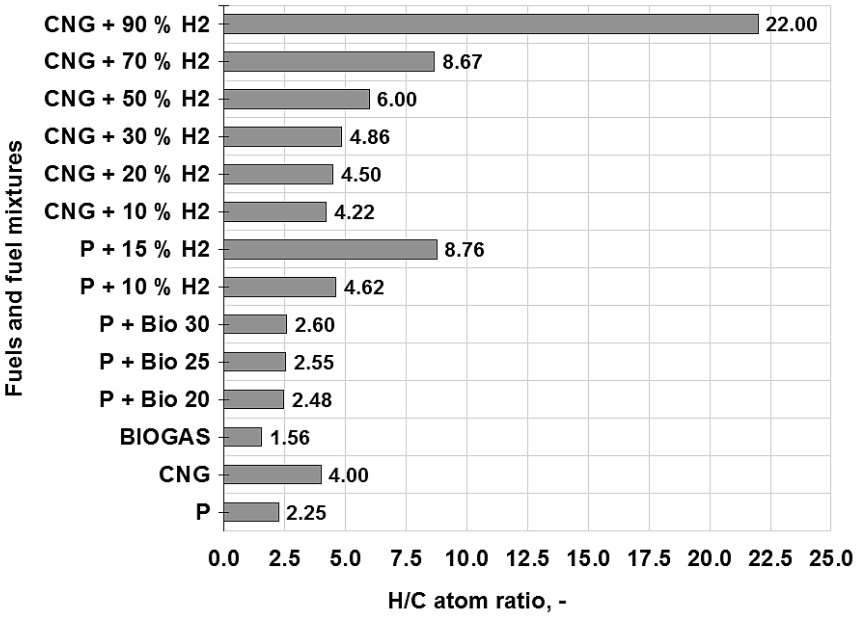

Fig. 2.7. Hydrogen and carbon atom ratio depending on hydrogen additive amount in a fuel

With increasing amount of hydrogen and increasing ratio of H/C, the exhaust gas emissions of CO_2 should reduce because of changing combustion chemical reactions.

2.7. CO_2 Emission Evaluation Depending on Gas Fuel Mixture

Exhaust gas element CO_2 is another parameter which as important evaluating ICE and trying to meet newest EU emission standards. The CO_2 emission according to mass for CNG and CNG / H_2 fuel mixtures was calculated using theoretical calculation formulas in this thesis work. Assuming that during combustion of 1 molecule CH_4 there is produced 1 molecule of CO_2:

$$CH_4 + 2(0_2 + 3.76N_2) \rightarrow CO_2 + 2H_2O + 7.52N_2 . \quad (2.12)$$

It was calculated that from 1 gram of CH_4 there is produced 2.75 g of CO_2 according to following formulas. The mole number from 1 gram of component is calculated by:

$$n = \frac{m_{fuel\ comp.}}{M_{fuel\ comp.}}. \tag{2.13}$$

Here $n_{fuel\ comp.}$ – mole number of a fuel component in 1 gram, moles; $m_{fuel\ comp.}$ – mass of a fuel component, g; $M_{fuel\ comp.}$ – molar mass of a component, g/mol.

The measured hourly fuel consumption (B_d) which were measured in kg/h were converted into dm^3/h. Using same methodology, like mentioned before, it is admitted that 1 mole of gas is equal to $V_m = 22.465\ dm^3$.

Natural gas is composed from methane (CH_4), ethane (C_2H_6), propane (C_3H_8), butane (C_4H_{10}). Measured dm^3/h fuel consumption was calculated in moles. The volume of each fuel component was calculated according to the fuel composition. According to proportion (e. g. 1 g of CH_4 = 2.75 g of CO_2) the total CO_2 amount which is produced during combustion was calculated for each natural gas element (ethane, propane, butane). The CO_2 emission amount was calculated for the *P* fuel, CNG + 10% H_2; CNG + 20% H_2; CNG + 30% H_2; CNG + 50% H_2; CNG + 70% H_2 and CNG + 90% H_2 fuel mixtures. Obtained results are presented in results chapter.

2.8. Numerical Simulation and Analysis of Engine Work Cycle

Engine work cycle simulation was performed using numerical simulation software *AVL BOOST*. This software is able to simulate engine thermodynamic processes during combustion in the cylinder.

The simulation of the thermodynamic state of the cylinder is based on the thermodynamics law (*AVL BOOST* Theory 2011):

$$\frac{d\left(m_c \cdot u\right)}{d\alpha} = -p_c \cdot \frac{dV}{d\alpha} + \frac{dQ_F}{d\alpha} - \sum \frac{dQ_w}{d\alpha} - h_{BB} \cdot \frac{dm_{BB}}{d\alpha} + \\ + \sum \frac{dm_i}{d\alpha} \cdot h_i - \sum \frac{dm_e}{d\alpha} \cdot h - q_{ev} \cdot f \cdot \frac{dm_{ev}}{dt}. \tag{2.14}$$

The sum of the in-flowing and out-flowing masses let to calculate the variation of the mass in the cylinder:

$$\frac{dm_c}{d\alpha} = \sum \frac{dm_i}{d\alpha} - \sum \frac{dm_e}{d\alpha} - \frac{dm_{BB}}{d\alpha} + \frac{dm_{ev}}{dt}. \tag{2.15}$$

Here $\frac{d(m_c \cdot u)}{d\alpha}$ – change of the internal energy in the cylinder; $-p_c \cdot \frac{dV}{d\alpha}$ – piston work; $\frac{dQ_F}{d\alpha}$ – fuel heat input; $\sum \frac{dQ_w}{d\alpha}$ – wall heat losses; $\frac{dm_{BB}}{d\alpha}$ – enthalpy flow due to blow-by; m_c – mass in the cylinder; u – specific internal energy; p_c – cylinder pressure; V – cylinder volume; Q_f – fuel energy; Q_W – wall heat loss; α – crank angle; h_{BB} – enthalpy of blow-by; $\frac{dm_{BB}}{d\alpha}$ – blow-by mass flow; dm_i – mass element flowing into the cylinder; dm_e – mass element flowing out of the cylinder; h_i – enthalpy of the in-flowing mass; h_e – enthalpy of the mass leaving the cylinder; q_{ev} – evaporation heat of the fuel; f – fraction of evaporation heat from the cylinder charge; m_{ev} – evaporating fuel.

Additional model and heat transfer explanation is presented in Annex A.4 (*AVL BOOST* simulation methodology).

2.8.1. Application of Vibe Function

The approximation of engine RoHR characteristics the Vibe function is used (Vibe 1970):

$$\frac{dx}{d\varphi} = \frac{a}{\Delta_{\varphi_c}} \cdot (m_v + 1) \cdot y^{m_v} \cdot e^{-a \cdot y^{(m_v+1)}}; \tag{2.16}$$

$$dx = \frac{dQ}{Q}. \tag{2.17}$$

Here Q – released heat amount from fuel which was used during engine work cycle; φ – crank angle; m_v – combustion intensity shape parameter; a – Vibe constant when 99.9% of fuel is burned, a = 6.905; y – relative combustion duration.

$$y = \frac{\varphi - \varphi_0}{\Delta_{\varphi_c}}. \tag{2.18}$$

Here φ_0 – start of combustion; $\Delta\varphi_c$ – combustion duration.

Integration of Vibe function gives the mass fuel burned MBF which combusted from start of combustion:

$$x = \int \frac{dx}{d\varphi} \cdot d\varphi = 1 - e^{-a \cdot y^{(m_v+1)}}. \tag{2.19}$$

In Fig. 2.8 there is presented the dependence of RoHR on different combustion intensity shape parameter m_v at different CAD.

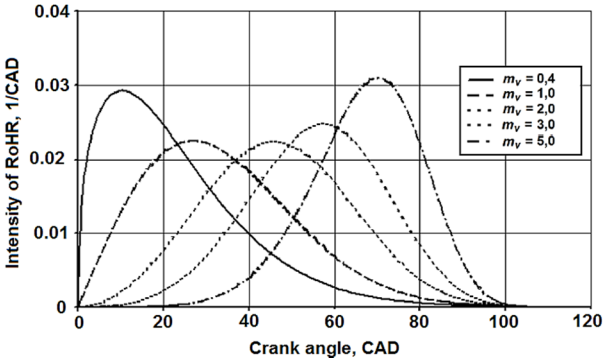

Fig. 2.8. The dependence of rate of heat release on different combustion intensity shape parameter m_v

With lower m_v values the combustion intensity is more concentrated at the beginning of combustion process and with increasing m_v values the combustion process has higher intensity at the middle or end of combustion.

2.8.2. Application of Vibe Two Zone Function

Numerical simulation and analysis process was done with *AVL BOOST* software where Vibe Two Zone function was used. Cylinder is divided into two zones where burned charge and unburned charge is present (*AVL BOOST* Theory 2011):

$$\frac{dm_b u_b}{d\varphi} = -p_c \frac{dV_b}{d\varphi} + \frac{dQ_F}{d\varphi} - \sum \frac{dQ_{W.b}}{d\varphi} + h_u \frac{dm_b}{d\varphi} - h_{BB.b} \frac{dm_{BB.b}}{d\varphi}; \qquad (2.20)$$

$$\frac{dm_u u_u}{d\varphi} = -p_c \frac{dV_u}{d\varphi} - \sum \frac{dQ_{W.u}}{d\varphi} - h_u \frac{dm_b}{d\varphi} - h_{BB.b} \frac{dm_{BB.b}}{d\varphi}. \qquad (2.21)$$

Here index b – burned zone; index u – unburned zone; $h_u \frac{dm_b}{d\varphi}$ – the enthalpy flow from the unburned to the burned zone due to conversion of a fresh charge to combustion products.

The cylinder volume should be equal to sum of the volume changes and the sum of the different zone volumes must be equal to the cylinder volume.

$$\frac{dV_b}{d\varphi} + \frac{dV_u}{d\varphi} = \frac{dV}{d\varphi}; \qquad (2.22)$$

$$V_b + V_u = V. \qquad (2.23)$$

Engine combustion analysis for *P + Bio* and CNG / H_2 fuel mixtures was performed using *AVL BOOST* utility BURN. The measured in-cylinder pressure traces were input into BURN utility and the inverse calculations were done. The software calculated RoHR of each desired fuel mixture which was tested during bench tests. Same calculation algorithms, like for the simulation, were used for RoHR calculation. The calculations are based on first law of thermodynamics and the same heat transfer models were used to calculate.

The calculations were performed when the high pressure rise appears – intake and exhaust valves are closed (time from intake valve closed IVC and exhaust valve open EVO).

The simulation of engine work cycles were performed with created simulation model in *AVL BOOST* software. Fig. 2.9 presents created *AVL BOOST* model for *Nissan HR16DE* 4 cylinder SI engine.

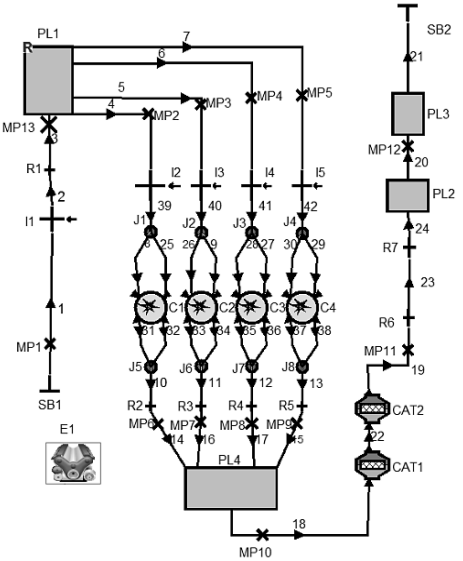

Fig. 2.9. Spark ignition *HR16DE* 4 cylinder engine numerical simulation model in *AVL BOOST* environment: SB – system boundaries; MP – measuring points; J – junctions; I – port fuel injectors, PL – plenum, R – restriction, CAT – catalytic converter, E1 – engine parameters

Such data was set in engine numerical model: engine technical parameters (bore, stroke, con-rod length, compression ratio, valve timing, cylinder head area above piston, piston surface area, engine speed, number of strokes, cylinders work cycle arrange, friction in engine at certain engine speed, intake and exhaust manifold volumes), fuel type (single fuel or fuel mixture composition and their lower

heating value, stoichiometric fuel ratio, fuel hourly or cycle amount), combustion characteristics (start of combustion, combustion duration, shape parameter m_v).

2.9. Reliability and Error Calculations of Experimental Research Data

2.9.1. Verification of Experimental Data Sample Normality

In order to get better understanding about obtained and calculated experimental data reliability it is important to evaluate the data sample normality and calculate standard deviation with error bar values.

Normal distribution N (μ, σ), μ – mean value, σ – standard deviation are applied very widly in statistical researches. However, the application of normal distribution is more applied when the taken sample, according to which the the m and s evaluation of normal distribution $N(\mu, \sigma)$ mean values μ and standard deviation σ are calculated, is distributed according to normal distribution.

There are more than 20 criterias to verify the normality of sample, starting from χ^2, Kolmogorov-Smirnov, Omega2, etc. The most widely applied and most powerful verification criterias for normality is Shapiro-Wilk criteria (Kobzar 2006).

The normality of sample is possible to verify by checking H_0 hypothesis against interfering H_1 hypothesis. H_0 hypothesis state that random value X is distributed according normal distribution $N(\mu, \sigma)$ of which mean value is μ and standard deviation is σ. H_1 hypothesis state that random value is not distributed according to $N(\mu, \sigma)$. These hypotheses shown as:

$$\begin{aligned} H_0 &: X \sim N(\mu, \sigma); \\ H_1 &: X \sim N(\mu, \sigma). \end{aligned} \tag{2.24}$$

If H_0 is accepted then it is possible to state that the studied data of sample is not contradicting H_0 hypothesis. Otherwise, when H_1 hypothesis is accepted the data of sample contradict H_0 hypothesis.

By applying Shapiro-Wilk criteria, the p value is calculated. If $p < p_{crit}$ then H_0 is rejected and H_1 hypothesis is accepted. If $p \geq p_{crit}$, then there is no reason to reject the H_0 hypothesis. Here $p_{crit} = 0.05$ – critical value.

Shapiro-Wilk criteria calculations were performed using software package *R* and *R Studio*, version 0.99.902.

2.9.2. Results of Experimental Data Sample Normality Calculations

The normality verification was done for *Nissan HR16DE* 4 cylinder engine test data as it had the greatest amount of sampled data. There were verified 96 measured samples of engine torque (M_e), 96 measured samples of engine fuel consumption (B_d) at $\lambda = 1$ conditions. Also verification was done for 129 measured samples of M_e, 129 measured samples of engine B_d at $\lambda = 1.4$ conditions. In overall, there were verified 450 samples. The size of every sample is $n_s = 10$ pcs.

Generally, the majority of M_e samples are distributed according to normal distribution. 11 torque samples were $p < p_{crit} = 0.05$ from 96 M_e samples at $\lambda = 1$ conditions. That means that H_0 hypothesis is rejected, showing that 11 samples are not distributed according to normal distribution. 17 M_e samples has $p < p_{crit} = 0.05$ from whole 129 samples at $\lambda = 1.4$ tested conditions. H_0 hypothesis is rejected for 17 samples.

However, more than half (55) of 96 B_d samples taken from $\lambda = 1$ conditions are not distributed according to normal distribution and almost all (115) B_d samples from 129 samples at $\lambda = 1.4$ conditions are not distributed according to normal distribution.

Therefore, the normal distribution can be just applied for M_e samples and statistics of mean values, standard deviation and for calculations of error margins of mean values. However, the normal distribution cannot be applied for B_d samples. At this case the confident interval of mean $\mu \in [m - s\beta, m + s\beta]$ cannot be related with accurate possibility, when β is a certain quintile for Student or Standard Normal Distribution (when the sample size is enough big).

2.9.3. Error Bar Calculation and Application for the Measured Values

According to statistical hypothesis evaluation it was obtained that normal distribution $N(\mu, \sigma)$ can be applied for M_e values. The example of normal distribution for M_e is presented in Fig. 2.10.

In this case the error bar is calculated by applying the Student distribution:

$$m - t_{p,d} \cdot \frac{s}{\sqrt{n}} \le \mu \le m + t_{p,d} \cdot \frac{s}{\sqrt{n}} . \tag{2.25}$$

Here n – sample size, $n = 10$; s – evaluation of standard deviation $S = \sqrt{\frac{1}{n-1}\sum_{i=1}^{n}(x_i - \mu)^2}$; m – evaluation of mean value ($m = \frac{\sum_i x_i}{n}$); $t_{p,d}$ –

Student distribution (with degree of freedom $d = n - 1$, d = 9 and quantile $p = 1 - \frac{\alpha_s}{2}$; α_s – significance level, α_s = 0.05).

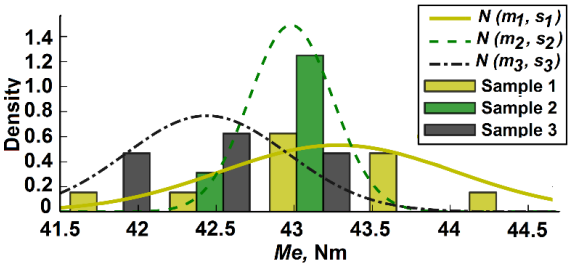

Fig. 2.10. Normal distribution of measured M_e values

The standard error of the mean value is calculated:

$$SE = \frac{s}{\sqrt{n}}. \tag{2.26}$$

Calculated values are presented as error bars in M_e, B_d, BSFC, η_e diagrams.

2.9.4. Errors of Calculated Parameters

The calculation methodology for engine P_e, BSFC and η_e of indirect measurement uncertainties calculated according to standard (JCGM 100: 2008) uncertainty calculation manual. These indirectly measured values calculated according to these formulas:

- Engine power P_e, kW

$$P_e = \frac{M_e \cdot n}{9549}. \tag{2.27}$$

- Brake specific fuel consumption BSFC, g/kWh

$$BSFC = \frac{B_d \cdot 9549}{M_e \cdot n}. \tag{2.28}$$

- Engine thermal efficiency η_e

$$\eta_e = \frac{3600 \cdot M_e \cdot n}{9549 \cdot B_d \cdot LHV}. \tag{2.29}$$

Here M_e – measured engine torque, Nm, M_e accuracy ±0,9 Nm, n_e – measured engine revolutions, rpm; B_d – measured engine fuel consumption, g/h, B_d accuracy ±0.10%; *LHV* – fuel lower hating value, *MJ/kg*.

It was accepted that engine *n* and LHV are accurate values and they are not influencing much the indirectly measured values. Engine M_e and B_d measured values can be measured inaccurately, therefore the uncertainty of these values have to be evaluated. It is admitted that M_e and B_d are not correlated values. The standard uncertainties of indirect measured value $u_c(f)$ are calculated according standard (JCGM 100: 2008) methodology:

$$u_c(f) = \sqrt{u_c^2(f)}. \tag{2.30}$$

Here $u_c^2(f)$ – dispersion of whole uncertainty.

$$u_c^2(f) = \sum_{i=1}^{N} \left(\frac{\partial f}{\partial x_i} \right)^2 u^2(x_i). \tag{2.31}$$

Here $f \in \{P_e, \text{BSFC}, \eta_e\}$ – indirect measured value function (e.g. engine P_e, *BSFC*, η_e); $u(x_i)$ – directly measured value standard uncertainties.

It is common to treat measured values as random values and their uncertainties are matching to standard deviations. $u(x_i)$ uncertainties or standard deviations depend on what is random value. If some certain measured value is distributed according to rectangular distribution then the standard deviation of this value is calculated (JCGM 100: 2008):

$$u(x_i) = \frac{a_d}{\sqrt{3}}. \tag{2.32}$$

Here a_d – rectangular distribution parameter.

If some certain measured value is distributed according to normal distribution then the standard deviation empirical estimation is calculated according to such standard procedure:

$$u(x_i) = s = \sqrt{\frac{1}{n_i - 1} \sum_{i=1}^{n_i} \left(m_i - x_{i,j} \right)^2}. \tag{2.33}$$

Here m_i – *i* sample empirical mean value,

$$m_i = \frac{1}{n_i} \sum_{i=1}^{n_i} x_{i,j}. \tag{2.34}$$

Here n_i – sample size , $x_{i,j}$ – random value *j* realization.

However, (2.33) is spot value, therefore for $u(x_i)$ uncertainty evaluation it is purposeful to take higher boundary of standard deviations confident interval:

$$u_{upp}\left(x_i\right)=\sqrt{\frac{\left(n_i-1\right)s^2}{x^2_{1-p,(n_i-1)}}}\,. \tag{2.45}$$

Here s – given in (2.33) formula, $p = 1 - \alpha_s/2$ quintile of $\chi^2_{1-p,(n-1)} - \chi^2$ distribution with $n - 1$ degree of freedom, $\alpha_s = 0{,}05$ – degree of confident.

Table 2.11. Error values of measured and calculated parameters

Parameter	Tested engines		
	Nissan HR16DE	*AVL* Single Cylinder	*F2BE0642H*
n, rpm	2000	1000	1500
M_e, Nm	42	–	–
M_e accuracy, %	2.15	–	–
ΔM_e, Nm	±0.9	–	–
P_e, kW	9.1	–	115
P_e accuracy, %	5.44	–	±1
ΔP_e, kW	±0.49	–	±1.15
P_i, kW	–	3.92	–
P_i accuracy, %	–	0.536	–
ΔP_i, kW	–	±0.0211	–
B_d, g/h	2016	496.8	24630
B_d accuracy, %	±0.10	±0.35	±0.10
ΔB_d, g/h	±1.52	±0.138	±24.63
BSFC, g/kWh	221.538	–	214.17
BSFC accuracy, %	5.794	–	1
ΔBSFC, g/kWh	±12.84	–	±2.14
ISFC, g/kWh	–	282.4	–
ISFC accuracy, %	–	2.207	–
ΔISFC, g/kWh	–	±6.23	–
η_e	0.2942	–	0.355
η_e accuracy, %	6.01	–	1.001
$\Delta\eta_e$	±0.0167	–	±0.0036
η_i	–	0.411	–
η_i accuracy, %	–	1.963	–
$\Delta\eta_i$	–	±0.0081	–

As it was mentioned before, majority of M_e samples were distributed according to normal distribution, while majority of B_d samples are not distributed according to normal distribution. Therefore, for uncertainty calculations $u_c(f)$ it is accepted that M_e uncertainty $u_{Me}(x_i)$ is calculated according to formula (2.35) and fuel consumption $u_{Bd}(x_i)$ uncertainty is calculated according to rectangular distribution (2.32). Further calculation explanations with particular example presented in Annex A.5 (Methodology for errors of calculated parameters).

The error values of measured and calculated parameters of other experimental tests were calculated and presented in Table 2.11. The calculations of error values for efficiency parameters η_e and η_i varied from 1% to 6% showing that such accuracy is acceptable for the analysis. The measurement of M_e, B_d of 4-cylinder engine *HR16DE*, measurement of P_i and B_d of single cylinder engine has a high accuracy, showing that the measured data is reliable and suitable for analysis.

2.10. Conclusions of the 2nd Chapter

Research methodology presentation and review lead to these chapter conclusions:

1. Evaluated different fuels features and applied theoretical and experimental assessment methods will give a better understanding about different fuels influence on engine combustion process, its influence on efficiency changes and exhaust gas emission formation.
2. Designed and mounted duel fuel injection system for biogas fuel as additive to petrol fuel. The equipment was also used for testing CNG / H_2 fuels. The control of injection system was able to control injection duration, injection timing, therefore it was possible to achieve a stoichiometric and lean burn combustion. Adopted experimental basis is valuable for the future fuel mixture tests.
3. Created and developed comprehensive SI numerical simulation and analysis numerical model in *AVL BOOST* software according to laboratory test engine is valuable tool for the combustion process analysis and prediction of engine efficient and ecological parameters, when different fuel types are applied.
4. Optical engine experimental basis and test methodology is beneficial for the full-scale investigation of gas DI system influence on the combustion behavior and combustion product formation.

3

Numerical and Experimental Research of Gaseous Fuel Mixtures Use in Spark Ignition Engine

Theoretical calculations, experimental investigation and numerical simulation results are presented in the third chapter. Investigated different gaseous fuel mixtures and their influence on the engine parameters, combustion process. In addition, results of low pressure gas DI system research is presented. Research results were published in following scientific publications – Sendžikienė *et al*. 2015, Rimkus, Melaika *et al*. 2016, Pukalskas *et al*. 2014, Melaika *et al*. 2016, Melaika *et al*. 2013. Pukalskas *et al. 2013*.

3.1. Biogas Fuel Use in a Dual Fuel System

Petrol (*P*) and petrol with additional feeds of biogas (*Bio*), which had a composition of 65% CH_4 / 35% CO_2, were tested during primary experiments with 4 cylinder SI *HR16DE* engine: petrol and 20 *l*/min. (*P* + *Bio* 20), 25 *l*/min. (*P* + *Bio* 25) and 30 *l*/min. (*P* + *Bio* 30) of biogas additive were tested.

Dependencies of engine M_e, η_e and BSFC on the added biogas feed and advance ignition angle are presented in Fig. 3.1. If the engine was fuelled with *P*, the maximum torque (M_e = 65.43 Nm) was achieved when the advance ignition

angle was 22 CAD bTDC (Fig. 3.1). If the biogas was added to the air inlet, M_{e_max} decreased. At 20 *l*/min. of *Bio* addition, the engine MBT 64.10 Nm (–2.03% lower comparing with *P* fuel) was achieved when the advance ignition angle was 24 CAD bTDC. With 25 *l*/min. biogas addition, the maximum torque M_e = 63.38 Nm (–3.13%) obtained when Θ = 26 CAD bTDC. The M_e = 62.90 Nm (–3.86%) was obtained when Θ = 26 CAD bTDC with 30 *l*/min.

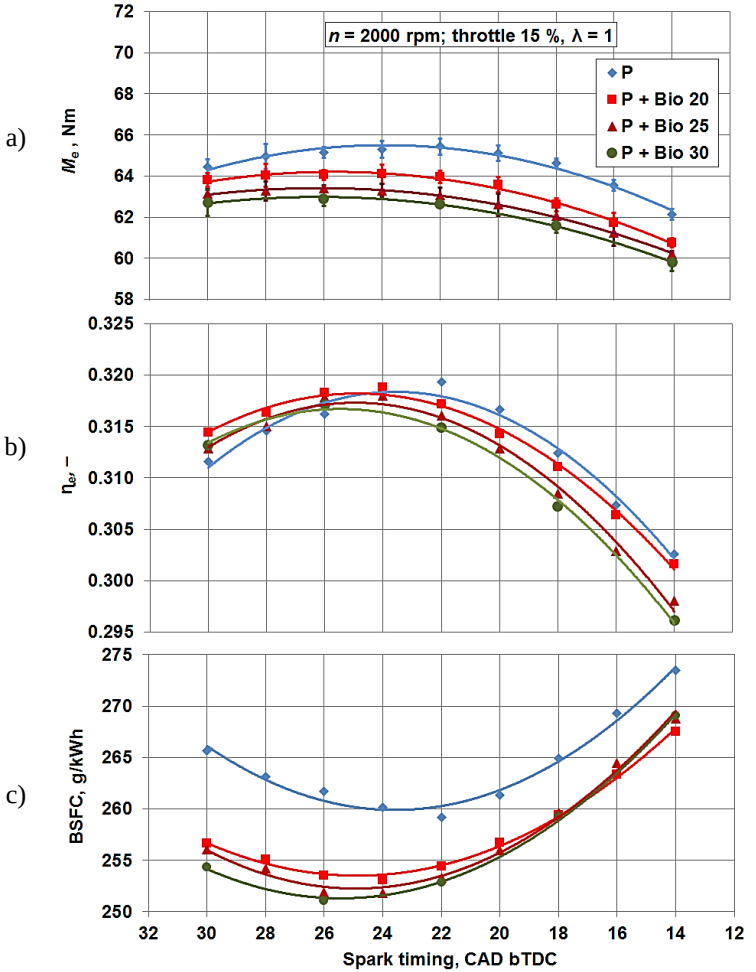

Fig. 3.1. Dependence of engine efficient indicators on different biogas feeds and spark timings: a) engine torque, b) efficiency, c) brake specific fuel consumption. Tested fuel *P* + *Bio*, engine speed 2000 rpm, throttle 15%, λ = 1

As the added biogas increased, the maximum engine torque M_e decreased, because the added gas feed consumed some volume of the cylinder and overall fuel LHV was lower which reduced E_c amount.

As a result, the cylinder volumetric efficiency worsens, and the amount of cyclic energy E_c contributed by the fuel decreases. 1% of biogas in the intake air volume reduced the engine capacity by 0.7–0.9% in the mode used in this study. Few studies' results show that increased content of CO_2 in gaseous fuels lowers the flame propagation speed at the flame front and decreases flame radius (Byun *et al*. 2015). In order to feed additional biogas and achieve maximum torque, the spark timing must be advanced by 2– 4CAD because the CH_4 and the CO_2 in the gas mixtures reduced the combustion intensity and increased the combustion duration.

When biogas was added to the feed, the maximum engine η_e slightly changes, and varies with CAD. If the highest amount of 30 *l*/min. of biogas is added, η_e = 0.317 at 26 CAD bTDC. If the highest amount of biogas was added, the energy efficiency η_e decreased up to ~ 1.25% with a steady advance ignition angle of 22 CAD bTDC, which is optimum for the engine fuelled with *P* fuel. Because of the high CO_2 content, biogas reduced the combustion speed of the combustible mixture. Therefore, to achieve a higher energy efficiency of the engine it is necessary to adjust the ignition angle which should be advanced.

If the engine was fuelled with *P*, η_e = 0.319 was achieved at 22 CAD bTDC. In order to be sure that obtained η_e results are correct, tests with *P* fuel were done at different engine loads and calculated η_e values were compared with other scientists' results (Yao *et al.* 2014) who made experimental investigation with the same SI *HR16DE* 4 cylinder engine. From Fig. 3.1 it is clear that with *P* fuel the maximum η_e = 0.319, which was reached at engine load 5.1 bar (calculated from M_e = 65.43 Nm, Fig. 3.1). Comparing with Yao *et al.* (2014) results, the differences between η_e values obtained in VGTU laboratory and other scientist tests are minor (Fig. 3.2). Therefore, it is possible to state that experimental data is correct and proper for further analysis.

Fig. 3.1 also shows how different biogas amount and advanced ignition angle has an influence on BSFC of petrol and biogas fuel mixture.

The electronic control system of the engine is adjusted to maintain a stoichiometric mixture (λ = 1); therefore, by increasing the added biogas (20 *l*/min., 25 *l*/min. and 30 *l*/min.), the intake air mass decreased and the total hourly *P* + *Bio* fuel mixture consumption decreased. Fuel mixture consumption also decreased because of the higher methane calorific value. The *P* fuel hourly consumption B_{d_P} also decreased. B_{d_P} and $BSFC_P$ consumptions are presented in Annexes in Fig. B.1. Similarly, biogas efficiently reduced the $BSFC_P$ by ~ 19%, ~ 25% and ~ 29%, respectively to mentioned fuel additions (Fig. B.1 in Annexes).

After assessment of the engine effective energy and consumed fuel mass, it was found that added biogas reduces the BSFC petrol / biogas fuel mixture consumption, when the ignition angle Θ is advanced. If the engine is fuelled with *P*, at 22 CAD, the minimum BSFC (259.2 g/kWh) is achieved (Fig. 3.1). In the cases of added biogas at 20 *l*/min., 25 *l*/min. and 30 *l*/min., with spark timing at 24 CAD, 24 CAD and 26 CAD, BSFC decreases by ~ 2.4%, ~ 2.85% and ~ 3.16%, respectively.

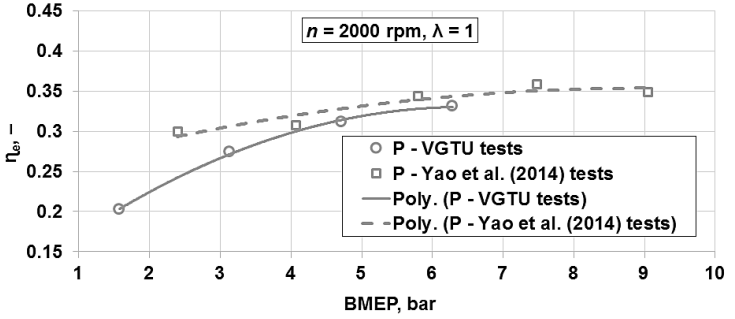

Fig. 3.2. Comparison of engine *HR16DE* obtained η_e values from two result sources: VGTU laboratory and Yao *et al.* (2014). Tested petrol fuel, engine speed 2000 rpm, λ = 1

Both the quantity of added biogas and the advance ignition angle Θ influenced the concentration of the engine exhaust gas. Fig. 3.3 presents biogas impact on hazardous (CO, CO_2, HC, NO_x) content in exhaust gas when spark timing was changed.

The CO content in the exhaust gases with spark timing 22–26 CAD bTDC, when the engine was fuelled with *P* fuel, was the lowest at 0.48% level. The CO content increased up to 0.63% (~ 31%), 0.76% (~ 58%) and 0.89% (~ 85%), respectively to added biogas feed of 20 *l*/min., 25 *l*/min. and 30 *l*/min. The quantity of an incomplete combustion product – CO increased in the exhaust gas because the added biogas worsened the combustion process in the engine cylinder. Whether accelerating or delaying combustion, the process worsened and the CO content increased as a result in the exhaust gas.

The CO_2 content was 14.7% when the engine was fuelled with *P* fuel at the same testing conditions. As the amount of added biogas increased (20 *l*/min., 25 *l*/min. and 30 *l*/min.), the CO_2 content increased also up to 14.78% (~ 0.5% higher), 14.77% (~ 0.5% higher) and up to 14.74% (~ 0.3% higher) in the exhaust gas, respectively to mentioned biogas additions. The increase of CO_2 is not high

because the CO_2 (30% according to molar mass) contained in biogas is compensated by elemental carbon particles (75%) contained in the methane (CH_4), comparing with *P* fuel (86%).

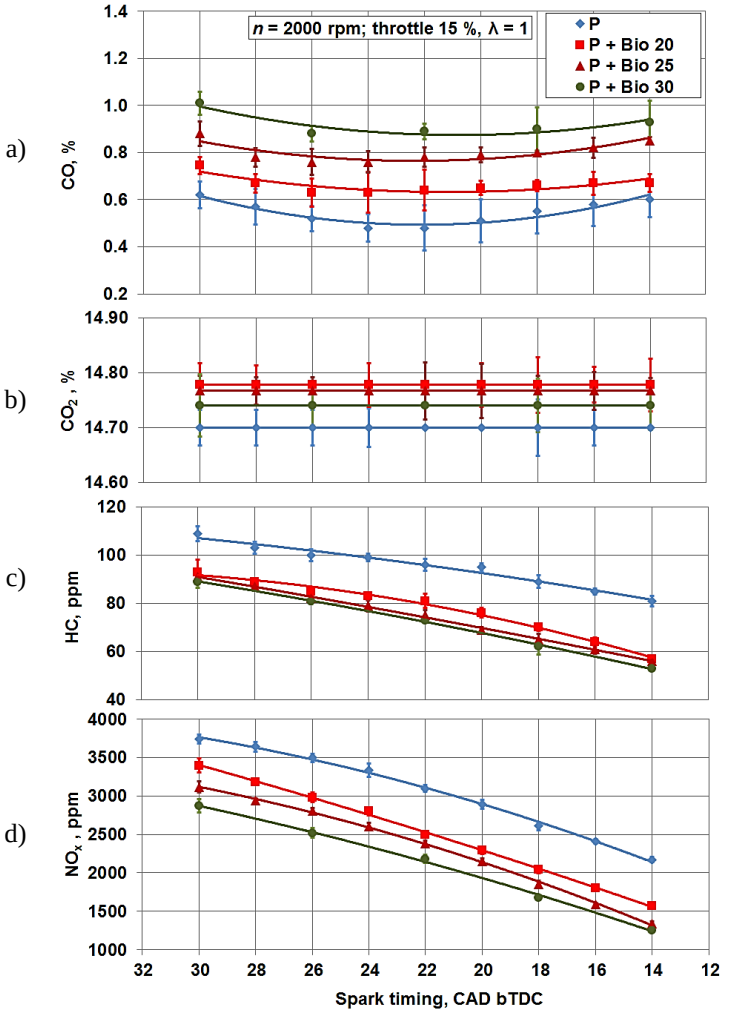

Fig. 3.3. Biogas impact on exhaust gas emissions when biogas feed and spark timing are being changed: a) CO emission, b) CO_2 emission, c) HC emission, d) NO_x emission. Tested fuel – petrol + biogas, engine speed 2000 rpm, throttle 15%, λ = 1

The unburnt HC content, under the optimum advance ignition angle – 22 CAD bTDC, if the engine was fuelled with *P* fuel, is 96 ppm (Fig. 3.3). As the

biogas content increased (20 *l*/min., 25 *l*/min. and 30 *l*/min.), the HC content decreased up to 81 ppm (–16%), 75 ppm (–22%) and 73 ppm (–24%), respectively. This can be explained by the simple molecular methane structure and better evaporation, compared with *P* fuel, which ensures a better combustion reaction.

If the engine was fuelled with *P* fuel, the NO_x content was 3098 ppm under the optimum spark timing (22 CAD bTDC) (Fig. 3.3). As the biogas content increased, the NO_x content decreased up to 2498 ppm (–19%), 2378 ppm (–23%) and 2181 ppm (–30%) according to biogas fuel feed. The decrease in NO_x content can be explained by the change of fuel content, which resulted in lower energy brought amount and lower methane combustion temperature. As the biogas has self-ignition temperature higher, lower NO_x emission also can be explained by small compression ratio (10.7:1) of a tested engine. Such technical parameter leads to a lower combustion temperature which results in engine power and thermal efficiency drop. Numerous research result data shows that engine efficiency values increases steadily with compression ratio up to value of 13:1 (Chandra *et al.* 2011; Yamasaki *et al.* 2013).

The maximum thermal efficiency η_e, with the added biogas feeds (20 *l*/min., 25 *l*/min. and 30 *l*/min.), was achieved when the advance ignition angle was 26 CAD bTDC. If the engine operated in this mode, the HC and the NO_x contents did not exceed the indices achieved using *P* under the optimum 22 CAD bTDC. The HC levels with 26 CAD bTDC were 85 ppm (–11%), 82 ppm (–15%) and 81 ppm (–17%) according to increased biogas feed inputs. The NO_x levels were 2984 ppm (–4%), 2810 ppm (–9%) and 2520 ppm (–18%) at the same tested fuel conditions.

3.2. Analysis and Simulation of Engine Work With Petrol / Biogas Fuel Mixtures Using *AVL BOOST* Software

In order to have a better overview of a combustion process, when *P* and biogas fuels were used, the *AVL BOOST* numerical simulation tool was applied which let to obtain such combustion data like RoHR, MBF, and temperature in cylinder ($T_{cyl.}$) during the combustion.

Pressure in cylinder respect to engine crank angle degree was traced by integrated pressure sensor in the spark plug. Experimental data show that at 15% open throttle and spark timing 22 CAD bTDC, while the engine was running on *P* only, the maximum 33.1 bar pressure was reached at 14.0 CAD aTDC in the cylinder (Fig. 3.4).

The pressure in cylinder decreased up to 32.2 bar (–2.8%) at 14.7 CAD aTDC, 31.1 bar (–6.0%) at 15.4 CAD aTDC and 29.4 bar (–11.1%) at 16.3 CAD aTDC while supplying additional biogas feeds (20 *l*/min., 25 *l*/min. and 30 *l*/min.), respectively. This result was obtained due to less E_c, which was brought by the fuel mixture to the cylinder, and slower combustion process, which also resulted in reduced η_e and M_e.

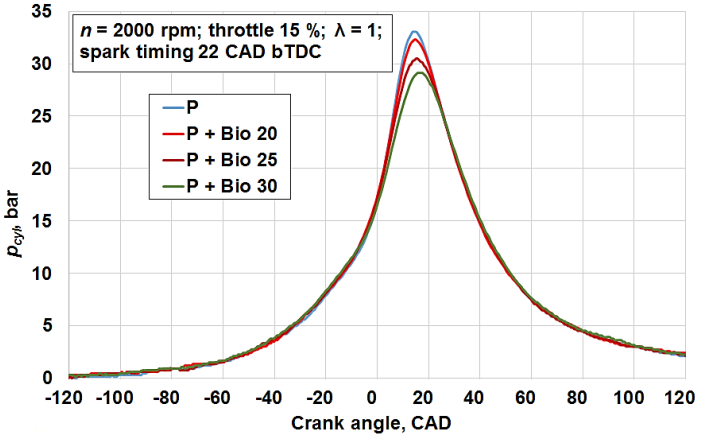

Fig. 3.4. Dependence of pressure in the cylinder on different fuel mixtures. Tested fuel – petrol + biogas, engine speed 2000 rpm, throttle 15%, λ = 1

Table 3.1. Combustion process parameters of different petrol and biogas fuel mixtures

Tested fuels	Indicator		
	Start of combustion φ_0, CAD bTDC	Comb. duration φ_z, CAD	Shape parameter (combustion intensity parameter) m_v
P	–18.2	37.3	2.65
P + *Bio* 20	–18.2	43.6	2.44
P + *Bio* 25	–18.1	46.8	2.31
P + *Bio* 30	–18.1	52.2	2.10

The start of combustion (φ_0), the duration of combustion (φ_z) in the cylinder and the combustion intensity coefficient (m_v) were determined, when the engine was running on *P* and on additionally supplied biogas amounts. Mentioned values are presented in Table 3.1.

The combustion parameters were obtained using the *AVL BOOST* utility BURN, using author research data such as the measured cylinder pressure, fuel

consumption and air consumption. The combustion start did not change and remained φ_0 = 18.1°–18.2° bTDC, whether the engine ran on *P* or on a *P* + *Bio* fuel mixture, at advanced ignition angle 22 CAD bTDC. However, the *P* and biogas fuel mixture combustion duration was longer by ~ 17%, ~ 26% and ~ 40% comparing with single tested *P* fuel. The spark timing was too late with the cases when different amounts of biogas were used. This occurred due to the decreased flame speed, which made the combustion process slower. Similar results can be found in other scientific research (Shrestha *et al*. 2001; Karim *et al.* 2011, where methane with different diluents were used in SI engine. Combustion duration became longer with increasing CO_2 amount in the fuel composition.

The combustion intensity coefficient m_v values for the cases with added biogas were less than for the *P* fuel (m_v = 2.65) by ~ 8%, ~ 13% and ~ 20%, according to different tested biogas feeds. Though, usually the lower m_v number means the increased combustion intensity at the earlier part of the combustion, but at these investigated particular cases, the combustion durations were longer with biogas additions, therefore the combustion intensity distributed over longer combustion durations.

The MBF, the RoHR and the temperature ($T_{Cyl.}$) in the cylinder were determined using *AVL BOOST* software with the Vibe two-zone combustion model. The combustion process parameters were obtained using the BURN utility when the engine ran on petrol and on additionally supplied biogases. Obtained data using numerical simulation software is presented in Fig. 3.5.

The highest RoHR (38.39 J/CAD) was reached at 2 CAD aTDC, when the engine was running on *P* fuel. At these conditions, the MBF was 0.767. The addition of biogases (20 *l*/min., 25 *l*/min. and 30 *l*/min.) caused the MBF at 2 CAD aTDC to decrease up to 0.656 (–14%), 0.612 (–20%) and 0.575 (–25%), respectively, because of slower combustion process of the combustible mixture. The RoHR decreased up to 30.26 J/CAD (–21%), 26.62 J/CAD (–31%) and 22.87 J/CAD (–40%). Significant decrease of RoHR indicates that the flame speed was lower because of decreased total petrol and biogas cyclic energy. What is more, CO_2 has higher heat capacity, which influenced in-cylinder temperature, and therefore RoHR reduced. The maximum RoHR of 31.57 J/CAD (–17%) was reached at 4 CAD aTDC and MBF = 0.742 when 20 *l*/min. biogas was added. Supplying 25 *l*/min. of biogas, the maximum RoHR of 28.73 J/CAD (–25%) was reached at 5 CAD aTDC and MBF = 0.737. Supplying 30 *l*/min. of biogas, the maximum RoHR of 25.25 J/CAD was reached at 6 CAD aTDC (–34%) and MBF = 0.728. As the amount of added biogas increased, the speed of the flame front propagation decreased, resulting in an increase of the combustion duration and decrease of MBF and RoHR. Similar MBF decrease trend can be found in Porpatham (2008) experimental results when different CO_2 and methane mixtures were supplied to the SI engine.

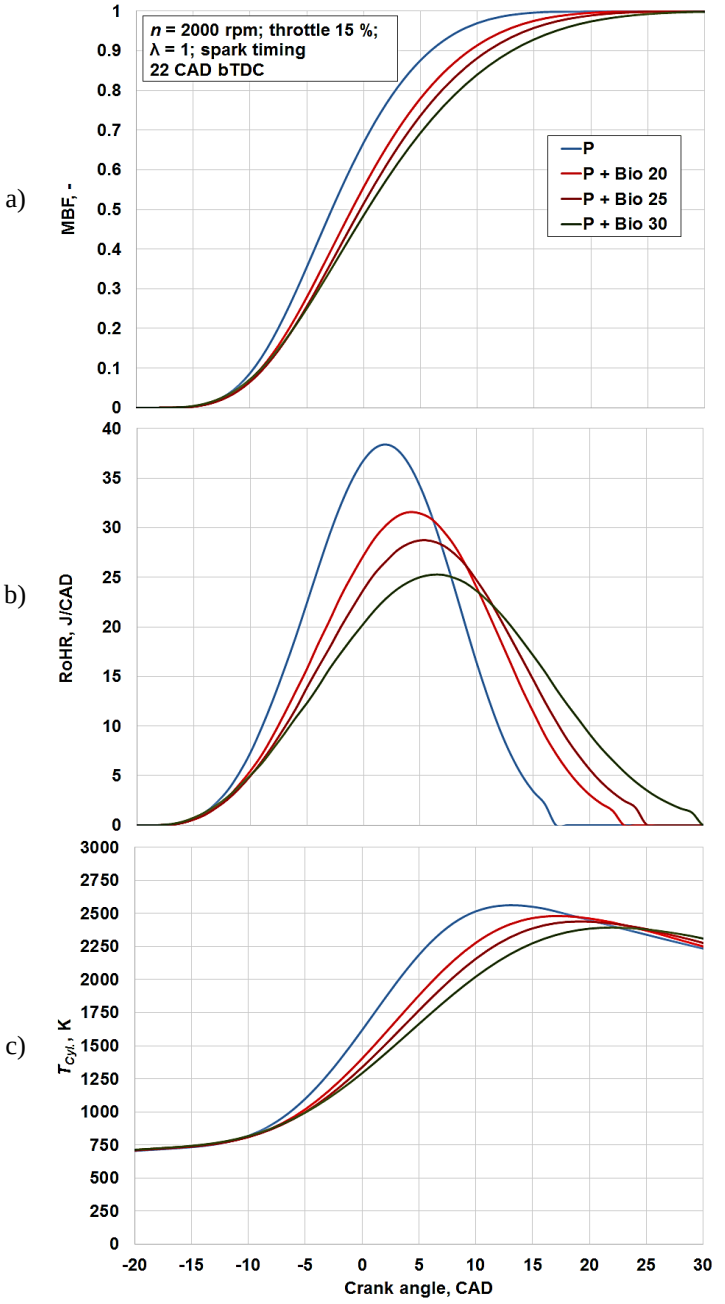

Fig. 3.5. Dependence of combustion parameters on different tested fuels: a) mass burned fraction, b) rate of heat release, c) temperature in the cylinder. Tested fuel – petrol + biogas, engine speed 2000 rpm, throttle 15%, λ = 1

The numerical simulation of the engine performance showed that the maximum temperature ($T_{Cyl.}$) in the cylinder was 2562.8 K at 13 CAD aTDC when petrol was used as the fuel. With the addition of biogas (20 *l*/min., 25 *l*/min. and 30 *l*/min.), the temperature in the cylinder reached 2481.1 K (–3.2%) at 17 CAD aTDC, 2440.2 K (–4.8%) at 19 CAD aTDC and 2394.0 K (–6.5%) at 22 CAD aTDC, respectively.

Added biogas reduced the maximum temperature in the cylinder, which reduced the NO_x concentration in the exhaust gas. Additionally supplied biogas reduced the combustion speed and the temperature, which decreased the engine torque M_e and the efficiency η_e. To achieve better engine energy characteristics, it is necessary to use the optimal (advanced) ignition timing for *P* and biogas combustible mixture.

3.3. Hydrogen Use in a Dual Fuel System

In order to have a better overview of combustion process with fuels having H_2 additive, which has better physical and chemical properties and which can improve combustion in cylinder, the numerical simulation was carried out using same *AVL BOOST* engine model. The model was created according real 4 cylinder SI *Nissan HR16DE* engine, which is set in VGTU, Internal Combustion Engine Laboratory.

The effective power of the engine was determined during bench tests as the engine was running on *P* fuel and under stoichiometric conditions. Obtained P_e = 11.91 kW. Combustion duration φ_c = 47 and combustion intensity parameter m_v = 2.5 was found after performing the analysis of engine duty cycle and following the scientific literature resources (Safari *et al.* 2009; Rakopoulos *et al.* 2010). The engine work cycle was simulated and the effective power of the engine P_e = 12.07 kW was achieved by using the aforementioned indicators and upon performing the analysis of combustion process. The difference from the measured one was only up to 1.3%, and it showed that the created numerical model is fairly accurate. As the H_2 concentration in the mixture varied and composition of combustible mixture was changed during the numerical simulation, the parameters were selected by taking into account the fact that H_2 increased combustion intensity and accelerated flame front propagation speed, and combustion intensity decreased in case of leaning the mixture (Heywood 1988).

Fig. 3.6 presents effective power dependence on H_2 concentration and A/F ratio. Numerical simulation revealed that engine P_e decreased by 9.5% (from 12.07 kW to 10.92 kW) with a case of stoichiometric mixture and additional 10% H_2 supply, and – P_e decreased 15.5% (from 12.07 kW to 10.2 kW) with a case of 15% H_2 supply.

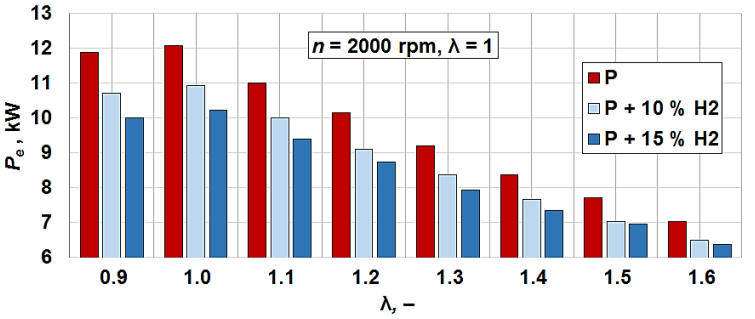

Fig. 3.6. Dependence of effective power on hydrogen concentration and air excess coefficient. Investigated petrol + hydrogen fuel mixtures, engine speed 2000 rpm, λ = 1

The estimated decrease in P_e was higher than the determined decrease in energy brought by fuel, while supplying H_2 gas, since H_2 changes the combustion parameters, and the identified spark timing Θ = 18 CAD bTDC was not optimal. Simulation results also confirmed the decrease of engine indicated thermal efficiency η_i from 0.351 for *P* fuel to 0.327 for *P* + 15% H_2 fuel mixture. More detailed η_i data presented in Annexes in Fig. B.2.

Real engine bench test was done with *P* fuel and the pressure trace was captured. In-cylinder pressure (p_{cyl}) with tested *P* fuel is presented in Fig. 3.7 and in Annexes in Fig. B.3, Fig. B.4.

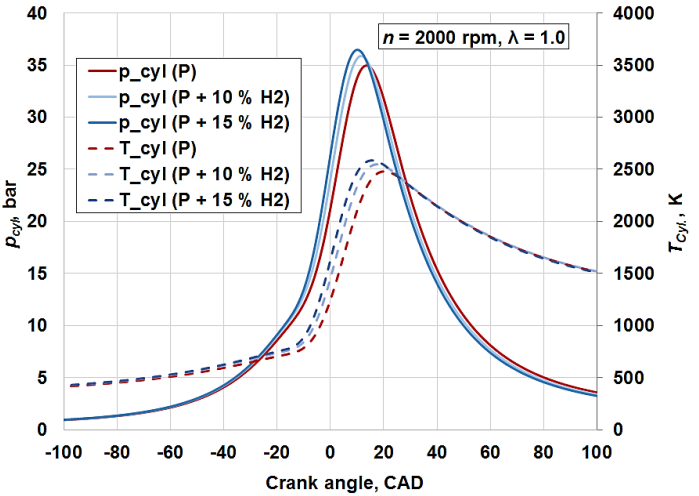

Fig. 3.7. Dependence of in-cylinder pressure (p_{cyl}) and temperature ($T_{cyl.}$) in cylinder on hydrogen concentration and air / fuel ratio. Investigated petrol + hydrogen fuel mixtures, engine speed 2000 rpm, λ = 1

Pressure peak for *P* fuel was p_{max} = 33.9 bar at stoichiometric conditions during the experimental tests, as crankshaft turned at 13.9 CAD aTDC (Annexes Fig. B.3). Using *AVL BOOST* simulation tool the cylinder peak pressure with *P* fuel reached p_{max} = 35.0 bar at 13.6 CAD aTDC. This confirmed the properly set modelling parameters. Further simulation results with H_2 additive at different A/F ratios are presented in Fig. 3.7, which shows the p_{cyl} and T_{cyl}.

As hydrogen concentration increased in the mixture, combustion became more intensive, the maximum pressure and temperature reached closer to the TDC. However, combustion intensity decreased and approached to optimum *P* fuel ignition advance angle with lean mixtures. Thus, it is possible to obtain the optimum η_i for a cycle by additional supply of H_2 and by leaning the combustible mixture without additional adjustment of combustion start. However, the parameters were obtained lower than in case of engine running on *P* fuel, since larger part of thermal energy transferred to environment due to higher combustion temperature of H_2.

Simulation results also revealed that additional supply of H_2 and increase of its quantity, there was an increase of NO_x concentration in exhaust gas. It was mostly affected by a free quantity of O_2 (excess air) during the combustion, combustion intensity, and maximum temperature. Fig. B.5 and Fig. B.6 (Annexes) presents NO_x and HC emission simulation results. HC concentration decreased in exhaust gas, when the fuel mixture was lean and the concentration of additionally supplied H_2 increased. Scientists also note that mixture with H_2 can combust even at high air excess (λ = 9.85), it is characterized by high diffusion (Gupta 2009). Furthermore, it increases combustion and temperature and, thus, improves oxidation of HC.

3.4. Research of CNG / Hydrogen Fuel Mixture Use in a Spark Ignition Internal Combustion Engine

3.4.1. Gaseous Fuel Mixtures Influence on Engine Parameters at Different Engine Loads and Air / Fuel Ratios

Assessment of natural gas and hydrogen fuel mixtures influence on ICE performance indicators was performed on the basis of bench tests and numerical simulation of SI engine *HR16DE*.

Primarily, experimental analysis was performed at constant engine speed (n = 2000 rpm), at different engine loads with different amounts of H_2 in natural gas fuel: 10% H_2, 20% H_2, 30% H_2, 50% H_2, 70% H_2 (Table 3.2). The percentages show the H_2 amount by volume of total CNG and H_2 fuel mixture. 90% H_2 fuel

mixture could not be tested at different engine loads due to too much advanced angle that was kept according to CNG angle. The combustion occurred not stable.

Four different engine loads (20 Nm / 1.56 bar; 40 Nm / 3.14 bar; 60 Nm / 4.72 bar; 80 Nm / 6.28 bar) were tested at stoichiometric conditions ($\lambda = 1$) during 4 cylinder engine experiments. In-cylinder pressure, exhaust gas concentration, A/F ratio, fuel and air mass flow were captured and analysed during the whole experimental study.

The best spark timings were set for *P* and CNG tests according to obtained best engine efficiency at stoichiometric conditions and low engine load (1.56 bar). *P* fuel spark timing was 30 CAD bTDC and spark timing for CNG was 32 CAD bTDC at 1.56 bar load. The difference of 2 CAD shows that CNG fuel probably has longer combustion duration and in order to reach best MBT the ignition timing should be advanced. The spark timing had to be retarded when the load increased, because the injected fuel mass was bigger and the fuel combusted faster. Such spark retard was obvious for both – *P* and CNG cases. The spark timing had to be advanced about few degrees for the CNG fuel in all tested loads at $\lambda = 1$.

In order to find out what was the influence on the engine parameters of CNG / H_2 fuel mixtures, the ignition timing was kept the same like for the CNG case for all tests with H_2 addition.

Table 3.2. Natural gas and hydrogen fuel mixture testing modes presented in dissertation work

Fuel	Engine speed, rpm	λ	Engine load, bar			
			1.56	3.14	4.72	6.28
			Spark timing, CAD bTDC			
P	2000	1.0	30	26	24	22
CNG			32	28	26	24
CNG + 10% H_2						
CNG + 20% H_2						
CNG + 50% H_2						
CNG + 70% H_2						

As it was mentioned in the methodology chapter before, the desirable λ value was achieved and controlled by oxygen sensor measurements in exhaust gas pipe. The engine ECU was controlling fuel injectors' injection duration in order to achieve the set λ value. To have a certain measurements, the air mass flow was measured. Fig B.7 (Annexes) shows the λ value dependence on different tested fuel mixtures at 1.56 bar engine load and 2000 rpm engine speed. The blue line shows desirable λ value (1 and 1.4). The orange line shows the lambda value which was calculated from the air mass and the fuel mass flow measurements. The air mass was measured with air mass flow meter *Bosch HFM 5*. The grey line

shows λ measurement obtained from the exhaust gas analyser. It is clear from presented figure in the Annexes that with changed fuel type, the measured lambda value according to air mass flow meter matched the desirable testing λ value with some minor deviations, which are in a range of air flow meter accuracy (≤3%). The λ measurements from the exhaust gas analyser had a great deviation, especially, when the λ = 1.4 and high H_2 concentrations were tested, because the λ value in the exhaust gas analyser is calculated according to input formula, which depends on fuel type. The deviation from desirable value was even more than 14% with tested 70% H_2 addition, therefore, the λ values from the exhaust gas analyser were not used in experimental test data analysis.

Engine B_d, BSFC and η_e are presented in Fig. 3.8. Hourly fuel consumption measurements showed that the highest fuel consumption was achieved with *P* fuel: 1.699 kg/h at 1.56 bar; 2.5092 kg/h at 3.12 bar; 3.2976 kg/h at 0.472 bar and 4.1148 kg/h at 0.628 bar. The fuel mass flow was lower using CNG fuel. The fuel consumption was 15.82% lower (1.4304 kg/h) at lowest load point, 16.09% lower (2.1054 kg/h) at 3.12 bar load; 15.92% lower (2.7726 kg/h) at 0.472 bar; 16.94% (3.4176 kg/h) at highest 6.28 bar engine load comparing with *P* fuel. Much lower CNG consumption can be influenced by a higher fuel LHV (~ 50.4 MJ/kg), therefore less fuel was needed to inject in order to achieve a desirable load.

It is possible to achieve even lower fuel consumption with H_2 addition. That means that the E_c in fuel is much higher comparing to *P* and CNG fuel. Hydrogen LHV is more than 120 MJ/kg. For this reason, the injected fuel mass reduced. Comparing with CNG fuel, the fuel consumption with 70% of H_2 in CNG gas was 18.67% lower (1.1634 kg/h) at 1.56 bar load; 19.61% lower (1.6926 kg/h) at 3.14 bar load; 19.71 % lower (2.225 kg/h) at 4.72 bar load and 19.41% (2.754 kg/h) lower at highest 6.28 bar engine load.

The BSFC calculations revealed (Fig. 3.8) that highest BSFC was for the *P* fuel. It was possible to achieve from ~ 14% to 16.6% lower BSFC using CNG fuel at different engine load points comparing with *P* fuel. The lowest BSFC was achieved with 70% H_2 addition in CNG gas: 19.7% lower at lowest engine point; 21.63% lower (203.703 g/kWh) at 3.14 bar; 21% lower (178.823 g/kWh) at 4.72 bar point and 20.34% lower (166.107 g/kWh) at highest engine load point.

Engine efficiency calculations show (Fig. 3.8) that with increasing engine load the engine efficiency was increasing. Engine thermal efficiency was lower with higher H_2 amount (e.g. 50%, 70%) in the fuel comparing with *P* and CNG test cases on λ = 1. Such efficiency drop can be caused by inefficiently used combustion process for the engine work, which was probably resulted by to early spark timing for the fuel mixtures with H_2 addition. In addition, it can be probably also explained by increased in-cylinder temperature which increased the wall heat losses due to reduced flame quenching distance in the cylinder.

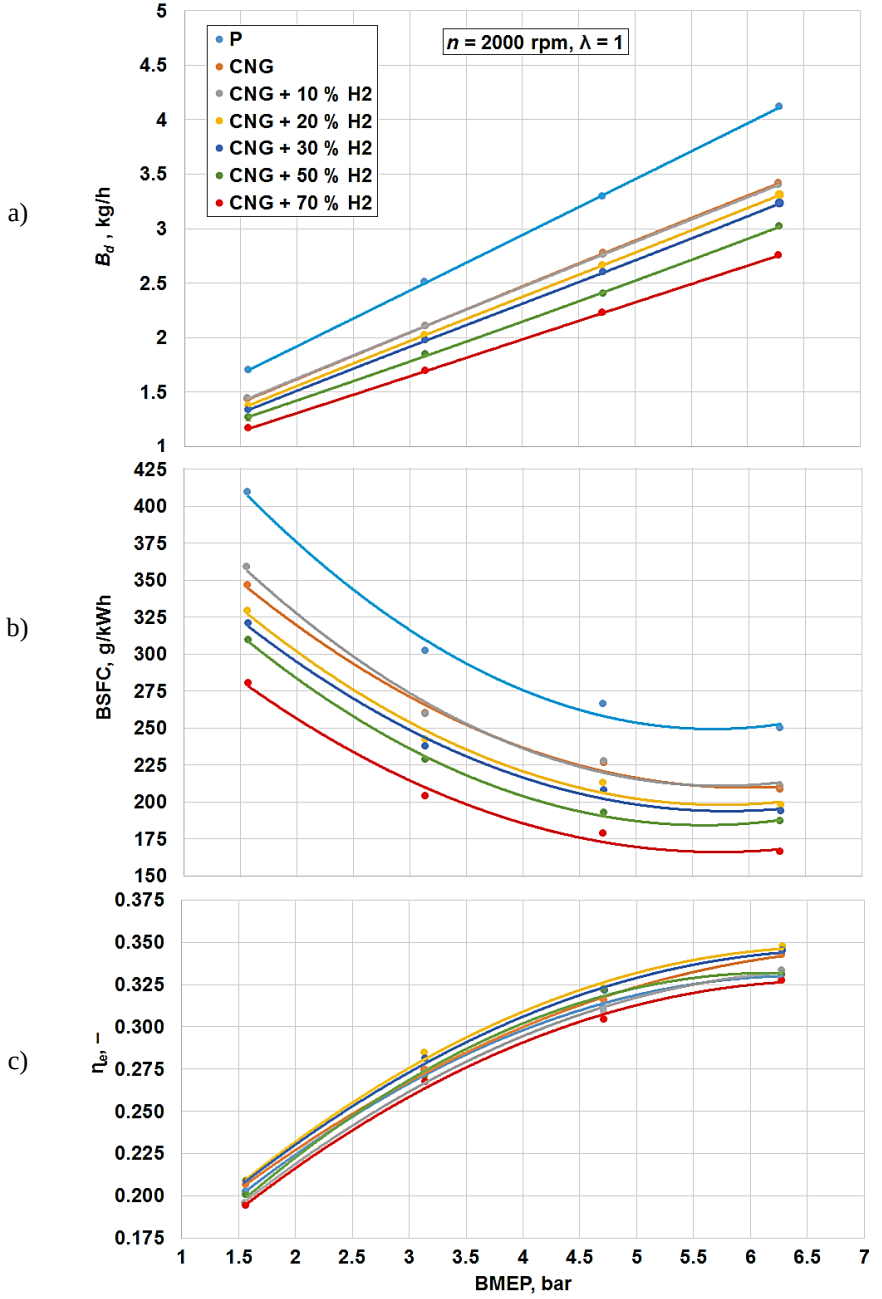

Fig. 3.8. Dependence of engine indicators on different engine loads and fuel mixtures: a) fuel consumption, b) brake specific fuel consumption, c) thermal efficiency. Tested fuels – petrol, natural gas, natural gas / hydrogen fuel mixtures; n = 2000 rpm, λ = 1

Exhaust gas emission analysis is presented in Fig. 3.9 which shows that with low amounts of H_2 in natural gas fuel, the concentration of CO was getting a little bit higher in some certain engine load points. But further increase of H_2 in the fuel mixture let to achieve lower CO concentrations than for *P* and CNG cases.

The emission of CO for CNG fuel was: 0.724%, 0.667%, 0.663%, and 0.534% accordingly to engine loads 1.56 bar, 3.14 bar, 4.72 bar, 6.28 bar. The CO emission was 0.484%, 0.427%, 0.445%, and 0.484% for the biggest H_2 amount (70%) in gaseous fuel. That was 33%, 35%, 34%, 9.4% lower comparing with CNG fuel according to mentioned engine loads.

The decrease of CO can be explained by better a combustion process due to H_2 additive, which increased flame temperature and resulted in a faster combustion. Also the H/C atom ratio was bigger in the fuel mixture when more H_2 was added (Fig. 2.7), less C atom element was present in a gaseous fuel. However, the CO emission was even higher than for CNG or *P* fuel with some H_2 additions, probably due to reduced flame quenching distance and burning oil film in the cylinder. Also it was impossible to reach zero CO emission with highest hydrogen additions because of same oil film issue. Such emission effect was also mentioned by Acikgoz *et al.* (2012).

The CO_2 emission data show (Fig. 3.9) that with CNG fuel it was possible to achieve lower CO_2 level because natural gas has less carbon in the fuel composition comparing with liquid fuels. The addition of H_2 let to achieve even lower emissions. It was possible to achieve 6.8–6.95% of CO_2 with highest H_2 amount at all engine loads at $\lambda = 1$. That was about 35% lower comparing with CNG fuel and about 51% lower comparing with *P* fuel.

Literature overview showed that the tests with H_2 up to 30% in the fuel mixture also let to reduce CO_2 and CO emissions, especially with lean burn combustion (Ceper *et al.* 2009).

HC emission curves show (Fig. 3.9) that the HC concentration was lower with gaseous fuels comparing with liquid *P* fuel. The data distribution of every fuel evenly distributed with predictable tendencies. The concentration of HC emission for *P* fuel was 98.1 ppm, 111.3 ppm, 117.9 ppm, 113.4 ppm according to tested loads (1.56 bar, 3.14 bar, 4.72 bar, 6.28 bar). The HC emission was 69.2 ppm, 71.8 ppm, 72.1 ppm, 68.9 ppm using CNG fuel, which means it was lower in 29.45%, 35.49%, 38.85%, and 39.24% comparing with *P* fuel.

The use of biggest amount of H_2 let to reach 30%, 37.18%, 38.28%, 41.94% reduction of HC comparing with CNG fuel at stoichiometric case. It was resulted by less C atoms in the fuel composition, which was changed by a bigger amount of H_2 element. It can be also explained by the fact that H_2 increased the flame propagation and reduced quenching distance which reduced a chance to have an incomplete combustion process.

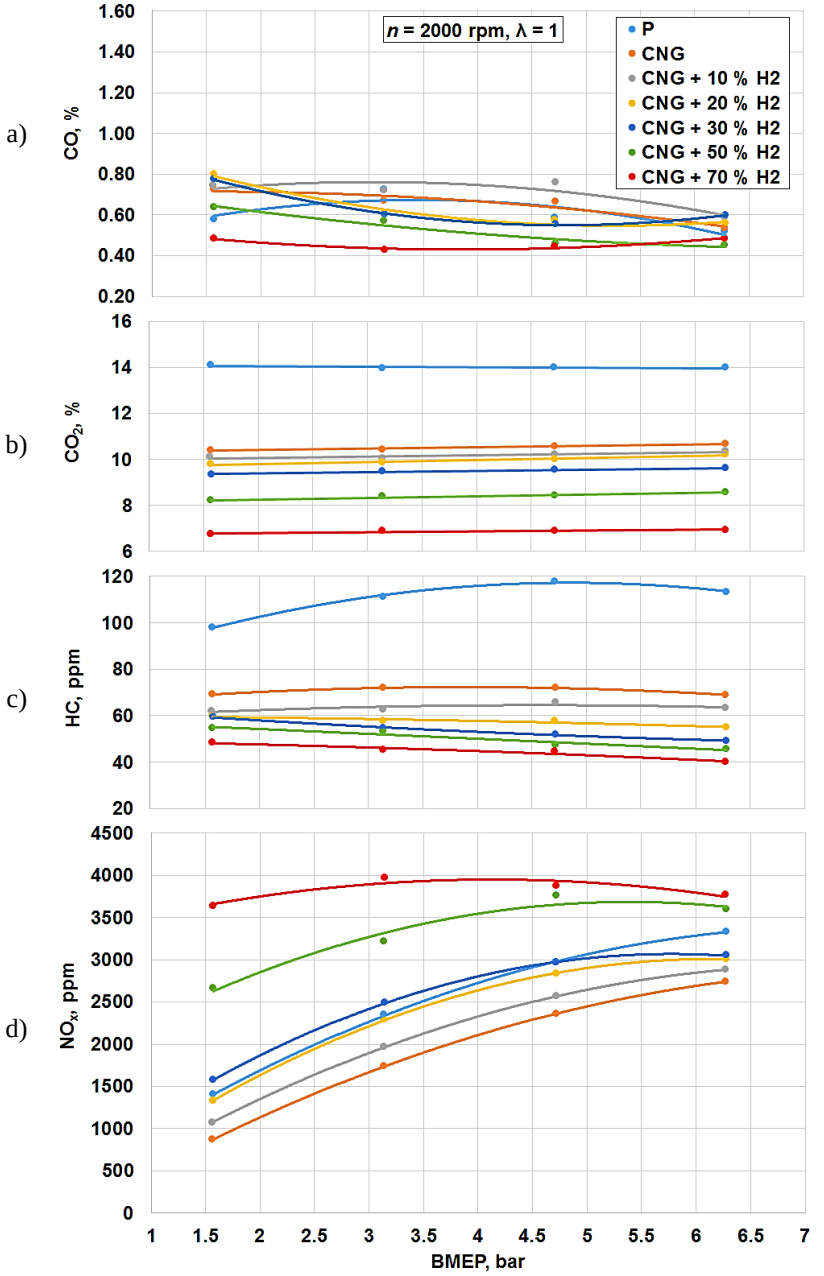

Fig. 3.9. Dependence of exhaust gas emissions on different engine loads and fuel mixtures: a) CO emission, b) CO_2 emission, c) HC emission, d) NO_x emission. Tested fuels – petrol, natural gas, natural gas / hydrogen fuel mixtures; n = 2000 rpm, λ = 1

Scientists also noted that with H_2 amount up to 20% it is not possible to achieve extremely low emissions without exhaust after treatment systems. In order to reduce HC, λ has to be less than 1.3 (Sierens *et al.* 2000).

The NO_x emission data is also presented in Fig. 3.9. The CNG fuel gave lowest NO_x emissions at λ = 1 case. It means that the combustion temperature should be lower which resulted in less NO_x formation. Increasing amount of H_2 gave negative effect for NO_x emissions. The flame temperature, which increased due to hydrogen addition, had a strong impact on NO_x formation mechanism. Highest NO_x emission numbers were obtained with 70% of H_2 in natural gas fuel mixture. The emission of NO_x increased from 871 ppm, 1743 ppm, 2356 ppm, 2742 ppm (at engine loads 1.56 bar, 3.14 bar, 4.72 bar, 6.28 bar) for CNG case up to 3638 ppm, 3871 ppm, 3869 ppm, 3767 ppm for 70% H_2 case at the same engine loads.

The increasing NO_x emission level was also observed by (Akansu *et al.* 2007, Moreno *et al.* 2012) due to increased combustion temperature in the cylinder.

Fig. 3.10 presents CO_2 hourly amount and brake specific CO_2 emission depending on different fuels and engine loads.

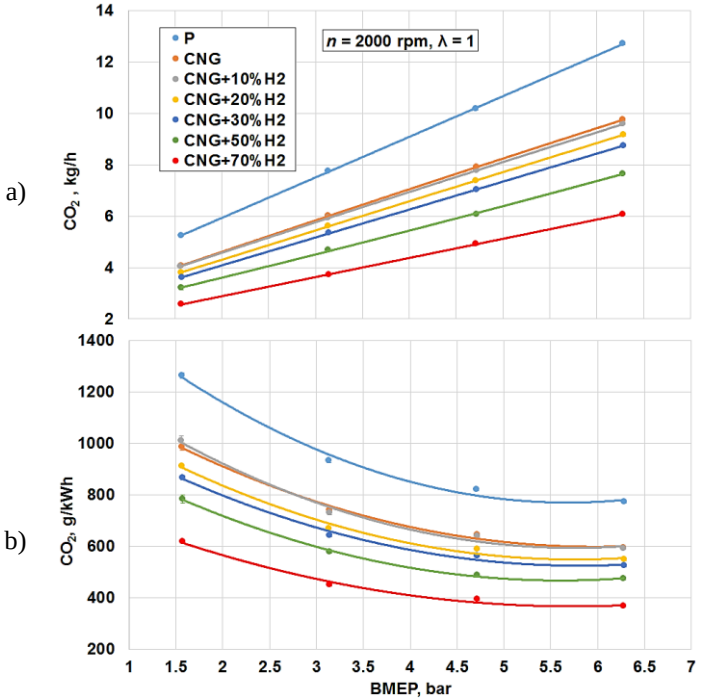

Fig. 3.10. Dependence of CO_2 emission on different engine loads and fuel mixtures: a) hourly emissions, b) brake specific emissions. Tested fuels – petrol, natural gas, natural gas / hydrogen fuel mixtures; n = 2000 rpm, λ = 1

CO_2 hourly emissions correlate with B_d values. Highest emission amount as for *P* fuel. CNG had the highest hourly emissions from all tested gaseous fuels. H_2 addition let to reduce CO_2 emissions. The reduction of CO_2 can be supported by H/C atom ratio calculations, which were presented in methodology chapter (Fig. 2.7). The H/C atom ratio directly depends on element composition by mass, therefore with increasing amount of H_2 in the fuel mixture, the fuel consumption decreased and H/C atom ratio was getting higher. In this case, the obtained CO_2 amount by mass also reduced with increasing H_2 additive in the fuel mixture. The CO_2 reduction was also influenced by reduced hourly fuel consumptions. Brake specific CO_2 emission tendencies also represent same tendencies like for the BSFC data (Fig. 3.8). With increased amount of H_2 up to 70% it is possible to reach lowest brake specific CO_2 emissions 366.242 g/kWh at $\lambda = 1$ while for the *P* fuel case the lowest numbers are 772.391 g/kWh.

The reduction of CO, CO_2 and HC was also observed by (Akansu *et al.* 2007) with increasing H_2 addition in CNG fuel. The decrease of CO_2 was also presented by (Mariani *et al.* 2013) when H_2 and CNG fuel mixtures were tested at different driving cycles and CO_2 emission was measured in g/km.

3.4.2. Gaseous Fuel Mixtures Influence on Engine Parameters when the Ignition Angle and Air / Fuel Ratio is Changed

Advanced ignition angle was changed for each tested fuel and fuel mixture during *HR16DE* engine experiments at different A/F ratio coefficients – $\lambda = 1$ and $\lambda = 1.4$. In-cylinder pressure, exhaust gas temperature, exhaust gas concentration, A/F ratio, fuel and air mass flow were measured and analysed during the whole experimental study. Engine was running at 15% opened throttle on both λ cases, keeping it stable. *P*, CNG and CNG with 10% H_2, 20% H_2, 30% H_2, 50% H_2, 70% H_2, 90% H_2 additions were tested at mentioned experimental conditions.

Fig. 3.11 shows engine torque dependence on different ignition angles, CNG / H_2 fuel mixtures at $\lambda = 1$ and at $\lambda = 1.4$. Highest engine torque was achieved with *P* fuel – 64.9 Nm at spark timing of 24 CAD bTDC. The MBT was ~ 61.85 Nm using CNG gas at ignition angle of 26 CAD bTDC. 2 degrees difference can be explained that natural gas combustion was slower and it combust longer. In order to reach MBT the ignition angle has to be advanced few degrees. However, the addition of 70% H_2 into natural gas let to reach highest ~63.03 Nm torque at 12 CAD bTDC ignition angle. Though it was lower than for the *P* fuel case, it was still the highest achieved M_e value among all tested gaseous fuels. The H_2 addition requires to retard the spark timing in order to achieve the highest M_e.

Engine M_e reduced for every tested fuel case at homogeneous lean burn conditions ($\lambda = 1.4$) comparing with $\lambda = 1$ tests. It was resulted due to less injected fuel and less performed work in cylinder.

a)

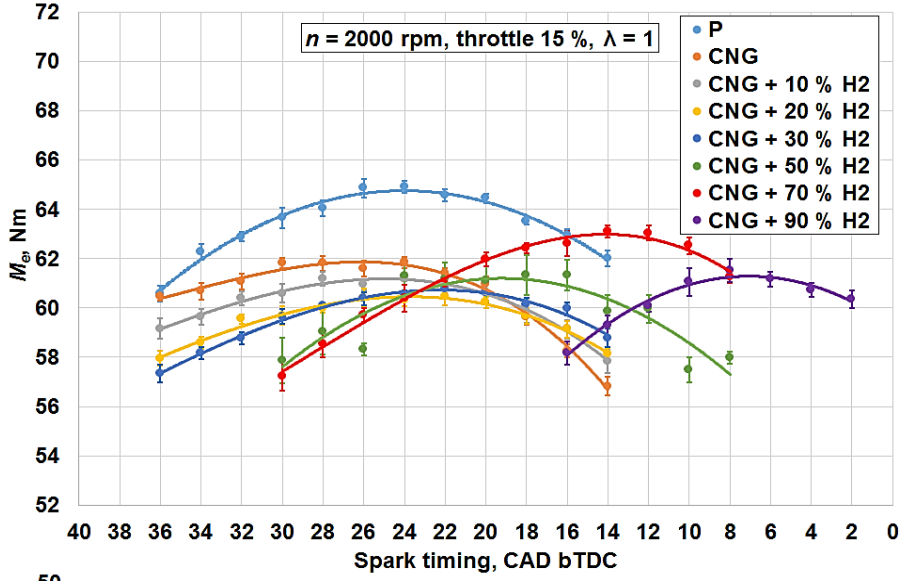

b)

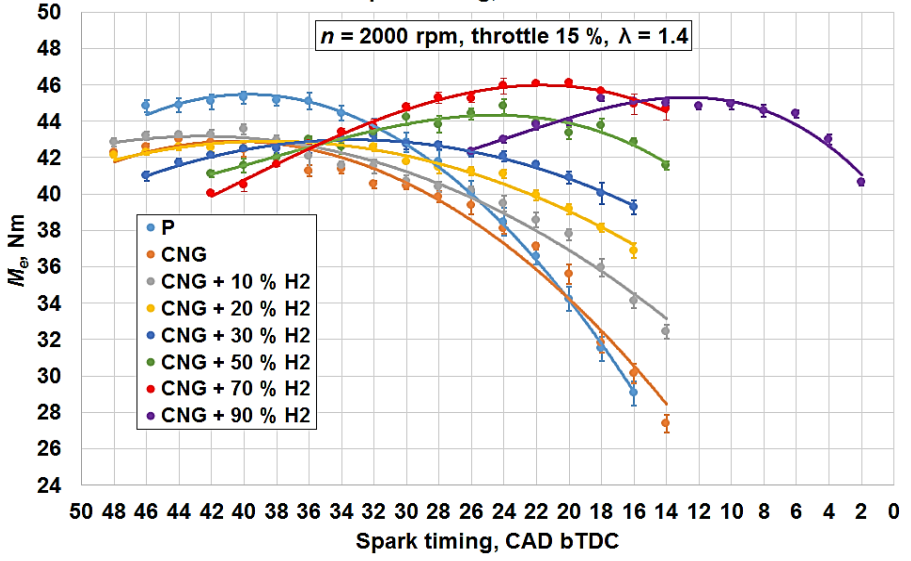

Fig. 3.11. Engine torque dependence on different ignition angles, fuel mixtures and air / fuel ratios. Tested fuels – petrol, natural gas, natural gas / hydrogen fuel mixtures; n = 2000 rpm, a) λ = 1 and b) λ = 1.4

Engine M_e = 45.28 Nm using P fuel at spark timing of 38 CAD bTDC. CNG fuel achieved 43 Nm at ignition angle of 38 CAD bTDC. However, the highest engine M_e was achieved with 70% H_2 fuel mixture – 46.12 Nm at 20 CAD bTDC.

In overall, the increase of H_2 additive in natural gas demands to retard spark timing due to faster H_2 and natural gas fuel mixture combustion.

Fig. 3.12 shows the dependence of achieved maximum engine M_{e_max} values on different tested CNG and H_2 fuel mixtures with different tested A/F ratio conditions. Interesting phenomena observed with different amount of H_2 in natural gas. H_2 concentrations 10% and 20% showed the engine M_{e_max} drop although the best ignition angles were obtained (24 CAD bTDC and 22 CAD bTDC) respectively). It means that the E_c, which was brought by the fuel mixture, was lower than with CNG fuel. But H_2 additions of 30%, 50% and 70% concentration showed increasing engine M_{e_max} tendency with best spark timings (22, 18 and 14 CAD bTDC accordingly). It can be explained by the increased E_c in the fuel mixtures. Although the fuel mixture with 90% H_2 addition has a little bit higher E_c, comparing with 70% addition, but this fuel mixture showed engine M_{e_max} decrease, when the best spark timing was applied (6 CAD bTDC). Same M_{e_max} drop and increase tendency was observed with different CNG and H_2 fuel mixtures at $\lambda = 1.4$ (Fig. 3.12). 10% H_2 and 20% H_2 additions were reducing the obtained M_{e_max} values to 42.96 Nm, however, engine M_{e_max} increased up to 46.12 Nm with 70% H_2 addition and it was even higher than with *P* fuel or CNG fuel.

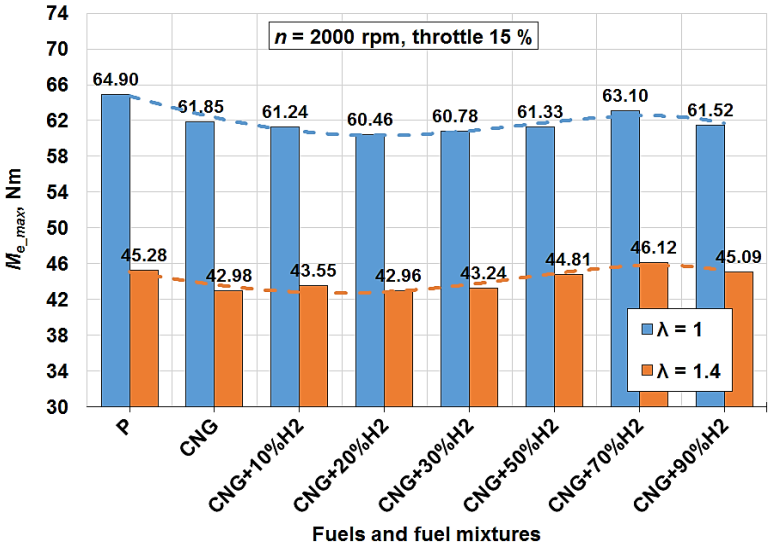

Fig. 3.12. Engine maximum torque dependence on different fuel mixtures and air / fuel ratios. Tested fuels – petrol, natural gas, natural gas / hydrogen fuel mixtures; n = 2000 rpm, $\lambda = 1$ and $\lambda = 1.4$

These experimental research findings can be supported by other scientists' works. It was proved that H_2 gives higher burning rate. In order to obtain M_{e_max}, the spark timing has to be retard (Nagalingman *et al.* 1983). It was also obtained similar engine power output tendencies. Tests up to ~ 26% of H_2 in CNG fuel let to extend lean burn limits (Huang *et al.* 2006). It was noticed that at specific excessive A/F ratios, engine power and engine efficiency decreased with H_2 fraction up to 20%. However, these parameters increased, when hydrogen fraction was increased more than 20%.

Fig. 3.13 shows the BSFC dependence on different ignition angles with different fuels and fuel mixtures at $\lambda = 1$ and $\lambda = 1.4$. Highest BSFC was obtained with *P* fuel. The highest BSFC was achieved with CNG from all tested gaseous fuels which had best BSFC point (221.24 g/kWh) when spark timing was set at 26 CAD bTDC. The lowest BSFC was achieved with 90% H_2 fuel mixture (132.07 g/kWh), which was 40.3% lower comparing with CNG fuel.

The highest BSFC was again – for *P* fuel (266.54 g/kWh) at tested $\lambda = 1.4$ point when the ignition angle was 36 CAD bTDC. CNG fuel reached lower BSFC – 224.21 g/kWh (40º bTDC). However, lowest BSFC was obtained with 90% H_2 fuel mixture (133.48 g/kWh), which was 40.46% lower comparing with CNG fuel.

Fig. 3.14 presents engine brake thermal efficiency dependence on different ignition angles and CNG / H_2 fuel mixtures at $\lambda = 1$ and $\lambda = 1.4$. Although highest engine M_{e_max} was achieved with 70% H_2 fuel mixture and lowest BSFC was achieved with 90% H_2 fuel mixture, the best engine η_e (0.328) at $\lambda = 1$ was achieved with 30% H_2 fuel mixture when the spark timing was 22 CAD bTDC. The lowest engine η_e was observed with 90% H_2 fuel mixture ($\eta_e = 0.312$).

The highest engine η_e was obtained with *P* fuel (0.311) at lean combustion conditions at around 40 CAD bTDC spark timing. The second best result was obtained with 70% H_2 fuel mixture ($\eta_e = 0.309$) and the lowest η_e was obtained with CNG and 10% H_2 fuel mixture – 0.216 and 0.295, respectively (Fig. 3.14). This shows that the highest engine η_e can be achieved with fuels which have biggest amount of energy, which is brought, by an injected fuel mass.

Scientists published similar engine η_e results with stoichiometric and lean burn cases when H_2 was used in CNG fuel. The thermal efficiency increased with increasing H_2 percentage up to certain concentration addition using stoichiometric (Dimapoulous *et al*. 2007) and lean fuel mixtures (Akansu *et al.* 2007). Using lean mixtures, the specific heat ratio values reduced more than for stoichiometric combustion. With rich mixtures, combustion is not complete, therefore there will be a decrease of η_e.

Fig. 3.15 presents the HC emission dependence on different spark timing and CNG / H_2 fuel mixture at different A/F ratios. The highest HC emissions were achieved with liquid *P* fuel (more than 120 ppm) at $\lambda = 1$ conditions. Although

the injected fuel mass reduced with λ = 1.4 case for *P* fuel, but the HC emission was highest from all tested fuels again and at some points higher than with λ = 1. Such phenomena probably influenced by worse combustion conditions: less fuel was injected, the fuel was combusting much slower in the cylinder, the flammability of the fuel mixture reduced, and the time for combustion chemical reactions was too short to have full combustion products.

a)

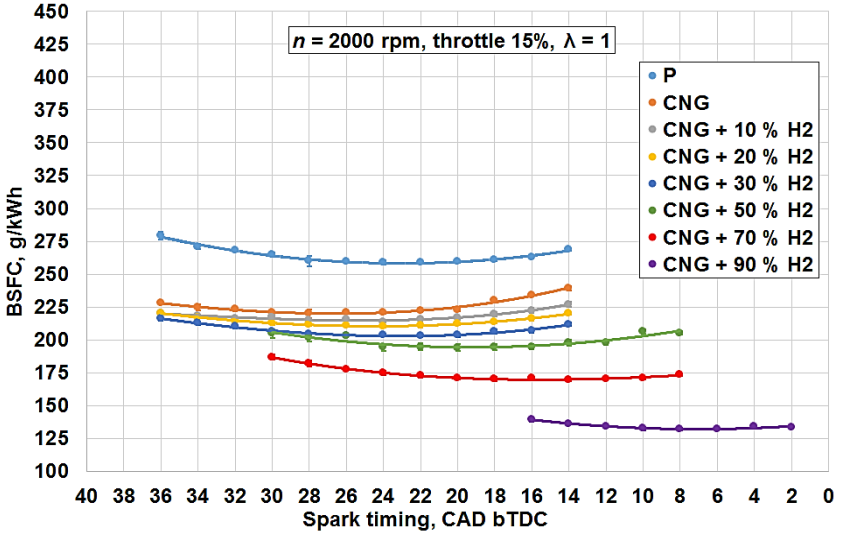

b)

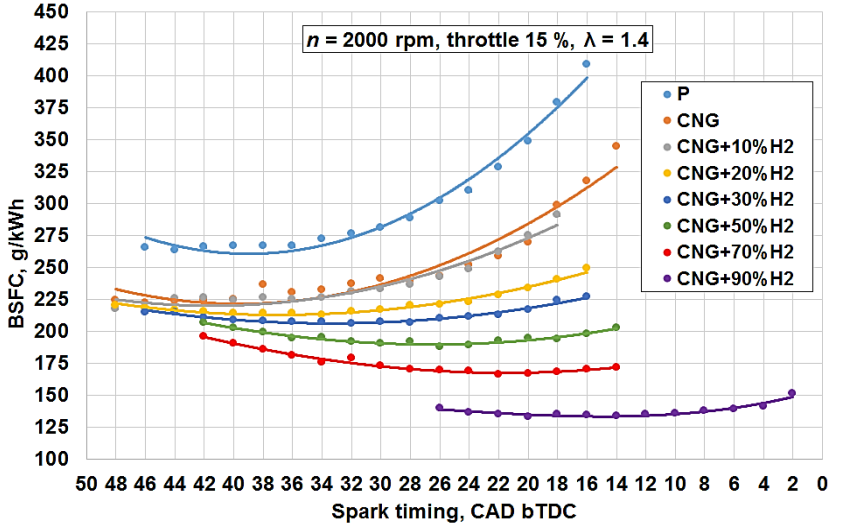

Fig. 3.13. Brake specific fuel consumption dependence on different ignition angles, fuel mixtures and air / fuel ratios. Tested fuels – petrol, natural gas, natural gas / hydrogen fuel mixtures; *n* = 2000 rpm, a) λ = 1 and b) λ = 1.4

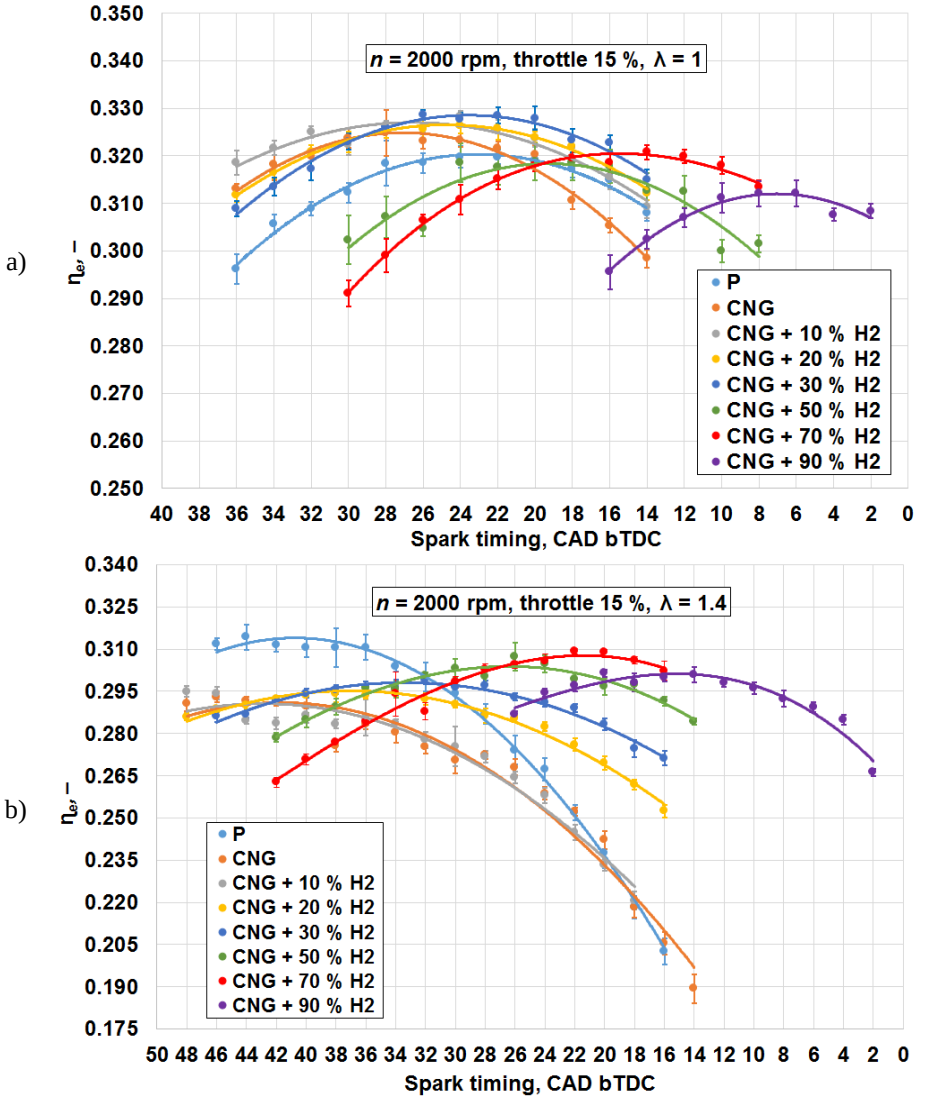

Fig. 3.14. Engine brake thermal efficiency dependence on different ignition angles, fuel mixtures and air / fuel ratios. Tested fuels – petrol, natural gas, natural gas / hydrogen fuel mixtures; n = 2000 rpm, a) $\lambda = 1$ and b) $\lambda = 1.4$

Similar tendencies were observed with CNG fuel. The HC emission was ~ 20% higher (more than 100 ppm) $\lambda = 1.4$ than for $\lambda = 1$. Lean conditions slow down the combustion of natural gas, which already has a fairly slower combustion comparing with *P* fuel at stoichiometric conditions.

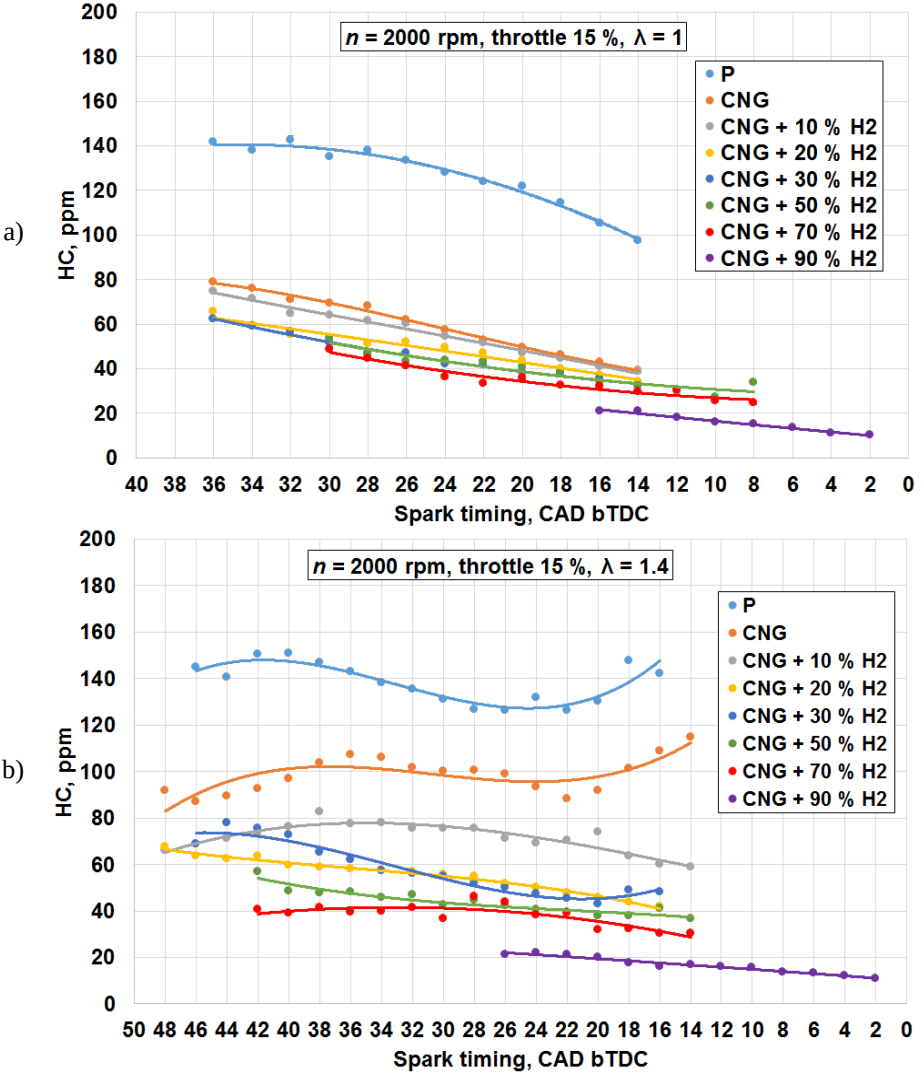

Fig. 3.15. HC emission dependence on different ignition angles, fuel mixtures and air / fuel ratios. Tested fuels – petrol, natural gas, natural gas / hydrogen fuel mixtures; n = 2000 rpm, a) λ = 1 and b) λ = 1.4

Comparing smaller amounts of H_2 in the fuel mixture (10% H_2, 20% H_2 and 30% H_2) the HC emission was higher at λ = 1.4 than for λ = 1. It can be explained that H_2 additive takes some volume of natural gas fuel. The E_c, which was brought by H_2, was quite low as H_2 has very low density. What is more, H_2 occupies natural

gas place and the fuel mixture has even less E_c by volume. In this case, the combustion and oxidation of mentioned fuels was much slower in the late cycle part, which had influence on increased HC emission. Another possible explanation could be that the flame quenching distance decreased with H_2 addition in the fuel. The flame approached closer to the cylinder wall, the wall temperature increased and the HC emission possibly increased due to lube oil. The HC emissions were very close between stoichiometric and lean burn cases with bigger H_2 concentrations (50%, 70%, 90%). In overall, the HC emissions were decreasing with increasing H_2 amount in CNG fuel at different A/F ratios. The H_2 was improving combustion characteristics, therefore hydrocarbons combusted better. Also the H/C atom ratio of the fuels were changing and the C element was less present in tested fuels with bigger H_2 concentrations.

Fig. 3.16 presents the NO_x emissions depending on different ignition angles, CNG / H_2 fuel mixtures and A/F ratios. The lowest NO_x emissions were achieved with CNG fuel at $\lambda = 1$. Increasing H_2 amount in natural gas, increased emissions, because the combustion temperature was getting higher. The retard ignition angle decreased NO_x emissions for all tested fuels, because the time to take O_2 atom and form NO elements reduced. The NO_x was ~ 2500 ppm with CNG at 26 CAD bTDC, where the highest η_e was achieved. The 10%, 20% and 30% H_2 additions gave lower NO_x emissions than for *P* fuel case. The emissions were more than 4000 ppm with highest 90% H_2 addition. The measurements for the 90 % H_2 addition could not be done due to exceeded exhaust gas analyser measuring range at some CAD spark timings. Such big increase of nitrous oxide directly related to very high combustion temperature, which occurred due to big H_2 concentration in the fuel and which increased the LHV.

NO_x emissions were lowest for *P* fuel, CNG and CNG + 10% H_2 fuel mixture at $\lambda = 1.4$, because the fuel mixtures were leaner and less fuel was injected which resulted in lower combustion temperature. The increase of H_2 in the fuel, increased the NO_x emissions. However, the emission level with higher H_2 concentrations were lower comparing with $\lambda = 1$ tests. The highest η_e was achieved at $\lambda = 1.4$ with 70% H_2 addition at spark timing of 20 CAD bTDC. At this measuring point the NO_x level was ~ 1000 ppm which was almost equal to *P* fuel level at ~ 40 CAD bTDC where the *P* fuel reached highest η_e and it was ~ 3 times lower comparing with *P* fuel at $\lambda = 1$.

Akansu (2007) points that with lean burn cases NO_x emission was achieved at low level. Scientists also noted that low NO_x emission can be achieved just with at least $\lambda = 1.5$ when H_2 amount was up to 20% (Sierens *et al.* 2000).

Fig 3.17 shows the dependence of exhaust gas temperature on different spark timing and tested fuels at stoichiometric ant lean burn conditions.

Measurements revealed that the exhaust gas temperature was reducing with increased H_2 concentration in natural gas. Although the combustion temperature

increased with increasing H_2 amount, – that can be explained by increased NO_x emissions, but the exhaust temperature was getting lower. It can be supported by increased combustion speed and shorter combustion duration. The more H_2 was present in the fuel mixture, the shorter combustion duration occurred, and the exhaust temperature was getting cooler earlier. The retard ignition timing gave later combustion. In this case the exhaust gas temperature increased.

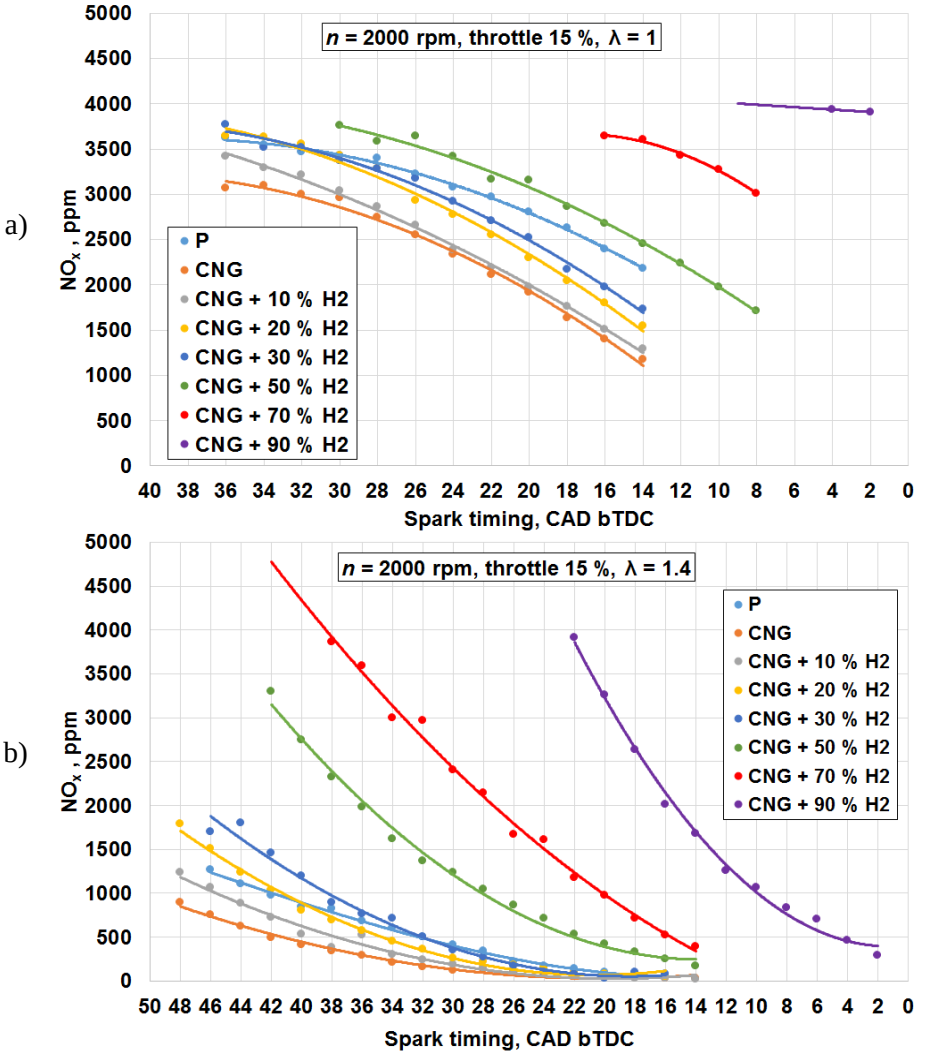

Fig. 3.16. NO_x emission dependence on different ignition angles, fuel mixtures and air / fuel ratios. Tested fuels – petrol, natural gas, natural gas / hydrogen fuel mixtures; n = 2000 rpm, a) λ = 1 and b) λ = 1.4

a)

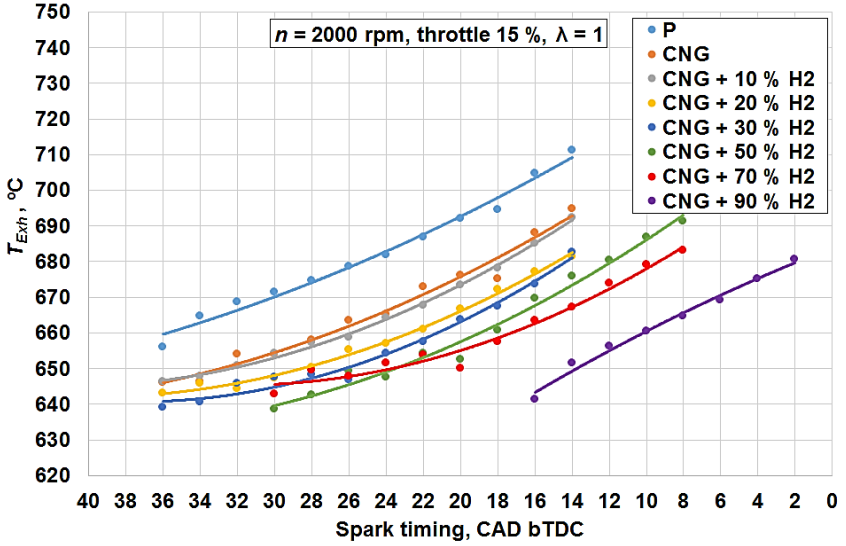

b)

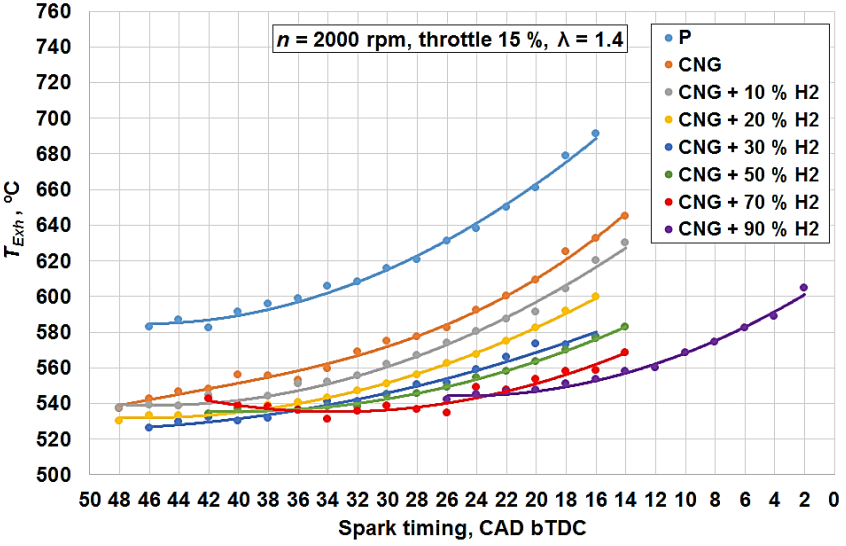

Fig. 3.17. Exhaust gas temperature dependence on different ignition angles, fuel mixtures and air / fuel ratios. Tested fuels – petrol, natural gas, natural gas / hydrogen fuel mixtures; n = 2000 rpm, a) $\lambda = 1$ and b) $\lambda = 1.4$

Homogeneous lean burn combustion measuring data showed that exhaust gas temperature reduced for all tested fuels due to less injected fuel and reduced combustion temperature comparing with $\lambda = 1$ measurements.

3.4.3. Research Data Analysis of Engine Running with Natural Gas / Hydrogen Fuel Mixtures Using *AVL BOOST* Software

AVL BOOST software was used to analyse combustion process and thermodynamic processes with different fuels and fuel mixtures in 4 cylinder SI *HR16DE* engine. The measured in cylinder pressure, fuel mass, air mass, fuel composition were set up in *AVL BURN* utility. Software was able to determine the combustion start, combustion duration in cylinder, also combustion intensity which is described as Factor m_v. *AVL BOOST* software used Vibe two zone combustion model.

The calculations were made at engine speed 2000 rpm, 1.56 bar (20 Nm) load at $\lambda = 1$ when spark timing was kept constant like CNG spark timing for all fuel mixtures with H_2 addition. The combustion duration became shorter with increased amount of H_2 in gas mixture (Fig. 3.18).

CNG combustion duration was ~ 66 CAD at 1.56 bar load. 10% H_2 addition shortened combustion ~ 3 CAD and 70% H_2 addition shortened it even 18 CAD. Similar results were obtained with higher engine load at $\lambda = 1$, just combustion duration became shorter for every fuel case because the injected fuel mass increased and it combusted faster. Shorter combustion duration with increasing amount of H_2 in CNG fuel was obtained also by (Mariani *et al.* 2013).

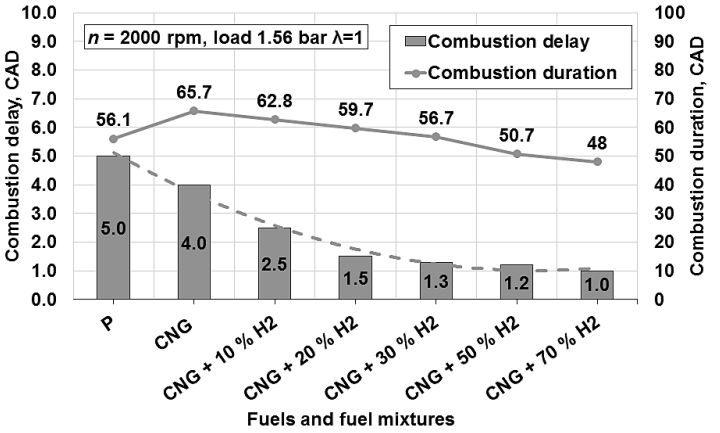

Fig. 3.18. Combustion delay and combustion duration dependence on different fuel mixtures. Tested fuels – petrol, natural gas, natural gas / hydrogen fuel mixtures; n = 2000 rpm, load 1.56 bar, $\lambda = 1$

Fig. 3.19 presents pressure in cylinder dependence on different fuel mixtures at $\lambda = 1$, at 1.56 bar engine load. The pressure rose earlier and more intensively with increasing H_2 amount in the fuel mixture. This was resulted by a higher H_2

LHV, which increased overall fuel mixture energy content (Fig. 2.6), and higher combustion speed. Combustion pressure increase was also described by Mariani (2013) where similar fuels (CNG, CNG + 15% H_2, CNG + 30% H_2) were tested and the pressure peak rise was obtained with increasing H_2 amount.

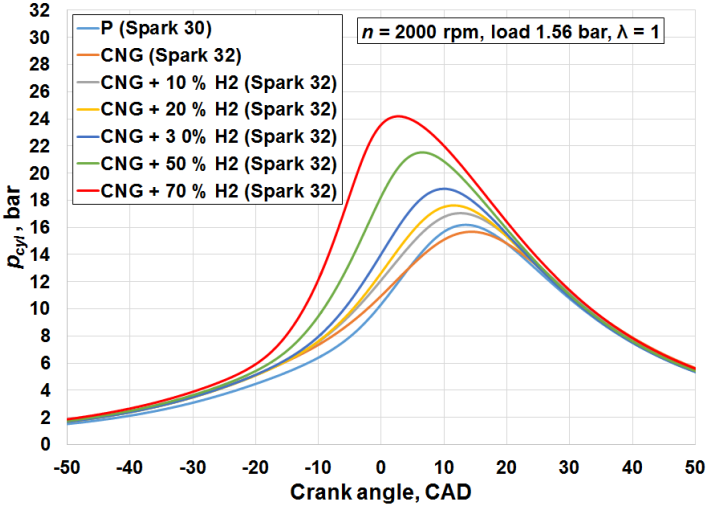

Fig. 3.19. In-cylinder pressure dependence on different fuel mixtures. Tested fuels – petrol, natural gas, natural gas / hydrogen fuel mixtures; n = 2000 rpm, load 1.56 bar, $\lambda = 1$

RoHR data for each fuel at $\lambda = 1$ is presented in Fig. 3.20. RoHR analysis showed that using CNG fuel instead of *P*, RoHR ($dQ/d\Phi$) reduced during combustion process. The combustion duration was longer than for *P* fuel. H_2 addition in the fuel mixture improved fuel mixture combustion: the RoHR was increasing and the duration was becoming shorter. Fig. 3.18 represent these combustion characteristic numbers. The RoHR reached maximum value of 20 J/deg with 70% H_2 addition, when CNG fuel RoHR was just 12 J/deg. Furthermore, the figure obviously shows that the start of combustion with H_2 addition became earlier. Scientists also noticed that the maximum value of heat release rate also increased in investigations with H_2 additions (Mariani *et al.* 2013).

Combustion analysis proved that combustion temperature became higher with increased H_2 amount in CNG / H_2 fuel mixture (Fig. 3.20). Increased combustion temperature influenced higher NO_x formation that was obvious from measured exhaust gas emissions (Fig. 3.16). From Fig. 3.20 it is also obvious that the temperature dropped earlier in the cylinder.

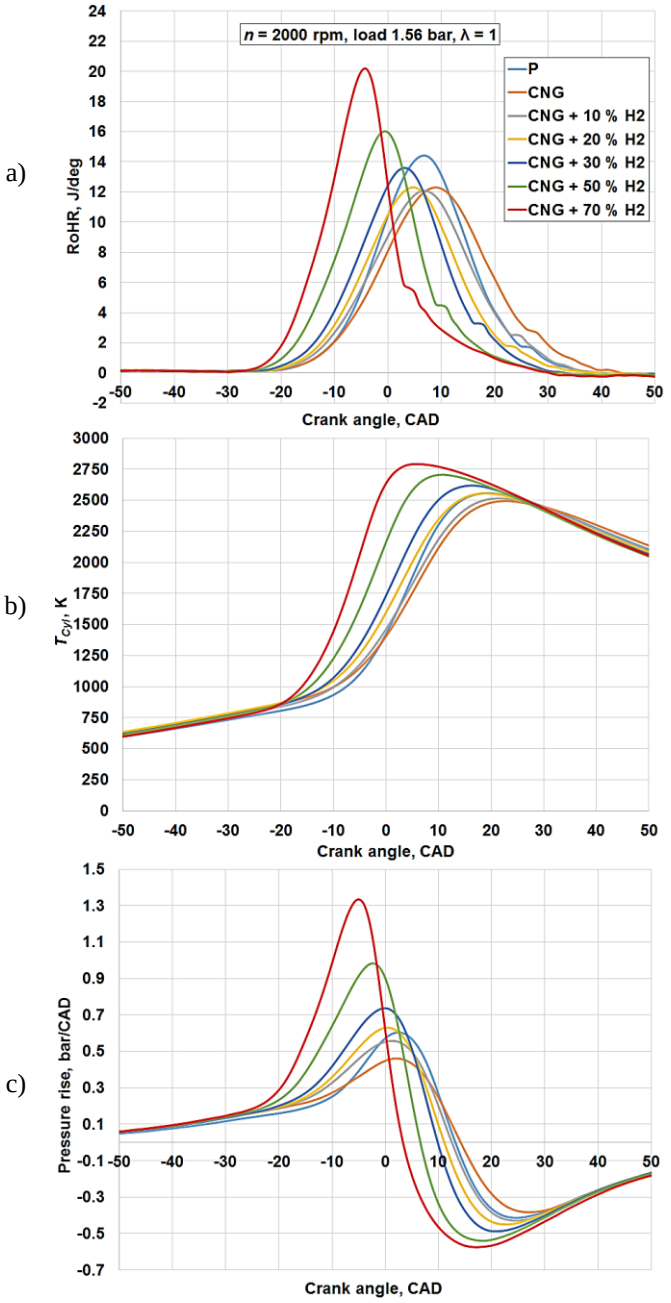

Fig. 3.20. Dependence of combustion parameters on different fuel mixtures: a) rate of heat release, b) temperature in cylinder, c) pressure rise. Tested fuels – petrol, natural gas, natural gas / hydrogen fuel mixtures; n = 2000 rpm, load 1.56 bar, λ = 1

H_2 combusted faster and the temperature decrease appeared earlier. Increased in-cylinder temperatures also explain increasing wall heat losses with higher H_2 concentrations (e.g. 50%, 70%) which resulted in reduced engine η_e at all tested engine loads.

Increased combustion speed with H_2 additive influenced pressure rise characteristics (Fig. 3.20). Pressure rise in cylinder showed that it was about 3 times bigger using CNG + 70% H_2 fuel, comparing with pure CNG fuel. Also it is obvious that peak of pressure rise was much before TDC which resulted in higher stress for engine parts and decreased MBT. These data analysis findings prove that the ignition timing has to be adjusted in case of H_2 addition in the fuel mixtures.

The change of ignition timing with different CNG / H_2 fuel mixtures showed that the spark ignition has to be retard in order to obtain best efficient parameters with increasing H_2 amount in the fuel (Fig. 3.11, Fig. 3.12, Fig. 3.14). As it was mentioned before, interesting phenomena observed with 70% H_2 addition at $\lambda = 1$ and $\lambda = 1.4$ conditions. The obtained M_e and η_e were highest with CNG + 7% H_2 fuel mixture among all tested CNG / H_2 fuel mixtures. The increasing values' tendencies were observed starting with 30% H_2 addition and reducing values with more than 70% H_2 addition. In order to have a more detailed explanation, the obtained combustion data is presented from analysis tool *AVL BOOST BURN*.

Combustion characteristics, like combustion delay and combustion duration, are given in Fig. 3.21. Gaseous CNG fuel had an increase of combustion delay comparing with liquid fuel ($\lambda = 1$). The combustion duration was also longer for tested CNG fuel. Increasing H_2 concentration in a fuel mixture decreased the combustion delay more than 84% if compared 90% H_2 addition in the fuel with pure CNG. Same tendencies observed as it was obtained with const. engine load (Fig. 3.18). The combustion duration also had a reduction tendency, when the H_2 concentration was increasing in the fuel mixture.

The combustion delay increased with increasing H_2 amount at lean combustion conditions ($\lambda = 1.4$), but the combustion duration was still reducing. The combustion duration was longer due to lower flame front speed inside the cylinder comparing with stoichiometric combustion. The combustion delay increased at $\lambda = 1.4$. It could be effected due to very lean conditions in combustion chamber as the fuel molecules are relatively far away from each other and the combustion reactions are slower than in stoichiometric conditions. Since the H_2 is very reactive molecule, the combustion delay started to decrease with very high H_2 concentration, due to increased H_2 amount by mass.

Fig. 3.22 represent another important combustion parameter – shape parameter m_v. As it was mentioned in methodology chapter, this number was used in Vibe formula to calculate the RoHR values. Also it is directly connected with RoHR shape form.

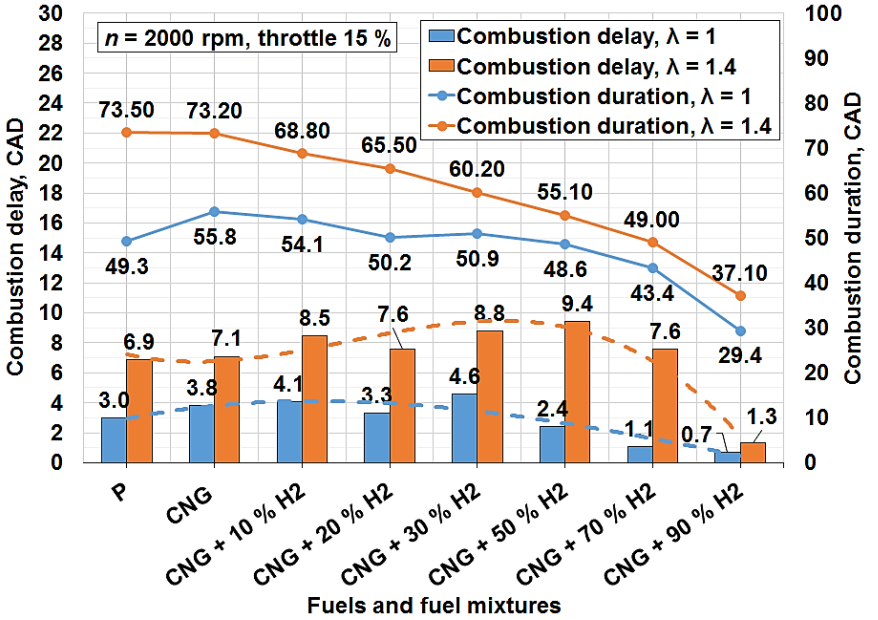

Fig. 3.21. Combustion delay and combustion duration dependencies on different fuel mixture and air / fuel ratios. Tested fuels – petrol, natural gas, natural gas / hydrogen fuel mixtures; n = 2000 rpm, throttle 15%, λ = 1 and λ = 1.4

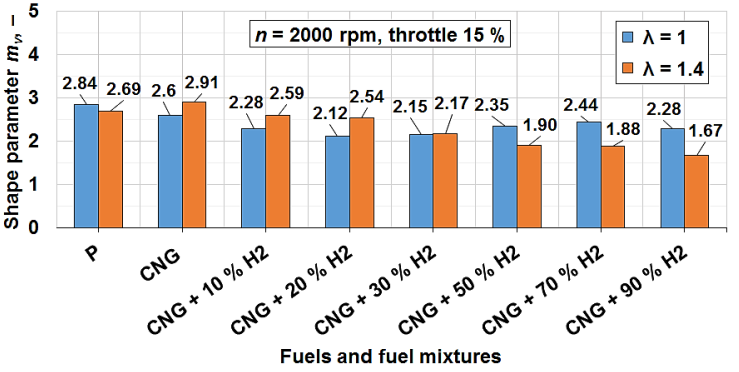

Fig. 3.22. m_v dependence on different fuel mixtures. Tested fuels – petrol, natural gas, natural gas / hydrogen fuel mixtures; n = 2000 rpm, throttle 15%, λ = 1

Fig. 3.23 and Fig. 3.24 present the pressure in cylinder, RoHR and pressure rise in cylinder dependencies on different tested fuel mixtures at 2000 rpm engine speed (λ = 1 and λ = 1.4) when throttle was kept const. 15% for all testing cases.

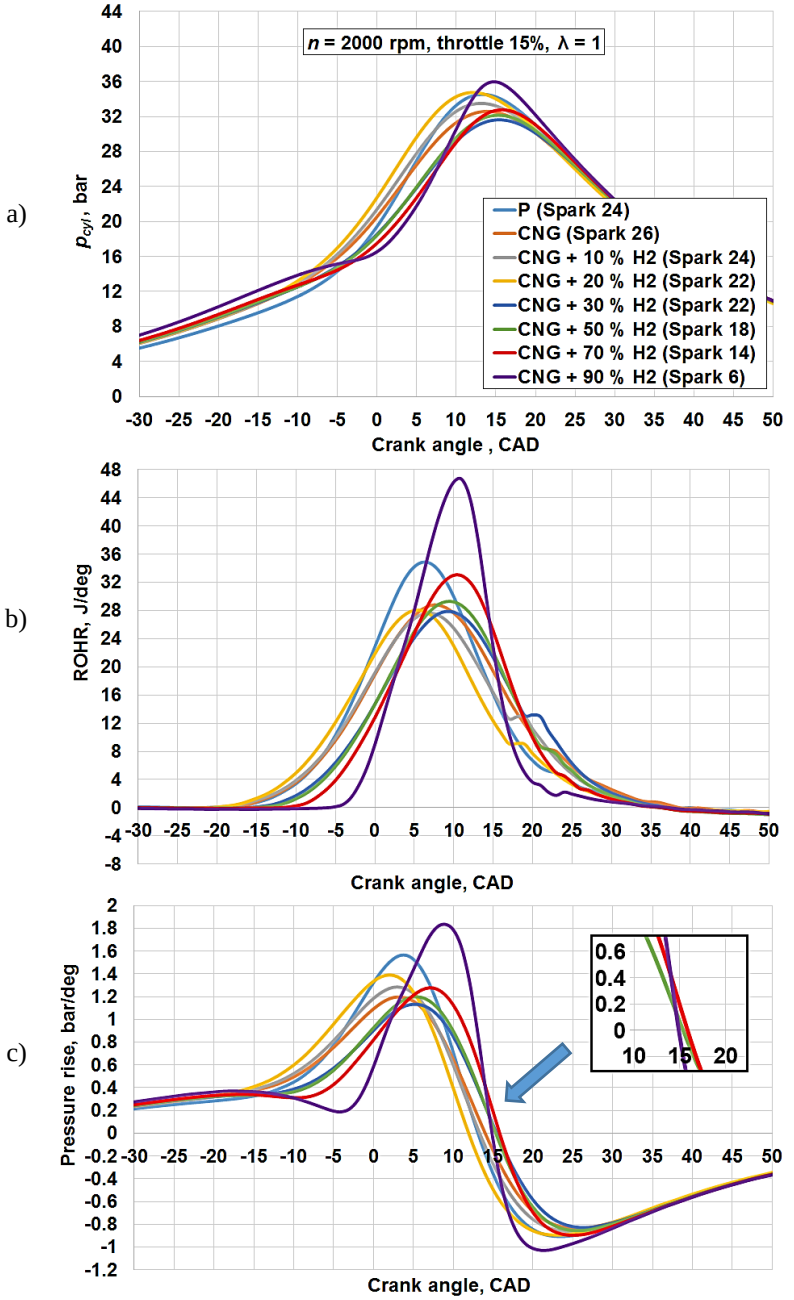

Fig. 3.23. Dependence of combustion parameters on different fuel mixtures: a) pressure in cylinder, b) rate of heat release, c) pressure rise. Tested fuels – petrol, natural gas, natural gas / hydrogen fuel mixtures; n = 2000 rpm, throttle 15%, λ = 1

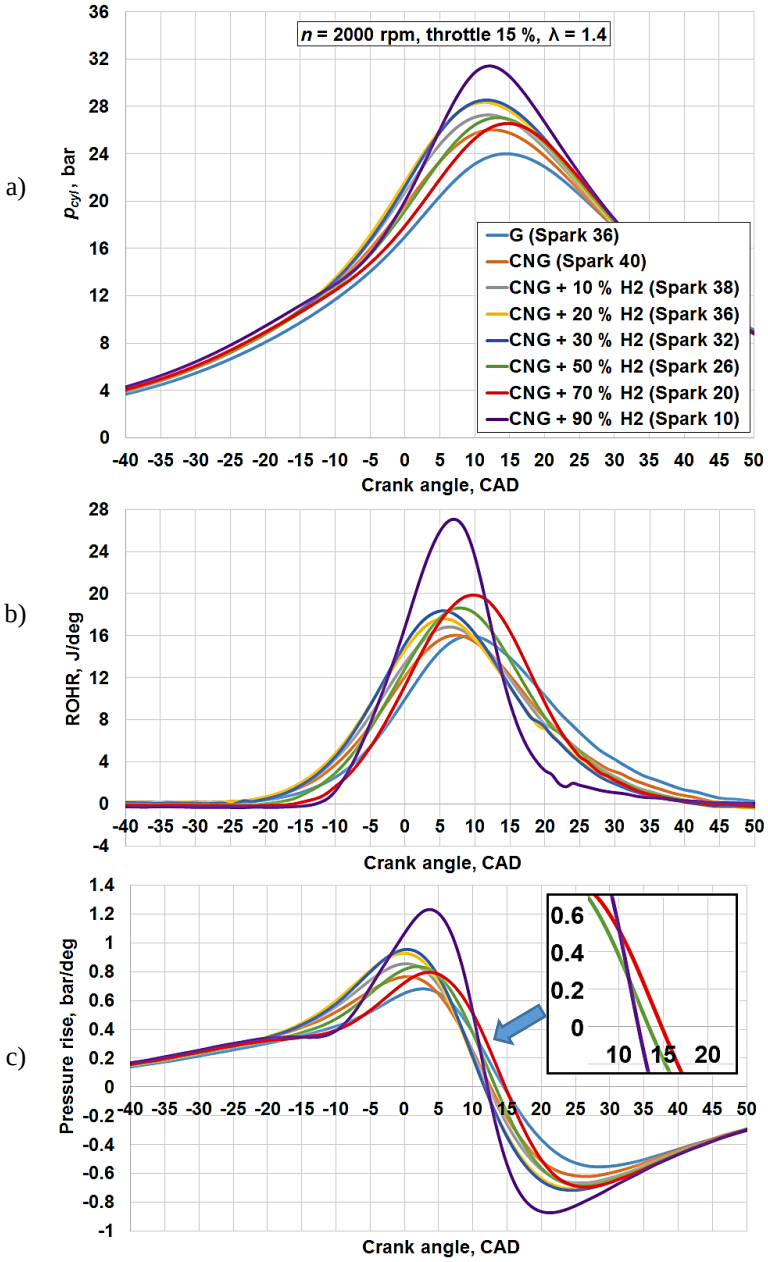

Fig. 3.24. Dependence of combustion parameters on different fuel mixtures: a) pressure in cylinder, b) rate of heat release, c) pressure rise. Tested fuels – petrol, natural gas, natural gas / hydrogen fuel mixtures; n = 2000 rpm, throttle 15%, λ = 1.4

The highest pressure in cylinder was obtained with 90% H_2 addition on both λ conditions. Also same tendencies observed with RoHR and pressure rise characteristics. It is obvious that with increasing H_2 content from 10% up to 30% by volume at $\lambda = 1$, the RoHR peak values were slightly lower than for CNG fuel, though the H_2 addition gave little earlier RoHR. The increasing amount of H_2 by volume was taking the volume in the combustion chamber and less fuel was injected in order to keep the desired A/F ratio. The E_c amount by mass, which was brought with injected fuel, was reducing, which can be supported by Fig. 3.26 which is presented in the next chapter. This resulted in reduced M_e and η_e. The parameter m_v reduced from 2.84 up to 2.12 with 20% H_2 (Fig. 3.22) at $\lambda = 1$ conditions. This showed that the combustion duration was getting shorter and the RoHR was more intense at the beginning of combustion which was a result of more reactive element H_2.

Homogeneous lean burn cases showed that start of combustion appears very late after spark timing. This can be caused due to very lean mixture that had much slower flame front speed. The combustion duration also was longer for *P* and CNG cases. H_2 addition helped to improve combustion process. The cylinder pressure and RoHR was higher with same H_2 concentrations (10%, 20%) at $\lambda = 1.4$ comparing with CNG fuel. The start of combustion appeared much earlier and the combustion duration was shorter (Fig 3.23, Fig. 3.24).

The cylinder pressure, RoHR and pressure rise were increasing with higher H_2 additions (more than 30%), because the E_c was higher with bigger H_2 concentrations. As it was mentioned before, the combustion duration was shorter due to increased flame speed. The combustion shape parameter m_v started to increase with bigger H_2 amount at $\lambda = 1$, because the RoHR distributed in shorter combustion duration period, but that does not mean that the combustion intensity reduced.

The m_v reduced evenly with increasing H_2 amount in all fuel mixtures at $\lambda = 1.4$ conditions. It can be explained by longer combustion duration due to rich air conditions. The RoHR distributed in longer combustion period and the combustion intensity characteristic was shifting more to the beginning of combustion due to increased H_2 concentrations. This can also be explained by higher air motion in the cylinder due to lean burn application. It is known that H_2 has very wide combustion limits in the air, therefore the air excess could improve the combustion with very high H_2 concentrations.

The H_2 increase more than 30% showed increasing M_e and η_e values (Fig. 3.11, Fig. 3.14). This tendency can be explained by an increasing H_2 content in the fuel mixture by mass and increased injected E_c amount by mass (Fig. 3.28). Though the 90% H_2 addition had also slightly bigger injected E_c amount by mass at stoichiometric conditions, but engine M_e reduced by ~ 2.5% and η_e reduced by ~ 2.7%. Such reduction of efficient parameters can be explained by too fast combustion process in the cylinder. This can be supported by pressure rise curves

(Fig. 3.24). The start of combustion with 90% H_2 was later ~ 7.7 CAD comparing with 70% H_2 addition. Due to big amount of H_2 the combustion was very intense and gave the highest RoHR, therefore the combustion duration was also shorter which gave biggest pressure rise among all tested fuels. What is more, the intense combustion gave very fast drop of pressure rise. The pressure rise reached 0 bar/deg. value at ~ 15 CAD aTDC, while 70% H_2 addition at this CAD moment still had ~ 0.3 bar/deg. pressure rise, which effected engine work positively. Such fast combustion speed increase and very fast drop did not give the efficient work on the piston move with CNG + 90% H_2 fuel mixture , therefore all efficient indicators were reducing.

3.4.4. Simulation of Engine Running with Natural Gas / Hydrogen Fuel Mixtures Using *AVL BOOST* Software

The experimental measurements showed that the highest engine M_e (63.10 Nm) was achieved with 70% H_2 addition among tested CNG / H_2 fuel mixtures at $\lambda = 1$. The M_e value was the highest (46.12 Nm) also with same fuel mixture among all tested fuels and fuel mixtures at lean conditions ($\lambda = 1.4$). As it was explained before the M_e increase with such particular fuel mixture can be explained by increased injected cycle energy. But with higher H_2 concentration the M_e started to reduce because of very intense combustion which gave negative effect.

In order to find out which CNG / H_2 fuel mixture gives the highest engine M_e and η_e, the numerical simulation *AVL BOOST* software was applied. The increase of M_e was observed from tested 20% H_2 addition up to 7% H_2 and decrease from 70% H_2 up to 90% H_2, therefore the simulated fuel mixtures were in mentioned ranges with presumption that they can give better effect than 70% H_2 addition in CNG fuel.

Combustion parameters (start of combustion, combustion duration, combustion intensity factor m_v) were determined by interpolation from already know values and their trend lines (Annexes Fig. B.8). Mentioned combustion values for 60% H_2, 65% H_2, 75% H_2, 80% H_2 and 85% H_2 additions were determined by the calculated mass content in the fuel mixture. Also fuel *LHV* and A/F ratios for mentioned fuel mixtures were determined and included into simulation process.

The numerical simulation was performed at the same engine speed $n = 2000$ rpm, when the air injection pressure was regulated in order to keep same $\lambda = 1$ conditions with determined fuel injection ratio with different CNG / H_2 fuel mixtures. Fig. 3.25 shows the simulated and obtained maximum M_e and BSFC values which are compared with experimental values.

Obtained simulation results showed that the differences between experimental and simulation are minor. The difference between simulated and experimental M_e values at 50% H_2, 70% H_2 and 90% H_2 were ~ 0.31%, 0.63%, ~ 0.49%

respectively, which show that the numerical model was fairly adequate and accurate. The differences between obtained BSFC simulated and experimental values had also minor margins.

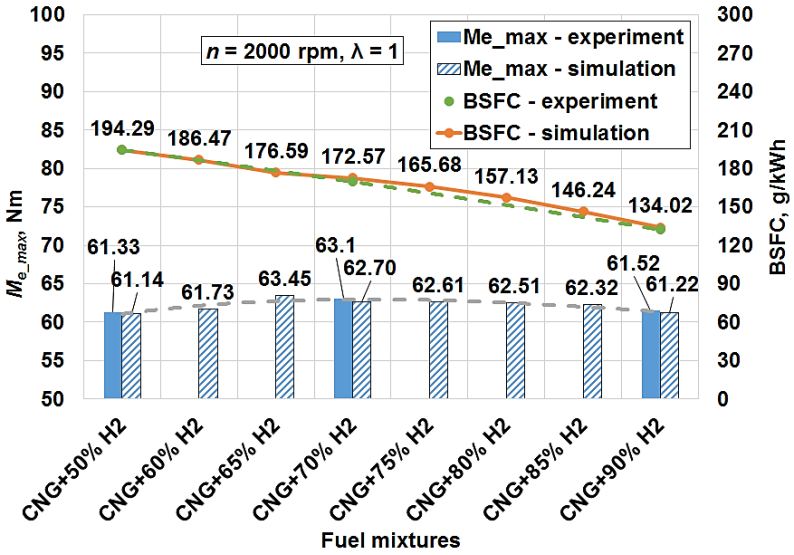

Fig. 3.25. Dependence of engine maximum torque M_{e_max} and brake specific fuel consumption on different fuel mixtures onbtained from simulation

Numerical simulation revealed same engine M_e increasing tendency up to 70% H_2 addition which was then reducing up to 90% H_2 additive. The highest simulated M_e meaning (63.45 Nm) was achieved with CNG + 65% H_2 fuel mixture wich was 1.2% higher comparing with 70% H_2 addition (62.70 Nm).

3.5. Generalized Comparison of Gaseous Fuel Research Results

Experimental measurements, numerical analysis and simulation revealed that gaseous fuel composition or additive characteristics have a great influence on engine efficient and ecological indicators.

In order to get a better understanding about different fuels influence on combustion behavior and emission formation, Fig. 3.26 represent the comparison of E_c values of all represented tested fuels in this work, when the engine was running

at the same conditions: n = 2000 rpm, throttle 15%, λ = 1. The calculations support obtained and given results.

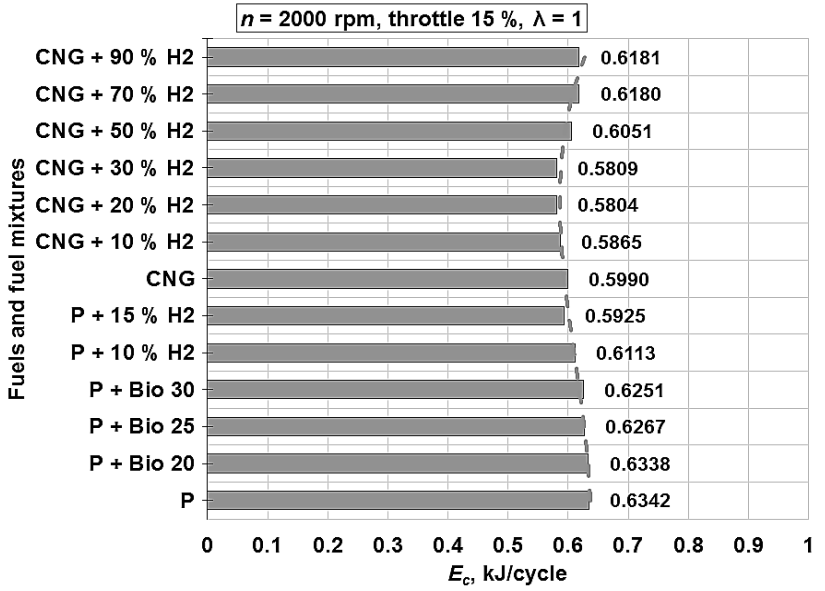

Fig. 3.26. Dependence of cyclic energy amount brought by fuel to the cylinder on different tested fuels and fuel mixtures. Engine n = 2000 rpm, throttle 15%, λ = 1

The injected cyclic energy reduced due to lower fuel mixture LHV and decreasing injected fuel mass with addition of biogas with different fuel feeds (*Bio* 20, *Bio* 25, *Bio* 30). The addition of more reactive element H_2 into the combustible mixture up to certain concentration (~ 20%) also reduced the E_c. Although the LHV of fuel mixtures increased, but H_2 took bigger volume in the cylinder due to its physical characteristics (low density), the injected fuel mass was decreasing and the energy which was brought by mass was also decreasing. It had an impact on engine M_e and η_e reduction. Furthermore, the analysis of emissions, like NO_x, showed substantial increase due to increased combustion temperature in cylinder.

With higher H_2 additions (> 30%) the E_c started to increase, as the H_2 part in the fuel according to mass was also increasing sharply. This was influenced by increasing LHV which let to obtain higher M_e and η_e, reduce CO, CO_2 but it increased NO_x emissions.

Fig. 3.27 presents the dependence of spark timing (when the MBT reached) and BSFC on different calculated MON and MN values at a certain engine regime – n = 2000 rpm, throttle 15%, λ = 1.

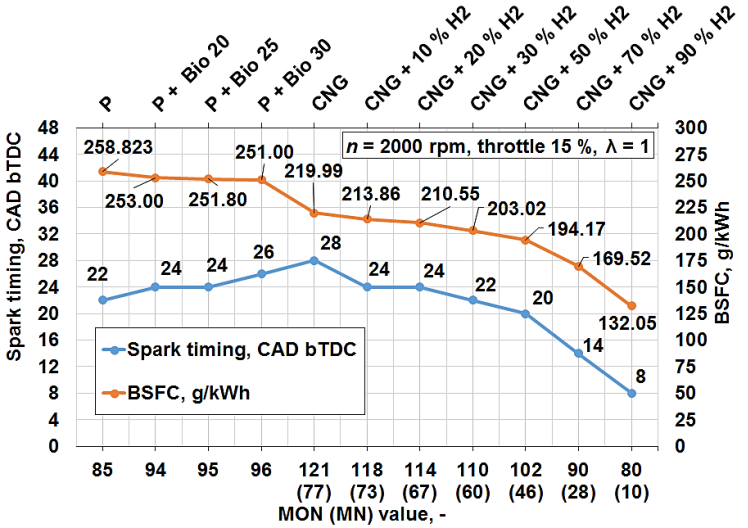

Fig. 3.27. Dependence of spark timing and brake specific fuel consumption on different calculated octane number and methane number values. Engine n = 2000 rpm, throttle 15%, λ = 1

This figure support the presented findings with researched fuels and their additions – biogas and H_2. When biogas addition was used (*Bio* 20, *Bio* 25, *Bio* 30) in a duel fuel system, the MON values increased, showing that the fuel was more knock resistant and spark timing had to be retard in order to obtain the MBT and lowest BSFC. The combustion intensity reduced and combustion duration became longer. It is possible to use engines having higher ε with such duel fuel system (*P* + *Bio*).

The most retard spark timing (28 CAD bTDC) was obtained with CNG fuel which had 121 MON (77 MN) showing that it was one of the slowest combustions. In order to obtain better η_e it is possible to use higher ε ratio engine (~12–13.5) as fuel has such high knock resisting limits. The H_2 addition reduced MON and MN up to 80 and 10, respectively, showing that fuel was less knock resistant and has improved combustion characteristics (shorter and faster combustion). In this case, the spark timing has to be retard essentially in order to achieve best efficient results. Although the combustion analysis did not show any auto-ignition or knock phenomena with high H_2 concentration additions, but the MON (MN) value calculations (Table 2.10) and other scientists' research analysis (Fig. 1.5, Fig. 1.6) revealed that such limits can be very close. The numerical simulation showed that most promising CNG / H_2 fuel mixture was obtained with ~ 65% H_2 addition in CNG fuel. The calculated MON value of such mixture should be between 95 and

100. In this case, higher compression ratio engine could be used in order to get much higher engine efficiency with mentioned fuel mixture.

3.6. Research of CNG and Hydrogen Fuel Mixture Use in Heavy Duty Vehicle

Heavy duty vehicle tests (6 cylinder engine *F2BE0642H*) were performed on vehicle dyno test bench. Table 3.3 presents testing modes with different CNG / H_2 fuel mixtures. The experiments were performed at const. rpm and load. The load was measured on wheels. Three different loads were run: 30 kW, 50 kW and 100 kW. The engine speed was kept at 1500 rpm which was in diapason of highest torque according to manufacturer engine characteristics. The bus engine had stoichiometric combustion ($\lambda = 1$) setup.

Fig. 3.28 presents different fuel mixtures influence on B_d, BSFC and engine η_e. The fuel consumption, as it was expected, increased with increasing power on wheels and engine load. Like previous results from 4 cylinder engine research revealed, the B_d decreased with increasing H_2 amount in CNG fuel. However, the decrease was insignificant.

The lowest B_d was obtained with CNG + 15% H_2 fuel mixture at different power modes. If compared with pure CNG fuel, the lowest B_d (13.87 kg/h) was with 15% H_2 addition at 30 kW power. With same fuel mixture the B_d = 16.546 kg/h at 50 kW power and B_d = 23.384 kg/h at 100 kW. Comparing with CNG that was 4.12%, 3.41% and 3.21% lower, respectively. Highest BSFC decrease was observed with same CNG + 15% H_2 fuel mixture at different power regimes.

Calculations revealed that highest thermal efficiency was achieved with CNG + 10% H_2 fuel mixture at three different obtained power loads. It was 1.17% (η_e = 0.17) at 30 kW, 0.42% (η_e = 0.237) at 50 kW and 0.30% (η_e = 0.335) at 100 kW higher comparing with CNG values (η_e = 0.168, η_e = 0.236, η_e = 0.334 according to mentioned loads).

Table 3.3. Heavy duty vehicle *Castrosua* testing modes with natural gas / hydrogen fuel mixtures

Gaseous fuel	Engine speed, rpm	λ	Load on wheels, kW		
CNG	1500	1.0	30	50	100
CNG + 5% H_2					
CNG + 10% H_2					
CNG + 15% H_2					
CNG + 20% H_2					

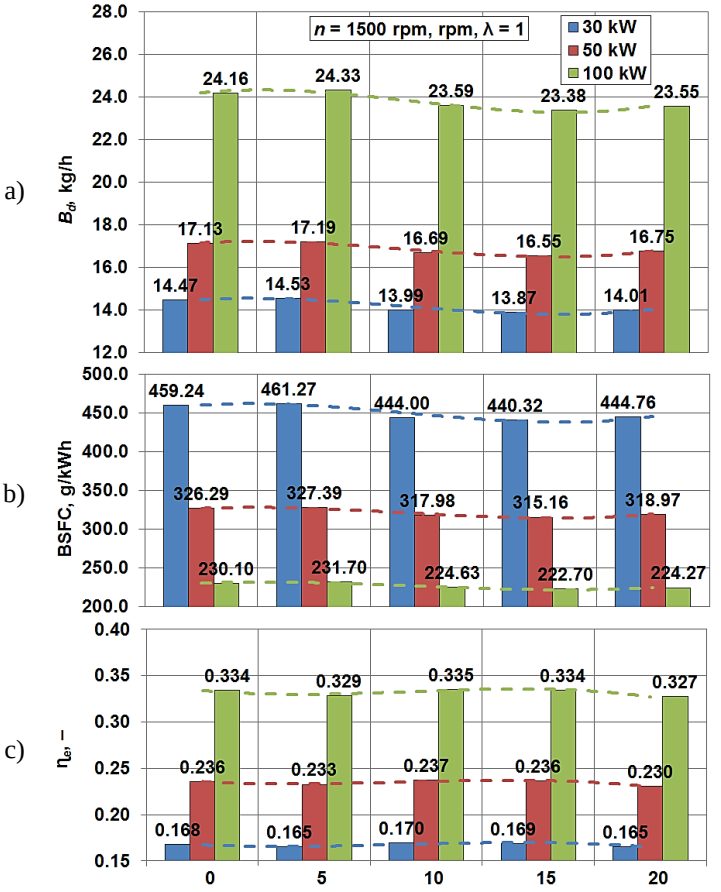

Fig. 3.28. Dependence of engine indicators on different tested loads and natural gas / hydrogen fuel mixtures: a) fuel consumption, b) brake specific fuel consumption, c) thermal efficiency.

The lowest η_e was for fuel mixtures with 5% H_2. However, results revealed that the η_e changes were minor and CNG / H_2 made insignificant influence on engine efficient work.

The exhaust gas emission variation due to different CNG / H_2 fuel mixture at different tested loads is presented in Fig. 3.29.

The concentration of CO with CNG fuel was ~ 0.58%. With increasing H_2 volume in the fuel mixture the CO emissions were decreasing at all power points. The lowest CO emission was achieved with 20% H_2 addition at 100 kW point (0.473%). It was 18.86% lower if compared with CNG case at same testing point (0.580%).

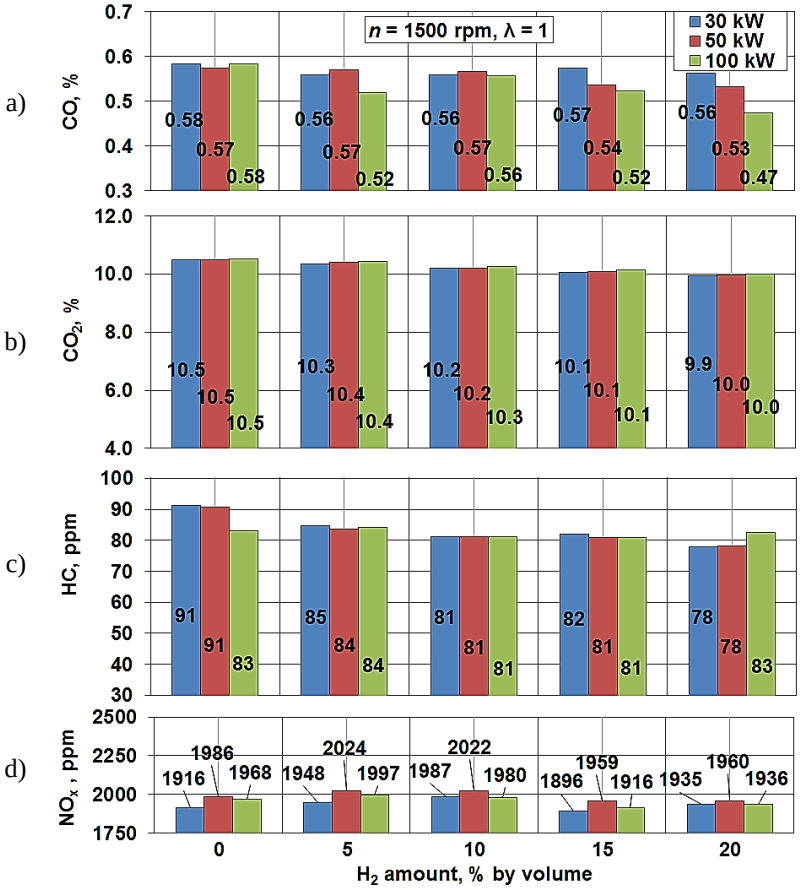

Fig. 3.29. Exhaust gas emission dependence on different tested loads and natural gas / hydrogen fuel mixtures: a) CO emission, b) CO_2 emission, c) HC emission, d) NO_x emission

The CO_2 emission was also decreasing steadily with increasing volume of H_2 in natural gas fuel. The CO_2 emission (10%) was 5.03% lower than using pure CNG (10.53%) with 20% H_2 addition at 100 kW power. Such emission was lowest from all tested engine loads. The CO and CO_2 emission decrease was possibly influenced by a better combustion process due to H_2 additive. What is more the H/C atom ratio in the fuel was bigger, less carbon element was present in gaseous fuel, and therefore less CO and CO_2 were formed.

The HC emission was also decreasing steadily at all load points with increasing H_2 amount in the fuel. This was also resulted because of H/C atom ratio changes in the fuel mixture and better combustion characteristics.

It should be noted that H_2 influence on NO_x emission formation was minor with increasing H_2 amount. The highest increase (2022 ppm) was observed with 10% of H_2 at 50 kW power. Comparing with CNG case (1986 ppm) at same load point it was just 1.82% higher. It was possible to achieve even lower NO_x emissions at all load points and increasing amount of H_2. For example, at 50 kW load point the 15% H_2 gave 1959.3 ppm comparing with 1985.7 ppm CNG case. That was 1.32% lower. It should be also noted that these results are different from results obtained with 4 cylinder *HR16DE* engine, where the NO_x formation was obviously increasing with increased H_2 volume in the fuel mixture. Since the heavy duty engine had an EGR system which returned some part of exhaust gas to the cylinder, the combustion temperature decreased. This resulted in stable NO_x emissions with all tested fuel mixtures although the H_2 concentration increased in the fuel mixtures. Dimapoulous *et al*. (2007) also stated that with optimal EGR and CNG / H_2 fuel mixture it is possible to achieve lower NO_x emissions. It was also noticed that NO_x emission was lower – even 15–20% in other research works (Raman *et al*. 1994; Raman 1997; Mhy Bus 2009).

3.7. Experimental Investigation of Methane Direct Injection System

Experimental tests were carried out using *AVL* optical single cylinder engine which has a possibility to observe a combustion process through the piston top – bottom view and cylinder liner – side view. Also other parameters like B_d, IMEP, p_{cyl}, CoV_{IMEP} and ISFC were measured or calculated.

During experiments pure (100%) CH_4 was used. Different engine speeds and loads were tested in order to get a better understanding about different combustion types with DI gas system. The combustion types were: homogeneous stoichiometric with stable $\lambda = 1$ value, homogeneous lean burn with stable $\lambda = 1.4$ value and stratified lean burn with λ value above 2. Different engine loads (~2.5, ~3.5 and ~5 bar IMEP) were tested at different engine speeds (1000, 1500 and 2000 rpm). Such experimental investigation plan was able to fulfill analysis of combustion on both low speeds and higher engine speeds.

Gas fuel injection timing (start of injection SOI) for stoichiometric cases were the same 280 CAD bTDC in all engine loads and speeds. The lean burn cases had 220 CAD bTDC and stratified cases had variable injection timing (depending on stratified case it varied from 36 to 65 CAD bTDC) in order to get proper stratification and enough stable combustion which could reach desirable load. The injector was electronically controlled from a *LabView* DI system module. The injector

current peak values (A), power supply voltage (V) and injector opening time (injection duration) in milliseconds (ms) was adjusted and optimized to get aimed points.

The intake air pressure had to be adjusted with throttle valve in order to reach desirable λ values at different loads for homogeneous stoichiometric and homogeneous lean burn cases. The stratified cases were run on wide open throttle (WOT).

3.7.1. Methane Direct Injection Tests at Different Engine Speeds and Loads

Intake air pressure and compression pressure measurements showed that in order to achieve stoichiometric combustion it had to be unthrottled. Lean burn and stratified combustion need more air, therefore it had to be throttled or even used WOT (Annexes Table B.1).

The injection duration shows that the shortest time for injection was needed for lean burn combustion (0.85, 1.07, 1.37 ms) for 2.5, 3.5 and 5 bar IMEP respectively. It was shorter than for stoichiometric combustion (0.96, 1.42, 2.4 ms) because the λ target was 1.4 in lean burn cases (Annexes Table B.1). It can be also seen from the intake pressure and compression pressure that more air was in taken into the cylinder.

The longest injection duration was achieved by stratified combustion (1.7, 2.3 and 3.1 ms respectively to mentioned loads above) (Annexes Table B.1). In order to achieve required load, the certain E_c with the fuel has to be brought into the cylinder. As stratified combustion required injection during compression stroke, the backpressure was quite high during compression stroke in the cylinder. The methane DI injector pressure was 18 bar, therefore the pressure difference was lower and the injection duration had to be enough long to inject the required fuel mass.

Fig. 3.30 presents the dependence of ISFC, η_i and CoV_{IMEP} on different engine loads and speeds for three different combustion types. Low engine speed tests showed that at all load points the highest indicated efficiency was achieved for stratified combustion (0.375, 0.373, 0.340). The lean burn combustion was at the middle (0.300, 0.318, and 0.336) and the lowest η_i was for stoichiometric combustion (0.255, 0.290, and 0.320). Measurements also showed that the highest ISFCs was obtained with the stoichiometric combustion cases (282.4 g/kWh, 248.8 g/kWh, 225.3 g/kWh) and this was expected as the throttle losses then are the highest. The reduced pumping losses and lower heat losses of the homogeneous lean burn combustion reduced ISFC to 239.7 g/kWh, 226.3 g/kWh, 214.3 g/kWh as compared with stoichiometric. However, it was impossible to reach higher 5 bar IMEP load with lean burn combustion.

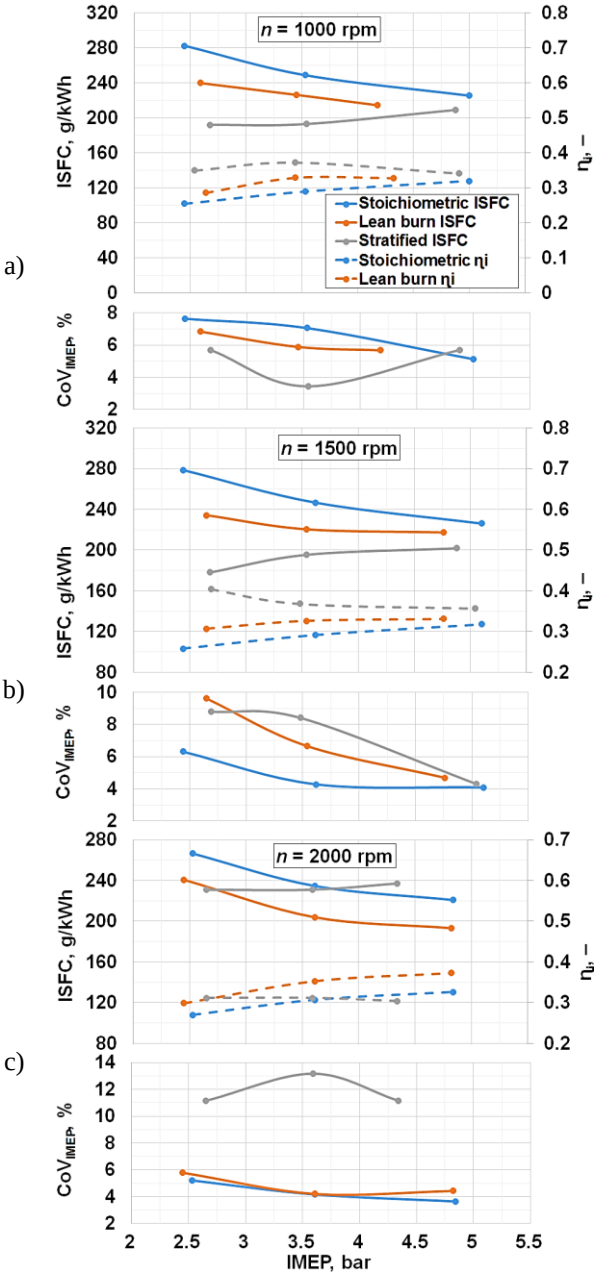

Fig. 3.30. Dependence of indicated specific fuel consumption, indicated efficiency and covariance of indicated mean effective pressure on different engine loads and speeds for three different combustion types: fuel 100% CH_4: a) n = 1000 rpm, b) n = 1500 rpm; c) n = 2000 rpm

Lowest B_d was obtained for stratified combustion as expected since there were no pumping losses at WOT and the heat losses were lower than in the stoichiometric cases. The ISFC were 192 g/kWh, 192.9 g/kWh, 209 g/kWh. Part of the lower heat losses are explained by the higher specific heat ratio during the compression stroke. If this indicated fuel consumption is multiplied by 1.18, P fuel equivalent values are obtained. Similar low specific fuel consumption tendency for stratified case with DI methane system was found by (Bohatsch 2011).

From the Fig. 3.30 can be seen that the η_i got lower and ISFC got higher for stratified combustion with increased engine load. Such behavior can be explained by increased E_c needed to achieve high loads and to achieve this, much more fuel is required. Therefore the injection timing had to be advanced and the injection duration had to be longer (Annexes Table B.1).

The best combustion stability (CoV_{IMEP}) was achieved for stratified cases. It was between 2.5–6%. Stoichiometric cases had 5.5–7.5% and lean burn cases had 5.5–7%.

The ignition timing had to be advanced with all combustion types at higher engine speed (1500 rpm) (Fig. 3.30 b)) in order to get enough time to ignite and combust the A/F mixture (Annexes Table B.1).

The start of injection for stoichiometric and lean burn cases remained the same, but for the stratified combustion the injection timing was advanced (42, 48 and 61 CAD bTDC for 2.5, 3.5 and 5 bar IMEP load) in order to have enough time to inject required fuel mass so that the engine loads could be achieved.

The injection durations for 1500 rpm were relatively lower comparing with 1000 rpm cases. It can be explained by lower heat losses because of less time due to higher engine speed.

Fig. 3.30 b) shows same tendency that with stratified case at 1500 rpm the η_i was highest (0.404, 0.368, 0.357) comparing with stoichiometric (0.258, 0.292, 0.318) and lean burn (0.307, 0.318, 0.336) at engine loads of 2.5, 3.5 and 5 bar IMEP accordingly.

The efficiency for stratified combustion started to drop with higher engine speed, although it was still higher than for stoichiometric and lean burn combustion. The ISFC values were getting higher with increased load in stratified cases (178.1 g/kWh, 195.4 g/kWh, 201.8 g/kWh). Again it can be explained by a need of more energy which should be brought with bigger fuel mass in order to achieve aimed engine load. The ISFC for stoichiometric combustion 278.7 g/kWh, 246.7 g/kWh, 226.1 g/kWh) and lean burn (234.3 g/kWh, 220.5 g/kWh, 217.4 g/kWh) were decreasing at higher IMEP.

The results showed that indicated efficiency for stratified combustion (0.312, 0.312, 0.304) was getting lower than for lean burn (0.299, 0.353, 0.373) at highest engine speed (2000 rpm) and at highest load were even lower than for stoichiometric conditions (0.270, 0.307, 0.326) (Fig. 3.30 c)). It was influenced by a

higher fuel consumption for stratified cases and the ISFC for stoichiometric and lean burn combustion were lower at higher loads comparing with stratified cases.

At highest engine speed the combustion stability for stratified combustion was very low. Diagrams shows that the CoV_{IMEP} was higher than 10% for all load points comparing with stoichiometric and lean burn which were between 3.5% and 6%.

3.7.2. Experimental Investigation of Spark Timing Influence on Engine Parameters with Direct Injection Methane System

In order to get better understanding about lean mixture combustion the investigation of spark timing influence on engine parameters was performed at 1500 rpm. Spark timing was changed from 30 CAD bTDC to 46 CAD bTDC for homogeneous lean burn combustion and from 28 CAD bTDC to 50 CAD bTDC for stratified combustion with 2 CAD step for both combustion cases (Fig. 3.31).

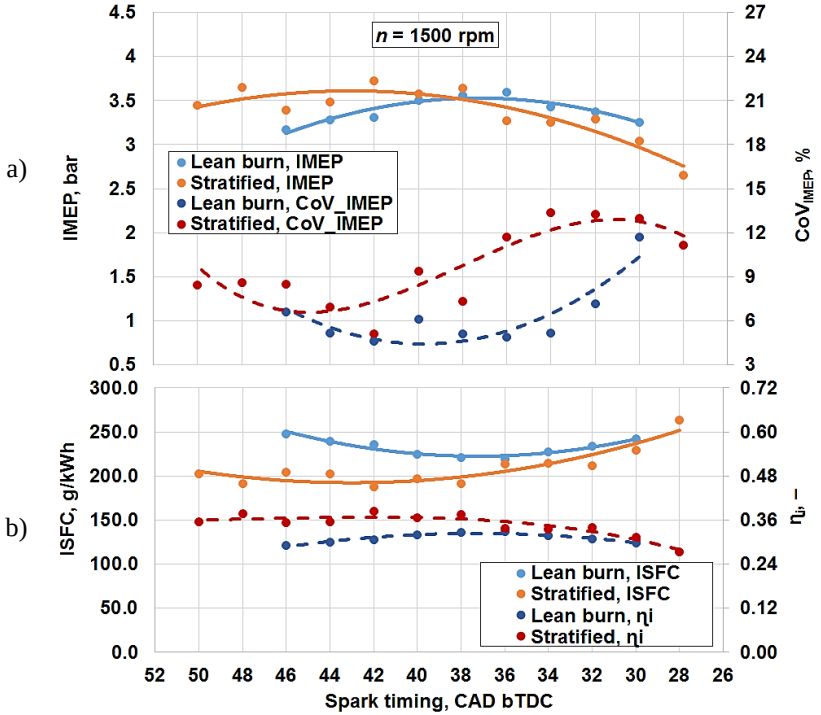

Fig. 3.31. Dependence of engine efficient parameters on spark timing and combustion type: a) indicated mean effective pressure and covariance of indicated mean effective pressure, b) indicated specific fuel consumption and indicated efficiency. Fuel 100% CH_4, n = 1500 rpm

The injection timing for lean burn was 220 CAD bTDC and for stratified type was 48 CAD bTDC. Fig. 3.31 shows that highest IMEP for lean burn combustion was obtained with spark timing at 36–38 CAD bTDC. Stratified combustion achieved mentioned parameters at almost similar CAD – 38–40 CAD bTDC. Methane did not have enough time to combust and achieve MBT with retarded spark timing therefore the IMEP was getting lower and the ISFC getting higher for both combustion types (Fig. 3.31).

Moreover, the retarded ignition timing influenced CoV_{IMEP} greatly. The coefficient for stratified case was more than 10% at ignition timing 24–36 CAD bTDC. Similar behavior observed for lean burn combustion. With more advanced angles than 40 CAD bTDC the ISFC started to increase for both combustions.

3.7.3. Air / Fuel Ratio Influence for Engine Parameters with Direct Injection Methane System in Lean Burn Combustion

The influence of A/F ratio coefficient (λ) on engine parameters is presented in Fig. 3.32.

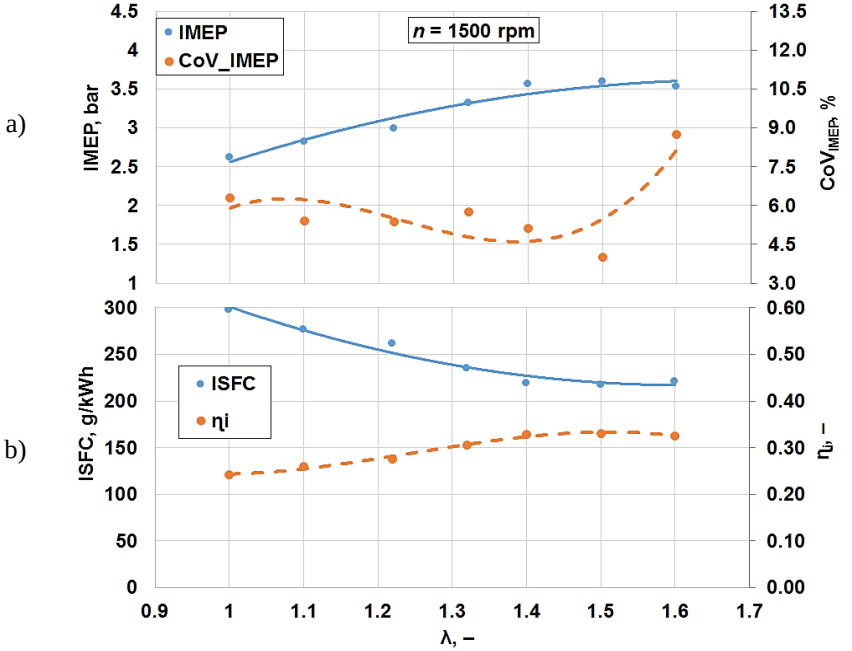

Fig. 3.32. . Dependence of engine efficient parameters on air / fuel ratio: a) indicated mean effective pressure and covariance of indicated mean effective pressure, b) indicated specific fuel consumption and indicated efficiency. Fuel 100% CH_4, n = 1500 rpm, lean burn combustion type

The homogeneous lean burn combustion type was tested at 1500 rpm engine speed with fixed injection timing 220 CAD bTDC, injection duration 1.07 and ignition timing 38 CAD bTDC. The A/F ratio was changed by throttle position which changed the air intake pressure.

The lowest IMEP and indicated efficiency was achieved when $\lambda = 1$. This point resulted also in highest ISFC (297.9 g/kWh). With leaner A/F mixture it was possible to achieve higher engine loads and lower ISFC. The lowest ISFC was achieved at $\lambda = 1.4$ and $\lambda = 1.5$. The indicated specific consumption was 217.4 g/kWh which was 27% lower comparing with $\lambda = 1$ case. The most stable combustion was possible to achieve (covariance of IMEP was around 4–5%) at mentioned λ value. The misfires started to occur and the CoV_{IMEP} was higher than 8% with leanest mixture ($\lambda = 1.6$). Also the ISFC was a little higher (221.1 g/kWh) comparing with $\lambda = 1.4$ and $\lambda = 1.5$. The same operation tendencies with lean burn engines were presented by Wartsila engine manufacturer (Wartsila Corporation 2015). Thermal efficiency can be increased when A/F ratio is adjusted to lean mixtures, especially with ultra-lean mixture (λ value 2.1–2.3). At such λ values high engine loads can be also obtained if misfire or knock is not appearing.

3.7.4. Injection Timing and Injection Duration Influence on Engine Parameters with Stratified Combustion Type

To get a better understanding about injection timing influence on engine efficiency in stratified combustion different injection timings were tested. Injection timing was changed from 32 CAD to 46 CAD bTDC for 1000 rpm and from 40 CAD to 56 CAD bTDC for 1500 rpm with 2 CAD step for both investigation cases. Spark timing remained the same in all tested cases. Ignition timing was 28 CAD bTDC at 1000 rpm and for 1500 rpm it was 38 CAD bTDC. The injection duration also remained the same for all injection timings. For 1000 rpm it was 2.4 ms and for 1500 rpm it was 2 ms.

Fig. 3.33 shows that at 1000 rpm highest IMEP can be achieved with 42 CAD bTDC and for 1500 rpm with 50 CAD bTDC. For 1000 rpm IMEP was 3.78 bar and for 1500 rpm it was 3.67 bar. In overall higher IMEP values were obtained with more advanced injection timings. It can be explained by a bigger injected fuel mass with more advanced angles. Fuel flow and λ values support this proposition. The fuel as injected during compression stroke in stratified combustion. The earlier injection timing was, the less compression pressure achieved, which resulted in lower backpressure. Therefore more fuel can be injected during the same injection duration comparing with retarded angles. The later fuel was injected, the bigger backpressure was achieved and it was hard to inject sufficient fuel mass into the cylinder.

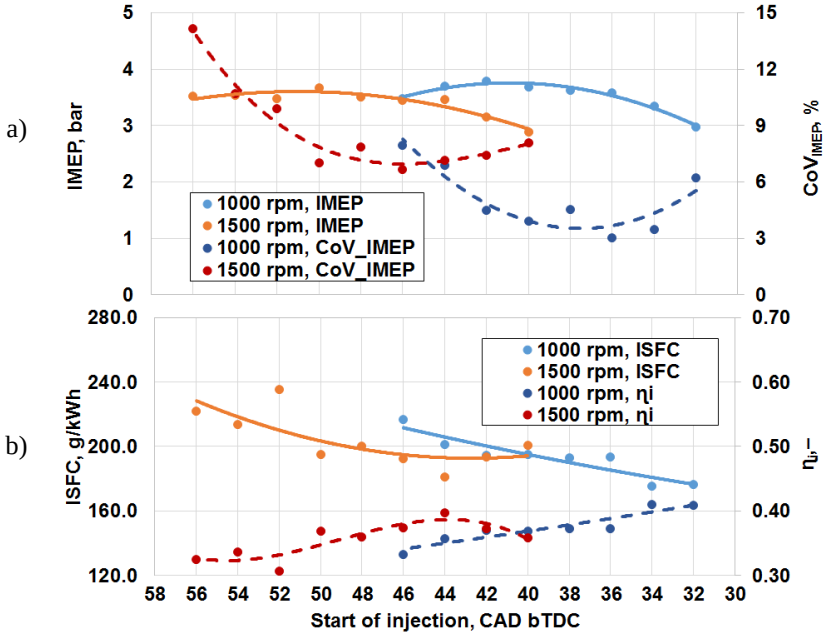

Fig. 3.33. Dependence of engine efficient parameters on start of injection and engine speed: a) indicated mean effective pressure and covariance of indicated mean effective pressure, b) indicated specific fuel consumption and indicated efficiency. Fuel 100% CH_4, stratified combustion type

Measured λ values prove this. λ values were 2.7–2.8 at late injection that means more air was present in cylinder than fuel. λ values got lower and achieved bellow 2 with advanced injection angle.

Although it is possible to achieve much higher IMEP with earlier timings, the combustion stability was getting worse. CoV_{IMEP} graph shows that the combustion stability coefficient was higher at highest achieved IMEP. In order to achieve most stable combustion injection timing has to be 36–38 CAD bTDC at 1000 rpm and 46–48 CAD bTDC. Such timing let to achieve relatively stable combustion without significant loss of engine power.

The very late injection timing (less than 32 CAD bTDC for 1000 rpm and less than 40 CAD bTDC for 1500 rpm) could not be achieved because misfires started to occur. This was resulted by not enough injected fuel before the ignition. The time between injection timing and spark timing was just 2 CAD. Therefore the dual coil system was not able to ignite mixture.

Fig. 3.34 can add more information about the backpressure influence on the injected fuel mass. This figure shows how the fuel flow and IMEP correlates with

start of injection and when the λ value 2.2 kept constant at 1500 rpm. Injection duration was adjusted in order to keep the same λ value.

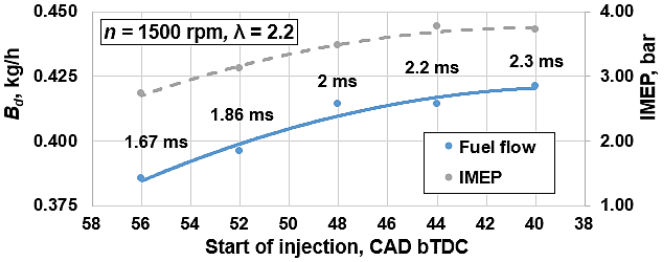

Fig. 3.34. Dependence of fuel flow and indicated mean effective pressure on start of injection when λ maintained const. by changing the injection duration (ms): fuel 100% CH_4, n = 1500 rpm, spark timing 38 CAD bTDC, λ = 2.2

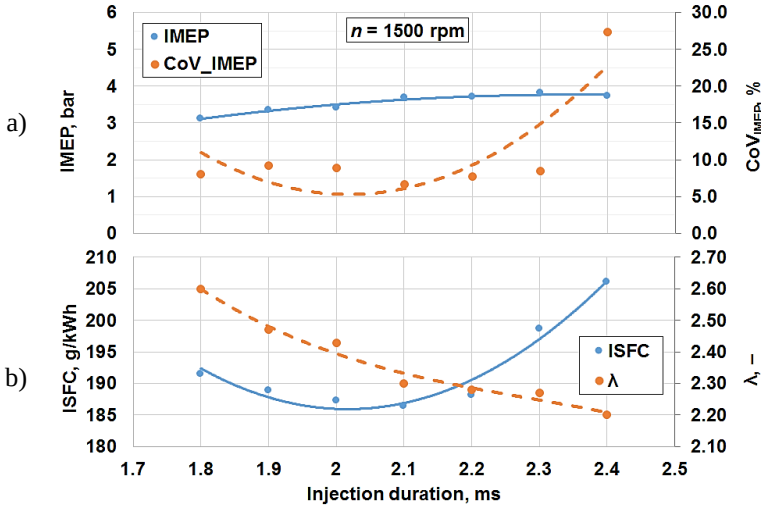

Fig. 3.35. Dependence of engine efficient parameters and combustible mixture on injection duration: a) indicated mean effective pressure and covariance of indicated mean effective pressure, b) indicated specific fuel consumption and air / fuel ratio. Fuel 100% CH_4, n = 1500 rpm, spark timing 38 CAD bTDC, injection duration 42 CAD bTDC

The backpressure got higher with later injection timing (40 CAD bTDC), therefore the injection duration had to be longer (2.3 ms) in order to achieve desirable λ. It is obvious that the backpressure was getting lower and the injection duration can be shortened with the most advanced injection timing (56 CAD bTDC) because there was no resistance for the fuel flow coming from the injector.

Fig. 3.35 shows the injection duration influence on engine efficient parameters. The injection duration was changed from 1.8 ms to 2.4 with 0.1 ms step. Engine speed was 1500 rpm, start of injection 42 CAD bTDC, spark timing 38 CAD bTDC. It was possible to achieve 3.12 bar IMEP with short injection timing (1.8 ms). At this point the fuel flow was the lowest but the ISFC was higher (191.4 g/kWh) comparing with longer injections. The λ value at this point was 2.6. The CoV_{IMEP} was 8.09 and it was relatively high. Almost highest ~ 3.8 bar IMEP was achieved with longest injection duration (2.4 ms), but the fuel flow and ISFC was highest. It also resulted in higher CoV_{IMEP}.

It can be explained by inefficient combustion because the ignition system was not able to ignite big amount of fuel at a later part of combustion. Best stable combustion with lowest ISFC and highest indicated efficiency was achieved with 2.1 ms injection duration when λ value was 2.3.

3.7.5. Stratified Combustion Cylinder Pressure and Heat Release Analysis

Since the stratified lean burn combustion is most promising due to lowest fuel consumptions and heat losses in cylinder, deeper combustion process analysis will be presented further.

Cylinder pressure and heat release analysis were performed for the stratified case at 1000 rpm, engine load 3.5 bar IMEP. Cylinder pressures were sampled for 50 combustion cycles. The cylinder pressure data were analysed using *MATLAB* software. The cylinder pressures for the 50 cycles together with a cycle-averaged mean value are shown in Fig. 3.36. The spark timing was 28 CAD bTDC.

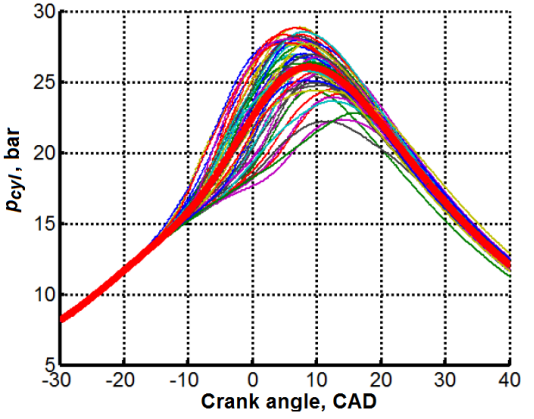

Fig. 3.36. Cylinder pressure traces with cycle-averaged mean value (thick red line) from 50 measured cycles for the stratified combustion case. Spark timing 28 CAD bTDC

The peak value of the mean pressure was obtained about ~ 9 CAD aTDC and the average peak pressure was 26 bar. Clearly, cycle-to-cycle variations are quite large and it is difficult to achieve really stable combustion. Similar issues with higher CoV_{IMEP} were faced by (Baratta *et al*. 2015) when late natural gas injection and fuel stratification were used.

CoV_{IMEP} is one of the parameters which is important for the drive ability of the vehicle. It was stated that CoV_{IMEP} values above 10% would give poor drivability (Haeng *et al*. 2007; Tadesse *et al*. 2009; Heywood 1988). This research results show that CoV_{IMEP} is lower than 10% for all combustion types. The stoichiometric and homogeneous lean burn resulted in a CoV_{IMEP} between 5 and 6%, which is considered as fairly stable combustion. These combustion modes were only included for comparisons of the fuel consumption. For the stratified case the start of injection of the fuel was late during the compression stroke, 36 CAD bTDC.

Different injection timings and spark timings were tested to achieve the most stable combustion. At the tested relatively low engine speed (1000 rpm), CoV_{IMEP} was 3.8% which can be considered as stable combustion. Variations in flow motion can be the major cause of the cyclic variations in combustion. Flame growth rate and the rate of early turbulent flame development are affected by the change in the local turbulence intensity and scales from one cycle to another. Higher cycle-to-cycle variability is achieved with very lean mixtures. Moreover, it is known that the mixture of methane and air has low burning speed comparing with petrol and air mixture. This resulted in lower flame propagation, occurrence of misfire, low mixture distribution quality (Haeng *et al*. 2007; Tadesse *et al*. 2009). In (Wang *et al*. 2007) research natural gas was injected at 18 bar with DI injector and they found CoV_{IMEP} between 1% and 6%.

In an experimental investigation of mixture formation and performance in a DI CNG engine was performed and it was shown that great cycle-to-cycle variation of the jet shape is apparent, even under steady-state engine operating conditions and fixed injection setups (Baratta *et al*. 2012). It was stated that combustion stability is influenced by mixture stratification at spark timing which varies from cycle-to-cycle.

The RoHR was calculated from the cylinder pressure traces and the result for the 50 combustion cycles together with a cycle-averaged mean value is shown in Fig. 3.37.

Here it is obvious that the combustion differs greatly between the different cycles. The RoHR has similarities to the heat release rate from a stratified system where liquid fuel is injected. Here, obviously there is no negative heat release rate when the fuel is injected as no fuel needs to be vaporized, in contrast to stratified systems with liquid injection where negative heat release rate is always present at the time of the fuel injection (Hemdal *et al*. 2011; Dahlander *et al*. 2015). The

similarities are instead that the heat release rate in the beginning of the combustion is generally higher than in the later part of the combustion. A well-mixed or premixed combustion system does not look like this, so the high cycle-to-cycle variations are due to variations in the A/F mixture. It is a known problem that it is difficult to mix gas-into-gas. The problem is that a gaseous fuel has less momentum than a liquid injected into air resulting in a poor penetration and momentum exchange between the fuel and air. Similar issues were found by Zoldak (2015) where the high density levels in combustion chamber result in strong aerodynamic drag and the injected plume loses its momentum, resulting in poor fuel penetration. The A/F mixture can vary greatly resulting in heat release curves that goes up and then down and then goes up again. The issue here is that there could be rich mixture present and this inevitably results in mixing controlled combustion with local rich conditions and therefore particle formation, as will be shown and supported by the combustion images and emission spectrum later. Fig. 3.38 shows relationship between combustion initiation timing and combustion phasing CA50 for the same data set.

CA10 (CAD where 10% of fuel mass burned) was plotted against CA50 (CAD where 50% of fuel mass burned) for each combustion cycle. The cycle-to-cycle variations are fairly high. The mean value of these individual combustion phasing's correspond to what is referred to as the combustion phasing. Fig. 3.38 shows that there is a correlation between CA10 and CA50, which means that in order to achieve a more stable combustion (cycle-averaged mean value of CA50s), the spread in CA10 must be smaller.

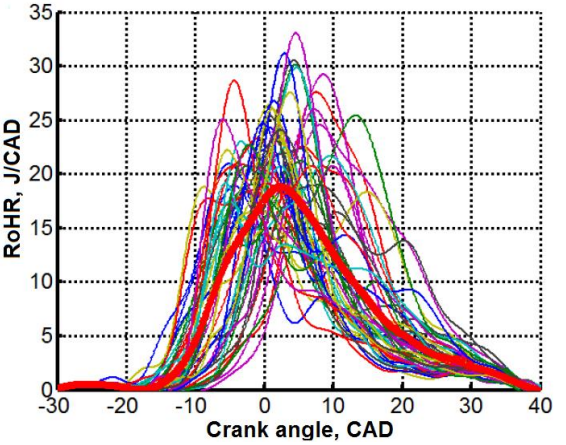

Fig. 3.37. Rate of heat release curves obtained from stratified combustion

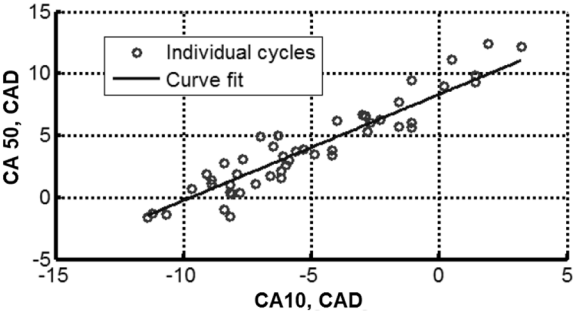

Fig. 3.38. Correlation between CA10 and combustion phasing CA50 of stratified combustion cases

The combustion phasing (mean value of individual value CA50) was 4.0 CAD aTDC.

3.7.6. Emission Spectroscopy

Using UV visible natural flame emission spectroscopy it is possible to get information about the presence of the typical species produced during the combustion process, which are indicative of the reacting conditions in the flame (Di Iorio *et al*. 2014). Emission spectroscopy was therefore performed to support the analysis of the combustion images. Flame radiant emission is agreed to be a combination of black body radiation from soot and chemiluminescent emission from electronically excited species: OH* (306.4 nm); CH* (431.5 nm); C_2 (516.5 nm) and CO_2 (broadband emission 340 to over 650 nm) (Pearse 1963).

In (Gupta *et al.* 2011) it was found that natural gas is clean burning and that the radiant emission is predominantly due to chemiluminescence. The emission spectrum were dominated by OH* and CO_2, whereas CH* and C2* had insignificant contributions (Gupta *et al*. 2011). Investigating gaseous fuels (methane and hydrogen blends) UV-visible spectroscopy showed radical species such as CN* and NH* at the spark timing, together with OH* and a background of CO_2 (Di Iorio *et al*. 2014). Later during the combustion OH* was the dominating peak on top of the broad feature of CO_2 and possibly HCO* and CH_2O* emission, while the CH* peak was very weak. In liquid fuel combustion at rich conditions, e.g. in diesel combustion, radiation from soot particles is dominated. The intensity of radiation from a black body vary with wavelength and temperature of the black body according to Planck's equation (Zhao *et al*. 1998).

Emission spectrum images were captured and from those, the emission spectrums were calculated by extracting data along a band (20 pixel rows) passing through the spark plug area, thus in the middle of the cylinder. The purpose was

to identify species and investigate the wavelength of the peaks over time. The results are shown in Fig. 3.39 to Fig. 3.41, where the emission spectrum for stratified combustion at three different time steps are presented: when the spark plasma occurs, when OH* starts to appear and when mixing controlled combustion is dominating and therefore soot formation occurs, respectively.

The average spectrum from 10 cycles does not clearly represent different species formation due to high cycle-to-cycle variations so the emission spectrum shown is from one combustion cycle. When the spark plasma starts (25.7 CAD bTDC), a clear CN* peak at ~ 370 nm can be observed, see Fig. 3.39.

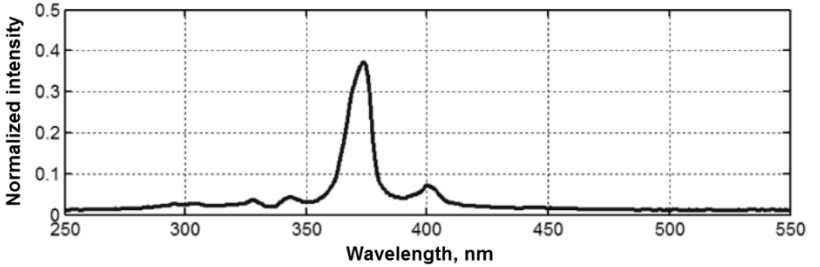

Fig. 3.39. Emission spectrum at 25.7 CAD bTDC. The spark plasma emits a distinct CN peak at around 370 nm

Together with the main CN* peak two more peaks from the violet band system can be observed at ~ 340 and ~ 405 nm (Robinson 1974) and a small peak, likely from NH* can be noted at ~ 330 nm. Synchronized High-speed color camera images and emission spectrum images were compared showing that the CN* peak was present for 5 ms and disappeared exactly when the spark plasma in the images disappeared. The long spark plasma duration of 5 ms is due to the dual coil ignition system.

The wavelengths were calibrated carefully with a Mercury lamp, but intensity calibration was not performed since the purpose was to investigate the wavelengths of the peaks. The intensity, on the other hand, of the CN* peak is govern by for example the A/F ratio, spark energy etc. and have been investigated in eg. (Fansler *et al*. 2002).

Later during the combustion, at 2.2 CAD bTDC, a clear high peak centered around 308 nm is seen, see Fig. 3.40. This peak is due to OH* and is typically found in high-temperature hydrocarbon combustion. The strong CN* peak and its satellites can still be observed. Less obvious is the emission from CO_2, here seen as a background like structure from 420 to 550 nm but also present under the CN* peaks. This broadband CO_2 emission is what the color video camera detect as blue light in the absence of soot radiation. Neither CH* peaks around 430 nm nor C_2* Swan band peaks around 460 and 520 nm could be observed. This is consistent

with previous investigations of natural gas / methane combustion (Di Ioro *et al*. 2014; Gupta *et al*. 2011), although the peaks often occurs in SI combustion with petrol as fuel (Hemdal *et al*. 2011; Catapano *et al*. 2013).

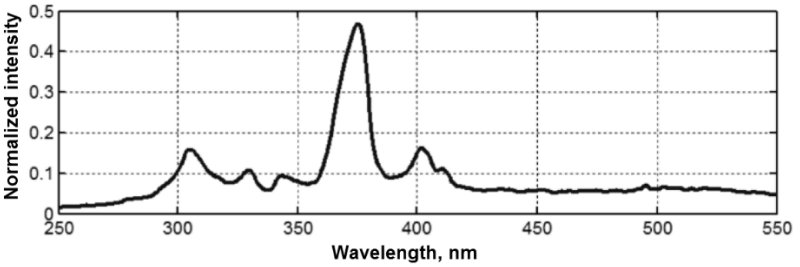

Fig. 3.40. Emission spectrum at 2.2 CAD bTDC showing OH* radicals at around 308 nm, CN* from the spark plasma at 370 nm, CO_2 presence in a range from 420 nm to 550 nm

At an even later combustion stage, 7.5 CAD aTDC soot starts to appear and this is seen as black body radiation, see Fig. 3.41.

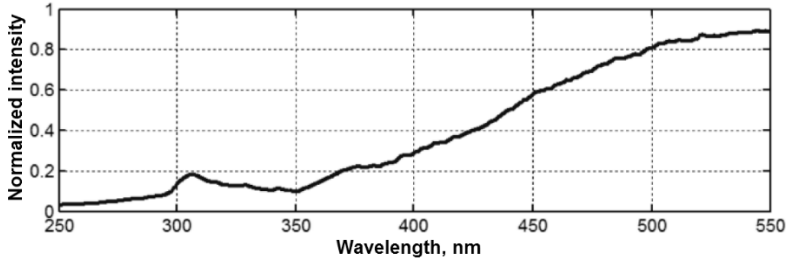

Fig. 3.41. Emission spectrum at 7.5 CAD aTDC. The signal intensity from hot burning soot particles is here completely dominating and the contribution from OH* radicals is relatively weak

The soot radiation is here very intense and the emission spectrum is accordingly dominated by a rising intensity from ~ 350 to 550 nm. This result can be explained by fuel-rich zones in the cylinder which causes mixing-controlled combustion and therefore soot. The OH* peak can still be clearly seen, while the CO_2 luminescence is hidden under the much stronger soot radiation (due to the broad peak and spectral overlap).

To summarize the emission spectrum analysis, CN* is seen from the spark plasma, slightly later OH* starts to occur in the flame along with broadband CO_2 emission, which is detected as blue light emission by the color video camera, whereas the UV emission of CN* and OH* is invisible to the color camera. Later

an intense yellow flame occurs as a result of thermal radiation from hot soot particles occurring at longer wavelengths than the chemiluminescence (Di Ioro *et al*. 2013).

3.8. Combustion Image Analysis

Images of the spark plasma and the whole combustion event were filmed with two different camera views, one through the quartz glass piston top (below view) and the other through the pent-roof window from the side (side view). Using two different cameras views enables identifying the location of the sources of particle formation which otherwise would not have been possible with only one camera view.

The combustion was filmed under 50 combustion cycles. Under these cycles the temperature of the piston top and the cylinder head surfaces increase. This limitation, always present in an optical engine, which has a minor effect on the results. This means that the results are not dependent on which cycles of the 50 combusting cycles the results are based on.

3.8.1. Spark Deflections

In stratified combustion systems, in the vicinity of the spark plug, the A/F ratio can vary greatly from cycle-to-cycle at the time of the ignition. Within each cycle it can vary between lean to rich conditions in both time and space. The reason is primarily the lack of mixing time but here it can also be due to the difficulty of mixing two gases (methane and air). One solution to achieve stable ignition under these conditions is to use a dual coil ignition system and such a system was used here.

The spark plasma is here greatly influenced by in-cylinder gas motion giving arise to dramatic, highly stochastic spark plasma deflections, see Fig. 3.42.

Such spark plasma deflections also makes the influence on better combustion stability because the plasma has surface fluctuations with combustible mixture and it is possible to ignite A/F mixture at different combustion chamber areas.

The dual coil ignition system gives a spark plasma which is available over a much longer time period than for a single coil ignition system. During the same combustion cycle, the plasma can occur between the middle electrodes and all three side electrodes as well as being greatly deflected, see Fig. 3.43.

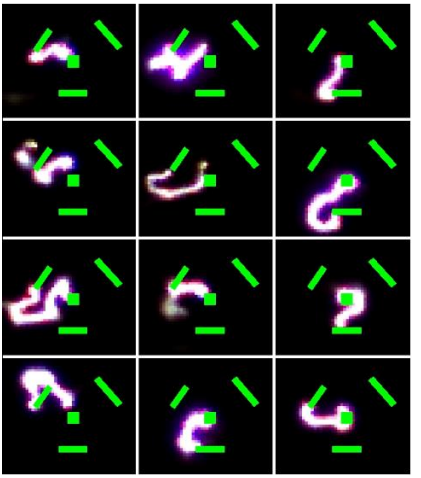

Fig. 3.42. An example of the stochastic spark plasma deflections from the dual-coil ignition system at 13 CAD bTDC

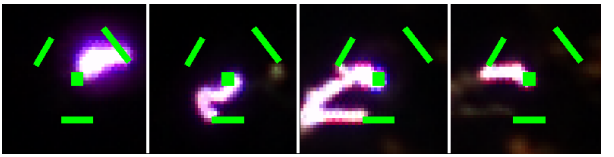

Fig. 3.43. Spark plasma deflections from the same combustion cycle at different timings

Thus, under its long lifetime, the plasma covers a great area. This is advantageous here since the A/F ratio in all stratified combustion systems varies around the spark at the time of ignition and since there are no misfires here, the plasma has found ignitable mixtures in all cycles.

3.8.2. Images through the Optical Piston – Below View

The images presented below are taken through the quartz glass piston top and are here denoted as below view images. Fig. 3.44 shows combustion images through the piston top at 1.6 CAD bTDC (26.4 CAD after spark timing).

The color scale has here been adjusted and gained in order to enable visualization of the weak blue signal. As seen, there is a mixture between well-mixed blue flame and yellow soot luminescence (mixing controlled combustion). This supports that the mixing between the air and fuel here is not sufficient to create a pre-mixed flame only. The blue flame is generally surrounding the areas where the soot has already begun to form. This early soot formation is occurring closer

towards the center. There are large cycle-to-cycle variations in the combustion. In some cycles, soot formation has already started to appear. The cycle-to-cycle variations are also supported by the cylinder pressure data, see Fig. 3.36. The reasons for the variations could be variations in the air flow, shot-to-shot variations in the injected methane as well as A/F mixing problems. Baratta (2015) noted that combustion stability was influenced by mixture stratification at spark timing. Other factors that can influence the variations in the mixture formation are the engine chamber geometry, especially the piston shape as well as the injector nozzle geometry.

From the emission spectroscopy, as it was mentioned before, from the early part of the combustion OH* radicals are present at around 308 nm, CO_2 is being formed according to the spectrum analysis in the range 350 nm to 550 nm. In the later part of the combustion soot luminescence is dominating (yellow / white in the images) and it is shown in the wavelength spectrum, see Fig. 3.41, as black body radiation. The well-mixed part of the combustion, blue parts in the images, continues and disappears at around ~ 26 CAD aTDC (~ 54 CAD after ignition timing) and after that the combustion is entirely dominated by mixing controlled combustion which is seen as soot luminescence.

Fig. 3.45 shows combustion images at a later stage, 41.6 CAD aTDC (69.6 CAD after ignition timing).

Here, the well-mixed (blue) part of the combustion is gone and only soot luminescence can be observed. After this, flame radiant emissions – soot is being present or formed, see Fig. 3.45. Soot formation typically occurs under fuel-rich conditions and at temperatures from around 1400 to 2000 K. This means that is here not possible to achieve a well-mixed A/F cloud. This results in mixing controlled combustion with too rich mixtures. Soot luminescence occurring especially during late stages of stratified combustion is not favorable and should be avoided since the temperature decreases and the oxidation slows down, resulting in increased PM emissions (Hemdal *et al*. 2013; Johansson *et al*. 2013). High temperature burning carbon particles appears as yellow-white color. As the flame temperature decrease, the radiation from the soot particle changes color through orange to red (Carlucci *et al*. 2010). During the expansion stroke, soot temperature reduces and therefore gives a lower signal making it difficult to visualize lower temperature soot.

The amount of soot luminescence in Fig. 3.45 differs less between the different combustion cycles than compared to earlier stage combustion, see Fig. 3.44. Analysing the cycle-averaged images show that the soot luminescence is slightly higher in south west direction of the spark plug, towards the exhaust valve.

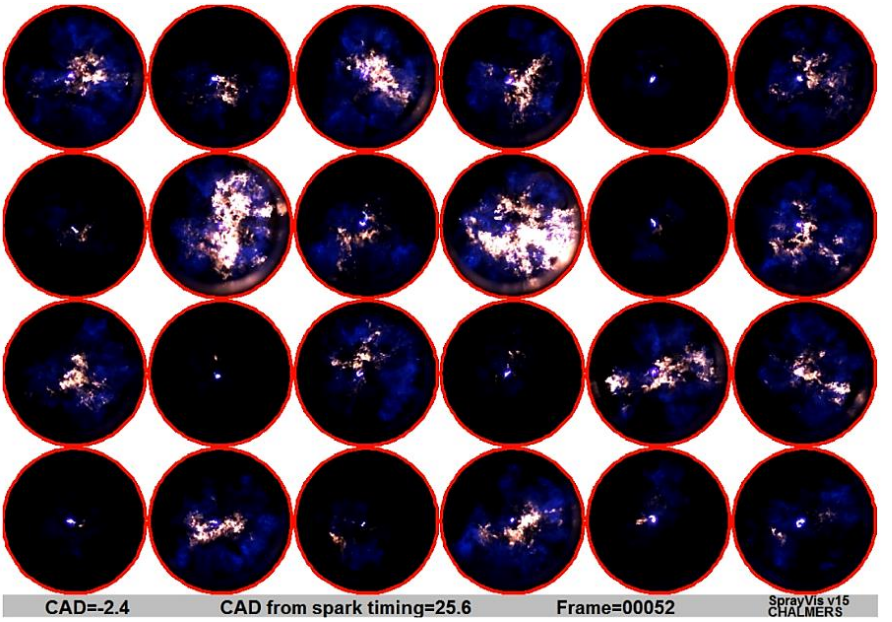

Fig. 3.44. Combustion images representing the early part of the combustion at 1.6 CAD bTDC (26.4 CAD after spark timing). 24 randomly selected combustion cycles. View through the piston

The reason for this is likely a combination of in-cylinder motion, mixing and turbulence in this very combustion geometry but this cannot be fully proved by the presented data.

Fig. 3.46 shows an example of the combustion where the well-mixed combustion, blue flame, is still present at 7.5 CAD aTDC. Also there is lot of soot formation at different locations.

This image was selected since it was filmed simultaneously with the spectrometer images and because it contains regions with blue flame with no soot (blue marked north of the spark plug), spark plug region with almost no blue flame and no soot (red marked) and finally a green marked area (south of the spark plug) where soot formation is dominating. Emissions spectrums were extracted from these three regions, from the corresponding spectrum image, and the result is shown in Fig. 3.47.

In all three regions there are OH* present in the combustion. This cannot be seen by the high-speed camera capturing the combustion images due to the short wavelength. The green spectrum represents the soot formation region south of the spark plug. It shows a typical curve for black body radiation (hot soot particulates) where the intensity increases with wavelength. It however also contains an OH* peak.

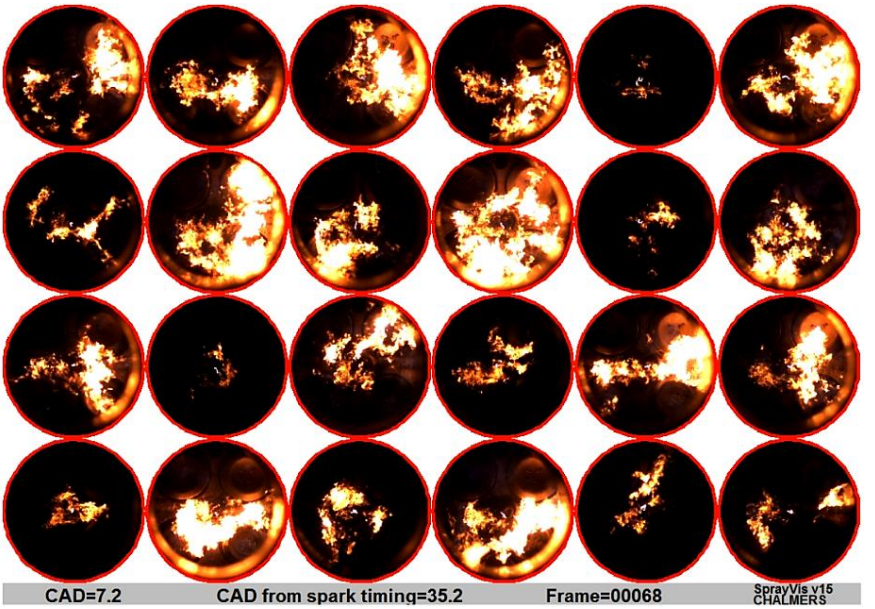

Fig. 3.45. Combustion images representing the later part of the combustion at 7.2 CAD aTDC (35.2 CAD after spark timing). 24 randomly selected combustion cycles. View through the piston

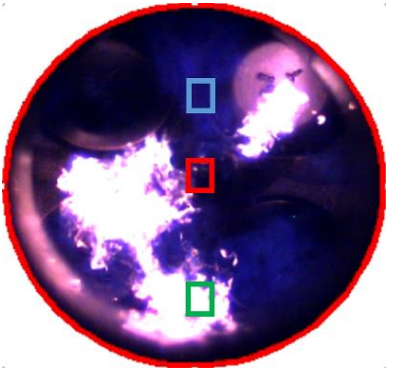

Fig. 3.46. Combustion image example at 7.5 CAD aTDC in which 3 different combustion areas have been color marked

The blue spectrum representing the blue flame from the area north of the spark plug has a weak broad band spectrum and an OH* peak. The weak broad band spectrum does not really increase with wavelength and therefore occurrence of blue flames means that there is no soot formation. The red spectrum representing the spark plug area is in general very weak here at this timing but it also has

an OH* peak. Since the blue flame has such a weak intensity over a wide wavelength range, regions with soot formation could also contain blue flames, but this cannot be proved due to the spectrum overlap with a strong black body radiation.

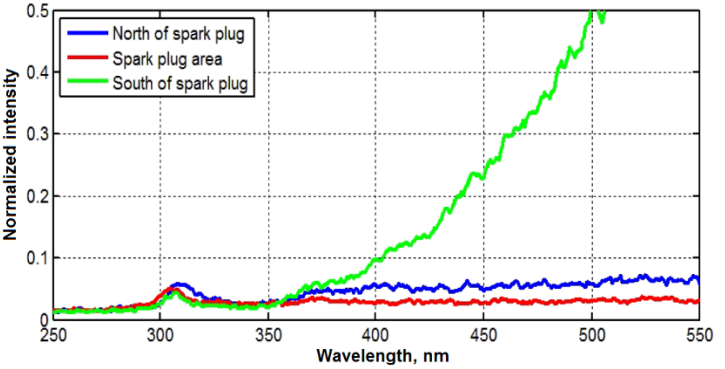

Fig. 3.47. Emission spectrum extracted from the three colors marked regions in Fig. 3.46

At an earlier stage of the combustion, CN* was observed in the vicinity of the plasma from the spark plug, as shown in the emission spectroscopy section. However, CN* was not present elsewhere in the combustion.

3.8.3. Images through the Pent Roof Window – Side View

The images presented here are taken through the cylinder liner's pent-roof window and the camera view is shown in Fig. 3.48. These images are denoted as side view images. An Ametec Vision Research Phantom Miro M310 camera with a Nikon 105 mm f/2 lens was used for the side view combustion images.

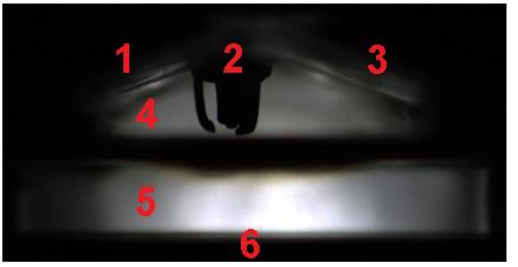

Fig. 3.48. Camera view for side view images: exhaust valves (1), spark plug (2), intake valves (3), pent-roof glass (4), cylinder liner glass (5) and piston (6)

Fig. 3.49 shows the combustion at a later stage, 41.6 CAD aTDC (69.6 CAD after spark timing). This is from the same timing as the below view combustion images shown in Fig. 3.45. The image shows (Fig. 3.49) occurrence of soot luminescence and large cycle-to-cycle variations in the combustion from 9 randomly selected cycles. The cycle variations are occurring in both time and space. Cycle-averages (not shown here) show that soot luminescence is not dominating in any particular location. The location of soot luminescence thus varies greatly in space but show no obvious soot luminescence around the spark plug (jet-flame) which in liquid based stratified system sometimes can be the case if too much liquid droplet hit the spark plug (Dahlander *et al*. 2015; Johansson *et al.* 2013).

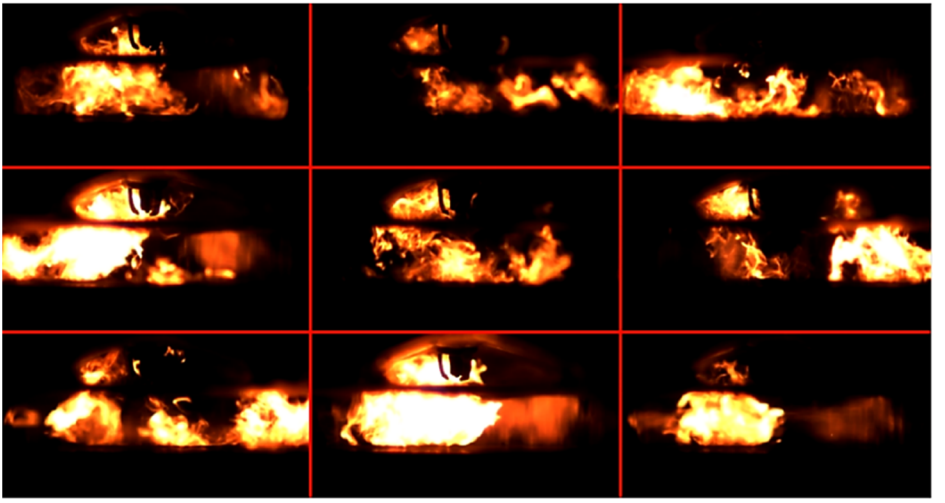

Fig. 3.49. Combustion images at 41.6 CAD aTDC (69.6 CAD after spark timing) in 9 randomly selected cycles, illustrating diffusion burn and the large cycle-to-cycle variations in the combustion in both time and space. Pictures through the pent-roof window (Side view)

There are no pool fires from the piston top following the piston during the expansion. This is expected since there is no liquid that can form liquid films on the piston. Soot formation instead occurs in the bulk flame and is very random, a result of poor mixing between the air and fuel. It should be noted that in this late combustion phase, soot luminescence is much less bright than in earlier stages of the combustion.

3.9. Conclusions of the 3rd Chapter

Experimental research, numerical simulation, theoretical analysis lead to such chapter conclusions:

1. Engine working with petrol and additionally supplied biogas (65% CH_4 / 35% CO_2), had lower rate of heat release and longer combustion duration, and therefore the advanced ignition angle should be adjusted in order to achieve highest engine efficiency. Biogas had also a positive influence on the exhaust gas emission (HC, NO_x) formation.
2. H_2 occupies certain amount of combustion chamber due to its low density when H_2 was used as a fuel additive (*P* + H_2, CNG / H_2) in PFI system. Due to physical and chemical H_2 features the combustion parameters (combustion intensity, duration) changed. Engine with *P* or CNG fuel adjustments cannot reach optimum effective and ecological parameters. Because of higher combustion temperature, the NO_x formation was bigger with increasing H_2 amount. Higher efficiency and lower exhaust gas emissions were obtained using optimum fuel mixture at stoichiometric and lean burn conditions.
3. Using methane direct injection system with stoichiometric, lean burn and stratified mixture combustion, the best effective engine parameters were achieved with stratified cases when the fuel was injected at late compression stroke phase. Indicated specific fuel consumptions for stratified combustion cases were ~ 30% lower than for stoichiometric mixture.
4. Duel coil ignition system makes the influence on better combustion stability because the spark plasma has surface fluctuations with combustible mixture and it is possible to ignite A/F mixture at different cylinder areas.
5. Soot formation was observed, when stratified combustion was applied with methane DI system. Soot formation was proved by emission spectroscopy.

General Conclusions

1. Applied theoretical calculation methods of LHV, MON, MN and H/C atom ratio for gaseous fuels and fuel mixtures, which revealed that with increasing amount of biogas in the fuel, the knock limits are increasing. Addition of highly reactive element H_2 in the fuel mixtures, has a reduction impact on MON and gives an increase tendencies for H/C atom ratio.
2. In order to achieve the highest engine efficiency with a duel fuel system (petrol / biogas), it requires spark timing advancement due to decreased rate of heat release and longer combustion duration. Although engine efficiency decreases by ~ 1.3% with the 30 *l*/min. biogas supply, but the HC, NO_x emission levels can be lowest among all tested petrol / biogas fuel mixtures.
3. Engines with higher compression ratio could be applied with duel fuel systems (petrol / biogas fuel mixtures) because the knock and auto-ignition limits of mentioned fuels are higher. This supported by MON calculation methodology. Theoretical analysis shows that higher compression ratio engines can achieve higher efficiency.
4. H_2 addition in natural gas fuel improves combustion process: the combustible mixture ignition delay reduces ~5 times for the stoichiometric conditions, the rate of heat release becomes higher and more intense, and the combustion duration become shorter ~47%. In order to achieve the best engine efficient

parameters, the new particular spark timings have to be determined and applied for different concentrations of H_2 in natural gas.

5. The highest engine efficiency was achieved with 30% H_2 addition at homogenous stoichiometric conditions ($\lambda = 1$) and the best efficiency was obtained with 70% H_2 addition in natural gas fuel mixture at lean burn conditions ($\lambda = 1.4$). Increasing amount of H_2 in the fuel mixture decreases the brake specific fuel consumptions and fuel with 90% H_2 addition shows the lowest results of mentioned indicator for stoichiometric and lean burn conditions.
6. Although H_2 increased the combustion intensity and combustion temperature, as could be predicted, which resulted in increased NO_x emission, but it is still possible to use H_2 additions up to 30% in the fuel mixtures and measured emissions will not exceed the liquid petrol exhaust gas emission values on both, – stoichiometric and lean burn conditions.
7. Engine measurements revealed that the maximum torque decreases with H_2 additions up to 20% in natural gas / hydrogen fuel mixtures, but the torque starts to increase steadily with higher H_2 concentrations and highest engine torque value can be achieved with 70% H_2 addition. Bigger amount of H_2 shows reduction tendency of mentioned indicator, which could be explained by too fast and too short combustion process.
8. In order to determine optimum natural gas / hydrogen fuel mixture, the numerical simulation model was developed and applied for the investigation. Numerical simulation results demonstrated that created model matches the experimental engine parameters and it was determined that the highest engine torque can be achieved with CNG + 65% H_2 fuel at stoichiometric conditions.
9. The study revealed that stratified combustion with methane DI in a SI engine is possible with relatively low (18 bar) fuel injection pressure, though some of ignition system changes have to be applied, like a dual-coil ignition system was needed to ensure a stable combustion.
10. Gas DI system with stratified combustion type, comparing with homogeneous stoichiometric and homogeneous lean burn, lets to achieve lower indicated specific fuel consumptions. However, combustion images, cylinder pressure data and heat release analysis showed that there are high cycle-to-cycle variations during stratified combustion cases. These findings show that the variations can be due to improper air / fuel mixing, air motion due to swirl in the cylinder.
11. The combustion photographs and the emission spectrums supported that soot formation appears in methane DI stratified mode. The source of soot formation was found to be randomly localized in the bulk flame. These findings illustrate the difficulty of achieving proper mixing between air and methane resulting in both cycle-to-cycle variations in the combustion and fuel rich areas which create a source of soot.

References

Acikgoz, B.; Celik, C. 2012. An experimental study on performance and emission characteristics of a methane-hydrogen fueled gasoline engine. *International Journal of Hydrogen Energy* 37: 18492–18497.

Akansu, S.O., Kahraman, N., Ceper, B. 2007. Experimental study on a spark ignition engine fuelled by methane-hydrogen mixtures. *International Journal of Hydrogen Energy* 32: 4279–4284.

Al-Alousi Y., Karim G. A. 1984. Some considerations of cyclic variations in spark ignition engines fuelled with gaseous fuels. *Proceedings of the SAE International Congress & Exposition. Detroit. February. SAE Paper No. 840232*.

Arthur M. Brownstein. 2015. *Renewable Motor Fuels*: 77–87.

Arunachalam, A.; Olsen, D. B. 2012. Experimental evaluation of knock characteristics of producer gas. *Biomass and bioenergy* 37: 169–176.

A-Aziz, A.; Firmansyah. 2009. The Effect of Fuel Rail Pressure on the Performance of a CNG-Direct Injection Engine. *SAE Technical Paper* 2009-01-149: 7 p.

AVL. 2011. *AVL Pressure sensors for combustion analysis. Product Catalog – Edition 2011*. Internet page: www.avl.com.

AVL BOOST v 2011.2. 2011. *AVL BOOST Theory*, Graz, Austria: 113 p.

AVL BOOST v 2011.2. 2011. *AVL BOOST Users Guide*, Graz, Austria: 297 p.

Bain, A.; Barclay, J.; Bose, T.; Edeskuty, F.; Fairlie, M.; Hansel, J.; Hay, D.; Swain, M. 1998. *Sourcebook for Hydrogen Applications*. Montreal, Tisec Inc.

Baratta, M.; Catania, A.; Spessa, E.; Herrmann, L.; Roessler, K. 2009. Multi-Dimensional Modeling of Direct Natural-Gas Injection and Mixture Formation in a Stratified-Charge SI Engine with Centrally Mounted Injector. *SAE International Journal Engines* 1(1): 607–626.

Baratta, M.; Rapetto, N. 2015. Mixture Formation Analysis in a Direct-Injection NG SI Engine Under Different Injection Timings. *Fuel* 159: 675–688.

Baratta, M.; Rapetto, N.; Spessa, E.; Fuerhapter, A.; Philipp, H. 2012. Numerical and Experimental Analysis of Mixture Formation and Performance in a Direct Injection CNG Engine. *SAE Technical Paper* 2012-01-0401: 23 p.

Bari, S. 1996. Effect of carbon dioxide on the performance of biogas diesel duel-fuel engine). *Renewable Energy, Volume* 9(1–4)*:* 1007–1010.

Bedoya, I. D.; Arrieta, A. A.; Cadavid, F. J. 2009. Effects of mixing system and pilot fuel quality on diesel-biogas dual fuel engine performance. *Bioresource Technology* 100: 6624–6629.

Bielaczyc, P.; Woodburn, J.; Szczotka, A. 2014. An assessment of regulated emissions and CO_2 emissions from a European light-duty CNG-fueled vehicle in the context of Euro 6 emissions regulations. *Applied Energy* 117: 134–141.

Bohatsch, S. 2011. Ein Injektorkonzept zur Darstellung eines ottomotorischen Brennverfahrens mit Erdgas-Direkteinblasung. *PhD Thesis, Institut fur Verbrennungsmotoren und Kraftfahrwesen der Universitat Stuttgart*: 121 p.

Boretti, A.; Lappas, P.; Zhang, B.; and Mazlan, S. 2013. CNG Fueling Strategies for Commercial Vehicles Engines – A Literature Review. *SAE Technical Paper* 2013–01 2812: 19 p.

Byun, J.S.; Park, J. 2015. Predicting the performance and exhaust NO_x emissions of a spark-ignition engine generator fuelled with methane based biogases containing various amounts of CO_2. *Journal of Natural Gas Science and Engineering* 22: 196–202.

Carlucci, A.; Laforgia, D.; Saracino, R.; Toto, G. 2010. Study of Combustion Development in Methane-Diesel Dual Fuel Engines, Based on the Analysis of In-Cylinder Luminance. *SAE Technical Paper* 2010-01-1297: *14 p.*

Carlucci, A. P.; Laforgia, D.; Saracino, R.; Toto, G. 2011. Combustion and emissions control in diesel-methane dual fuel engines: The effects of methane supply method combined with variable in-cylinder charge bulk motion. *Energy Conversion and Management* 52: 3004–3017.

Catapano, F.; Di Iorio, S.; Sementa, P.; Vaglieco, B. M. 2013. Characterization of CH_4 and CH_4/H_2 Mixtures Combustion in a Small Displacement Optical Engine. *SAE International Journal of Fuels and Lubricants* 6(1): 24–33.

Catapano, F.; Sementa, P.; Vaglieco, B. M. 2013. Optical characterization of bio-ethanol injection and combustion in a small DISI engine for two wheels vehicles. *Fuel* 106: 651–666.

Ceper, B. A.; Akansu, S. O.; Kahraman, N. 2009. Investigation of cylinder pressure for H_2/CH_4 mixtures at different loads. *International Journal of Hydrogen Energy* 34: 4855–4861.

Chandra, R.; Vijay, V. K.; Subbarao, P. M. V.; Khura, T. K. 2011. Performance evaluation of a constant speed IC engine on CNG, methane enriched biogas and biogas. *Applied Energy* 88: 3969–77.

Chiodi, M.; Berner, H.; Bargende, M. 2006. Investigation on different Injection Strategies in a Direct-Injected Turbocharged CNG-Engine. *SAE Technical Paper* 2006-01-3000: 18 p.

D'Andrea, T.; Henshaw, P. F.; Ting, D. S. K. 2004. The addition of hydrogen to a petrol-fuelled SI engine. *International Journal of Hydrogen Energy* 29: 1541–1552.

Dahlander, P.; Hemdal, S. 2015. High-Speed Photography of Stratified Combustion in an Optical GDI Engine for Different Triple Injection Strategies. *SAE Technical Paper* 2015-01-0745: 14 p.

Dahlstrom, J.; Tunestal, P.; Johansson, B. 2013. Reducing the Cycle-Cycle Variability of a Natural Gas Engine Using Controlled Ignition Current. *SAE Technical Paper* 2013-01-0862: 12 p.

Das, L. M.; Gulati, R.; Gupta, P. K. A. 2000. Comparative evaluation of the performance characteristics of a spark ignition engine using hydrogen and compressed natural gas as alternative fuels. *International Journal of Hydrogen Energy* 25: 783–793.

Dimopoulos, P.; Rechsteiner, C.; Soltic, P.; Laemmle, C.; Boulouchos, K. 2007. Increase of passenger car engine efficiency with low engine-out emissions using hydrogen-natural gas mixtures: A thermodynamic analysis. *International Journal of Hydrogen Energy* 32: 3073–3083.

Di Iorio, S.; Sementa, P.; Vaglieco, B. M.; Catapano, F. 2014. An experimental investigation on combustion and engine performance and emissions of a methane-petrol dual-fuel optical engine. *SAE Technical Paper* 2014-01-1329: 11 p.

Di Ioro, S.; Sementa, P.; Vaglieco, B. M. 2014. Experimental Investigation on the Combustion Process in a Spark Ignition Optically Accessible Engine Fueled With Methane/Hydrogen Blends. *International Journal of Hydrogen Energy* 39: 9809–982.

Di Iorio, S.; Sementa, P.; Vaglieco, B. 2013. Experimental Investigation of a Methane-Petrol Dual-Fuel Combustion in a Small Displacement Optical Engine. *SAE Technical Paper* 2013-24-0046: 9 p.

Doornbos, G.; Hemdal, S.; Dahl, D. 2015. Reduction of Fuel Consumption and Engine-out NO_x Emissions in a Lean Homogeneous GDI Combustion System, Utilizing Valve Timing and an Advanced Ignition System.*SAE Technical Paper* 2015-01-0776: 11 p.

European Commision. 2013. *Communication from the Commission to the European Parliament, The Council, The European Economic and Social Committee and the Committee of the Regions. Clean Power for Transport: A European alternative fuels strategy*. Brussels.

European Commision. 2011. *Transport 2050.* Brussels.

European Commision. 2011. *White Paper. Roadmap to a Single European Transport Area – Towards a competitive and resource efficient transport system.* Brussels.

European Parliament and the Council of the European Union. 2007. *Regulation (Ec) No 715/2007 of the European Parliament and of the Council of 20 June 2007 on type approval of motor vehicles with respect to emissions from light passenger and commercial vehicles (Euro 5 and Euro 6) and on access to vehicle repair and maintenance information.* Official Journal of the European Union.

European Parliament and the Council of the European Union. 2009. *Regulation (Ec) No 595/2009 of the European Parliament and of the Council of 18 June 2009 on type-approval of motor vehicles and engines with respect to emissions from heavy duty vehicles (Euro VI) and on access to vehicle repair and maintenance information and amending Regulation (EC) No 715/2007 and Directive 2007/46/EC and repealing Directives 80/1269/EEC, 2005/55/EC and 2005/78/EC.* Official Journal of the European Union.

Fansler, T. D.; Stojkovic, B.; Drake, M. C.; Rosalik M. E. 2002. Local fuel concentration measurements in internal combustion engines using spark-emissions spectroscopy. *Applied Physics* B (75): 577–590.

Genchi, G.; Pipitone, E. 2014. Octane rating of natural gas-gasoline mixtures on CFR engine. *SAE International Journal of Fuels and Lubricants*: 10 p.

Karavalakis, G.; Durbin, T. D.; Villela, J. M.; Miller, W. 2012. Air pollutant emissions of light-duty vehicles operating on various natural gas compositions. *Journal of Natural Gas Science and Engineering* 4: 8–16.

Glassman, I.; Yetter, R. A. 2008. *Combustion. Fourth edition.* Elsevier. ISBN: 978-0-12-088573-2, 773 p.

Gupta, S. B. 2009. *Hydrogen fuel: production, transport, and storage.* Boca Raton: Taylor & Francis Group, CRC Press.

Gupta, S. B.; Bihari, P. B.; Biruduganti, M.S.; Sekar, R. R.; Zigan, J. 2011. On Use of CO_2 Chemiluminescence for Combustion Metrics in Natural Gas Fired Reciprocating Engines. *Proceedings of the Combustion Institute* 33: 3131–3139.

Haeng, M. C.; He, B. 2007. Spark ignition natural gas engines – A review. *Energy Conversion and Management* 48: 608–618.

Hemdal, S.; Andersson, M.; Dahlander, P.; Ochoterena, R.; Denbratt, I. 2011. In-Cylinder Soot Imaging and Emissions of Stratified Combustion in a Spark-Ignited Spray-Guided Direct-Injection Petrol Engine. *International Journal of Engine Research* 12: 549–563.

Heywood, J. B. 1988. *Internal Combustion Engine Fundamentals*. McGraw-Hill.

Holladay, J. D.; Hu, J.; King, D. L. 2009. An Overview of Hydrogen Production Technologies. *Catalysis Today* 139: 244–60.

Huang, Z.; Wang, J.; Liu, B.; Zeng, K.; Yu, K.; Jiang, D. 2007. Combustion characteristics of a direct-injection engine fuelled with natural gas-hydrogen blends under different ignition timings. *Fuel* 86: 381–7.

Huang, K. Z. Z.; Liu, B.; Liu, L.; Jiang, D.; Ren, Y.; Wang, J. 2006. Combustion Characteristics of a Direct-Injection Natural Gas Engine under Various Fuel Injection Timings. *Applied Thermal Engineering* 26: 806–813.

Huang, Z.; Liu B., Zeng, K.; Huang, Y.; Jiang, D.; Wang, X.; Miao, H. 2006. Experimental study on engine performance and emissions for an engine fuelled with natural gas-hydrogen mixtures. *Energy Fuels* 20(5): 2131–6.

Ji, Ch.; Liu, X.; Gao, B.; Wang, Sh.; Yang, J. 2013. Numerical investigation on the combustion process in a spark-ignited engine fueled with hydrogen-petrol blends. *International Journal of Hydrogen Energy* 38: 11149–11155.

Ji, Ch.; Wang, Sh. 2011. Effect of hydrogen addition on lean burn performance of a spark-ignited petrol engine at 800 rpm and low loads. *Fuel* 90: 1301–1304.

Jingding, L.; Linsong, G.; Tianshen, D. 1998. Formation and restraint of toxic emissions in hydrogen-petrol mixture fueled engines. *International Journal of Hydrogen Energy* 23(10): 971–975.

Johansson, A.; Hemdal, S.; Dahlander, P. 2013. Experimental Investigation of Soot in a Spray-Guided Single Cylinder GDI Engine Operating in a Stratified Mode. *SAE Technical Paper* 2013-24-0052: 10 p.

Kahraman, E.; Ozcanlıb, S., C.; Ozerdem, B. 2006. An experimental study on performance and emission characteristics of a hydrogen fuelled spark ignition engine. *International Journal of Hydrogen Energy* 32: 2066–2072.

Kakaee, A.; Paikani, A.; Ghajar, M. 2014. The Influence of Fuel Composition on the Combustion and Emission Characteristics of Natural Gas Fueled Engines. *Renewable and Sustainable Energy Reviews* 38: 64–78.

Kalam, M. A.; Masjuki, H. H. 2011. An Experimental Investigation of High Performance Natural Gas Engine with Direct Injection. *Journal of Energy* 36: 3563–3571.

Karavalakis, G.; Durbin, T.D.; Villela, M.; Miller, J.W. 2012. Air pollutant emissions of light-duty vehicles operating on various natural gas compositions. *Journal of Natural Gas Science and Engineering* 4: 8–16.

Karim, G. A. 2011.The combustion of bio-gases and low heating value gaseous fuel mixtures. *International Journal of Green Energy* 8: 372–82.

Karim, G. A. 2003. Hydrogen as a spark ignition engine fuel. *International Journal of Hydrogen Energy* 28: 569–577.

Karim, G. A.; Wierzba, I.; Al-Alousi, Y. 1996. Methane-Hydrogen mixtures as fuels. *International Journal of Hydrogen Energy* 21: 625–31.

Keršys, A.; Kalisinskas D.; Pukalskas S.; Vilkauskas, A.; Keršys, R.; Makaras, R. 2013. Investigation of the influence of hydrogen used in internal combustion engines on exhaust emission. *Maintenance and reliability. Eksploatacja i niezawodność*. *Lublin: Polish Maintenance Society* 4(15): 384–389.

Khalil, E.B.; Karim, G. A. 2002. A Kinetic Investigation of the Role of Changes in the Composition of Natural Gas in Engine Applications. *ASME Vol.* 124: 404–411.

Kistler. 2016. *Engine Combustion Analysis. Engine Pressure Measurement for Research and Development*. Internet page: https://www.kistler.com/?type=669&fid=42&model=download&callee=frontend.

Kobzar, A.I. 2006. *Applied mathematical statistics. For engineers and scientists.* M .: Fizmalit: 816 p.

Korakianitis, T.; Namasivayam, A. M.; Crookes, R. J. 2011. Natural-gas fueled spark-ignition (SI) and compression-ignition (CI) engine performance and emissions. *Progress in Energy and Combustion Science* 37: 89–112.

Kovács, V. B.; Török, Á. 2010. Investigation on transport related biogas utilization. *Transport* 25: 77–80.

Larsen, J. F.; Wallace, J. S. 1997. Comparison of emissions and efficiency of a turbo-charged lean-burn natural gas and hythane-fueled engine. *Journal of Engineering for Gas Turbines and Power* 119: 218–26.

Lee, Y. J.; Kim, G.C. 2000. Effect of Gas Composition on NGV Performance. *Seoul 2000 FISITA World Automotive Congress*: 1–6.

Leiker, M.; Christoph, K.; Rankl, M.; Cartellieri, W.; Pfeifer, U. 1972. Evaluation of anti-knocking property of gaseous fuels by means of methane number and its practical application to gas engines. *ASME Diesel and Gas Engine Power Conference and Exhibit*: 1–17.

Li, R.; Chen, S.; Li, X.; Lar, J. S.; He, Y.; Zhu, B. 2009 Anaerobic codigestion of kitchen waste with cattle manure for biogas production. *Energy Fuels* 23: 2225–8.

Liu, Y.; Yeom, J.; Chung, S. 2013. A study of spray development and combustion propagation processes of spark-ignited direct injection (SIDI) compressed natural gas (CNG). *Mathematical and Computer Modelling* 57: 228–244.

Ma, F.; Ding. S.; Wang, Y.; Wang, M.; Jiang, L.; Naeve, N. 2009. Performance and emission characteristics of a spark-ignition (SI) hydrogen-enriched compressed natural gas (HCNG) engine under various operating conditions including idle conditions. *Energy Fuels* 23: 3113–3118.

MacLeana, H. L.; Lave L. B. 2003. Evaluating Automobile Fuel / Propulsion System Technologies. *Progress in Energy Combustion Science* 29: 1–69.

Makarevičienė ,V.; Sendžikienė, E.; Pukalskas, S.; Rimkus, A.; Vėgneris, R. 2013. Performance and emission characteristics of biogas used in diesel engine operation. *Energy Conversion and Management* 75: 224–33.

Malenshek, M.; Olsen, D. B. 2009. Methane number testing of alternative gaseous fuels. *Fuel* 88: 650–656.

Mardi, K. M.; Khalilarya, Sh.; Nemati, A. 2014. A numerical investigation on the influence of EGR in a supercharged SI engine fueled with petrol and alternative fuels. *Energy Conversion and Management* 83: 260–269.

Mariani, A.; Morrone, B.; Unich, A. 2012. Numerical evaluation of internal combustion spark ignition engines performance fuelled with hydrogen-natural gas blends. *International Journal of Hydrogen Energy* 37: 2644–2654.

Mariani, A.; Prati, M.V.; Unich, A.; Morrone, B. 2013. Combustion analysis of a spark ignition i. c. engine fueled alternatively with natural gas and hydrogen-natural gas blends. *International Journal of Hydrogen Energy* 38: 1616–1623.

Matthews, R.; Chiu, J.; Hilden, D. 1996. CNG Compositions in Texas and the Effects of Composition on Emissions, Fuel Economy, and Driveability of NGVs. *SAE Technical paper. Topics in Alternative Fuels and Their Emissions* (SP-1208): 1–18.

McAllister, S.; Chen, J.; Fernandez-Pello, A. C. 2011. *Fundamentals of Combustion Processes.* Springer. ISBN 978-1-4419-7942-1: 302 p.

Mhy Bus. 2009. *Methane and Hydrogen blend for Public Transport City Bus. Road Test Results in Public Transport with Hydromethane*. www.mhybus.eu: 16 p.

Mokhatab, S.; Poe, W. A.; Mak, J. Y. 2015. *Handbook of Natural Gas Transmission and Processing (Third Edition)*: 1–36.

Moreno, F.; Arroyo, J.; Munoz, M.; Monne, C. 2012. Combustion analysis of a spark ignition engine fueled with gaseous blends containing hydrogen. *International Journal of Hydrogen Energy* 37: 13564–13573.

Motec. 2016. *Engine Management and Data Acquisition Systems. Bosch LSU 4.9 sensor product data sheet.* www.motec.com/filedownload.php/?docid=3525

Nagalingam, B.; Duebel, F.; Schmillen, K. 1983. Performance study using natural gas, hydrogen-supplemented natural gas and hydrogen in AVL research engine, *Hydrogen Energy* 8: 715–735.

NGVA Europe, 2013. *Internet page: http://www.ngvaeurope.eu/members/presentations/ROBERT_STAIMER–MAN.pdf*

Obiols, J.; Soleri, D.; Dioc, N.; Moreau, M. 2011. Potential of Concomitant Injection of CNG and Petrol on a 1.6 L Petrol Direct Injection Turbocharged Engine. *SAE Technical Paper* 2011-01-1995: 16 p.

Pearse, R. W. B.; Gaydon, A. G. 1963. T*he Identification of Molecular Spectra: Third Edition*: ISBN041214350X: 333 p.

Polcyn, N.; Lai, M.; Lee, P. 2014. Investigation of Ignition Energy with Visualization on a Spark Ignited Engine powered by CNG. *SAE Technical Paper* 2014-01-1331: 8 p.

Porpatham, E.; Ramesh, A.; Nagalingam, B. 2008. Investigation on the effect of concentration of methane in biogas when used as a fuel for a spark ignition engine. *Fuel* 87: 1651–9.

Porpatham, E.; Ramesh, A.; Nagalingam, B. 2012. Effect of compression ratio on the performance and combustion of a biogas fuelled spark ignition engine. *Fuel* 95: 247–56.

Raheman, H.; Subhrajit, M. 2012. Biogas production potential of jatropha seed cake. *Biomass & Bioenergy* 37: 25–30.

Rakopoulos, C., D.; Kosmadakis, G., M.; Pariotis, E., G. 2010. Evaluation of a combustion model for the simulation of hydrogen spark-ignition engines using a CFD code. *International Journal of Hydrogen Energy* 35: 12545–12560.

Ramadhas, A. S. 2011. *Alternative Fuels for Transportation*, New York, 2011: 463 p.

Raman, V.; Hansel, J.; Fulton, J.; Lynch, F.; Bruderly, D. 1994. Hythane – an ultraclean transportation fuel. *Proceedings of 10th World Hydrogen Conference*, Cocoa Beach, Florida, USA.

Raman, V. 1997. The Emerging Applications of Hydrogen in Clean Transportation. *American Chemical Society Conference*, San Francisco: 611–615.

Reynolds, C.; Evans, R.; Andreassi, L.; Cordiner, S.; Mulone, V. 2005. The Effect of Varying the Injected Charge Stoichiometry in a Partially Stratified Charge Natural Gas Engine. *SAE Technical Paper* 2005-01-0247: 13 p.

Rimkus, A. 2013. *Improvement of efficiency of operation of an internal combustion engine by using Brown gas.* Dissertation Thesis, Vilnius Gediminas Technical University: 140 p.

Rimkus, A.; Pukalskas, S.; Matijošius, J. 2011. The research on efficiency of using HHO gas (oxyhydrogen) in petrol internal combustion engines [CD]. *International Conference on Hydrogen Production (ICH$_2$P-11)*, June 2011, Thessaloniki, Greece.

Rimkus, A.; Pukalskas, S.; Matijošius, J.; Sokolovskij, E. 2013. Betterment of ecological parameters of a diesel engine using brown's gas. *Journal of Environmental Engineering and Landscape Management* 2(21): 133–140.

Ristovski, Z. D.; Morawska, L.; Hitchins, J.; Thomas, S.; Greenaway, C.; Gilbert, D. 2000. Particle Emissions from Compressed Natural Gas Engines. *Journal of Aerosol Science* 31: 403–13.

Robinson, J.W. 1974. *Handbook of Spectroscopy. Volume I*: 796 p. ISBN 0-8493-0331-1.

Rulkens, W. 2008. Sewage sludge as a biomass resource for the production of energy: overview and assessment of the various options. *Energy Fuels* 22: 9–15.

Ryan, T. W.; Callahan, T. J.; King, S. R. 1993. Engine Knock Rating of Natural Gases—Methane Number. *Journal of Engineering for Gas Turbines and Power. ASME Vol.* 115: 769–776.

Safari, H.; Jazayeri, S., A.; Ebrahimi, R. 2009. Potentials of NO_x emission reduction methods in SI hydrogen engines: Simulation study. *International Journal of Hydrogen Energy* 34: 1015–1025.

Shrestha, S. O. B.; Karim, G.A. 2001. Predicting the effects of the presence of diluents with methane on spark ignition engine performance. *Applied Thermal Engineering* 21: 331–342.

Sierens, R.; Rosseel, E. 2000. Variable composition hydrogen/natural gas mixtures for increased engine efficiency and decreased emissions. *Journal of Engineering for Gas Turbines and Power* 122: 135–40.

Stanmore, B. R.; Brilhac, J. F.; Gilot, P. 2001. The Oxidation of Soot: A Review of Experiments, Mechanisms and Models. *Carbon* 39 (15): 2247–2268.

Stojkovic, B. D.; Fansler, T. D.; Drake, M. C.; Sick, V. 2005. High-Speed Imaging of OH* and Soot Temperature and Concentration in a Stratified-Charge Direct-Injection Petrol Engine. *Proceedings of the Combustion Institute* 30 (2): 2657–2665.

Soberanis, M. A.; Fernandez, A. M. 2010. A review on the technical adaptations for internal combustion engines to operate with gas/hydrogen mixtures. *International Journal of Hydrogen Energy* 35: 12134–12140.

Standard EN 16726: 2015. *Gas infrastructure – Quality of gas – Group H*, 49 p.

Standard ISO 15403: 2006. *Natural gas – Natural gas for use as a compressed fuel for vehicles – Part 1: Designation of the quality*, 32 p.

Standard ISO 6976: 2005. *Natural gas – Calculation of calorific values, density, relative density and Wobbe index from composition*, 48 p.

Standard JCGM 100: 2008. *Evaluation of measurement data – Guide to the expression of uncertainty in measurement*, 132 p.

Subramanian, K. A.; Vinaya, C.; Mathad, V. K.; Vijay, P.; Subbarao, M. V. 2013. Comparative evaluation of emission and fuel economy of an automotive spark ignition vehicle fuelled with methane enriched biogas and CNG using chassis dynamometer. *Applied Energy* 105: 17 p.

Talal. F.; Buttsworth, Y. D. R.; Saleh Khalid, H.; Yousif, B. F. 2010. Biogas-diesel engine performance and exhaust emission analysis with the aid of artificial neural network. *Applied Energy* 87: 1661–9.

Tadesse, G.; Aziz, A. R. A. 2009. Effect of Boost Pressure on Engine Performance and Exhaust Emissions in Direct-Injection Compressed Natural Gas (CNG-DI) Spark Ignition Engine. *SAE Technical Paper* 2009-32-0135: 10 p.

Thipse, S.; Sonawane, S.; D' Souza, A.; Rairikar, S. 2015. Injection Strategies, Optimization and Simulation Techniques on DI CNG Technology. *SAE Technical Paper* 2015-26-0046: 12 p.

Tricase, C.; Lombardi, M. 2009. State of the art and prospects of Italian biogas production from animal sewage: technical-economic considerations. *Renewable Energy* 34: 477–85.

Vibe, I. I. 1970. *Brennverlauf und Kreisprozeß von Verbrennungsmotoren.* Berlin: Verlag Technik, 286 p.

Wasiu, A. B.; Aziz, A.; Rashid, H. M.R. 2012. The Effect of Carbon Dioxide Content-Natural Gas on the Performance Characteristics of Engines: A Review. *Journal of Applied Sciences* 12 (23): 2346–2350.

Wang, J.; Huang, Z.; Fang, Y.; Liu, B.; Zeng, K.; Miao, H.; Jiang, D.; 2007. Combustion behaviors of a direct-injection engine operating on various fractions of natural gas-hydrogen blends. *International Journal of Hydrogen Energy* 32: 3555–3564.

Wärtsilä Corporation. 2015. *Wärtsilä 50DF Engine. Engine technology. [Online]* [Referred 2015 12 27]. Available: http://www.wartsila.com/docs/default–source/Power–Plants–documents/w%C3%A4rtsil%C3%A4–50df.pdf?sfvrsn=2

Yadollahi, B.; Boroomand, M. 2011. The Effect of Piston Head Geometry on Natural Gas Direct Injection and Mixture Formation in a SI Engine with Centrally Mounted Single-Hole Injector. *SAE Technical Paper* 2011-01-2448: 13 p.

Yamasaki, Y.; Kanno, M.; Suzuki, Y.; Kaneko, S. 2013. Development of an engine control system using city gas and biogas fuel mixture. *Applied Energy* 101: 465–74.

Yao, C.; Li, X.; Zang, R.; Xu, Y. Research on the performance of an electronically controlled spark ignition engine fuelled with hydrogen-rich gases. *Proceedings of IMechE Part D: Journal of Automobile Engineering 2014,* Vol. 228 (9): 1084–1094.

Zachariah-Wolff, J.L.; Egyedi, T. M.; Hemmes, K. 2007. From natural gas to hydrogen via theWobbe index: The role of standardized gateways in sustainable infrastructure transitions. *International Journal of Hydrogen Energy* 32: 1235–1245.

Zhao, H. 2010. *Advanced Direct Injection Combustion Engine Technologies and Development. Volume 1: Petrol and Gas Engines*: 298 p.

Zhao, H.; Ladommatos, N. 1998. Optical Diagnostics for Soot and Temperature Measurement in Diesel Engines. *Progress in Energy and Combustion Science* 24 (3): 221–255.

Zoldak, P.; Joseph, J.; Shelley, W.; Johnson, J.; Naber, J. 2015. Characterization of Partially Stratified Direct Injection of Natural Gas for Spark-Ignited Engines. *SAE Technical Paper* 2015-01-0937: 15 p.

List of Publications by the Author on the Topic of the Dissertation

Papers in the Reviewed Scientific Journals

Sendžikienė, E.; Rimkus, A.; Melaika, M.; Makarevičienė, V.; Pukalskas, S. 2015. Impact of biomethane gas on energy and emission characteristics of a spark ignition engine fuelled with a stoichiometric mixture at various ignition advance angles. *Fuel* 162: 194–201. ISSN 0016-2361.

Rimkus, A.; Melaika, M.; Matijošius, J.; Mikaliūnas, Š.; Pukalskas, S. 2016. Investigation of combustion, performance and emission characteristics of spark ignition engine fuelled with buthanol – gasoline mixture and a hydrogen enriched air. *Advances in science and technology-research journal (ASTRJ)* 10: 102–108. ISSN 2080-4075.

Pukalskas, S.; Rimkus, A.; Melaika, M.; Bogdanovičius, Z.; Matijošius, J. 2014. Numerical investigation on the effects of gasoline and hydrogen blends on si engine combustion. *Agricultural engineering. Research papers* 46: 66–77. ISSN 1392-1134.

Latakas, J.; Pukalskas, S.; Rimkus, A.; Melaika, M.; Vėgneris, R.; Stravinskas, P. 2014. Vandenilio dujų įtaka dyzelinio vidaus degimo variklio efektyvumo rodikliams. *Science – future of Lithuania: civil and transport engineering, aviation technologies* 6(5): 558–563. ISSN 2029-2341.

Jasilionis, A.; Nagurnas, S.; Melaika, M. 2012. Matematinės statistikos metodų taikymas analizuojant variklių technines charakteristikas. *Science – future of Lithuania: civil and transport engineering, aviation technologies* 4(4): 351–355. ISSN 2029-2341.

Papers in other reviewed publications

Melaika, M.; Dahlander, P. 2016. Experimental investigation of methane direct injection with stratified charge combustion in optical SI single cylinder engine. *SAE technical papers*: 1–13. ISSN 0148-7191.

Rimkus, A.; Melaika, M.; Matijošius, J.; Mikaliūnas, Š.; Pukalskas, S. 2016. Analysis of combustion process of spark ignition engine fuelled with buthanol – petrol mixture and a HHO enriched air. *Innovative technologies in engineering production (ITEP 2016)*: 6–10. ISBN 9788089276516.

Rimkus, A.; Berioza M.; Melaika, M.; Juknelevičius, R. Bogdanovičius, Z. Improvement of the compression-ignition engine indicators using dual fuel (diesel and liquefied petroleum gas). *Transbaltica 2015: proceedings of the 9th international scientific conference* 134: 30–39. ISSN 1877-7058.

Kriaučiūnas, D.; Pukalskas, S.; Melaika, M. 2015. Skaitinė „Audi Coupe“ 2,3 l kibirkštinio variklio, veikiančio vandenilio ir benzino mišiniais, analizė. *Proceedings of 18th Lithuanian conference of young scientists "Science – future of Lithuania"*: 185–190. ISSN 2029-7149.

Melaika, M.; Rimkus, A.; Pukalskas, S.; Žaglinskis, J. 2013. Simulation of parameters of SI engine using H_2 and CH_4 fuel blends. *Transport Means 2013: proceedings of the 17th international conference*: 13–16. ISSN 1822-296X.

Morkūnas, D.; Nagurnas, S.; Rimkus, A.; Melaika, M. 2013. Uždegimo žvakių įtaka benzininio variklio su dujine įranga darbui. *Proceedings of 16th Lithuanian conference of young scientists "Science – future of Lithuania"*: 241–246. ISSN 2029-7157.

Pukalskas, S.; Bogdanovičius, Z.; Matijošius, J.; Melaika, M.; Rimkus, A.; Vėgneris, R.; Stravinskas, P. 2013. Biometano ir benzino mišinio įtakos kibirkštinio uždegimo variklio veikimo parametrams tyrimai. *Proceedings of 16th Lithuanian conference of young scientists "Science – future of Lithuania"*: 177–181. ISSN 2029-7157.

Summary in Lithuanian

Įvadas

Problemos formulavimas

Didėjant žmonių populiacijai žemėje didėja ir iškastinių degalų poreikis. Tai ypač juntama dabar, kai žmonių pragyvenimo lygis vis labiau kyla, o su juo kartu didėja ir sunaudojamos energijos poreikis (Korakianitis *et al*. 2011; Wasiu *et al*. 2012). Vystantis pramonei stengiamasi pereiti prie alternatyvių degalų panaudojimo. Žemės klimatas keičiasi dėl didėjančių šiltnamio efektą sukeliančių dujų emisijų, atsiranda vis daugiau žmonių sveikatos sutrikimų dėl užteršto oro miestuose. Neįmanoma staigiai globaliu mastu pereiti prie elektromobilių ir alternatyvių degalų šaltinių, todėl vienas iš lengvesnių būdų yra pereinamuoju laikotarpiu naudoti paprastesnės molekulinės struktūros degalus – gamtines dujas. Taip pat siekiant plačiau naudoti alternatyviuosius degalus yra būtina panaudoti energetiškai patrauklų ir švarų kurą – vandenilį.

Transporto priemonės, varomos gamtinėmis dujomis ar biodujomis, į aplinką išmeta žymiai mažesnius kietųjų dalelių ir azoto oksidų kiekius palyginus su kitais degalais varomomis transporto priemonėmis. Tačiau gamtinės dujos ir biodujos turi ir neigiamą savybę – jų degimo liepsnos greitis yra mažesnis, o panaudojus didesnį oro / degalų santykį gali prasidėti degimas su pertrūkiais.

Dujinių variklių charakteristikas galima gerinti gerinant degalų savybes bei variklio techninius parametrus. Šiame disertaciniame darbe yra pateikti abiejų gerinimo būdų teoriniai ir eksperimentiniai tyrimai. Moksliškai ištirti degalų mišiniai sudaryti iš tradicinių iškastinių degalų (SGD) ir priedo (H_2). Taip pat darbe pateikiami tyrimai su biodujomis,

kurios panaudotos dviguboje degalų tiekimo sistemoje su benzininiais degalais. Darbe pateikiami ir tyrimų rezultatai, gauti išbandžius dujų tiesioginį įpurškimą (DI) su santykinai žemu įpurškimo slėgiu.

Darbo aktualumas

Per pastaruosius dvidešimt metų netvarus energijos panaudojimas kelia susirūpinimą ne tik dėl klimato kaitos, bet ir dėl energijos tiekimo (Malenshek *et al.* 2009). Išleidus pirmąjį teršalų emisiją reglamentuojantį standartą Europos Sąjungoje ir Europos Ekonominėje Bendrijoje 1993 m. bei kiek vėliau pasirašius Kyoto Protokolą 1997 m., pagaliau imta plačiau ir išsamiau tirti bei naudoti alternatyviuosius degalus, kuriais vidaus degimo varikliuose būtų siekiama pakeisti tradicinius degalus. Būtent šie dokumentai privertė visas dalyvaujančias šalis mažinti šiltnamio efektą sukeliančias dujas.

Dabartiniai gamtinių dujų varikliai, dirbantys stechiometrinio mišinio pagrindu, dažniausiai pasiekia stabilų degiojo mišinio degimą, tačiau susiduriama su didele degalų sąnaudų ir deginių emisijos problema, lyginant su lieso degimo varikliais ($\lambda > 1,4$). Tačiau naudojant lieso degimo variklius susiduriama su degimo proceso stabilumo ir variklio galios praradimo iššūkiais. Vienas iš būdų pagerinti šiuos rodiklius yra vandenilio, turinčio geresnes fizikines ir chemines savybes, panaudojimas.

Siekiant pagerinti vidaus degimo variklių efektyviuosius rodiklius, yra būtina tirti ir vystyti pažangesnes degalų įpurškimo sistemas. Vienas iš būdų spręsti susidariusias efektyvumo problemas yra gamtinių dujų tiesioginio įpurškimo sistemos panaudojimas. Tiesioginis įpurškimas užtikrina geresnį cilindrų pripildymą oru, geresnį degiojo mišinio formavimą.

Disertacinis darbas yra reikšmingas savo išsamiais tyrimais, kurie apima: naujus degalų mišinius, kurie gali būti panaudoti jau esamuose ir būsimuose lengvojo ir sunkiojo transporto varikliuose, bei naujo tipo įpurškimo technologijas, kurios gali būti pritaikytos naujos kartos varikliuose. Paminėtos tyrimų kryptys yra glaudžiai susijusios viena su kita, nes dujinių degalų mišiniai gali būti naudojami ir dujų tiesioginio įpurškimo sistemose.

Tyrimo objektas

Dujinių degalų ir jų mišinių, kurių pagrindą sudaro metano dujos, degimo procesas kibirkštinio uždegimo vidaus degimo variklyje su dviguba degalų tiekimo sistema, dujų tiesioginiu įpurškimu arba dvigubos apvijos uždegimo sistema.

Darbo tikslas

Pritaikant teorinio vertinimo, skaitinio modeliavimo ir eksperimentinių tyrimų metodikos algoritmą nustatyti kibirkštinio uždegimo vidaus degimo variklio, veikiančio dujiniais degalais, efektyviųjų ir ekologinių rodiklių bei degalų degimo proceso gerinimo priemones.

Darbo uždaviniai

Siekiant įgyvendinti iškeltą tikslą, formuluojami šie disertacinio darbo uždaviniai:

1. Įvertinti skirtingų dujinių degalų ir jų mišinių savybes ir parinkti šių savybių vertinimo metodus. Išplėtoti eksperimentinių ir skaitinių tyrimų metodiką, kai kibirkštiniame uždegimo variklyje yra taikomos skirtingos degalų tiekimo ir uždegimo sistemos.
2. Įvertinti benzinui, gamtinėms dujoms bei šių degalų mišinių su biodujomis ar ypatingai reaktyviu vandenilio elementu būdingus žemutinio degalų šiluminingumo, H/C atomų santykio ir MON (MN) teorinio skaičiavimo rezultatus bei juos palyginti su eksperimentiškai gautais duomenimis.
3. Pritaikyti dvigubą degalų įpurškimo sistemą benzino ir biodujų degalų mišinių panaudojimui bei, panaudojus skaitinio vertinimo metodiką, įvertinti šių mišinių įtaką šilumos išsiskyrimo greičiui, degimo trukmei, intensyvumui. Eksperimentiškai nustatyti jų įtaką variklio ekologiniams ir efektyviesiems rodikliams, kai panaudojami skirtingi variklio valdymo parametrai.
4. Eksperimentiškai įvertinti ypatingai reaktyvaus H_2 elemento įtaką benzino ir gamtinių dujų degimo procesui, variklio efektyviesiems ir ekologiniams rodikliams, kai kibirkštinio uždegimo variklyje naudojama kolektorinė dujinių degalų įpurškimo sistema. Pritaikius išplėtotą teorinę ir skaitinio modeliavimo metodiką nustatyti efektyviųjų rodiklių atžvilgiu optimalų degalų mišinį.
5. Pritaikyti optinių tyrimų metodiką ir įvertinti žemo slėgio (18 bar) dujų tiesioginio įpurškimo sistemos įtaką metano degimo procesui ir degimo produktų formavimuisi optiniame vieno cilindro variklyje, kai naudojami skirtingi degimo būdai ir uždegimo sistemos.

Tyrimų metodika

Šiame darbe pritaikyti teorinio vertinimo, eksperimentiniai ir skaitinio modeliavimo tyrimų metodai. Darbe pateikti žemutinio degalų šilumingumo, vandenilio / anglies atomų santykio skaičiavimai. Teorinių MON, MN skaičiavimų, eksperimentinių duomenų normalumo ir skaičiuojamųjų rodiklių neapibrėžčių skaičiavimų rezultatai nustatyti pagal ISO EN standartus, kurie pateikti disertaciniame darbe. Eksperimentai su gamtinių dujų ir vandenilio mišiniais, taip pat benzino ir biodujų mišiniais atlikti su 4 cilindrų kibirkštinio uždegimo varikliu, kuris turi kolektorinę dujų įpurškimo sistemą. Cilindro slėgio duomenų surinkimui naudotos *LabView, AVL DiTEST* ir *AVL Indicom* programos. Degalų purkštuvams ir kibirkšties momentui valdyti naudota *MoTEC, LabView* sistemos. Siekiant gauti degimo proceso duomenis ir sumodeliuoti variklio darbo procesą su skirtingais degalų mišiniais, skaitinio modeliavimo variklio modelis išplėtotas ir pritaikytas *AVL BOOST* programa. Gamtinių dujų ir vandenilio mišiniai išbandyti sunkiasvorėje transporto priemonėje panaudojant galios matavimo stendą. Metano tiesioginio įpurškimo eksperimentiniai bandymai atlikti su optiniu vieno cilindro kibirkštinio uždegimo vidaus degimo varikliu. Degimo procesas ir degimo liepsnos emisijos spektroskopija fiksuota per stiklinį stūmoklio paviršių ir stiklinę cilindro įvorę, panaudojant greito filmavimo kameras, kurių vaizdai vėliau apdoroti naudojant *MATLAB* programą.

Mokslinis naujumas

1. Pritaikyta teorinio MON ir MN skaičiavimo metodika pagal EN ISO standartą dujiniams degalams ir jų mišiniams. Gauti teorinio vertinimo rezultatai leido papildyti ir geriau įvertinti eksperimentinių tyrimų rezultatus.
2. Išplėtota ir pritaikyta eksperimentinių tyrimų metodika su dviguba dujinių degalų įpurškimo sistema, skirta skystų ir dujinių degalų panaudojimui (benzinas / biodujos, benzinas / gamtinės dujos, benzinas / vandenilis).
3. Taikyta eksperimentinių tyrimų metodika stendiniams variklių tyrimams su gamtinių dujų / vandenilio degalų mišiniais, kuriuos sudaro vandenilis nuo 10 % iki 90 % pagal tūrį degalų mišinyje, bei išplėtota ir pritaikyta skaitinio modeliavimo metodika, nustatant optimalų gamtinių dujų / vandenilio degalų mišinį.
4. Pritaikyta metano tiesioginio įpurškimo sistema su santykinai mažu degalų įpurškimo slėgiu (18 bar), ir ištirta jo įtaka variklio efektyviesiems rodikliams, panaudojus skirtingus degiojo mišinio degimo būdus.
5. Sluoksniuoto degiojo mišinio degimo pritaikymas su žemo slėgio įpurškimo sistema (18 bar) ir optinių tyrimų metodikos pritaikymas metano tiesioginio įpurškimo ir dvigubos apvijos uždegimo sistemos tyrimams.

Darbo rezultatų praktinė reikšmė

1. Ištirti skirtingi benzino / biodujų, benzino / vandenilio, gamtinių dujų / vandenilio degalų mišiniai kibirkštinio uždegimo variklyje su degalų įpurškimu į kolektorių. Gauti rezultatai rodo, kad panaudojus skirtingus alternatyvius dujinius degalus pasiekiamos mažesnės lyginamosios degalų sąnaudos, mažesnė išmetamųjų deginių emisija, todėl minėti degalai gali būti pritaikyti lengvosiose ir sunkiasvorėse transporto priemonės. Norint pasiekti didžiausią variklio efektyvumą su dujiniais degalais būtina reguliuoti uždegimo paskubos kampą, oro pertekliaus koeficientą. Išvados rodo, kad, norint pasiekti mažesnes NO_x, suodžių emisijas išmetamosiose dujose, yra būtini tolimesni tyrimai variklio valdymo sistemoms ir degalų tiekimo sistemoms tobulinti.
2. Gauti teorinių ir eksperimentinių tyrimų rezultatai pritaikomi optimizuojant jau esamų kogeneracinių jėgainių, miesto viešojo ir kitų transporto priemonių vidaus degimo variklius, veikiančius gamtinių dujų, biodujų degalais. Gauti rezultatai suteikia pagrindą tęsti tolimesnius dujinių degalų mišinių, pažangesnių įpurškimo ir uždegimo sistemų tyrimus, kurie leistų pasiekti didesnį vidaus degimo variklio efektyvumą ir žemesnį išmetamų deginių emisijos lygį.
3. Siekiant išanalizuoti skirtingų dujinių degalų mišinių įtaką degimo procesui ir nustatyti optimalų degalų mišinį, sukurtas ir išplėtotas kibirkštinio uždegimo variklio skaitinis modelis naudojant *AVL BOOST* programą. Išplėtotas modelis ir metodika tinkami tiriant ir kitokių dujinių degalų mišinių (biodujų, benzino / biodujų, gamtinių dujų / vandenilio) koncentracijų ar sudėčių įtaką variklio darbo procesui.
4. Optinių ir emisijos spektro eksperimentinių tyrimų rezultatai, gauti išbandžius metano tiesioginį įpurškimą optiniame vieno cilindro variklyje, leidžia tobulinti

įpurškimo sistemas ir palyginti skirtingus degimo tipus bei tobulinti efektyvesnius gamtinių dujų variklius su tiesioginiu degalų įpurškimu.

Ginamieji teiginiai

1. Benzino ir biodujų degalų mišinyje didinant biodujų kiekį iki 30 *l*/min., degalų oktaninis skaičius didėja iki 96. Pridedant reaktyvų vandenilio elementą į gamtines dujas (90 %) degalų mišinio oktaninis skaičius sumažėja iki 80. Degalų antidetonacinių savybių pasikeitimas turi įtakos degimo procesams eksperimentiškai tirtuose kibirkštinio uždegimo varikliuose.
2. Išplėtota ir pritaikyta VDV eksperimentinių tyrimų ir skaitinio modeliavimo metodika leidžia nustatyti optimalų gamtinių dujų / vandenilio degalų mišinį, kuris leidžia pasiekti geresnius VDV efektyviuosius rodiklius.
3. Naudojant degalų mišinius su maža vandenilio koncentracija stechiometriniame arba lieso degimo mišinyje įmanoma pasiekti HC, NO_x ir CO_2 emisijos ribas, neviršijančias benzininių degalų deginių emisijos.
4. Stechiometrinėmis sąlygomis naudojant gamtinių dujų / vandenilio degalų mišinius su labai didele H_2 koncentracija (90 %) kibirkštinio uždegimo variklio sukimo momentas, naudingumo koeficientas mažėja, o NO_x emisija deginiuose labai išauga (> 4000 ppm).
5. Pritaikyti teorinio skaičiavimo ir skaitinio modeliavimo metodų rezultatai rodo, kad didžiausią variklio sukimo momentą galima pasiekti su ~ 65 % H_2 priedu gamtinėse dujose.
6. Naudojant žemo slėgio (18 bar) tiesioginio įpurškimo sistemą kibirkštinio uždegimo variklyje su sluoksniuotu CH_4 dujinių degalų degimu pasiekiamos iki ~ 30 % mažesnės indikatorinės degalų sąnaudos ir iki ~ 36 % didesnis VDV indikatorinis efektyvumas palyginus su reikšmėmis, gautomis išbandžius homogeninį stechiometrinį ir homogeninį liesą degimą.
7. Taikant degimo proceso šviesos emisijos spektro tyrimų metodą eksperimentiniuose variklio bandymuose su metano tiesioginio įpurškimo sistema nustatyta, kad dėl nepakankamo oro ir degalų susimaišymo cilindre sluoksniuoto degimo metu susidaro suodžių židiniai. Taip pat degimo metu užfiksuoti tarpiniai degimo produktai – OH* ir CN* radikalai.

Darbo rezultatų aprobavimas

Disertacinio darbo tematika paskelbta 12 mokslinių straipsnių: vienas – mokslo žurnale, įtrauktame į *Thomson ISI Web of Science ISI* duomenų bazėse, du – tarptautinių konferencijų recenzuotų darbų leidiniuose (*Thomson Reuters data base Proceedings*); keturi – kitų tarptautinių duomenų bazių leidiniuose; vienas – recenzuojamame moksliniame žurnale; keturi – konferencijų medžiagose.

Tyrimų rezultatai disertacijos tematika paskelbti aštuoniose konferencijose:

1. „Inovatyvios technologijos inžinerinėje gamyboje ITEP 2016“. Žilina, Slovakija.
2. SAE Pasaulinis kongresas „Powering Possibilities 2016. SAE International“, Detroitas, Mičigano valstija, JAV.

3. „Mokslas – Lietuvos ateitis: 18-oji jaunųjų mokslininkų konferencija. Transporto inžinerija ir vadyba“, 2015. Vilnius, Lietuva.
4. „Transbaltica 2015: 9-oji tarptautinė mokslinė konferencija“. Vilnius, Lietuva.
5. Tarptautinė mokslinė konferencija „Mobile Machines 2014”. Kaunas, Lietuva.
6. „Transport Means 2013: 17-oji tarptautinė konferencija“. Kaunas, Lietuva.
7. „Mokslas – Lietuvos ateitis: 16-oji jaunųjų mokslininkų konferencija. Transporto inžinerija ir vadyba“, 2013. Vilnius, Lietuva.
8. *AVL* Tarptautinė pažangių modeliavimo technologijų vartotojų konferencija „*AVL* Advanced Simulation Technologies International User Conference”, 2013. Gracas, Austrija.

Disertacijos struktūra

Darbą sudaro įvadas, trys pagrindiniai skyriai, bendrosios išvados, literatūros sąrašas, autoriaus publikacijų disertacijos tema sąrašas, santrauka lietuvių kalba ir 4 priedai. Disertacijos apimtis (be priedų) – 157 puslapiai, 56 sunumeruotos formulės, 66 iliustracijos ir 16 lentelių. Rengiant disertaciją panaudoti 134 literatūros šaltiniai.

Padėka

Autorius dėkoja moksliniam vadovui doc. dr. Saugirdui Pukalskui už pagalbą rengiant disertaciją, dr. Alfredui Rimkui už vertingus patarimus tyrimų metu, prof. Ingemar Denbratt ir doc. dr. Petter Dahlander už šiltą sutikimą ir suteiktą galimybę atlikti tyrimus Čalmerso technologijų universitete, Pauliui Stravinskui (VGTU) ir Eugenio De Benito Sienes (Čalmerso technologijų universitetas) už pagalbą ruošiantis eksperimentams, įmonei „SG dujos Auto“ už bendradarbiavimą ir suteiktą galimybę atlikti tyrimus jų laboratorijoje.

1. Dujinių degalų aktualumo, savybių ir panaudojimo transporte analizė

Europos pramonė ir transportas yra priklausomi nuo importuojamos naftos kiekio. Siekiant sumažinti Europos priklausomybę nuo importuojamos naftos kiekio ir iki 2050 m. 60 % sumažinti transporto priemonių išmetamo anglies dvideginio kiekį, 2013 m. Europos Komisija priėmė išsamią konkurencingos transporto sistemos kūrimo strategiją „Transportas 2050“ (Europos Komisija 2013). Vienas iš šios strategijos pagrindinių tikslų – perpus sumažinti automobilių, naudojančių tradicinius degalus (dyzeliną, benziną) kiekį miestų transporto srautuose iki 2030 m. bei galutinai tokius automobilius eliminuoti iki 2050 m.

Deja, nėra vieno paprasto sprendimo, kurį priėmus būtų galima pašalinti visas su transportu, degalais bei tarša susijusias problemas, nes tiek alternatyvių degalų prieinamumas, tiek jų kaina skiriasi priklausomai nuo transporto rūšies (vandens, automobilių, laivų, geležinkelio). Alternatyvių degalų nauda pirmiausiai būtų pastebima didžiuosiuose miestuose, kur teršalų emisija bei alternatyvių degalų pasirinkimas yra didesnis.

Europoje plačiai naudojamas alternatyvus kuras – suslėgtos gamtinės dujos (SGD) (Kakaee *et al.* 2014). Jos išgaunamos ne tik iš didelių iškastinio kuro rezervų, bet taip pat

kaip biometanas iš paprasčiausių organinių atliekų. Gamtinės dujos yra vertinamos kaip alternatyvus kuras diversifikuojantis visą transporto degalų industriją. Varikliai, varomi SGD degalais, į aplinką išmeta žymiai mažesnius išmetamų deginių kiekius nei daugelis tradiciniais degalais varomų variklių. Pastaruoju metu pastebimas ženklus viešojo bei aptarnaujančio transporto augimas miestuose. Panaudojus SGD minėtose transporto priemonėse galėtų padidėti energijos suvartojimo efektyvumas (Europos Komisija 2013; Brownstein 2015).

Gamtines dujas sudaro metanas (CH_4), kurio procentinė dalis gamtinėse dujose paprastai svyruoja nuo 75 % iki 98 %, papildomi komponentai (etanas, propanas, butanas) bei priemaišos (azotas, anglies dvideginis), kurių koncentracija mišinyje gali būti įvairi. Komponentų bei priemaišų koncentracija gamtinėse dujose gali būti įvairi, ir tai daugiausiai priklauso nuo geografinio šaltinio, nuo gavybos metų laiko bei taikomos dujų gamybos metodikos (Mokhatab *et al.* 2015; Wasiu *et al.* 2012; Karavalakis *et al.* 2012; Kakaee *et al.* 2014).

Lyginant metano dujas su benzinu, metanas turi žymiai didesnį oktaninį skaičių. Metanui jis yra > 130, o benzinui – ~ 86. Didesnis degalų oktaninis skaičius leidžia panaudoti variklius su žymiai didesniu suslėgimo laipsniu, todėl yra galimybė pasiekti didesnį variklio efektyvumą. Varikliui veikiant gamtinėmis dujomis turi būti pritaikytos tam tikros variklio techninės modifikacijos (Boretti *et al.* 2013; Reynolds *et al.* 2005). Tipinės dujinių variklių suslėgimo laipsnio reikšmės svyruoja nuo 10:1 iki 13:1.

Lyginant benzininius ir dyzelinius variklius su gamtinių dujų varikliais, pastarųjų išmetamų deginių (angliavandenilių, anglies monoksido, anglies dvideginio, azoto oksidų bei kietųjų dalelių) emisija yra žymai mažesnė (Kakae *et al.* 2014).

Gamtinių dujų sudėtis turi didelę įtaką degalų antidetonacinėms ir savaiminio užsiliepsnojimo savybėms. Didėjant reaktyvesnių elementų kiekiui dujų sudėtyje oktaninis skaičius ir metano skaičius mažėja, todėl variklio suslėgimo laipsnis turi būti mažinamas (Malenshek *et al.* 2009; Ryan *et al.* 1993).

Biodujos dėl didelio CO_2 kiekio degaluose turi ypatingai mažą energijos kiekį, vertinant jas pagal tūrį. Šių dujų degimo greitis yra mažesnis palyginus su gryno metano degimo greičiu. Biodujų energijos kiekis labai priklauso nuo metano kiekio dujų mišinyje. Nustatyta, kad, panaudojus biodujas su nedideliu metano kiekiu mišinyje, CO_2 emisija išmetamosiose dujose padidėja (Makarevičienė *et al.* 2013, Kovács *et al.* 2010), tačiau taip pat nustatyta, kad panaudojus biodujas variklių NO_x emisija mažėja. Nereakcingas elementas CO_2 degalų mišinyje degimo metu absorbuoja dalį išsiskyrusios šilumos ir sumažina bendrai visą degimo temperatūrą, kuri tiesiogiai įtakoja NO_x formavimąsi (Makarevičienė *et al.* 2013; Talal *et al.* 2010). Nustatyta, kad šiluminės ir kinetinės reakcijos tarp skystų ir dujinių degalų prailgina degimo gaišties periodą (Carlucci *et al.* 2011).

Siekiant panaudoti kuo daugiau naujų alternatyvių degalų šaltinių, vandenilis yra vienas perspektyviausių elementų ir energijos akumuliatorių. Vandenilis gali pasitarnauti mažinant šiltnamio efektą sukeliančias dujas bei didinant variklių efektyvumą.

Vandenilio atomai yra labai reaktyvūs. Uždegus vandenilio ir oro mišinį, per trumpą laiko tarpą degimo metu išsiskiria didžiulis energijos kiekis. Vandenilio degimo greitis yra ~ 1,85 m/s palyginus su benzino 0,42 m/s ir dyzelino 0,38 m/s greičiu. Vandenilio degimo trukmė yra trumpesnė negu benzino (Ramadhas 2011, Mardi *et al.* 2014). Vandenilio priedas dėl padidėjusio degalų mišinio degimo greičio sutrumpina gaišties periodą ir

sutrumpina liepsnos plitimo trukmę (Ji *et al.* 2013; Ji *et al.* 2010; Rimkus *et al.* 2013). Tačiau vandenilio panaudojimas gali turėti ir neigiamos įtakos variklio rodikliams. Gali sumažėti variklio galingumas, sukimo momentas dėl vandenilio fizikinių ir cheminių savybių (Kahraman *et al.* 2006).

Panaudojant vandenilio ir gamtinių dujų degalų mišinius galima sumažinti CO, CO_2, HC emisijas (Larsen *et al.* 1997), tačiau išauga azotų oksidų emisija dėl padidėjusios degimo temperatūros (D'Andrea *et al.* 2004). Nustatyta, kad, norint pasiekti didžiausią variklio efektyvumą panaudojant vandenilį kaip priedą degalų mišiniuose, yra būtina teisingai nustatyti kibirkšties uždegimo momentą (Dimapoulous *et al.* 2007; Karim *et al.* 2003).

Kitas būdas pasiekti variklio didesnį efektyvumą yra tobulesnių ir naujų degalų įpurškimo ir valdymo sistemų kūrimas ir vystymas. Nustatyta, kad, naudojant dujinių degalų kolektorinį įpurškimą, dujos užima tam tikrą tūrį oro įsiurbimo kolektoriuje. Užimamas tūris kolektoriuje gali būti didesnis palyginus su skystais degalais.

Dujų tiesioginis įpurškimas į variklio cilindrą yra vienas iš būdų padidinti variklio efektyvumą, pasiekti geresnį degiojo mišinio formavimąsi cilindre, pasiekti didesnį sukimo momentą, sumažinti siurbimo nuostolius (Zhao 2010). Degimo procesas cilindre labai priklauso nuo tokių parametrų: purkštuvo antgalio, įpurškimo slėgio, įpurškimo laiko ir trukmės, variklio galvutės ir stūmoklio geometrinės formos (A-Aziz *et al.* 2009, Di Iorio *et al.* 2014, Baratta *et al.* 2009). Taikant degalų tiesioginio įpurškimo būdą susiduriama su suodžių formavimosi problema (Stojkovic *et al.* 2005). Ši problema aktuali ir dujiniams degalams, kai panaudojamas sluoksniuotas degimas – degalai įpurškiami suslėgimo takto pabaigoje.

Tiriant skirtingus dujinių degalų mišinius ir degalų įpurškimo sistemas būtina įvertinti reguliuojamų parametrų (uždegimo paskubos kampas, įpurškimo trukmė ir laikas, degiojo mišinio sudėtis, degalų mišinio sudėtis) įtaką variklio efektyvumui ir ekologiniams rodikliams.

2. Dujinių degalų degimo procesų tyrimų metodologija

Tyrimai atlikti 2012–2016 metais. Eksperimentai atlikti su 3 skirtingais varikliais:

- 4 cilindrų *HR16DE* kibirkštinio uždegimo variklis, naudojamas *Nissan Qashqai* transporto priemonėje. Tyrimai atlikti VGTU VDV tyrimų laboratorijoje. Tyrimai atlikti su benzino / biodujų, benzino / vandenilio ir gamtinių dujų / vandenilio degalų mišiniais.
- *AVL* vieno cilindro kibirkštinio uždegimo variklis. Tyrimai atlikti Čalmerso technologijų universitete, Degimo procesų tyrimų katedroje, Švedijoje. Tyrimai atlikti su grynu metanu (100 % CH_4).
- *Castrosua City Versus* miesto autobusas su 6 cilindrų kibirkštinio uždegimo VDV (variklis *F2BE0642H*). Tyrimai atlikti įmonėje „SG dujos Auto", Pabradės mieste. Tyrimai atlikti su gamtinių dujų / vandenilio mišiniais.

S.2.1 lentelėje pateikti išbandyti skirtingi degalų tipai, degalų mišiniai su skirtingais bandymų varikliais ir degalų įpurškimo sistemomis.

S.2.1 lentelė. Ištirtos skirtingos degalų rūšys su skirtingais varikliais

Varikliai	Degalų įpurškimas	Oro tiekimas	Degalai	Degalų žymėjimas
4 cilindrų variklis *HR16DE*	Kolektorinis įpurškimas	Atmosferinis	Benzinas	*P*
			Benzinas + Biodujos	*P* + *Bio*
			Benzinas + Vandenilis	*P* + H_2
			Suslėgtos gamtinės dujos	CNG
			Suslėgtos gamtinės dujos + Vandenilis	CNG + H_2
1 cilindro *AVL* optinis variklis	Tiesioginis įpurškimas	Atmosferinis	Metanas	CH_4
6 cilindrų *F2BE0642H* variklis	Kolektorinis įpurškimas	Turbokompresorinis	Suslėgtos gamtinės dujos	CNG
			Suslėgtos gamtinės dujos + Vandenilis	CNG + H_2

S.2.2 lentelėje pateikti bandytų variklių su skirtingais dujiniais degalais ir jų mišiniais techniniai parametrai. Eksperimentai atlikti su 4 cilindrų *HR16DE* varikliu panaudojant kolektorinio įpurškimo sistemą. Išbandyti degalai – benzinas / biodujos, gamtinės dujos / vandenilis. Bandymuose su 1 cilindro optiniu varikliu išbandytos metano dujos su tiesioginio įpurškimo sistemą ir dvigubos apvijos uždegimo sistema. 6 cilindrų variklis bandytas, panaudojant gamtinių dujų / vandenilio mišinius.

S.2.2 lentelė. Eksperimentiškai bandyti kibirkštinio uždegimo varikliai

Rodikliai	*Nissan HR16DE*	*AVL* 1 cilindro variklis	*F2BE0642H*
Cilindrų skaičius	4	1	6
Cilindro skersmuo, mm	78	83	115
Stūmoklio eiga, mm	83,6	90	125
Litražas, dm^3	1,598	0,487	7,790
Maksimali galia, kW (min^{-1})	84 (6000)	-	213 (2000)
Maksimalus sukimo momentas, Nm (min^{-1})	156 (4400)	-	1100 (1100–1850)
Suslėgimo laipsnis, ε	10,7	9,89	11,5
Švaistiklio ilgis, mm	130	139,5	-
Vožtuvų skaičius cilindrui, vnt.	4	4	4

Siekiant papildyti eksperimentinių tyrimų rezultatus apskaičiuoti tokie degalų rodikliai: žemutinis degalų šilumingumas, H/C atomų santykio skaičius, oktaninis ir metano

skaičiai, siekiant papildyti eksperimentinių tyrimų rezultatus ir turėti geresnį supratimą apie dujinių degalų degimo procesą. Oktaninis ir metano skaičių nustatymas atliktas pagal ISO 15403–2006, EN 16726:2015 standartus. Išplėtotas ir pritaikytas skaitinio modeliavimo modelis *AVL BOOST* aplinkoje (S.2.1 pav.), siekiant nustatyti optimalų dujinių degalų mišinį

S.2.2 paveiksle pateiktoje schemoje pristatytas optinių ir emisijos spektrinių tyrimų būdas, taikytas dujų tiesioginio įpurškimo tyrimuose. Bandymuose naudotas sąlyginai žemo įpurškimo slėgio (18 bar) purkštuvas. Degimo procesas fiksuotas greito filmavimo kameromis.

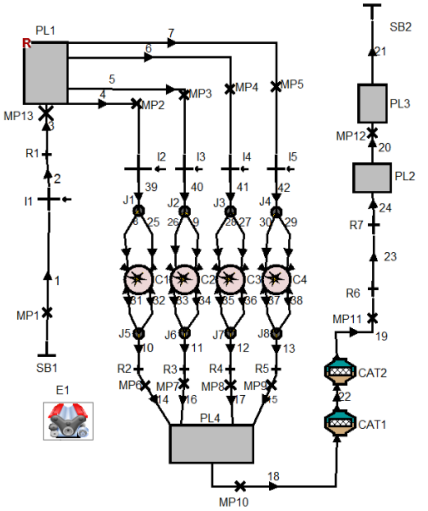

S.2.1 pav. Kibirkštinio uždegimo variklio *HR16DE* skaitinis *AVL BOOST* aplinkoje

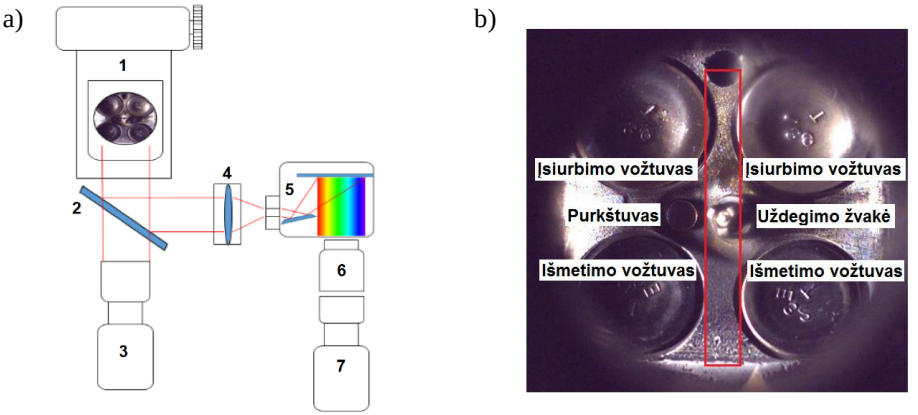

S.2.2 pav. Optiniai tyrimai taikyti tiesioginio įpurškimo sistemos bandymų metu: a) optinės įrangos išdėstymo schema, b) degimo kameros vaizdas iš variklio apačios

S.2.2 paveiksle pateikta įrangos išdėliojimo schema, kurioje: 1 – optinis vieno cilindro variklis, 2 – spindulio skaidytuvas, 3 – greito filmavimo kamera, skirta fiksuoti degimo procesą, 4 – fokusavimo lęšis, 5 – atspindinti difrakcinė gardelė, 6 – vaizdo stiprintuvas, 7 – greito filmavimo kamera, skirta fiksuoti šviesos emisijos spektrą.

3. Dujinių degalų mišinių panaudojimo kibirkštinio uždegimo vidaus degimo variklyje skaitinis ir eksperimentinis tyrimas

Atlikus eksperimentus su benzino ir biodujų degalų mišiniais nustatyta, kad uždegimo paskubos kampo keitimas turi įtakos nustatant maksimalius efektyviuosius variklio rodiklius. Variklio maksimalus sukimo momentas ($M_{e\_maks.}$) mažėjo (~ 4 %), naudojant biodujas (30 *l*/min. biodujų) kartu su benzinu dviguboje degalų tiekimo sistemoje. Uždegimo paskubos kampas turėjo būti ankstinamas 4º, lyginant su gautais rezultatais išbandžius benziną. Įpurkštos biodujos į įsiurbimo kolektorių užėmė tam tikrą tūrį cilindre, variklio valdymo blokas įpurkšdavo mažesnį kiekį benzino, todėl bendras degalų mišinio šilumingumas mažėjo. Cilindrų pripildymas blogėjo, tai sumažino ir ciklinį įpurškiamų degalų kiekį (E_c).

Biodujų priedas sumažino variklio efektyvumą (sumažėjo ~ 1,3 %) esant optimaliam benzino 22º prieš viršutinį rimties tašką (VRT) kampui. Degalų mišinio degimo greitis sumažėjo dėl didelio CO_2 kiekio, esančio biodujose. Siekiant išgauti aukštesnį variklio η_e būtina ankstinti uždegimo kampą.

Variklio elektroninis valdymo blokas palaikė stechiometrinį mišinį ($\lambda = 1$). Didinant biodujų kiekį degalų mišinyje, įsiurbiamas oro kiekis mažėjo, nes dujos užėmė dalį įsiurbimo kolektoriaus ir cilindro tūrio. Valdymo blokas įpurkšdavo mažiau degalų, o tai sumažino degalų mišinio valandines degalų sąnaudas.

CO ir CO_2 deginių emisija didėjo didinant biodujų kiekį degalų mišinyje. CO didėjo dėl pablogėjusio degimo proceso, kuriam turėjo įtakos CO_2 priedas degalų mišinyje. CO_2 emisijos padidėjimas 0,5 % yra labai mažas. Šiam nedideliam padidėjimui galėjo turėti įtakos metanas, kuris turi paprastesnę molekulinę struktūrą, lyginant su benzino degalų molekuline struktūra. Biodujų priedas sumažino HC ir NO_x emisiją. NO_x emisija mažėjo dėl sumažėjusios degimo temperatūros, kurią sumažino biodujose esantis CO_2 bei sumažėjęs degalų mišinių šilumingumas.

Benzino ir biodujų degalų mišinių degimo proceso analizė parodė, kad biodujos, kurių sudėtis yra 65 % CH_4 / 35 % CO_2, lėtino degimo procesą cilindre. Degimas prasidėdavo vėliau ir vyko ilgiau, todėl sukuriamas naudingas darbas cilindre buvo neefektyviai panaudojamas. Ankstinant uždegimo paskubos kampą įmanoma pasiekti geresnį variklio efektyvumą su biodujų priedu negu su standartiniu uždegimo kampu, tinkamu benzinui. Bandant benzino ir biodujų degalų mišinį ir ankstinant uždegimo paskubos kampą pasiektos mažesnės išmetamų deginių emisijos.

Atlikus oktaninio skaičiaus bei metano skaičiaus skaičiavimus nustatyta, kad biodujų priedas didina oktaninį skaičių (S.3.2 pav.). Tai reiškia, kad mišinio antidetonacinės savybės didėja. Padidėjus oktaniniam skaičiui, varikliui būtų galima taikyti aukštesnį suslėgimo laipsnį. Tai padidintų variklio efektyvumą.

Gamtinių dujų ir vandenilio (CNG + H_2) degalų mišinių bandymai atlikti su skirtingomis variklio apkrovomis (1,56, 3,14, 4,72, 6,28 bar) esant optimaliam CNG dujų uždegimo kampui. Bandymai taip pat atlikti su skirtingais degalų mišiniais keičiant uždegimo paskubos kampą ir palaikant tą pačią akseleratoriaus sklendės padėtį (15 %). Bandymai atlikti su stechiometriniu ($\lambda = 1$) ir liesu ($\lambda = 1{,}4$) degalų mišiniu. Eksperimentiniai tyrimai parodė, kad didžiausios degalų sąnaudos pasiektos su benzinu bei gamtinėmis dujomis. Didinant H_2 kiekį gamtinėse dujose degalų sąnaudos mažėjo, nes vandenilio apatinis degalų šilumingumas didino bendrą degalų mišinio šilumingumą. Padidėjus degalų šilumingumui mažėjo degalų E_c.

H_2 priedas gamtinėse dujose sumažino CO, CO_2 ir HC deginių emisiją, lyginant su benzino ir CNG deginių emisija. CNG + H_2 degalų mišiniai yra paprastesnės molekulinės struktūros, kuri keitėsi didinant H_2 priedą degaluose. Didinant H_2 kiekį H / C atomų santykis didėjo. Tai mažino minėtų deginių emisiją, tačiau padidėjusi degimo temperatūra ir intensyvumas padidino NO_x emisijas.

Panaudojus vandenilio priedą gamtinių dujų mišinyje nustatyta, kad padidėja degimo temperatūra cilindre, padidėja šilumos išsiskyrimo greitis bei sutrumpėja gaišties periodas. Naudojant vandenilį degalų mišiniuose, dėl pasikeitusio degimo proceso yra būtina vėlinti uždegimo paskubos kampą, jeigu norima pasiekti didesnį variklio efektyvumą ir mažesnes išmetamųjų deginių emisijas. Eksperimentinių bandymu metu nustatyta, kad didžiausias variklio sukimo momentas pasiektas su CNG + 70 % H_2 degalų mišiniu (S.3.1 pav.).

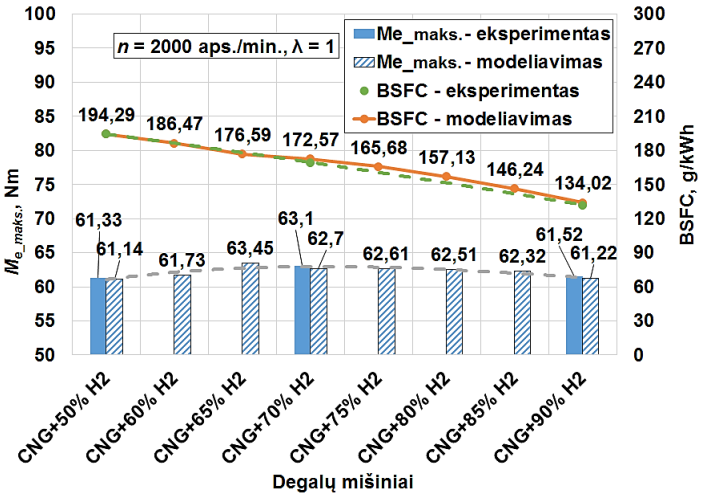

S.3.1 pav. Variklio maksimalaus sukimo momento ir lyginamųjų degalų sąnaudų priklausomybė nuo skirtingų eksperimentiškai ir skaitiniu būdu tirtų gamtinių dujų / vandenilio mišinių

Pritaikyta išplėtota skaitinio modeliavimo metodika ir panaudotos degimo procesų rodiklių reikšmės skaitiniame variklio modelyje nustatant optimalų degalų mišinį. Skaitinio modeliavimo būdu nustatyta, kad optimalus gamtinių dujų ir vandenilio mišinys yra su 65 % H_2 priedu (S.3.1 pav.).

Oktaninio skaičiaus ir metano skaičiaus teorinis vertinimas parodė, kad vandenilio priedas mažina degalų antidetonacines savybes (S.3.2 pav.), todėl varikliai su aukštais suslėgimo laipsniais bei didelėmis vandenilio koncentracijomis degalų mišiniuose negali būti naudojami dėl padidėjusios tikimybės atsirasti detonaciniams reiškiniams cilindre. Naudojant vandenilio priedą būtina vėlinti uždegimo paskubos kampą dėl išaugusio degimo greičio ir degimo intensyvumo. Uždegimo momento reguliavimas leistų pasiekti didžiausią variklio efektyvumą.

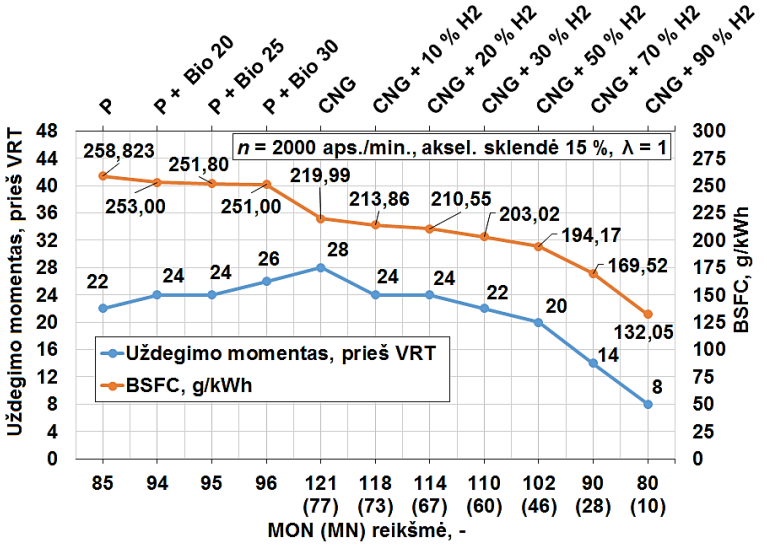

S.3.2 pav. Uždegimo paskubos kampo ir lyginamųjų degalų sąnaudų priklausomybė nuo degalų oktaninio (metano) skaičiaus ir degalų mišinio, kai variklio sūkiai n = 2000 aps./min., aksel. sklendė 15 %, λ = 1

Atliekant metano dujų (100 % CH_4) tiesioginio įpurškimo sistemos tyrimus nustatyta, kad 18 bar įpurškimo slėgis yra įmanomas naudojant tiek stechiometrinį, tiek lieso degimo, tiek sluoksniuotą degųjį mišinį. Eksperimentinių bandymų metu nustatyta, kad kompresijos slėgio ir įpurškimo slėgio skirtumas turi didelę įtaką įpurškiamų degalų kiekiui ir įpurškimo trukmei. Nustatyta, kad ilgiausia įpurškimo trukmė turi būti taikoma sluoksniuotam degimui. Geriausi efektyvieji rodikliai (mažiausios degalų sąnaudos ir indikatorinės lyginamosios degalų sąnaudos) pasiekti su sluoksniuotu degimu. Naudojant minėtą degimo būdą sumažėja siurbimo nuostoliai, pagerėja cilindro pripildymas oru, sumažėja šilumos nuostoliai į cilindro sieneles. Priklausomai nuo variklio apkrovos ir sūkių, lyginant stechiometrinį degimą su sluoksniuotu, sluoksniuoto degimo metu galima pa-

siekti iki ~ 30 % žemesnes indikatorines lyginamąsias degalų sąnaudas. Didelę įtaką degimo proceso stabilumui turi ir oro pertekliaus koeficientas, uždegimo paskubos kampas, įpurškimo trukmė bei variklio sūkiai.

Analizuojant metano sluoksniuotą degimo procesą ir panaudojus degimo proceso spektrinę analizę, nustatyta, kad skirtingose variklio degimo kameros vietose vienu metu gali būti ir OH* (~ 308 nm), CN* (~ 370 nm) radikalų, CO_2 (420–550 nm) bei suodžių židinių (350–550 nm) (S.3.3 pav.).

Siekiant užtikrinti stabilų sluoksniuotą degimą panaudota dvigubos apvijos uždegimo sistema su trijų elektrodų uždegimo žvake. Naudojant šią uždegimo sistemą žvakės plazma degė ilgesnį laiką ir apėmė didesnį degimo kameros tūrį, todėl buvo įmanoma uždegti oro / degalų mišinį visais fiksuotais degimo proceso atvejais.

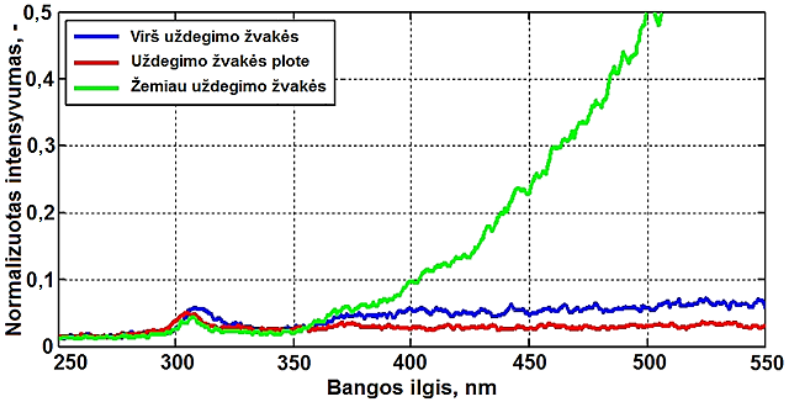

S.3.3 pav. Emisijos spektras išmatuotas trijuose skirtinguose optinio variklio cilindro plotuose

Degimo proceso, cilindro slėgio ir šilumos išsiskyrimo analizė parodė, kad, naudojant tiesioginį įpurškimą su sluoksniuotu degimu cilindre, pasireiškia dideli cikliniai degimo proceso svyravimai, kurių atsiradimui galimai turi įtakos netinkamas oro / degalų mišinio susimaišymas cilindre.

Bendrosios išvados

1. Pritaikyti teorinio LHV, MON, MN ir H/C atomų santykio skaičiavimai dujiniams degalams ir jų mišiniams atskleidė, kad su didėjančiu biodujų kiekiu degalų mišinyje antidetonacinės ribos didėja. Pridedant ypatingai reaktyvų H_2 elementą į degalų mišinį pastebimas oktaninio skaičiaus sumažėjimas bei H/C atomų santykio didėjimas.
2. Norint pasiekti aukščiausią variklio efektyvumą, panaudojus biodujas dviguboje degalų tiekimo sistemoje kartu su benzinu, yra būtina paankstinti kibirkšties uždegimo momentą dėl sumažėjusio šilumos išsiskyrimo greičio ir ilgesnės degimo

trukmės. Nors didžiausias biodujų (30 *l*/min.) priedas ~ 1,3 % sumažina variklio efektyvumą, tačiau HC ir NO_x deginių koncentracija išmetamosiose dujose gaunama mažiausia iš išbandytų degalų mišinių.

3. Dviguba degalų tiekimo sistema (benzinas + biodujos) gali būti naudojama varikliuose su aukštesniu suslėgimo laipsniu, nes, kaip parodė MON teorinio skaičiavimo rezultatai, minėtų degalų detonacinės ir degalų savaiminio užsiliepsnojimo ribos yra aukštesnės. Teoriniai tyrimai rodo, kad aukštesnio suslėgimo laipsnio varikliai pasiekia didesnį efektyvumą.
4. H_2 priedo panaudojimas gamtinėse dujose pagerina degimo procesą: degiojo mišinio gaišties periodas sutrumpėja ~ 5 kartus esant stechiometrinėms degimo sąlygoms, šilumos išsiskyrimo greitis padidėja ir tampa intensyvesnis, degimo trukmė sutrumpėja ~ 47 %. Norint pasiekti geriausius variklio efektyviuosius rodiklius, uždegimo momentas turi būti vėlinamas ir pritaikomas atitinkamai H_2 priedo koncentracijai gamtinėse dujose.
5. Aukščiausias variklio η_e pasiekiamas su 30 % H_2 priedu stechiometrinėmis degiojo mišinio sąlygomis ($\lambda = 1$), o pats didžiausias η_e lieso degimo sąlygomis ($\lambda = 1,4$) pasiektas su 70 % H_2 koncentracija gamtinių dujų / vandenilio degalų mišinyje. Didinant H_2 kiekį degalų mišinyje, lyginamosios degalų sąnaudos mažėja, o mažiausios šio rodiklio reikšmės gaunamos su 90 % H_2 priedu tiek stechiometrinėmis, tiek lieso degimo sąlygomis.
6. H_2 padidina degimo intensyvumą ir degimo temperatūrą, kaip ir buvo galima prognozuoti. Padidėjusi degimo temperatūra suintensyvina NO_x formavimąsi variklio cilindre, tačiau naudojant H_2 degalų mišiniuose iki 30 % išmatuota NO_x deginių emisija tiek stechiometrinis, tiek lieso degimo sąlygomis neviršija gauto emisijos lygio bandant benziną.
7. Variklio maksimalaus sukimo momento matavimai parodė, kad momentas mažėja panaudojant gamtinių dujų ir vandenilio mišinius, kuriuose yra iki 20 % H_2, tačiau, didinant H_2 koncentraciją, momentas nuosekliai didėja, ir didžiausia reikšmė pasiekiama kai H_2 sudaro 70 %. Didesnis H_2 kiekio panaudojimas rodo maksimalaus sukimo momento mažėjimo tendencijas, nes degimo proceso metu pasiekiamas per didelis degimo greitis bei per trumpa degimo trukmė.
8. Siekiant nustatyti optimalų gamtinių dujų / vandenilio degalų mišinį, tyrimuose išplėtotas ir pritaikytas skaitinio modeliavimo modelis. Skaitinio modeliavimo rezultatai parodė, kad sukurtas modelis atitinka eksperimentinio variklio rodiklius. Nustatyta, kad didžiausias variklio sukimo momentas pasiekiamas su SGD + 65 % H_2 degalų mišiniu stechiometrinėmis sąlygomis.
9. Tyrimai parodė, kad sluoksniuotas degimas su metano tiesioginiu įpurškimu yra įmanomas kibirkštinio uždegimo vidaus degimo variklyje esant sąlyginai žemam (18 bar) degalų įpurškimo slėgiui. Siekiant užtikrinti stabilų degimo procesą cilindre turi būti naudojama dvigubos apvijos uždegimo sistema.
10. Dujų tiesioginė įpurškimo sistema su sluoksniuotu degimu, lyginant su homogeniniu stechiometriniu ir homogeniniu liesu degimu, leidžia pasiekti mažesnes indikatorines lyginamąsias degalų sąnaudas. Tačiau sluoksniuoto degimo proceso

vaizdinė medžiaga, slėgio cilindre, šilumos išsiskyrimo greičio duomenys parodė, kad cikliniai degimo proceso svyravimai yra dideli. Minėtiems svyravimams turi įtakos netinkamas oro / degalų sumaišymas ir oro sūkuriavimas cilindre.

11. Užfiksuoti degimo proceso vaizdai ir emisijos spektro analizė rodo, kad suodžių židiniai formuojasi metano sluoksniuoto degimo metu atsitiktiniame liepsnos degimo židinyje. Šie rezultatai parodo, kaip sunkiai pasiekiamas tinkamas oro ir metano maišymasis, kuris turi įtakos tiek cikliniams degimo proceso svyravimams, tiek riebaus mišinio zonoms, kurios yra suodžių susidarymo židiniai variklio cilindre.

Annexes[1]

Annex A. Research Methodology of Gaseous Fuels and Fuel Injection Systems

Annex B. Experimental and Simulation Results Obtained from Gaseous Fuel Tests

Annex C. Agreements of Co-Authors to Provide Published Materials in the Dissertation

Annex D. Copies of Scientific Publications by the Author on the Topic of the Dissertation

[1]The annexes are supplied in the enclosed compact disc

Mindaugas MELAIKA

RESEARCH OF A COMBUSTION PROCESS
IN A SPARK IGNITION ENGINE, FUELLED
WITH GASEOUS FUEL MIXTURES

Doctoral Dissertation

Technological Sciences,
Transport Engineering (03T)

Mindaugas MELAIKA

DUJINIŲ DEGALŲ MIŠINIŲ DEGIMO PROCESO
KIBIRKŠTINIO UŽDEGIMO VARIKLYJE TYRIMAI

Daktaro disertacija

Technologijos mokslai,
Transporto inžinerija (03T)

2016 12 23. 14,5 sp. l. Tiražas 20 egz.
Vilniaus Gedimino technikos universiteto
leidykla „Technika“,
Saulėtekio al. 11, 10223 Vilnius,
http://leidykla.vgtu.lt
Spausdino UAB „BMK leidykla“,
Jasinskio g. 16, 01112 Vilnius